



Universiteit  
Leiden  
The Netherlands

## **Innate immunity, developmental speed and their trade-offs in two hexapod models**

Cheng, S.

### **Citation**

Cheng, S. (2023, November 28). *Innate immunity, developmental speed and their trade-offs in two hexapod models*. Retrieved from <https://hdl.handle.net/1887/3665319>

Version: Publisher's Version

License: [Licence agreement concerning inclusion of doctoral thesis in the Institutional Repository of the University of Leiden](#)

Downloaded from: <https://hdl.handle.net/1887/3665319>

**Note:** To cite this publication please use the final published version (if applicable).

Innate immunity, developmental speed  
and their trade-offs in two hexapod  
models

Shixiong Cheng

Cheng, S

Innate immunity, developmental speed and their trade-offs in two hexapod models

PhD thesis, Faculty of Science, Leiden University, Leiden, the Netherlands

Cover design and layout: Shixiong Cheng

Front cover: stills from two live imaging movies of *Tribolium castaneum* embryos at the same timepoint. Up is a wild type, and below is an embryo from the Crispr line that carries a deletion in a regulatory region of *Cyp18a1* (Chapter 4). The wildtype embryo is at the retracted germband stage, whereas the CRISPR embryo develops faster and is already undergoing dorsal closure.

Printed: Ridderprint | [www.ridderprint.nl](http://www.ridderprint.nl)

ISBN: 978-94-6483-432-1

© 2023 by Shixiong Cheng. All right reserved.

# Innate immunity, developmental speed and their trade-offs in two hexapod models

## Proefschrift

ter verkrijging van  
de graad van doctor aan de Universiteit Leiden,  
op gezag van rector magnificus prof.dr.ir. H. Bijl,  
volgens besluit van het college voor promoties  
te verdedigen op dinsdag 28 november 2023  
klokke 13:45 uur

door

Shixiong Cheng  
geboren te Gansu, China  
in 1993

**Promotor**

Prof. dr. H. P. Spaink

**Co-promotor**

Dr. M. van der Zee

**Promotiecommissie**

Prof. dr. A. H. Meijer

Prof. dr. M. K. Richardson

Dr. D. E. Rozen

Prof. dr. B. Wertheim (University of Groningen)

Prof. dr. B. J. Zwaan (Wageningen University & Research)

## Table of Contents

Chapter 1	General introduction	7
Chapter 2	Immune competence in eggs of the springtail <i>Orchesella cincta</i>	31
Chapter 3	Correlated responses to selection for embryonic developmental time in <i>Tribolium castaneum</i>	43
Chapter 4	A novel allele of large effect that alters developmental time and mediates trade-offs	63
Chapter 5	Summary, discussion and perspective	153
	Nederlandse samenvatting	163
	Curriculum Vitae	167
	List of publications	169



# Chapter 1

## General introduction

### The success of the insects

#### The earth's largest and most diverse group of organisms

Insects underwent unparalleled diversification and make up more than half of all animal species. Insects (Insecta or Hexapoda) are the largest class of the phylum Arthropoda, which is itself the largest of all animal phyla. According to the estimates from Grimaldi, 64 percent of described around 1.5 million species on earth are arthropods, of which more than 87 percent are insects (Grimaldi and Engel, 2005) (Figure 1-1). Globally, over one million species of insect have been described to date. The total amount of insect species is believed to vary from 2.5 to 5.5 million. It is also estimated that the number of living individual insects has reached 10 quintillion at this moment (Berenbaum, 1996; Stork, 2018). Insects have shown an incredible diversity, abundance and biomass over time. They occur in practically all habitats all over the earth (Price, 1997). Before providing some hypotheses for this spectacular success, I first introduce the taxonomy of insects in more detail, and discuss their importance for humans.

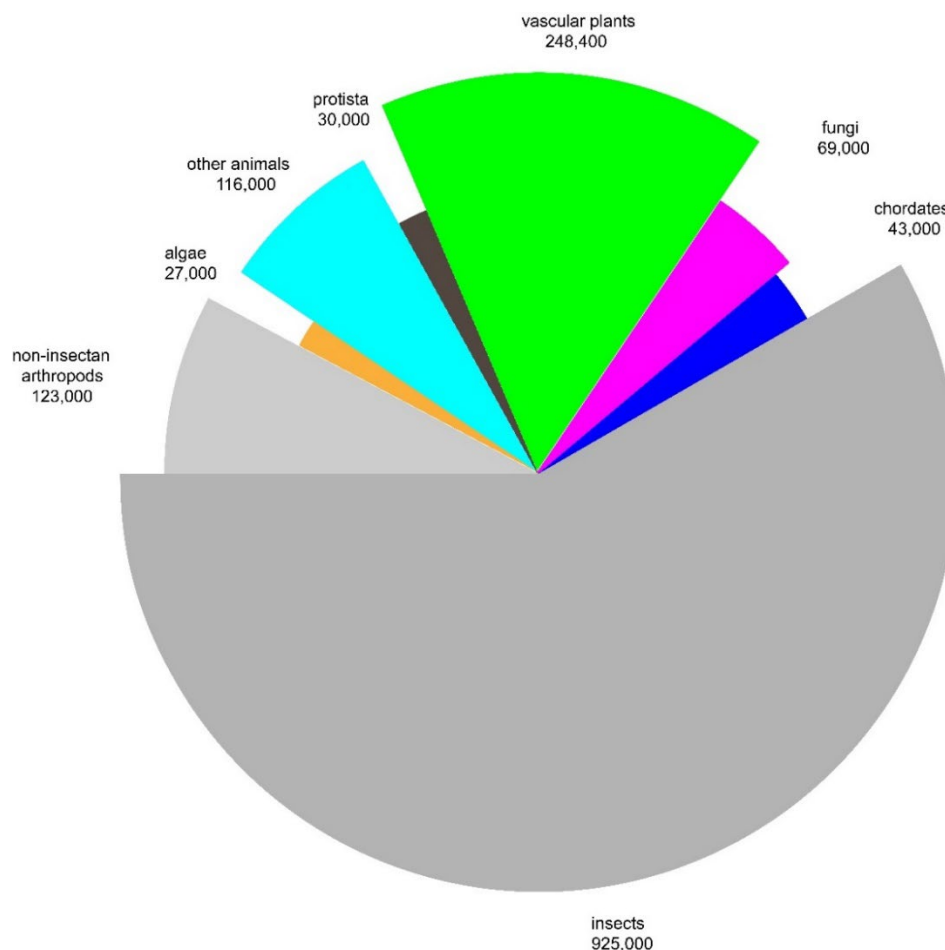




Figure 1-1. Relative proportions of described eukaryote taxa, with species numbers [summarized by (Grimaldi and Engel, 2005)].

## Classification

The subphylum Hexapoda consists of four groups: Insecta, Collembola, Protura, and Diplura. The subphylum name refers to the most distinctive feature: the presence of six legs in the three consolidated segments of the thorax. The mouthparts of insects are ectognathous, while the other groups are endognathous. These non-insect hexapods are called the Entognatha and lack wings. In particular, Collembola (springtails) are extremely abundant in soil and are found in almost all terrestrial environments. I will study the immune competence of one springtail, *Orchesella cincta*, in Chapter 2. Collembola comprise more than 82 percent of all described entognathan species. Strikingly, insects comprise more than 99 percent of the Hexapod species and are thus the largest class (Zhang, 2011; Zhang, 2013) (Figure 1-2).

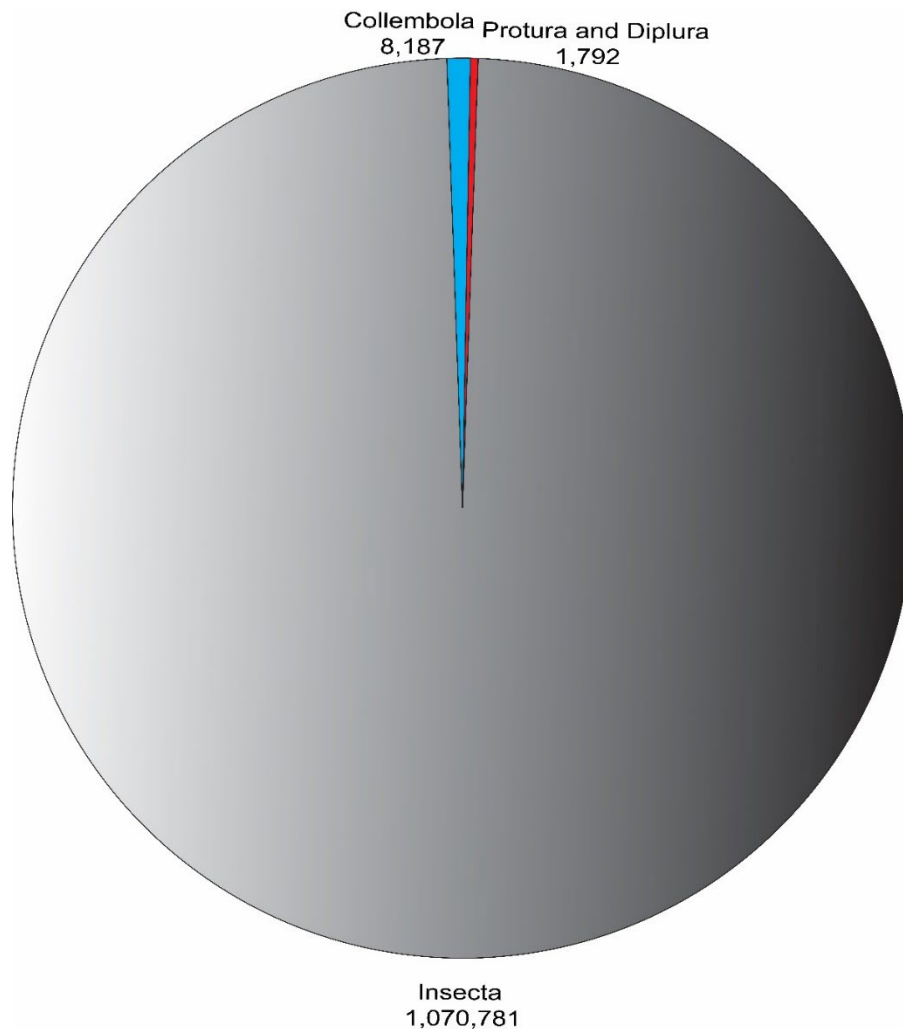


Figure 1-2. Relative proportions of described species in the subphylum Hexapoda, with species numbers [adopted from (Zhang, 2011; Zhang, 2013)].

Insects have an exoskeleton and three pairs of walking legs. The class Insecta is divided into two subclasses: Apterygota (primitively wingless insects) and Pterygota (winged or secondarily wingless insects). The Apterygota is a kind of small, agile insects. The Apterygota consist of the Archaeognatha

(known as jumping bristletails) and the Zygentoma (known as silverfish and firebrats). There is no metamorphosis in apterygotes as their nymphs are similar to adults. The Pterygota include the majority of species in the class Insecta. Most of them have wings, while a few species lost their wings secondarily due to adaptation to the living environment. One typical characteristic of the Pterygota is the metamorphosis, namely the larva does not have wings. Some insects undergo several nymphal stages into the adult by a series of molts (incomplete metamorphosis), while others undergo complete metamorphosis through a pupal stage.

Incomplete metamorphosis includes three stages: egg, nymph, and adult in insect development. When these insects hatch from the egg, the nymph resembles the miniature adult. This type of insects are also called the hemimetabolous insects which contain orders of Hemiptera (true bugs), Orthoptera (grasshoppers, locusts and crickets), Mantodea (praying mantis), and so on. In contrast, holometabolous insects undergo complete metamorphosis. Their life cycle consists of four distinct stages: egg, larva, pupa, and adult. The pupa is a tough capsule (cocoon) formed by the hardening of the larval skin. Recent classifications showed that 39 insect orders exist in total, of which four orders are holometabolous insects but comprise over 80% of insect species. These orders are the Coleoptera, Diptera, Lepidoptera, and Hymenoptera (Zhang, 2011; Zhang, 2013) (Figure 1-3).

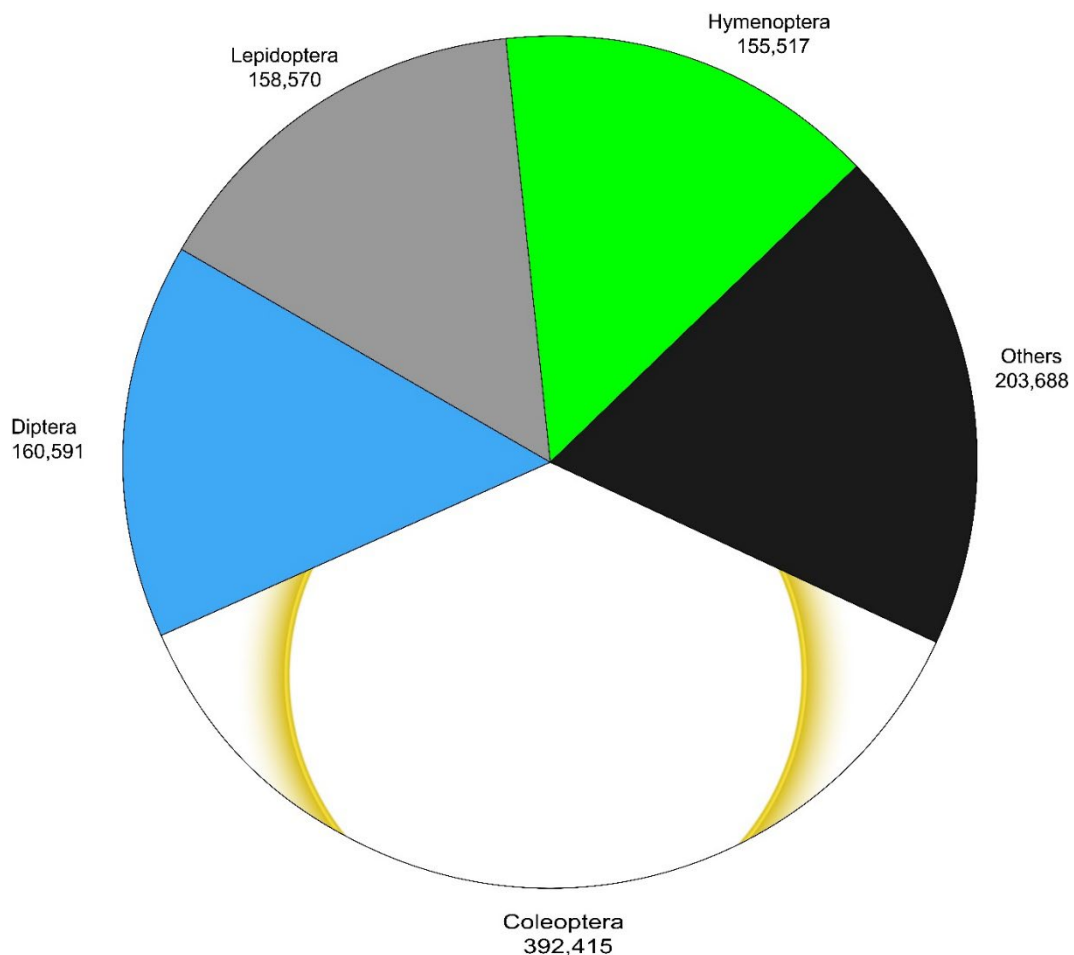


Figure 1-3. Relative proportions of named species in the orders in the Insecta, with species numbers [adopted from (Zhang, 2011; Zhang, 2013)].

Diptera, normally known as true flies only use a single pair of wings to fly and their hindwings have evolved into halteres that act as assistance for balance during flight. The fruit fly *Drosophila melanogaster*, one of the most thoroughly studied organisms by humans, belongs to this insect order. The knowledge on development and genetics is mostly based on experiments done on *D. melanogaster* (Dubrovsky, 2005).

Coleoptera, commonly known as beetles, are the largest insect order and account for approximately 37% of insect species. The most characteristic and diagnostic feature of beetles is the hardening of the forewings into elytra (Crowson, 2013). The red flour beetle *Tribolium castaneum* belongs to this order. In the last decades, *T. castaneum* has emerged as a powerful model system for studying evolutionary and developmental biology. The development of *T. castaneum* is evolutionary more primitive than that of *D. melanogaster* even though they are both holometabolous. For example, *Drosophila* undergoes long-germ embryogenesis. This means that it patterns the future segments (head, thorax and abdomen) simultaneously at the blastoderm stage, before gastrulation. *Tribolium* and most other insects undergo short-germ embryogenesis, patterning only the anterior segments (head and thorax) at the blastoderm stage, while the remaining segments develop from a posterior growth zone after gastrulation (Brown et al., 2009; Rosenberg et al., 2009).

Lepidoptera consist of butterflies and moths. The most obvious features of them are the scales which cover the body and wings and are the source of various color patterns, and a proboscis (Powell, 2009).

Hymenoptera are one of the most species-rich insects orders, only behind Coleoptera and Lepidoptera. This order includes all wasps, bees and ants, of which many are eusocial. A series of hooks act as a key feature of this order to connect the hind wings and the fore wings (Quicke, 2009). In the updated classification, the order Hymenoptera is consisted of two suborders (Symphyta and Apocrita) (Aguiar et al., 2013).

In addition to the above mentioned 4 holometabolous orders, there are 35 orders in the Insecta. Insects adapted to every land and freshwater habitat. Whether we like them or not, they interact with other species as well as humans in countless ways.

## **Importance**

Insects perform crucial ecological functions in all terrestrial ecosystems. For instance, butterflies and moths play a crucial role in the natural ecosystem as pollinators and herbivores (Ahmed et al., 2015). Hymenoptera play vital roles as pollinators as well (Peters et al., 2017) and bees are regarded as the most known and understood insect pollinators (Gill et al., 2016; Sanchez-Bayo and Goka, 2014). Insects are also crucial in the nutrient cycle by eating dead animals, plants, fungi or decaying organic matter. Thus, insects act as primary or secondary decomposers in nature. At the same time, insects are very important food sources for many amphibians, reptiles, birds, and mammals (Pough, 1991; Rytönen et al., 2019).

From a human perspective, insects can be beneficial or harmful. Harmful insects include blood-feeding insects like mosquitoes, because they can be vectors of disease. For example, human malaria is a vector-borne disease caused by the infection with the protist *Plasmodium* (Chulay et al., 1986; Kaaya, 1989). The World Health Organization (WHO) estimates that there are hundreds of millions of malaria cases and more than half a million deaths each year (Emerson et al., 2022; Organization,

2022). Additionally, some insects can cause allergic or adverse reactions through their bite or sting. These insects include Anoplura (lice), Siphonaptera (fleas), and Hemiptera (bed bugs) (Sarwar, 2015).

Harmful insects also include agricultural pests such as locusts. The impact of locusts dates back millennia and locusts continue a major economic pest of agricultural crops today throughout the world (Le Gall et al., 2019). Zhang et al. reported that locusts and grasshoppers (Orthoptera: Acridoidea) are among the most dangerous polyphagous pests of agricultural crops (Zhang et al., 2019). Insects consume up to 20% of global crops (Oerke et al., 2012). As insects perform better at higher temperature, a global mean surface temperature increase of 2-degree Celsius is predicted to rise crop losses to 46% for wheat, 31% for corn and 19% for rice (Deutsch et al., 2018). So, insect pest management and control are essential sociological challenges associated with our economics and politics (Shelton et al., 2002).

But in general, only 0.1% of insect species constitute pests and produce damage, disease, or even death to humans, livestock, crops, and manufactured goods. About 1% species of insects interact with humans directly or indirectly (Gillott, 2005). Most of them are beneficial.

For agricultural crops, for instance, insects are essential pollinators. Thus, insect pollinators play a crucial role in affecting human food supplies. Insects also produce commercially valuable products, as do honey bees, silkworms, lac insects, and pella wax scale insects etc. (Gillott, 2005). Honey has served humans for many thousands of years and is nevertheless still an irreplaceable product. Silk production greatly affected human history, during which the Silk Road increased the connections among the world. Lac is a product from lac scale insects mainly made in India and a component of shellac. Beeswax is a naturally occurring wax produced by worker honey bees of the genus *Apis*, and used for constructing the honeycombs where to store honey and pollen as well as house their larvae (Buchwald et al., 2006). In the past decades, the total production of beeswax exceeded 60 kilo tons worldwide per year (see in the Food and Agriculture Organization Corporate Statistical (FAOSTAT) database (<http://faostat.fao.org/>), which is more than doubled in 1960s (Phiri et al., 2022). Owing to its higher melting point than any other wax (about 63-65 °C), beeswax was used for candles in the past, which therefore remain upright in hot season. At present, beeswax has many uses in cosmetics and body products, in the food industry, in pharmacy, in medicine, and in research exploiting its antimicrobial activity (Fratini et al., 2016; Tulloch, 1980).

Insects themselves are also important biological control agents of agricultural pests. Hymenoptera are widely used as parasites of pests (Dongol et al., 2014). It is worth noting that Hymenopteran parasitoids make up nearly 78% of the estimated insect parasitoid species and often cause host death (Abram et al., 2019; Feener Jr and Brown, 1997). There are a range of control methods available to pest insects, including chemical, biological, microbial, genetic, and physical control etc. Each of them has its advantages and disadvantages in use in a certain situation. The use of chemicals is the oldest approach of pest control either to kill or to repel harmful insect pests. However, today, insecticide resistance is an increasing problem both in many insect vectors of disease and agricultural pests, threatening effective insect pest management and control (Gillott, 2005; Hemingway and Ranson, 2000; Roush and Tabashnik, 2012). It is worth recognizing the role of insects in developing ecofriendly approaches for the control of pests in future.

Another potential use of insects is the feeding of livestock. This is because insects are rich in proteins, essential amino acids, fat and active substances (such as polyunsaturated fatty acids, antimicrobial peptides) (Józefiak et al., 2016). Until now, one of the most popular nutrient insects, the yellow mealworm *Tenebrio molitor*, is a valuable food source for fish, poultry, and human pets (Khosravi et al., 2018; Peng et al., 2019). From another perspective, a variety of insects, including butterflies, are sometimes used for decoration.

Finally, insects (e.g. the fruit fly *Drosophila melanogaster*) are also important in research, and are used to study for instance human pathogens such as human immunodeficiency virus (HIV) or diseases such as cancer (Bairagi, 2019; Mirzoyan et al., 2019). Common characteristics of many insects, including short generation time and high fecundity, make them widely reared globally under laboratory conditions for both teaching and research. Studies of the fruit fly *Drosophila melanogaster* have provided crucial data to genetics, and developmental biology and behavioral biology (Mirzoyan et al., 2019; Ugur et al., 2016). The red flour beetle *T. castaneum* is the second most important model insect after *Drosophila*, and has provided a lot of information for fundamental and applied research (Campbell et al., 2021). Techniques such as RNA interference (RNAi) and CRISPR/Cas are well-established in *Tribolium* (Grau et al., 2017). In addition to *Tribolium*, non-model insects like the cowpea seed beetle *Callosobruchus maculatus*, the yellow mealworm *T. molitor*, the pea aphid *Acyrtosiphon pisum*, the milkweed bug *Oncopeltus fasciatus*, the tobacco hornworm *Manduca sexta* etc., are also proving to be valuable research models (Beck and Blumer, 2020).

In conclusion, without insects, many of plants including crops would not survive, and ecosystems will collapse. However, a 27 years long study in Germany showed a seasonal decline of 76% in flying insect biomass, and worse in mid-summer (82%) (Hallmann et al., 2017). A recent study showed that terrestrial insect abundance declined by 9% on average per decade, while freshwater insect abundance increased by 15%, which has raised concerns among scientists (Dornelas and Daskalova, 2020; van Klink et al., 2020). There is no doubt that the attention of the public should continuously be drawn to insects.

### **Traits may explain the extraordinary success of insects**

Over the last century, many hypotheses have been formulated to explain the success of insects. Several authors had suggested that the small body size of insects and their co-evolution with plants contributed (Gillott, 2005; Grimaldi and Engel, 2005; Novotny et al., 2006). Four key evolutionary innovations and their corresponding taxa have commonly been recognized as major contributors to this great diversification of hexapods (Figure 1-4): (i) the Insecta possesses the insect body ground plan or *Bauplan*, (ii) the Pterygota possesses wings, (iii) the Neoptera possesses wing folding, and (iv) the Holometabola possesses complete metamorphosis (Mayhew, 2002; Mayhew, 2007; Nicholson et al., 2014; Waegele and Bartolomaeus, 2014). The insect *Bauplan* (i) includes specialized legs, external mouthparts, an ovipositor and an eleven-segmented abdomen that allow accessibility to diverse ecological niches. Flight (ii) provides great conveniences for insects to forage, avoid enemies and expand their distribution range. Wing folding (iii) allows neopterous insects to exploit more concealed places such as holes, without damaging their wings; and complete metamorphosis (iv) contributes to the utilization of different food sources for insects at different developmental stages (Rolff et al., 2019). There is no doubt that these characters have contributed a lot to the success of insect. Fossil

evidence also confirmed the importance of the origin of wings and complete metamorphosis for insect diversity (Nicholson et al., 2014).

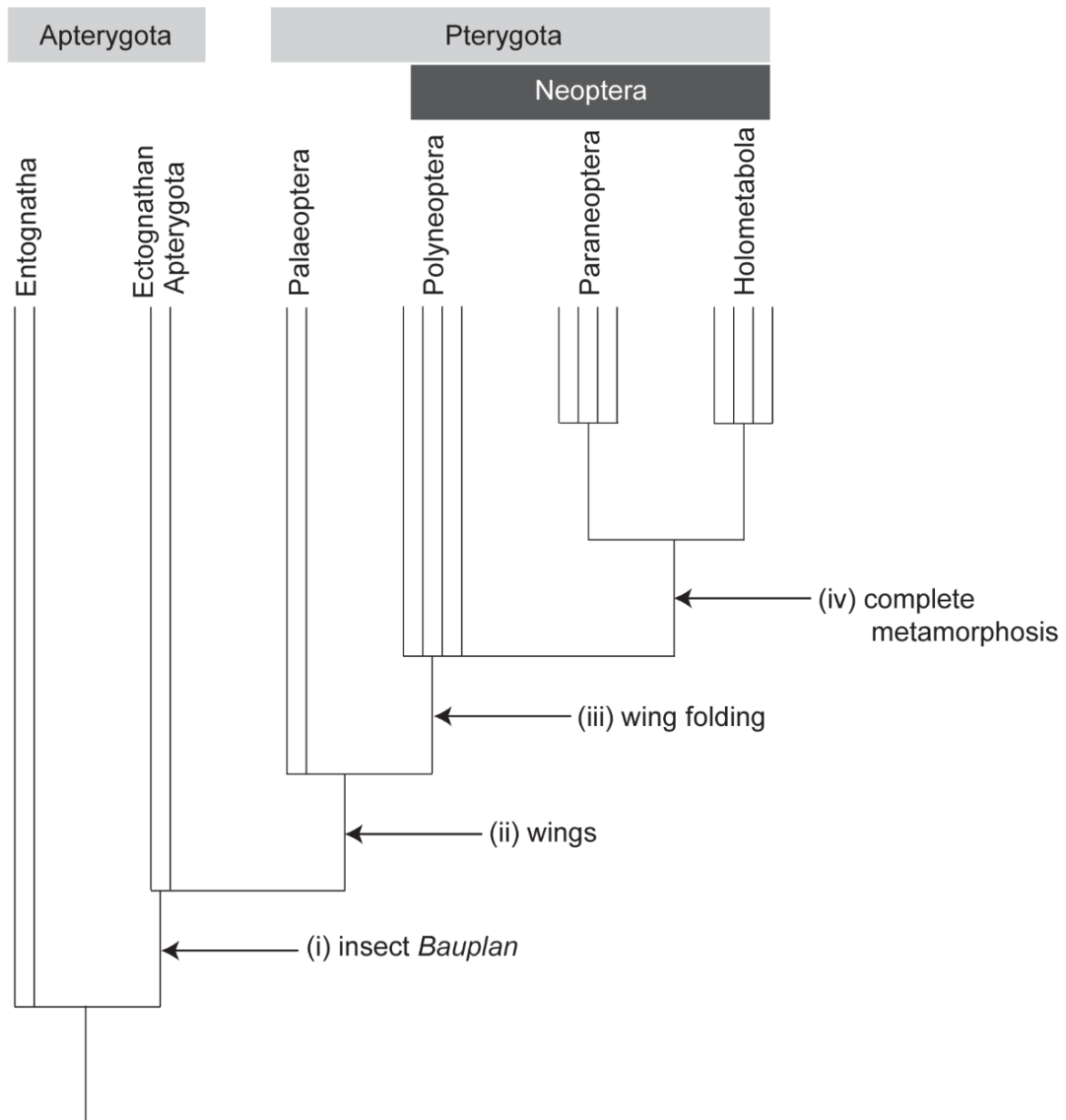


Figure 1-4. Four key evolutionary innovations and their corresponding taxa. Holometabola is also referred to as Endopterygota. Adopted from (Nicholson et al., 2014).

However, all these traits are based on traits of adult insects. In contrast to most other arthropods, there is no parental care in the majority of insects (Rezende et al., 2016). Crustaceans, for instance, usually carry their eggs with them (Sastry et al., 1983). Therefore, if insects eggs would not be adapted to the diverse habitats, insects would never have been so successful. Zeh et al. (1989) proposed that attributes of the egg stage must not be overlooked for the unparalleled diversification of insects. Egg-stage characters include maternal effects such as the ovipositor and architecture of the eggshell; and zygotic characters such as the amnion and serosa. These characters were proposed to have enabled the expansion of insects into previously inaccessible niches, and to allow rapid and extensive divergence. Additionally, the self-sufficient eggs may be associated with the low incidence of postzygotic parental

egg care among insects compared to other terrestrial arthropods (Zeh et al., 1989). Thus, egg-stage characters may have made significant contributions to the extraordinary success of the insects.

## **Development of insect eggs**

### **Structure of insect eggs**

The size of insect eggs varies greatly among species. For instance, the eggs of the desert locust (*Schistocerca gregaria*) are around 7-8 mm in length while the eggs of the egg parasitoid *Trichogramma dendrolimi* are around 0.2-0.3 mm long (Maeno et al., 2020; Zhou et al., 2020). The shapes of insect eggs are also diverse. The most common shape is oval (Figure 1-5). The egg is covered by a protective egg shell, called the chorion, which is secreted by exocrine glands before oviposition. The chorion layer has a complex structure and is the interface between the egg and the environment. The other layer, the vitelline envelope, is a relatively simple proteinaceous layer outside the oocyte (Jagadeeshan and Singh, 2007; Margaritis et al., 1980). Beneath these eggshells, the serosal cuticle is secreted by the extraembryonic serosa and becomes the innermost eggshell layer, which serves to protect insect eggs from desiccation, physical insult and bacterial infection (Jacobs et al., 2013; Jacobs et al., 2014a). The extraembryonic epithelium, the serosa, enfolds the embryo and yolk in almost all insect eggs. At the same time, the other extraembryonic membrane, the amnion, covers the embryo ventrally. Thus, the serosa and the amnion form a bilayer to protect normal development of the embryo. Strikingly, both of them rupture and withdraw actively in late embryogenesis (Hilbrant et al., 2016; Rezende et al., 2008).

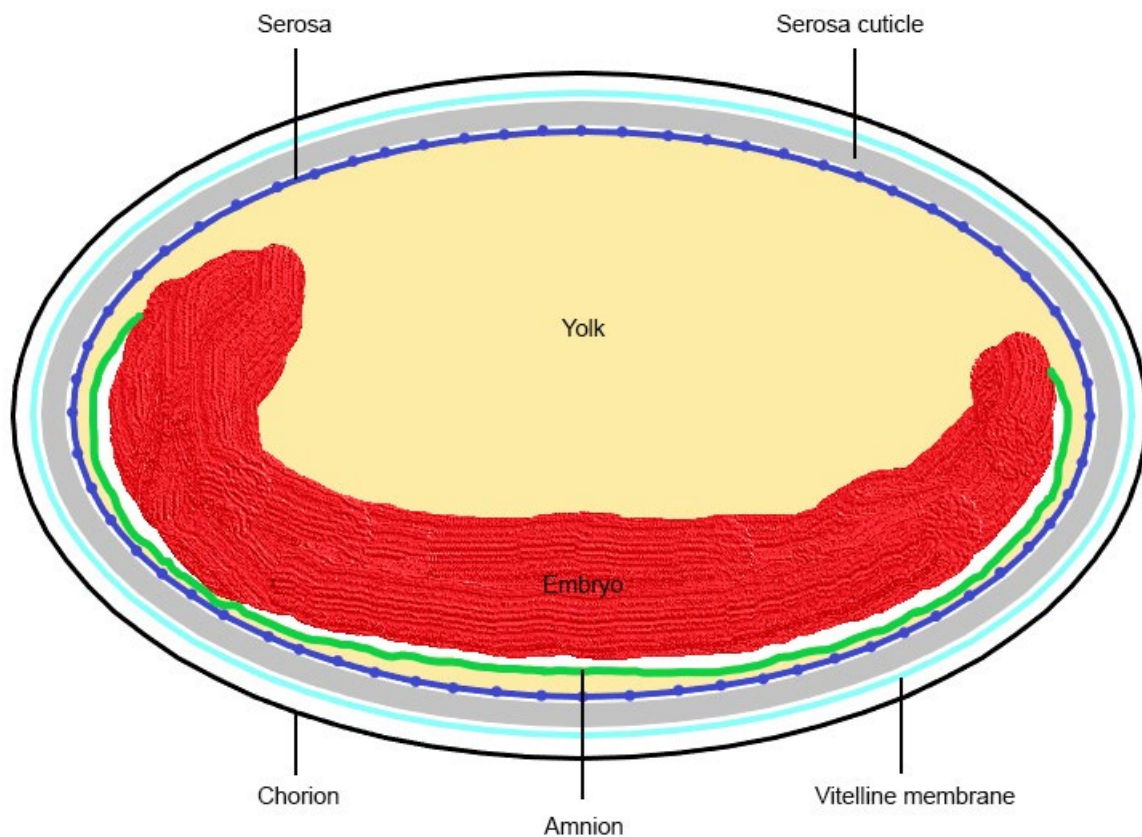


Figure 1-5. Schematic structure of holometabolous insect egg. Adopted from (Jacobs et al., 2015).

### Early embryonic development of insect eggs

Although parthenogenesis occurs in quite some insects (e.g. aphids, ants and bees), embryonic development of insects generally begins after the eggs are fertilized. Within the fertilized egg, the single nucleus divides hundreds of times into many cells in the yolk. After this, these nuclei move to the egg periphery of the yolk, become enclosed by cell membranes and form a single cell layer surrounding the yolk, called the blastoderm. Subsequently, the cells begin to differentiate, with a subset of cells giving rise to the embryo or germ and the remaining cells giving rise to the serosa. Exceptionally, *Drosophila* eggs only develop a small dorsal region as an extraembryonic tissue called the amnioserosa (Benton, 2018; Schmidt-Ott et al., 2010).

Next follows gastrulation, a process that is accompanied by a considerable longitudinal stretching of the germ Anlage. Before gastrulation, a strip of cells along the ventral midline is specified as the presumptive mesoderm. Gastrulation then begins with cellular invagination to form two germ layers. The outer layer is the ectoderm, and the inner germ layer is the mesoderm, which arises from the internalization of mesodermal cells. Subsequently, the serosal cells migrate over, and then surround the embryo and yolk, forming a complete, final barrier to protect the embryo from injury (Figure 1-6A) (Roth, 2004). At the same time, the amnion forms a fluid-filled cavity (amniotic cavity) to protect the embryo.



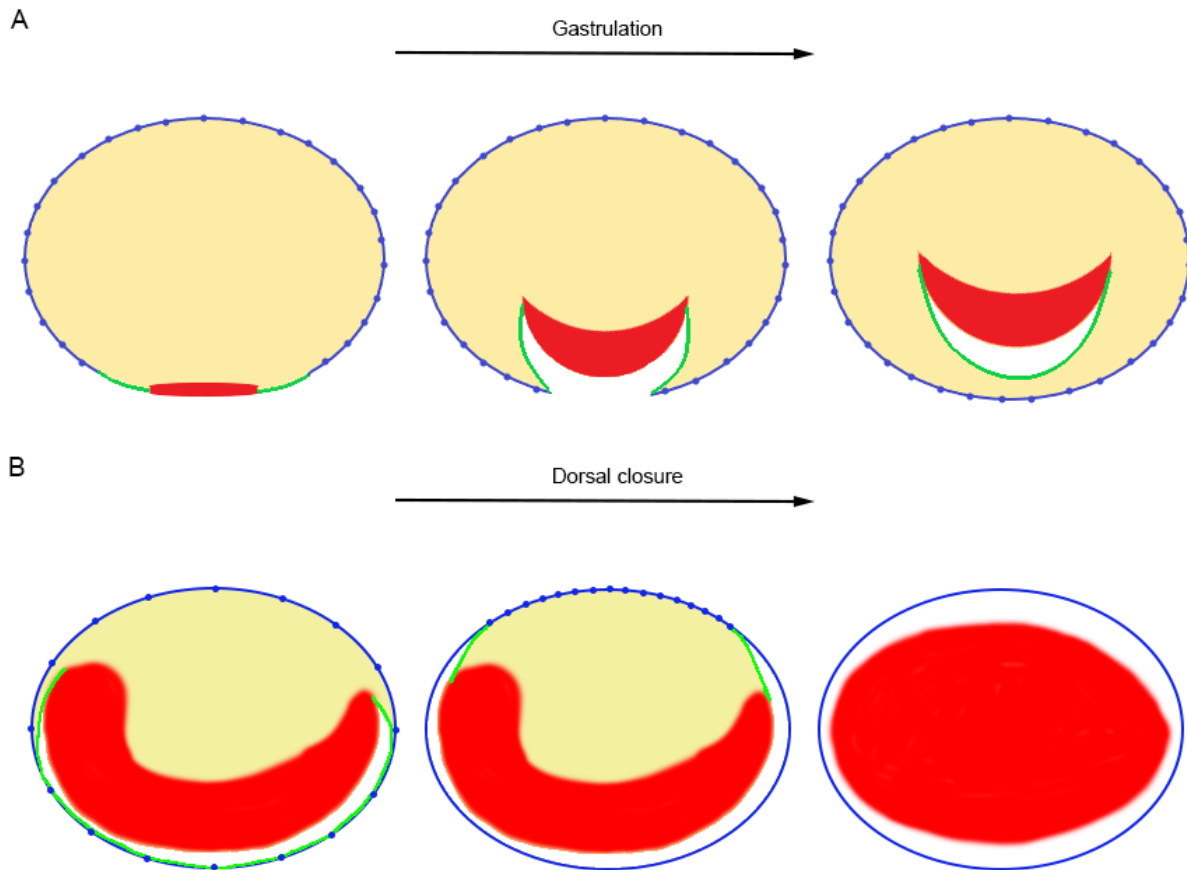


Figure 1-6. A, Formation of the complete serosa during gastrulation. B, Fate of the serosa during dorsal closure. Key: Yolk = light yellow; germ band/embryo = red; amnion = green; serosal cells = blue dots; serosal cuticle = blue ovals.

After gastrulation, segments are added one by one from a posterior growth zone, and appendages form on some of the segments. Strikingly, the serosa always surrounds the embryo and yolk prior to dorsal closure (Benton et al., 2013; Münster et al., 2019; Panfilio, 2008). Just before dorsal closure, however, the amnion and serosa actively rupture and withdraw into the body (Figure 1-6B). Then, two edges of the germ band meet and fuse along the dorsal midline, internalizing the yolk (Hilbrant et al., 2016; Sander, 1976).

## Function of the serosa

### An evolutionary novelty in insect eggs

It has been reported that there is a correlation between the capacity of arthropod eggs to develop in terrestrial environments, and the presence of a serosa which completely envelops the embryo and yolk (Jacobs et al., 2013). The higher flies (Diptera), including *Drosophila*, are unique among insects in that they have secondarily lost the serosa and formed a single dorsal extraembryonic epithelium called the amnioserosa (Jacobs et al., 2013; Rafiqi et al., 2008). This might explain why eggs of these flies

cannot survive easily outside humid environments. Most chelicerates, myriapods and crustaceans do not have the serosa at all. They have a single extraembryonic tissue which covers the dorsal yolk but that never enfolds the embryo (Figure 1-7). Thus, the serosa is considered to be an evolutionary novelty in insect eggs.

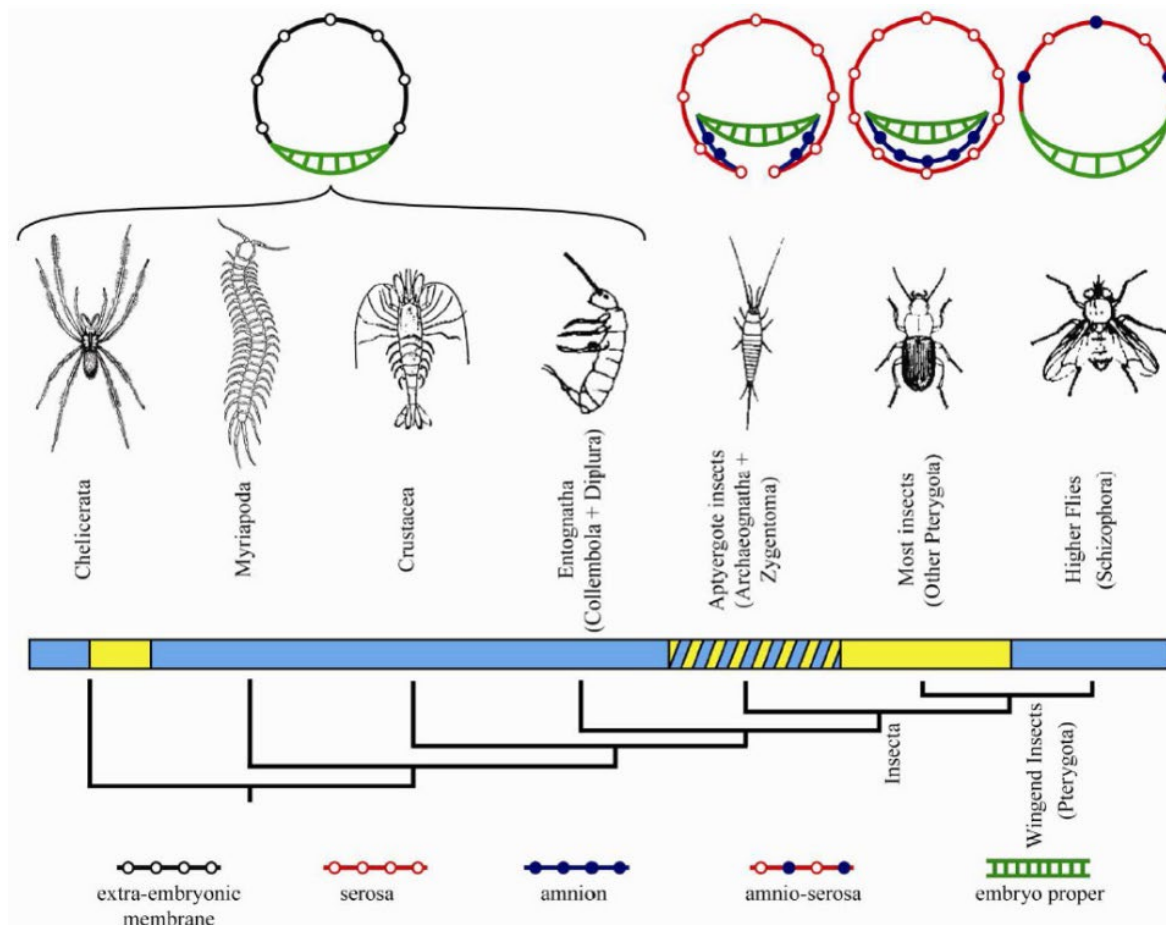


Figure 1-7. Phylogeny of all major arthropod groups. The bar under the groups shows the egg lives in aquatic (blue), terrestrial (yellow) or humid environments (striped). The top row shows a schematic overview of the egg, focusing on the serosa/amnion and embryo (from (Jacobs et al., 2013)).

## Function of the serosa

It is impossible to assess function of the serosa in *Drosophila* because it is absent. However, the serosa is present in the second most important insect model species *T. castaneum*. In 2005, van der Zee *et al.* developed a technique using parental RNAi with the gene *Zerknullt1* (*Tc-zen1*) to remove the serosa from *Tribolium* eggs, without damaging the maternal eggshell layers. As a consequence, in parental *Tc-zen1* RNAi eggs, the amnion only covers the yolk at the dorsal side (van der Zee *et al.*, 2005). These serosa-less eggs are prone to desiccation and infection (Jacobs *et al.*, 2013; Jacobs *et al.*, 2014a). It is particularly the secreted serosal cuticle that protects *Tribolium* eggs from desiccation (Jacobs *et al.*, 2013). In the egg of mosquitoes, desiccation resistance also coincides with the formation of the serosal chitinized cuticle (Goltsev *et al.*, 2009; Rezende *et al.*, 2008). At the same time, the serosa

promotes correct dorsal closure by pulling the amnion and embryo dorsally (Jacobs et al., 2013; van der Zee et al., 2005).

Another important function of the serosa in insect eggs is as barrier to infection. The NF- $\kappa$ B homologue Dorsal, a transcription factor entering the nucleus upon Toll signaling, is present in the serosa during early *Tribolium* development (Chen et al., 2000). Also, antimicrobial protein mRNAs and lysozyme are expressed only in extraembryonic tissues of immune-challenged the tobacco hornworm *M. sexta* eggs (Gorman et al., 2004).

In response to infections, the serosa mounts a full-range immune response protecting the embryo in the red flour beetle (*T. castaneum*) (Jacobs et al., 2013; Jacobs et al., 2014a), the tobacco hornworm (*Manduca sexta*) (Gorman et al., 2004), the milkweed bug (*O. fasciatus*) and the migratory locust (*Locusta migratoria*) (Jacobs et al., 2022). Interestingly the carrion beetle *Nicrophorus vespilloides* has a serosa, but it does not mount an immune response (Jacobs et al., 2014b). The eggs of *T. castaneum*, *O. fasciatus* and *L. migratoria* possess the extraembryonic serosa. *Drosophila* eggs have lost the serosa, desiccation resistance and immune competence altogether (Jacobs et al., 2013; Rafiqi et al., 2008). In chapter 2, I will investigate if the serosa is a prerequisite for an inducible innate immune response in the springtail *O. cincta*.

Like the *Drosophila* embryo, the *Nicrophorus* egg exhibits a remarkably faster embryonic development compared to other insect taxa (Fernández-Moreno et al., 2007). *Drosophila* eggs develop extremely quickly and hatch within 24 hours at 25 °C. *Nicrophorus* eggs hatch in two days at 25 °C which is also much more rapid than in other insect taxa. On the contrary, *Tribolium*, *Manduca*, *Oncopeltus* and *Locusta* eggs have a slow embryonic development. Embryonic development in *Tribolium*, *Oncopeltus* and *Manduca* is approximately 3–6 times slower than *Nicrophorus* (Chipman, 2017; Howe, 1956; Kingsolver and Nagle, 2007). Embryogenesis of *L. migratoria* takes 14–15 days at 30 °C (Tanaka, 2017). Thus, immune competence seems to trade-off with developmental speed. This trade-off may have driven the loss of the serosa in higher flies. In chapter 3, I will investigate whether immune competence trades off with developmental speed in lines of *Tribolium castaneum* that have been selected for fast or slow development.

## Insect immunity

Insects rely completely on the innate immune system when infected by pathogens (Charles and Killian, 2015). The two components of the innate immune system are cellular and humoral elements (Tsakas and Marmaras, 2010). For cellular immunity, pathogenic microorganisms are eliminated by phagocytes, such as the hemocytes of *Drosophila* (Kim and Kim, 2005) and mosquito (Hillyer and Strand, 2014). For humoral immunity, microbes are eliminated mainly by antimicrobial peptides (AMPs) that are secreted into the haemolymph. The systemic cooperation of the cellular and humoral immune components contributes to protection against pathogenic microorganisms (Tsakas and Marmaras, 2010; Yang et al., 2021). For instance, pro-phenoloxidase (PPO), the inactive zymogen form of phenoloxidase (PO), is synthesized and stored in hemocytes (cellular). Upon infection, however, the activation of PPO to the active PO is executed by humoral immune reactions (González-Santoyo and Córdoba-Aguilar, 2012; Yang et al., 2021).

The innate immune system is activated by pattern-recognition receptors (PRRs) that recognize specific pathogen-associated molecular patterns (PAMPs). These PAMPs are mainly peptidoglycans, that are present on both pathogenic and non-pathogenic bacteria (Janeway Jr and Medzhitov, 2002).

Diaminopimelic (DAP) type peptidoglycans of Gram negative bacteria mainly activate the IMD pathway, while Lysine (Lys) type peptidoglycans of Gram positive bacteria mainly activate the Toll pathway. Through a cytoplasmic signaling cascade, this leads to the nuclear localization of NF- $\kappa$ B that inducing the expression of effectors such as antimicrobial peptides, prophenoloxidasases, or other genes involved in the oxidative response such as the Dual oxidase (DUOX) (Davis and Engström, 2012; Ferrandon, 2013; Lemaitre and Hoffmann, 2007; Ligoxygakis, 2013).

In insects, a potent immune response has been identified in post-embryonic development in many species. In Table 1-1, I present a selection of immune studies in larvae and adults of the most used insect models. In eggs, however, innate immunity has only been experimentally demonstrated in a few insect species to date, including the tobacco hornworm *M. sexta* (Gorman et al., 2004), *T. castaneum* (Jacobs et al., 2014a), *T. molitor* (Jacobs et al., 2017), the milkweed bug *O. fasciatus* and the migratory locust *L. migratoria* (Jacobs et al., 2022). These eggs do have a serosa as described under ‘Function of the serosa’. Thus, the serosa seems to be a prerequisite for an inducible innate immune response. In chapter 2, I will test this hypothesis by investigating the immune response in *Orchesella cincta*, a species outside of the insects that does not have a serosa.

Table 1-1. A few examples of studies describing the immune response of insects during post-embryonic development.

Common name	Scientific name	References
Fruit fly	<i>Drosophila melanogaster</i>	(Ghosh et al., 2015; Hoffmann, 2003; Jacobs and van der Zee, 2013)
Red flour beetle	<i>Tribolium castaneum</i>	(Altincicek et al., 2008; Behrens et al., 2014; Bi et al., 2019; Choi et al., 2022; Contreras et al., 2013; Jacobs et al., 2014a; Jacobs and van der Zee, 2013; Milutinović et al., 2013; Zou et al., 2007)
Yellow mealworm	<i>Tenebrio molitor</i>	(Johnston et al., 2014)
Monarch butterfly	<i>Danaus plexippus</i>	(Lindsey and Altizer, 2009)
Tobacco budworm	<i>Heliothis virescens</i>	(Barthel et al., 2015)
Honey bees	<i>Apis mellifera</i>	(Barribeau et al., 2015; Evans et al., 2006)
Red imported fire ant	<i>Solenopsis invicta</i>	(Holmes and Johnston, 2023; Schluns and Crozier, 2009; Wei et al., 2021)
Kissing bugs	<i>Rhodnius prolixus</i> and <i>Triatoma infestans</i>	(Lobo et al., 2015; Salcedo-Porras and Lowenberger, 2019; Vieira et al., 2015)
Migratory locust	<i>Locusta migratoria</i>	(Mullen and Goldsworthy, 2003; Zhang et al., 2015)

## Evolutionary trade-offs

All living organisms are subject to finite resources. This means that life-history traits (or fitness components) are often negatively related to each other, resulting in trade-offs. At its core, a trade-off is a process of optimization and occurs when a beneficial change in one life-history trait is linked to a detrimental change in another (Stearns, 1989). So, trade-offs are typically seen as the result of tactical or strategic choices over limited resources of organisms. In other words, these trade-offs are the manifestation of the resource allocation of organisms. For instance, investment in immune defense must reduce investment in traits. Thus, trade-offs are used to optimize the competing requirements of life-history traits, such as growth, maintenance and reproduction, preventing sole allocation of limited resources to a single trait (Adamo et al., 2001; Bolund, 2020; Schmid-Hempel, 2005) (Figure 1-8). Trade-offs have played a key role in the development of life-history theory and interpretation (Zera and Harshman, 2001).

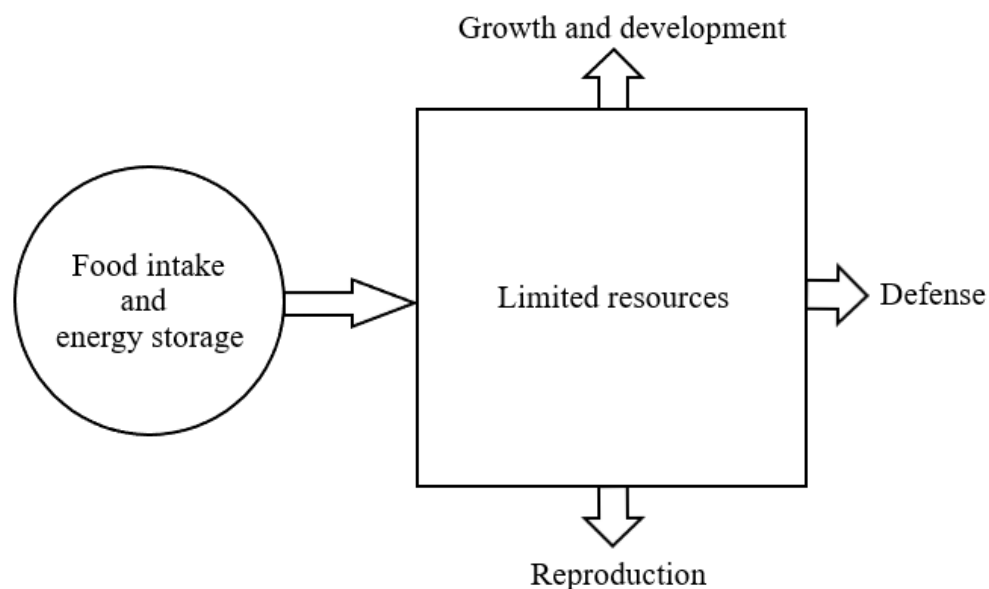


Figure 1-8. A conceptual diagram of trade-offs associated with the allocating of limited resources to competing physiological functions. Adopted from (Züst and Agrawal, 2017).

In the absence of trade-offs, an organism could maximize all its fitness components simultaneously and therefore become a ‘Darwinian Demon’ that reproduces directly after being born, lives forever and produces infinitely many offspring (Bonsall et al., 2004; Stearns, 1992). However, such an organism would not exist in nature. All living organisms undergo birth, development, growth, reproduction and death. The evolutionary trade-offs are ubiquitous and of fundamental importance in the evolution of life-history traits. Insects need to perform multiple tasks during their lifetime, such as growth, maintenance and defense. Such functional trade-offs must exist in insects. Evolutionary trade-offs

have been widely investigated in a diverse range of insect species, such as the tobacco hornworm *M. sexta* (Diamond and Kingsolver, 2011; Mira and Bernays, 2002), parasitoid wasps (e.g. *Aphaereta minuta*) (Jervis et al., 2008; Schwenke et al., 2016), and the fruit fly *D. melanogaster* (Ahmed et al., 2020; Chippindale et al., 1996). For instance, shorter developmental time is predicted to lead to reduced adult weight and fecundity.

In many organisms, the most prominent trade-off between life-history traits is associated with the cost of reproduction which has two major parts: costs paid for survival, such as parental survival; and costs paid for reproduction, such as fecundity (Stearns, 1989). A classic example of this kind of trade-off is that long-lived flies have decreased early fecundity in the fruit fly *D. melanogaster* (Djawdan et al., 2004; Leroi et al., 1994; Zwaan et al., 1995). The trade-off between reproduction and immune responses has been observed in a diversity of insects, probably owing to the alternative allocation of resources (Schwenke et al., 2016). In recent years, it has been demonstrated that reproduction trades off with many other life-history traits in insects, such as survival, maintenance, migration, flight capability (or dispersal), longevity and body structures (Ellers, 1996; Hanski et al., 2006; Langelotto et al., 2000; Lin et al., 2016; Rodrigues and Flatt, 2016; Tanaka and Suzuki, 1998; Wilson et al., 2020).

However, what remains unclear is whether there are any proximate mechanisms underlying these trade-offs. These proximate mechanisms could be shared across insect taxa (Harshman and Zera, 2007; Schwenke et al., 2016). In insects, most decisions on physiological, developmental, and behavioral events are mediated by hormones (Gade et al., 1997; Ketterson and Nolan, 1999; Lösel and Wehling, 2003; Stearns, 1989). There are two major classes of hormone in insects: (i) the true hormones produced by conventional glandular tissues comprising the prothoracic glands for ecdysteroids and the corpora allata for juvenile hormones; (ii) the neuropeptide hormones produced by the neurosecretory cells that reside in the central nervous system. Molting and metamorphosis are the best studied hormonal-stimulated events in the life cycle of insects, of which ecdysone executes these events, and juvenile hormone modulates ecdysteroid action. By contrast, most insect hormones are neurosecretory products. They play a crucial role in physiological, developmental, and behavioral processes controlled by the neurosecretory cells in the central nervous system (Gade et al., 1997; Nijhout, 1998; Rolff et al., 2019). However, it is still unknown how so many hormones cooperate to mechanistically regulate the trade-off in a molecular network. In chapter 4, I will study the genetic basis of different developmental speed caused by altered ecdysone pulses.

## **Aim and outline of this thesis**

The general aim of this work is to investigate:

- 1) the relation between the presence of a serosa and the innate immune response in the eggs of hexapoda;
- 2) the trade-offs between developmental speed and other life history traits including immune competence, pupal weight and fecundity;
- 3) the genetic basis of this trade-off in insects.

In **Chapter 2**, I ask whether focus on the evolution of the immune competence in eggs of a very basal non-insect springtail (*Orchesella cincta*), which belongs to the closely related hexapod subclass Collembola (Figure 1-7) that do not have a serosa. We do not find any evidence for maternal provision of antimicrobials to *Orchesella* eggs in zone-of-inhibition assays of egg extracts. However, we find that *Orchesella* eggs can upregulate immune genes after bacterial challenge in the absence of a serosa. Thus, I conclude that the serosa is not an absolute prerequisite for an innate immune response in insect eggs.

In **Chapter 3**, I ask what trade-offs are associated with increased developmental speed. We set up an evolutionary experiment comparing fast vs. slow embryonic development in the model organism *T. castaneum*. We do not find a trade-off between immune defense and embryonic development time in the selection populations. We do demonstrate a strong negative correlation between fast embryonic development and early fecundity. These results broaden our understanding of trade-offs between fitness components in life-history theory.

In **Chapter 4**, I analyze the genetic underpinning of fast embryonic development in *T. castaneum*. I identify two genomic regions under the selection by pooled resequencing. Using qPCR and a small-scale RNAi screen, we identify two alleles: a deletion upstream of the ecdysone-degrading enzyme *cytochrome18a1*, and a region upstream of *melted*, a gene involved in insulin signaling (Baker and Thummel, 2007; Teleman et al., 2005). The first allele is associated with a peak of ecdysone that induces dorsal closure during embryonic development. This is a major finding, as ecdysone is mainly known from larval and pupal development of insects (Dubrovsky, 2005; Moeller et al., 2017; Robbins et al., 1968). Finally, I confirm the functionality of the deletion upstream of *cytochrome18a1* using Crispr/cas9 technology. This deletion advances ecdysone peaks and also mediates the trade-off with pupal weight and fecundity.

In **Chapter 5**, I discuss the results in an evolutionary perspective.

## References

- Abram, P. K., Brodeur, J., Urbaneja, A. and Tena, A.** (2019). Nonreproductive effects of insect parasitoids on their hosts. *Annual Review of Entomology*, 259-276.
- Adamo, S. A., Jensen, M. and Younger, M.** (2001). Changes in lifetime immunocompetence in male and female *Gryllus texensis* (formerly *G. integer*): trade-offs between immunity and reproduction. *Animal Behaviour* **62**, 417-425.
- Aguiar, A. P., Deans, A. R., Engel, M. S., Forshage, M., Huber, J. T., Jennings, J. T., Johnson, N. F., Lelej, A. S., Longino, J. T. and Lohrmann, V.** (2013). Order Hymenoptera. In: Zhang, Z.-Q.(Ed.) *Animal Biodiversity: An Outline of Higher-level Classification and Survey of Taxonomic Richness* (Addenda 2013). *Zootaxa* **3703**, 51-62.
- Ahmed, M. Z., Araujo-Jnr, E. V., Welch, J. J. and Kawahara, A. Y.** (2015). Wolbachia in butterflies and moths: geographic structure in infection frequency. *Frontiers in Zoology* **12**, 1-9.
- Ahmed, S. M. H., Maldera, J. A., Kronic, D., Paiva-Silva, G. O., Pénalva, C., Teleman, A. A. and Edgar, B. A.** (2020). Fitness trade-offs incurred by ovary-to-gut steroid signalling in *Drosophila*. *Nature* **584**, 415-419.
- Altincicek, B., Knorr, E. and Vilcinskis, A.** (2008). Beetle immunity: Identification of immune-inducible genes from the model insect *Tribolium castaneum*. *Developmental & Comparative Immunology* **32**, 585-595.

- Bairagi, S. H.** (2019). Insects with Potential Medicinal Significance: A Review. *Biomedical Journal of Scientific & Technical Research* **16**, 12024-12027.
- Baker, K. D. and Thummel, C. S.** (2007). Diabetic larvae and obese flies—emerging studies of metabolism in *Drosophila*. *Cell metabolism* **6**, 257-266.
- Barribeau, S. M., Sadd, B. M., du Plessis, L., Brown, M. J., Buechel, S. D., Cappelle, K., Carolan, J. C., Christiaens, O., Colgan, T. J. and Erler, S.** (2015). A depauperate immune repertoire precedes evolution of sociality in bees. *Genome biology* **16**, 1-21.
- Barthel, A., Staudacher, H., Schmaltz, A., Heckel, D. G. and Groot, A. T.** (2015). Sex-specific consequences of an induced immune response on reproduction in a moth. *BMC evolutionary biology* **15**, 1-12.
- Beck, C. W. and Blumer, L. S.** (2020). Advancing Undergraduate Laboratory Education Using Non-Model Insect Species. *Annual Review of Entomology* **66**.
- Behrens, S., Peuß, R., Milutinović, B., Eggert, H., Esser, D., Rosenstiel, P., Schulenburg, H., Bornberg-Bauer, E. and Kurtz, J.** (2014). Infection routes matter in population-specific responses of the red flour beetle to the entomopathogen *Bacillus thuringiensis*. *BMC genomics* **15**, 1-17.
- Benton, M. A.** (2018). A revised understanding of *Tribolium* morphogenesis further reconciles short and long germ development. *PLoS biology* **16**, e2005093.
- Benton, M. A., Akam, M. and Pavlopoulos, A.** (2013). Cell and tissue dynamics during *Tribolium* embryogenesis revealed by versatile fluorescence labeling approaches. *Development* **140**, 3210-3220.
- Berenbaum, M. R.** (1996). *Bugs in the system: insects and their impact on human affairs*: Basic Books.
- Bi, J., Feng, F., Li, J., Mao, J., Ning, M., Song, X., Xie, J., Tang, J. and Li, B.** (2019). AC-type lectin with a single carbohydrate-recognition domain involved in the innate immune response of *Tribolium castaneum*. *Insect molecular biology* **28**, 649-661.
- Bolund, E.** (2020). The challenge of measuring trade-offs in human life history research. *Evolution and Human Behavior* **41**, 502-512.
- Bonsall, M. B., Jansen, V. A. and Hassell, M. P.** (2004). Life history trade-offs assemble ecological guilds. *Science* **306**, 111-114.
- Brown, S. J., Shippy, T. D., Miller, S., Bolognesi, R., Beeman, R. W., Lorenzen, M. D., Bucher, G., Wimmer, E. A. and Klingler, M.** (2009). The red flour beetle, *Tribolium castaneum* (Coleoptera): a model for studies of development and pest biology. *Cold Spring Harbor Protocols* **2009**, pdb. emo126.
- Buchwald, R., Breed, M. D., Greenberg, A. R. and Otis, G.** (2006). Interspecific variation in beeswax as a biological construction material. *Journal of experimental biology* **209**, 3984-3989.
- Campbell, J. F., Athanassiou, C. G., Hagstrum, D. W. and Zhu, K. Y.** (2021). *Tribolium castaneum*: A Model Insect for Fundamental and Applied Research. *Annual review of entomology* **67**.
- Charles, H. M. and Killian, K. A.** (2015). Response of the insect immune system to three different immune challenges. *Journal of insect physiology* **81**, 97-108.
- Chen, G., Handel, K. and Roth, S.** (2000). The maternal NF-kappaB/dorsal gradient of *Tribolium castaneum*: dynamics of early dorsoventral patterning in a short-germ beetle. *Development* **127**, 5145-5156.
- Chipman, A. D.** (2017). *Oncopeltus fasciatus* as an evo-devo research organism. *genesis* **55**, e23020.
- Chippindale, A. K., Chu, T. J. and Rose, M. R.** (1996). Complex trade-offs and the evolution of starvation resistance in *Drosophila melanogaster*. *Evolution* **50**, 753-766.
- Choi, B., Park, W.-R., Kim, Y.-J., Mun, S., Park, S.-J., Jeong, J.-H., Choi, H.-S. and Kim, D.-K.** (2022). Nuclear receptor estrogen-related receptor modulates antimicrobial peptide expression for host innate immunity in *Tribolium castaneum*. *Insect Biochemistry and Molecular Biology*, 103816.
- Chulay, J. D., Schneider, I., Cosgriff, T. M., Hoffman, S. L., Ballou, W. R., Quakyi, I. A., Carter, R., Trostler, J. H. and Hockmeyer, W. T.** (1986). Malaria transmitted to humans by



- mosquitoes infected from cultured *Plasmodium falciparum*. *The American journal of tropical medicine and hygiene* **35**, 66-68.
- Contreras, E., Rausell, C. and Real, M. D.** (2013). Proteome response of *Tribolium castaneum* larvae to *Bacillus thuringiensis* toxin producing strains. *PloS one* **8**, e55330.
- Crowson, R. A.** (2013). *The biology of the Coleoptera*: Academic press.
- Davis, M. M. and Engström, Y.** (2012). Immune response in the barrier epithelia: lessons from the fruit fly *Drosophila melanogaster*. *Journal of innate immunity* **4**, 273-283.
- Deutsch, C. A., Tewksbury, J. J., Tigchelaar, M., Battisti, D. S., Merrill, S. C., Huey, R. B. and Naylor, R. L.** (2018). Increase in crop losses to insect pests in a warming climate. *Science* **361**, 916-919.
- Diamond, S. E. and Kingsolver, J. G.** (2011). Host plant quality, selection history and trade-offs shape the immune responses of *Manduca sexta*. *Proceedings of the Royal Society B: Biological Sciences* **278**, 289-297.
- Djawdan, M., Sugiyama, T. T., Schlaeger, L. K., Bradley, T. J. and Rose, M. R.** (2004). Metabolic aspects of the trade-off between fecundity and longevity in *Drosophila melanogaster*. In *Methuselah flies: A case study in the evolution of aging*, pp. 145-164: World Scientific.
- Dongol, T., Dhananjaya, B., Shrestha, R. K. and Aryal, G.** (2014). Pharmacological and immunological properties of wasp venom. *Pharmacology and Therapeutics*, 47-81.
- Dornelas, M. and Daskalova, G. N.** (2020). Nuanced changes in insect abundance. *Science* **368**, 368-369.
- Dubrovsky, E. B.** (2005). Hormonal cross talk in insect development. *Trends in Endocrinology & Metabolism* **16**, 6-11.
- Ellers, J.** (1996). Fat and eggs: an alternative method to measure the trade-off between survival and reproduction in insect parasitoids. *Netherlands Journal of Zoology* **46**, 227-235.
- Emerson, C., Meline, J., Linn, A., Wallace, J., Kapella, B. K., Venkatesan, M. and Steketee, R.** (2022). End Malaria Faster: Taking Lifesaving Tools Beyond “Access” to “Reach” All People in Need. *Global Health: Science and Practice* **10**.
- Evans, J., Aronstein, K., Chen, Y. P., Hetru, C., Imler, J. L., Jiang, H., Kanost, M., Thompson, G., Zou, Z. and Hultmark, D.** (2006). Immune pathways and defence mechanisms in honey bees *Apis mellifera*. *Insect molecular biology* **15**, 645-656.
- Feener Jr, D. H. and Brown, B. V.** (1997). Diptera as parasitoids. *Annual review of entomology* **42**, 73-97.
- Fernández-Moreno, M. A., Farr, C. L., Kaguni, L. S. and Garesse, R.** (2007). *Drosophila melanogaster* as a model system to study mitochondrial biology. In *Mitochondria*, pp. 33-49: Springer.
- Ferrandon, D.** (2013). The complementary facets of epithelial host defenses in the genetic model organism *Drosophila melanogaster*: from resistance to resilience. *Current opinion in immunology* **25**, 59-70.
- Fratini, F., Cilia, G., Turchi, B. and Felicioli, A.** (2016). Beeswax: A minireview of its antimicrobial activity and its application in medicine. *Asian Pacific Journal of Tropical Medicine* **9**, 839-843.
- Gade, G., Hoffmann, K.-H. and Spring, J. H.** (1997). Hormonal regulation in insects: facts, gaps, and future directions. *Physiological reviews* **77**, 963-1032.
- Ghosh, S., Singh, A., Mandal, S. and Mandal, L.** (2015). Active hematopoietic hubs in *Drosophila* adults generate hemocytes and contribute to immune response. *Developmental cell* **33**, 478-488.
- Gill, R. J., Baldock, K. C., Brown, M. J., Cresswell, J. E., Dicks, L. V., Fountain, M. T., Garratt, M. P., Gough, L. A., Heard, M. S. and Holland, J. M.** (2016). Protecting an ecosystem service: approaches to understanding and mitigating threats to wild insect pollinators. In *Advances in ecological research*, pp. 135-206: Elsevier.
- Gillott, C.** (2005). *Entomology*: Springer Science & Business Media.
- Goltsev, Y., Rezende, G. L., Vranizan, K., Lanzaro, G., Valle, D. and Levine, M.** (2009). Developmental and evolutionary basis for drought tolerance of the *Anopheles gambiae* embryo. *Developmental biology* **330**, 462-470.

- González-Santoyo, I. and Córdoba-Aguilar, A.** (2012). Phenoloxidase: a key component of the insect immune system. *Entomologia Experimentalis et Applicata* **142**, 1-16.
- Gorman, M., Kankanala, P. and Kanost, M.** (2004). Bacterial challenge stimulates innate immune responses in extra-embryonic tissues of tobacco hornworm eggs. *Insect molecular biology* **13**, 19-24.
- Grau, T., Vilcinskis, A. and Joop, G.** (2017). Probiotic *Enterococcus mundtii* isolate protects the model insect *Tribolium castaneum* against *Bacillus thuringiensis*. *Frontiers in microbiology* **8**, 1261.
- Grimaldi, D. and Engel, M. S.** (2005). *Evolution of the Insects*: Cambridge University Press.
- Hallmann, C. A., Sorg, M., Jongejans, E., Siepel, H., Hofland, N., Schwan, H., Stenmans, W., Müller, A., Sumser, H. and Hörden, T.** (2017). More than 75 percent decline over 27 years in total flying insect biomass in protected areas. *PLoS one* **12**, e0185809.
- Hanski, I., Saastamoinen, M. and Ovaskainen, O.** (2006). Dispersal-related life-history trade-offs in a butterfly metapopulation. *Journal of animal Ecology* **75**, 91-100.
- Harshman, L. G. and Zera, A. J.** (2007). The cost of reproduction: the devil in the details. *Trends in ecology & evolution* **22**, 80-86.
- Hemingway, J. and Ranson, H.** (2000). Insecticide resistance in insect vectors of human disease. *Annual review of entomology* **45**, 371-391.
- Hilbrant, M., Horn, T., Koelzer, S. and Panfilio, K. A.** (2016). The beetle amnion and serosa functionally interact as apposed epithelia. *Elife* **5**, e13834.
- Hillyer, J. F. and Strand, M. R.** (2014). Mosquito hemocyte-mediated immune responses. *Current opinion in insect science* **3**, 14-21.
- Hoffmann, J. A.** (2003). The immune response of *Drosophila*. *Nature* **426**, 33-38.
- Holmes, V. R. and Johnston, J. S.** (2023). Differential Gene Expression of Innate Immune Response Genes Consequent to *Solenopsis invicta* Virus-3 Infection. *Genes* **14**, 188.
- Howe, R.** (1956). The effect of temperature and humidity on the rate of development and mortality of *Tribolium castaneum* (Herbst)(Coleoptera, Tenebrionidae). *Annals of Applied Biology* **44**, 356-368.
- Jacobs, C. G., Braak, N., Lamers, G. E. and van der Zee, M.** (2015). Elucidation of the serosal cuticle machinery in the beetle *Tribolium* by RNA sequencing and functional analysis of Knickkopf1, Retroactive and Laccase2. *Insect biochemistry and molecular biology* **60**, 7-12.
- Jacobs, C. G., Gallagher, J. D., Evison, S. E., Heckel, D. G., Vilcinskis, A. and Vogel, H.** (2017). Endogenous egg immune defenses in the yellow mealworm beetle (*Tenebrio molitor*). *Developmental & Comparative Immunology* **70**, 1-8.
- Jacobs, C. G., Rezende, G. L., Lamers, G. E. and van der Zee, M.** (2013). The extraembryonic serosa protects the insect egg against desiccation. *Proceedings of the Royal Society B: Biological Sciences* **280**, 20131082.
- Jacobs, C. G., Spaik, H. P. and van der Zee, M.** (2014a). The extraembryonic serosa is a frontier epithelium providing the insect egg with a full-range innate immune response. *elife* **3**, e04111.
- Jacobs, C. G., van der Hulst, R., Chen, Y.-T., Williamson, R. P., Roth, S. and van der Zee, M.** (2022). Immune function of the serosa in hemimetabolous insect eggs. *Philosophical Transactions of the Royal Society B* **377**, 20210266.
- Jacobs, C. G. and van der Zee, M.** (2013). Immune competence in insect eggs depends on the extraembryonic serosa. *Developmental & Comparative Immunology* **41**, 263-269.
- Jacobs, C. G., Wang, Y., Vogel, H., Vilcinskis, A., van Der Zee, M. and Rozen, D. E.** (2014b). Egg survival is reduced by grave-soil microbes in the carrion beetle, *Nicrophorus vespilloides*. *BMC Evolutionary Biology* **14**, 1-8.
- Jagadeeshan, S. and Singh, R. S.** (2007). Rapid evolution of outer egg membrane proteins in the *Drosophila melanogaster* subgroup: a case of ecologically driven evolution of female reproductive traits. *Molecular biology and evolution* **24**, 929-938.
- Janeway Jr, C. A. and Medzhitov, R.** (2002). Innate immune recognition. *Annual review of immunology* **20**, 197-216.
- Jervis, M. A., Ellers, J. and Harvey, J. A.** (2008). Resource acquisition, allocation, and utilization in parasitoid reproductive strategies. *Annu. Rev. Entomol.* **53**, 361-385.

- Johnston, P. R., Makarova, O. and Rolff, J.** (2014). Inducible defenses stay up late: temporal patterns of immune gene expression in *Tenebrio molitor*. *G3: Genes, Genomes, Genetics* **4**, 947-955.
- Józefiak, D., Józefiak, A., Kierończyk, B., Rawski, M., Świątkiewicz, S., Długosz, J. and Engberg, R. M.** (2016). 1. Insects—a natural nutrient source for poultry—a review. *Annals of Animal Science* **16**, 297-313.
- Kaaya, G. P.** (1989). A review of the progress made in recent years on research and understanding of immunity in insect vectors of human and animal diseases. *International Journal of Tropical Insect Science* **10**, 751-769.
- Ketterson, E. D. and Nolan, J., Val** (1999). Adaptation, exaptation, and constraint: a hormonal perspective. *the american naturalist* **154**, S4-S25.
- Khosravi, S., Kim, E., Lee, Y. S. and Lee, S. M.** (2018). Dietary inclusion of mealworm (*Tenebrio molitor*) meal as an alternative protein source in practical diets for juvenile rockfish (*Sebastes schlegeli*). *Entomological Research* **48**, 214-221.
- Kim, T. and Kim, Y.** (2005). Overview of innate immunity in *Drosophila*. *Journal of biochemistry and molecular biology* **38**, 121.
- Kingsolver, J. G. and Nagle, A.** (2007). Evolutionary divergence in thermal sensitivity and diapause of field and laboratory populations of *Manduca sexta*. *Physiological and Biochemical Zoology* **80**, 473-479.
- Langellotto, G. A., Denno, R. F. and Ott, J. R.** (2000). A trade-off between flight capability and reproduction in males of a wing-dimorphic insect. *Ecology* **81**, 865-875.
- Le Gall, M., Overson, R. and Cease, A. J.** (2019). A global review on locusts (Orthoptera: Acrididae) and their interactions with livestock grazing practices. *Frontiers in Ecology and Evolution* **7**, 263.
- Lemaitre, B. and Hoffmann, J.** (2007). The host defense of *Drosophila melanogaster*. *Annu. Rev. Immunol.* **25**, 697-743.
- Leroi, A. M., Chen, W. R. and Rose, M. R.** (1994). Long-term laboratory evolution of a genetic life-history trade-off in *Drosophila melanogaster*. 2. Stability of genetic correlations. *Evolution* **48**, 1258-1268.
- Ligoxygakis, P.** (2013). Genetics of immune recognition and response in *Drosophila* host defense. *Advances in Genetics* **83**, 71-97.
- Lin, X., Yao, Y., Wang, B., Emlen, D. J. and Lavine, L. C.** (2016). Ecological trade-offs between migration and reproduction are mediated by the nutrition-sensitive insulin-signaling pathway. *International journal of biological sciences* **12**, 607.
- Lindsey, E. and Altizer, S.** (2009). Sex differences in immune defenses and response to parasitism in monarch butterflies. *Evolutionary Ecology* **23**, 607-620.
- Lobo, L. S., Luz, C., Fernandes, E. K., Juárez, M. P. and Pedrini, N.** (2015). Assessing gene expression during pathogenesis: Use of qRT-PCR to follow toxin production in the entomopathogenic fungus *Beauveria bassiana* during infection and immune response of the insect host *Triatoma infestans*. *Journal of invertebrate pathology* **128**, 14-21.
- Lösel, R. and Wehling, M.** (2003). Nongenomic actions of steroid hormones. *Nature reviews Molecular cell biology* **4**, 46-55.
- Maeno, K. O., Piou, C. and Ghaout, S.** (2020). The desert locust, *Schistocerca gregaria*, plastically manipulates egg size by regulating both egg numbers and production rate according to population density. *Journal of Insect Physiology* **122**, 104020.
- Margaritis, L., Kafatos, F. and Petri, W.** (1980). The eggshell of *Drosophila melanogaster*. I. Fine structure of the layers and regions of the wild-type eggshell. *Journal of cell science* **43**, 1-35.
- Mayhew, P. J.** (2002). Shifts in hexapod diversification and what Haldane could have said. *Proceedings of the Royal Society of London. Series B: Biological Sciences* **269**, 969-974.
- (2007). Why are there so many insect species? Perspectives from fossils and phylogenies. *Biological Reviews* **82**, 425-454.
- Milutinović, B., Stolpe, C., Peuß, R., Armitage, S. A. and Kurtz, J.** (2013). The red flour beetle as a model for bacterial oral infections. *PloS one* **8**, e64638.
- Mira, A. and Bernays, E. A.** (2002). Trade-offs in host use by *Manduca sexta*: Plant characters vs natural enemies. *Oikos* **97**, 387-397.

- Mirzoyan, Z., Sollazzo, M., Allocca, M., Valenza, A. M., Grifoni, D. and Bellosta, P.** (2019). *Drosophila melanogaster*: A model organism to study cancer. *Frontiers in Genetics* **10**, 51.
- Moeller, M. E., Nagy, S., Gerlach, S. U., Soegaard, K. C., Danielsen, E. T., Texada, M. J. and Rewitz, K. F.** (2017). Warts signaling controls organ and body growth through regulation of ecdysone. *Current Biology* **27**, 1652-1659. e1654.
- Mullen, L. and Goldsworthy, G.** (2003). Changes in lipophorins are related to the activation of phenoloxidase in the haemolymph of *Locusta migratoria* in response to injection of immunogens. *Insect biochemistry and molecular biology* **33**, 661-670.
- Münster, S., Jain, A., Mietke, A., Pavlopoulos, A., Grill, S. W. and Tomancak, P.** (2019). Attachment of the blastoderm to the vitelline envelope affects gastrulation of insects. *Nature* **568**, 395-399.
- Nicholson, D. B., Ross, A. J. and Mayhew, P. J.** (2014). Fossil evidence for key innovations in the evolution of insect diversity. *Proceedings of the Royal Society B: Biological Sciences* **281**, 20141823.
- Nijhout, H. F.** (1998). *Insect hormones*: Princeton University Press.
- Novotny, V., Drozd, P., Miller, S. E., Kulfan, M., Janda, M., Basset, Y. and Weiblen, G. D.** (2006). Why are there so many species of herbivorous insects in tropical rainforests? *science* **313**, 1115-1118.
- Oerke, E.-C., Dehne, H.-W., Schönbeck, F. and Weber, A.** (2012). *Crop production and crop protection: estimated losses in major food and cash crops*: Elsevier.
- Organization, W. H.** (2022). World malaria report 2021. 2021. *Reference Source*.
- Panfilio, K. A.** (2008). Extraembryonic development in insects and the acrobatics of blastokinesis. *Developmental biology* **313**, 471-491.
- Peng, B.-Y., Su, Y., Chen, Z., Chen, J., Zhou, X., Benbow, M. E., Criddle, C. S., Wu, W.-M. and Zhang, Y.** (2019). Biodegradation of polystyrene by dark (*Tenebrio obscurus*) and yellow (*Tenebrio molitor*) mealworms (Coleoptera: Tenebrionidae). *Environmental science & technology* **53**, 5256-5265.
- Peters, R. S., Krogmann, L., Mayer, C., Donath, A., Gunkel, S., Meusemann, K., Kozlov, A., Podsiadlowski, L., Petersen, M. and Lanfear, R.** (2017). Evolutionary history of the Hymenoptera. *Current Biology* **27**, 1013-1018.
- Phiri, B. J., Fèvre, D. and Hidano, A.** (2022). Uptrend in global managed honey bee colonies and production based on a six-decade viewpoint, 1961–2017. *Scientific Reports* **12**, 21298.
- Pough, F. H.** (1991). Recommendations for the care of amphibians and reptiles in academic institutions. *ILAR Journal* **33**, S1-S21.
- Powell, J. A.** (2009). Lepidoptera: moths, butterflies. In *Encyclopedia of insects*, pp. 559-587: Elsevier.
- Price, P. W.** (1997). *Insect ecology*: John Wiley & Sons.
- Quicke, D. L.** (2009). Hymenoptera: Ants, Bees, Wasps. In *Encyclopedia of Insects*, pp. 473-484: Elsevier.
- Rafiqi, A. M., Lemke, S., Ferguson, S., Stauber, M. and Schmidt-Ott, U.** (2008). Evolutionary origin of the amnioserosa in cyclorrhaphan flies correlates with spatial and temporal expression changes of zen. *Proceedings of the National Academy of Sciences* **105**, 234-239.
- Rezende, G. L., Martins, A. J., Gentile, C., Farnesi, L. C., Pelajo-Machado, M., Peixoto, A. A. and Valle, D.** (2008). Embryonic desiccation resistance in *Aedes aegypti*: presumptive role of the chitinized serosal cuticle. *BMC developmental biology* **8**, 1-14.
- Rezende, G. L., Vargas, H. C. M., Moussian, B. and Cohen, E.** (2016). Composite eggshell matrices: Chorionic layers and sub-chorionic cuticular envelopes. In *Extracellular composite matrices in arthropods*, pp. 325-366: Springer.
- Robbins, W., Kaplanis, J., Thompson, M., Shortino, T., Cohen, C. and Joyner, S.** (1968). Ecdysones and analogs: effects on development and reproduction of insects. *Science* **161**, 1158-1160.
- Rodrigues, M. A. and Flatt, T.** (2016). Endocrine uncoupling of the trade-off between reproduction and somatic maintenance in eusocial insects. *Current opinion in insect science* **16**, 1-8.
- Rolff, J., Johnston, P. R. and Reynolds, S.** (2019). Complete metamorphosis of insects. *Philosophical Transactions of the Royal Society B* **374**, 20190063.

- Rosenberg, M. I., Lynch, J. A. and Desplan, C.** (2009). Heads and tails: evolution of antero-posterior patterning in insects. *Biochimica et Biophysica Acta (BBA)-Gene Regulatory Mechanisms* **1789**, 333-342.
- Roth, S.** (2004). Gastrulation in other insects. *Gastrulation: from cells to embryos* **105**, 121.
- Roush, R. and Tabashnik, B. E.** (2012). *Pesticide resistance in arthropods*: Springer Science & Business Media.
- Rytkönen, S., Vesterinen, E. J., Westerduin, C., Leviäkangas, T., Vatka, E., Mutanen, M., Välimäki, P., Hukkanen, M., Suokas, M. and Orell, M.** (2019). From feces to data: A metabarcoding method for analyzing consumed and available prey in a bird-insect food web. *Ecology and evolution* **9**, 631-639.
- Salcedo-Porras, N. and Lowenberger, C.** (2019). The innate immune system of kissing bugs, vectors of chagas disease. *Developmental & Comparative Immunology* **98**, 119-128.
- Sanchez-Bayo, F. and Goka, K.** (2014). Pesticide residues and bees—a risk assessment. *PloS one* **9**, e94482.
- Sander, K.** (1976). Morphogenetic movements in insect embryogenesis. In *Symposia of the Royal Entomological Society of London*.
- Sarwar, M.** (2015). Direct Possessions of Insect Arthropods on Humans Owing to Allergen, Bloodsucking, Biting, Envenomation and Stinging Side By Side Case Diagnosis and Treating. *International Journal of Bioinformatics and Biomedical Engineering* **1**, 331-337.
- Sastry, A., Vernberg, F. and Vernberg, W.** (1983). Ecological aspects of reproduction. *The biology of Crustacea* **8**, 179-270.
- Schluns, H. and Crozier, R. H.** (2009). Molecular and chemical immune defenses in ants (Hymenoptera: Formicidae). *Myrmecological News* **12**, 237-249.
- Schmid-Hempel, P.** (2005). Evolutionary ecology of insect immune defenses. *Annu. Rev. Entomol.* **50**, 529-551.
- Schmidt-Ott, U., Rafiqi, A. M. and Lemke, S.** (2010). Hox3/zen and the evolution of extraembryonic epithelia in insects. *Hox Genes*, 133-144.
- Schwenke, R. A., Lazzaro, B. P. and Wolfner, M. F.** (2016). Reproduction–immunity trade-offs in insects. *Annual review of entomology* **61**, 239-256.
- Shelton, A. M., Zhao, J.-Z. and Roush, R. T.** (2002). Economic, ecological, food safety, and social consequences of the deployment of Bt transgenic plants. *Annual review of entomology* **47**, 845-881.
- Stearns, S. C.** (1989). Trade-offs in life-history evolution. *Functional ecology* **3**, 259-268.
- (1992). *The evolution of life histories*: Oxford university press Oxford.
- Stork, N. E.** (2018). How many species of insects and other terrestrial arthropods are there on Earth? *Annual review of entomology* **63**, 31-45.
- Tanaka, S.** (2017). Locusta migratoria (Orthoptera: Acrididae) embryos monitor neighboring eggs for hatching synchrony. *Journal of orthoptera research*, 103-115.
- Tanaka, S. and Suzuki, Y.** (1998). Physiological trade-offs between reproduction, flight capability and longevity in a wing-dimorphic cricket, Modicogryllus confirmatus. *Journal of Insect Physiology* **44**, 121-129.
- Teleman, A. A., Chen, Y.-W. and Cohen, S. M.** (2005). Drosophila Melted modulates FOXO and TOR activity. *Developmental cell* **9**, 271-281.
- Tsakas, S. and Marmaras, V.** (2010). Insect immunity and its signalling: an overview. *Invertebrate Survival Journal* **7**, 228-238.
- Tulloch, A. P.** (1980). Beeswax—composition and analysis. *Bee world* **61**, 47-62.
- Ugur, B., Chen, K. and Bellen, H. J.** (2016). Drosophila tools and assays for the study of human diseases. *Disease models & mechanisms* **9**, 235-244.
- van der Zee, M., Berns, N. and Roth, S.** (2005). Distinct functions of the Tribolium zerku llt genes in serosa specification and dorsal closure. *Current Biology* **15**, 624-636.
- van Klink, R., Bowler, D. E., Gongalsky, K. B., Swengel, A. B., Gentile, A. and Chase, J. M.** (2020). Meta-analysis reveals declines in terrestrial but increases in freshwater insect abundances. *Science* **368**, 417-420.
- Vieira, C. S., Mattos, D. P., Waniek, P. J., Santangelo, J. M., Figueiredo, M. B., Gumiel, M., Da Mota, F. F., Castro, D. P., Garcia, E. S. and Azambuja, P.** (2015). Rhodnius prolixus

- interaction with *Trypanosoma rangeli*: modulation of the immune system and microbiota population. *Parasites & vectors* **8**, 1-13.
- Waegele, J. W. and Bartolomeaus, T.** (2014). *Deep Metazoan Phylogeny: the Backbone of the Tree of Life: new insights from analyses of molecules, morphology, and theory of data analysis*: Walter de Gruyter.
- Wei, Z., Ortiz-Urquiza, A. and Keyhani, N. O.** (2021). Altered expression of chemosensory and odorant binding proteins in response to fungal infection in the red imported fire ant, *Solenopsis invicta*. *Frontiers in Physiology* **12**, 596571.
- Wilson, J. K., Ruiz, L. and Davidowitz, G.** (2020). Within-host competition drives energy allocation trade-offs in an insect parasitoid. *PeerJ* **8**, e8810.
- Yang, L., Qiu, L. M., Fang, Q., Stanley, D. W. and Ye, G. Y.** (2021). Cellular and humoral immune interactions between *Drosophila* and its parasitoids. *Insect Science* **28**, 1208-1227.
- Zeh, D. W., Zeh, J. A. and Smith, R. L.** (1989). Ovipositors, amnions and eggshell architecture in the diversification of terrestrial arthropods. *The Quarterly Review of Biology* **64**, 147-168.
- Zera, A. J. and Harshman, L. G.** (2001). The physiology of life history trade-offs in animals. *Annual review of Ecology and Systematics* **32**, 95-126.
- Zhang, L., Lecoq, M., Latchinsky, A. and Hunter, D.** (2019). Locust and grasshopper management. *Annual review of entomology* **64**, 15-34.
- Zhang, W., Chen, J., Keyhani, N. O., Zhang, Z., Li, S. and Xia, Y.** (2015). Comparative transcriptomic analysis of immune responses of the migratory locust, *Locusta migratoria*, to challenge by the fungal insect pathogen, *Metarhizium acridum*. *BMC genomics* **16**, 1-21.
- Zhang, Z.-Q.** (2011). *Animal biodiversity: An outline of higher-level classification and survey of taxonomic richness*: Magnolia press.
- (2013). Phylum Arthropoda. In: Zhang, Z.-Q.(Ed.) *Animal Biodiversity: An Outline of Higher-level Classification and Survey of Taxonomic Richness* (Addenda 2013). *Zootaxa* **3703**, 17–26-17–26.
- Zhou, J. C., Liu, Q. Q., Wang, Q. R., Ning, S. F., Che, W. N. and Dong, H.** (2020). Optimal clutch size for quality control of bisexual and Wolbachia-infected thelytokous lines of *Trichogramma dendrolimi* Matsumura (Hymenoptera: Trichogrammatidae) mass reared on eggs of a substitutive host, *Antheraea pernyi* Guérin-Méneville (Lepidoptera: Saturniidae). *Pest management science* **76**, 2635-2644.
- Zou, Z., Evans, J. D., Lu, Z., Zhao, P., Williams, M., Sumathipala, N., Hetru, C., Hultmark, D. and Jiang, H.** (2007). Comparative genomic analysis of the *Tribolium* immune system. *Genome biology* **8**, 1-16.
- Züst, T. and Agrawal, A. A.** (2017). Trade-offs between plant growth and defense against insect herbivory: an emerging mechanistic synthesis. *Annual review of plant biology* **68**, 513-534.
- Zwaan, B., Bijlsma, R. and Hoekstra, R.** (1995). Direct selection on life span in *Drosophila melanogaster*. *Evolution* **49**, 649-659.



# Chapter 2

## Immune competence in eggs of the springtail

### *Orchesella cincta*

Shixiong Cheng, Annika Koumans, Nisanth Ponnar and Maurijn van der Zee

#### Abstract

The serosa is an extraembryonic epithelium unique to insect eggs. In the beetle *Tribolium castaneum*, this epithelium can mount an immune response protecting the embryo. Here, we expand our studies beyond the insects, and investigate the immune response in eggs of the springtail *Orchesella cincta* belonging to the closely related hexapod subclass Collembola that do not possess a serosa. Although qPCR could not detect significant upregulation of immune genes in adults, we did find significant upregulation of four out of the thirteen investigated antimicrobial peptides in eggs upon challenge with a mix of Gram positive and Gram negative bacteria. In line with the presence of this inducible response in eggs, we found no evidence for maternal provision of antimicrobials to the eggs in zone-of-inhibition assays of egg extracts. We conclude that mothers do not load their eggs with antimicrobials, and that *O. cincta* eggs can upregulate immune genes upon infection, without the requirement of a serosa. The exact tissue expressing these immune genes in the egg remains to be determined.

#### Introduction

The serosa is an extraembryonic epithelium that covers the yolk and embryo in insect eggs (Panfilio, 2008; Roth, 2004). It is an evolutionary innovation of the insects and is not present in the other arthropods, such as crustaceans and entognatha (Jacobs et al., 2013; Machida and Ando, 1998). As the serosa secretes a cuticle, it protects the egg against desiccation (Hinton, 1981; Jacobs et al., 2013; Rezende et al., 2008; Vargas et al., 2014). Hence, the serosa was probably crucial for the terrestrial radiation of the insects (Jacobs et al., 2013; Zeh et al., 1989).

The serosa also provides the holometabolous beetle *Tribolium castaneum* with a potent, full range immune response. The serosa can express massive amounts of antimicrobial peptides (AMPs) when challenged with a mix of Gram positive and Gram negative bacteria. Bacteria propagate twice as fast in serosa-less eggs (Jacobs et al., 2014a). Induced expression of functional AMPs in the serosa was also recently found in the hemimetabolous insects *Oncopeltus fasciatus* and *Locusta migratoria* (Jacobs et al., 2022). In addition, induction of antimicrobial peptides could be detected in egg fractions that contained the yolk and serosa of the moth *Manduca sexta*, but not in fractions only containing isolated germ bands (Gorman et al., 2004). Thus, the serosa provides the insect egg with an innate immune response.



Strikingly, the eggs of well-studied model organism *Drosophila* do not show an immune response after bacterial infection (Jacobs and van der Zee, 2013). *Drosophila* eggs do not have a serosa, as *Drosophila* belongs to the Schizophoran flies, the only group of insects that secondarily lost the serosa in evolution (Rafiqi et al., 2008; Schmidt-Ott, 2000). Absence of an immune response in Schizophoran flies may be compensated by maternal investments, as maternal antimicrobial peptides have been found in the outer chorion of eggs of the Mediterranean fruit fly *Ceratitidis capitata* (Marchini et al., 1997). Thus, the presence of an inducible immune response in the egg correlates with the presence of a serosa, and eggs without a zygotic immune response seem to require maternal protection. Indeed, arthropod groups without a serosa, such as the crustaceans, do large maternal investments in egg protection (Sastry et al., 1983).

To test the hypothesis that the serosa is a prerequisite for an inducible innate immune response, we investigate the immune response in eggs and maternal protection in the springtail *Orchesella cincta*. *O. cincta* is a wingless, soil-dwelling entognathan and is not an insect, but belongs to the closely related hexapod subclass Collembola (springtails) that do not possess a serosa (Anderson, 1973; Jacobs et al., 2013; Machida and Ando, 1998) (Figure 1-7). Consequently, we do not expect an inducible immune response in these eggs. We perform qPCR on 13 predicted AMPs and one metallothionein after bacterial challenge, and use zone-of-inhibition assays to test the presence of maternal antimicrobials. Surprisingly, we did not find a significant immune response in adults. We did, however, find significant upregulation of 4 AMPs in *Orchesella* eggs after infection. Together with the absence of maternal protection, this indicates that *Orchesella* eggs can mount a zygotic immune response and that the serosa is not required for this.

## Materials and Methods

### Rearing of the springtails and egg collection

The springtails (*Orchesella cincta*) were obtained from the Animal Ecology Department of Vrije University Amsterdam and kept at 80% humidity and 20 degrees Celsius in 16 cm wide plastic container tubes, closed with netting on top and Paris plaster at the bottom, under a photoperiod of 16h light and 8h dark. Wetted twigs from a location without heavy metal or insecticide contamination were provided. The colony was sprayed with tap water three times a week. To obtain eggs, 3 males and 3 females were put in similar 5 cm wide container tubes.

### Bacterial challenge experiment

*Micrococcus luteus* or *Escherichia coli* cultures were grown overnight in LB medium while shaking at 200 rpm at 37°C. Cultures were centrifuged at 2000 rpm for 10 min at room temperature to harvest bacteria, and pellets were mixed 1:1. For infection of adults, three springtails were put in a petri dish and cooled for 3 min on ice. They were then pricked in the abdomen with a tungsten needle that was either sterile (control) or dipped in the bacterial suspension (bacterial prick). Adults stick to the needle and were carefully put into a small container with help of a brush.

For infection of eggs, 300 3-4 day old eggs were selected that showed hair-like protrusions of the blastodermal cuticle and polar caps (Vargas et al., 2021). Similar to the adults, eggs were pricked with a tungsten needle that was either sterile (control) or dipped in the bacterial suspension (bacterial

prick). The eggs were then placed on wetted filter paper in a petri dish. Both the adults and the eggs were incubated for 6 h in the climate room (see materials and methods section 2.1) before RNA extraction. The experiments were performed in three biological replicates (each including control and bacterial prick).

## Selection of immune genes and their primers

We found 9 annotated AMPs in the *Orchesella cincta* genome (Faddeeva-Vakhrusheva et al., 2016), and found 7 others by BLAST (see results section 3.1, Table 2-2). Primers were designed using the NCBI primer design tool. Wherever possible, primers were chosen around an intron to avoid amplification from genomic DNA. In addition, we included the stress-induced metallothionein (MT) gene (Timmermans et al., 2005), and used beta-actin as normalizer gene (de Boer et al., 2009). All primers are listed below:

Table 2-1. Primers used for qPCR.

Gene name	Forward primer (5'-3')	Reverse primer (5'-3')
<b><i>Orchesella cincta</i></b>		
<i>Beta-actin</i>	CCGTAAGGATCTGTATGCCAACA	CCAGGGCAGTGATCTCCTTTT
<i>AMP1a</i>	TACGGGAGAAGTTTGCCTGG	CTGTTTGCCAGGAGGTACA
<i>AMP1b2</i>	CCGAATCAAGGGAGAAGGCT	AGACCACTTGGAAACATCGCA
<i>AMP1b3</i>	TGCATACTCCTGGTCACCTTG	CGTGTTCCACATGGTCCAAC
<i>AMP1b4</i>	TGTCGATTTGCTGGTGAGGG	AGGTCCAACATCGCACTCTC
<i>AMP1b5</i>	TTGCCACCTTTGCGTAATC	TCACAAAGGTCAGCGGTACG
<i>AMP2a</i>	GTCTCGGAAAATGGGCCAGA	ACGAAGCGTCAATGTCCTGA
<i>AMP2b</i>	TTGCACACGCGAAAGAAGTG	GCAAGAGTGCCTCCTCCATT
<i>Defensin</i>	TTGCAATCGGCATGCTGGAG	CCCTCAAACCTGGGCCAACA
<i>Diapausin1</i>	CTGCTCACTTTGGCTTTCGT	CCTGCAGCATTTCGTTGATCTC
<i>Diapausin2</i>	GCTTTCGTTCTGATTGCCACT	AGCCCTGCAGCATTTCATTGAT
<i>MT</i> *)	GGCAAATCGCCCACTTGTT	CCTTGCAGACACAATCTGGACC
<i>Toxin1</i>	ACACTCCAGTTCAACCCTGC	ATGAGCTTGACAGCACACGA
<i>Toxin2</i>	AGTGCAACCATGCAACAACC	CCCTTCCACCCTTGTAACCG
<i>Toxin3</i>	CCTTCTTGCAGTCCTCTTTCG	GGAGTGTCTCGGCGTTTGTA

\*) *Metallothionein*

## RNA extraction and qPCR

Total RNA of was extracted using trizol extraction (Invitrogen) after which the RNA was purified and DNA digested on column with the RNeasy kit (Qiagen). The quality of RNA preparation was confirmed spectro-photometrically. One microgram of total RNA was used for cDNA synthesis. First strand cDNA was synthesized in the Promega Reverse Transcription system (Promega, Madison, USA). Each qPCR mixture (10 µl) contained 5 ng of cDNA, and the real-time detection and analyses were done based on SYBR green dye chemistry using the SsoAdvanced Universal SYBR Green Supermix (Bio-Rad) and a CFX96 thermocycler (Bio-Rad). Thermal cycling conditions used were 95 °C for 30 s, then 40 cycles of 95°C for 15 s, 60°C for 30s, 72°C for 30 s; this was followed by dissociation analysis of a ramp from 65 to 95 °C with a read every 0.5 °C. Relative quantification for

each mRNA was done using the Livak-method (Livak and Schmittgen, 2001). Total RNA for each sample was measured by qPCR twice (technical replication).

## Data analysis of qPCR

Fold change upregulation of the immune genes upon bacterial challenge was calculated using the  $2^{-\Delta\Delta C_T}$  method with the sterile prick samples as calibrator (Livak and Schmittgen, 2001). Statistical difference between the  $\Delta C_T$  values of the bacterial prick and the sterile prick samples was calculated using T-tests (SPSS software, version 27.0). The level of significance was defined as  $P < 0.05$ .

## Inhibition zone assays

In order to check whether the mother provides antimicrobials to the egg, antimicrobial activity of egg extracts was tested in an inhibition zone assay (Dubuffet et al., 2015; Moret and Schmid-Hempel, 2000) with a few modifications. Briefly, egg extracts was prepared by smashing eggs into an acetic acid solution (0.05%, 100 eggs in 50  $\mu$ l) followed by centrifuging at 3500 g for 2 min. Supernatants was collected and divided into 5 aliquots, and kept at  $-20^\circ\text{C}$ . Methanol was used as the other extraction liquid. Bacteria (*E. coli* and *M. luteus*) were cultured overnight and then seeded to 1% LB-agar soft plates at a final concentration of  $10^5$  microorganisms/ml, respectively. Then, 5  $\mu$ l 0.05% acetic acid solution with egg extracts was applied on filter discs that were placed on the seeded LB agar plates. Plates were incubated at  $37^\circ\text{C}$  for 24 or 48 h according to the tested microorganism after which the diameter of inhibition zones was measured. 5  $\mu$ l 0.05% acetic acid solution and methanol acted as negative controls. The assays were conducted in triplicate.

## Results

### Identification of antimicrobial peptides in the *Orchesella cincta* genome

In total, we found 16 potential antimicrobial peptides in the *Orchesella cincta* genome (Table 2-2). Nine of them were annotated as such in the NCBI protein database: One (Ocin01\_18400-PA) was annotated as Defensin J1-1; two (Ocin01\_05907-PA and Ocin01\_07323-PA) were annotated as antimicrobial peptide 1; two (Ocin01\_04461-PA and Ocin01\_19094-PA) were annotated as antimicrobial peptide 2; two (Ocin01\_19250-PA and Ocin01\_13871-PA) were annotated as diapause specific protein; and two (Ocin01\_16060-PA and Ocin01\_13870-PA) were annotated as Toxin-like peptide AaF1CA1. In addition, we found 4 other peptides by blast that were highly similar to antimicrobial peptide 1 (Ocin01\_19760-PA, Ocin01\_17792-PA, Ocin01\_15366-PA and Ocin01\_20115-PA). We called them AMP1b2 to AMP1b5. And we found one that was very similar to Toxin-like peptide AaF1CA1 (Ocin01\_19251-PA). We called it Toxin3. We also blasted known antimicrobial peptides from other arthropods (Mylonakis et al., 2016) in the *Orchesella* genome, but found no additional potential AMPs, except for two peptides (Ocin01\_14538-PA and Ocin01\_18172-PA) that were similar to Drosomycin. We did, however, find no expression of these two genes by qPCR. We also did not find any expression of Ocin01\_07323-PA (AMP1b1). These genes were excluded for further analysis, but we added the reported stress-induced metallothionein gene (Timmermans et al., 2005).

Table 2-2. Potential antimicrobial peptides in the *Orchesella cincta* genome.

Gene name	NCBI annotation	GenBank	Collembolomics	Remark
<i>Defensin</i>	Defensin J1-1	ODM88282.1	Ocin01_18400-PA	
<i>AMP1a</i>	Antimicrobial peptide 1	ODN00764.1	Ocin01_05907-PA	
<i>AMP1b1</i>	Antimicrobial peptide 1	ODM99353.1	Ocin01_07323-PA	No expression detected by qPCR
<i>AMP1b2</i>	Hypothetical protein	ODM86921.1	Ocin01_19760-PA	Found similar to AMP1b1 by BLAST
<i>AMP1b3</i>	Hypothetical protein	ODM88896.1	Ocin01_17792-PA	Found similar to AMP1b1 by BLAST
<i>AMP1b4</i>	Hypothetical protein	ODM91321.1	Ocin01_15366-PA	Found similar to AMP1b1 by BLAST
<i>AMP1b5</i>	Hypothetical protein	ODM86567.1	Ocin01_20115-PA	Found similar to AMP1b1 by BLAST
<i>AMP2a</i>	Antimicrobial peptide 2	ODN02227.1	Ocin01_04461-PA	
<i>AMP2b</i>	Antimicrobial peptide 2	ODM87588.1	Ocin01_19094-PA	
<i>Diapausin1</i>	Diapause specific peptide	ODM87430.1	Ocin01_19250-PA	
<i>Diapausin2</i>	Diapause specific peptide	ODM92813.1	Ocin01_13871-PA	
<i>Toxin1</i>	Toxin-like peptide AaF1CA1	ODM90622.1	Ocin01_16060-PA	
<i>Toxin2</i>	Toxin-like peptide AaF1CA1	ODM92816.1	Ocin01_13870-PA	
<i>Toxin3</i>	Hypothetical protein	ODM87431.1	Ocin01_19251-PA	Found similar to Toxin2 by BLAST
<i>Drosomycin1</i>	Hypothetical protein	ODM92144.1	Ocin01_14538-PA	No expression detected by qPCR
<i>Drosomycin2</i>	Hypothetical protein	ODM88510.1	Ocin01_18172-PA	No expression detected by qPCR

## The expression of potential immune genes in adults and eggs upon bacterial challenge

Surprisingly, we did not find significant upregulation of AMPs upon infection of adults (Figure 2-1). Although some upregulations were on average high (*toxin3* was upregulated 56.1-fold upon infection), this was not significant because of the large spread among the biological replicates. We did, however find significant upregulation of 4 AMPs in eggs, namely of *antimicrobial peptide 1a* (*AMP 1a*, 4.3-fold), *antimicrobial peptide 1b4* (*AMP 1b4*, 5.2-fold), *antimicrobial peptide 2b* (*AMP 2b*, 9.7-fold) and *toxin1* (5.3-fold). The upregulation of *toxin1* in eggs was also significantly higher than in adults. This means that *Orchesella* eggs can upregulate some immune genes upon infection, despite absence of a serosa (Anderson, 1973).

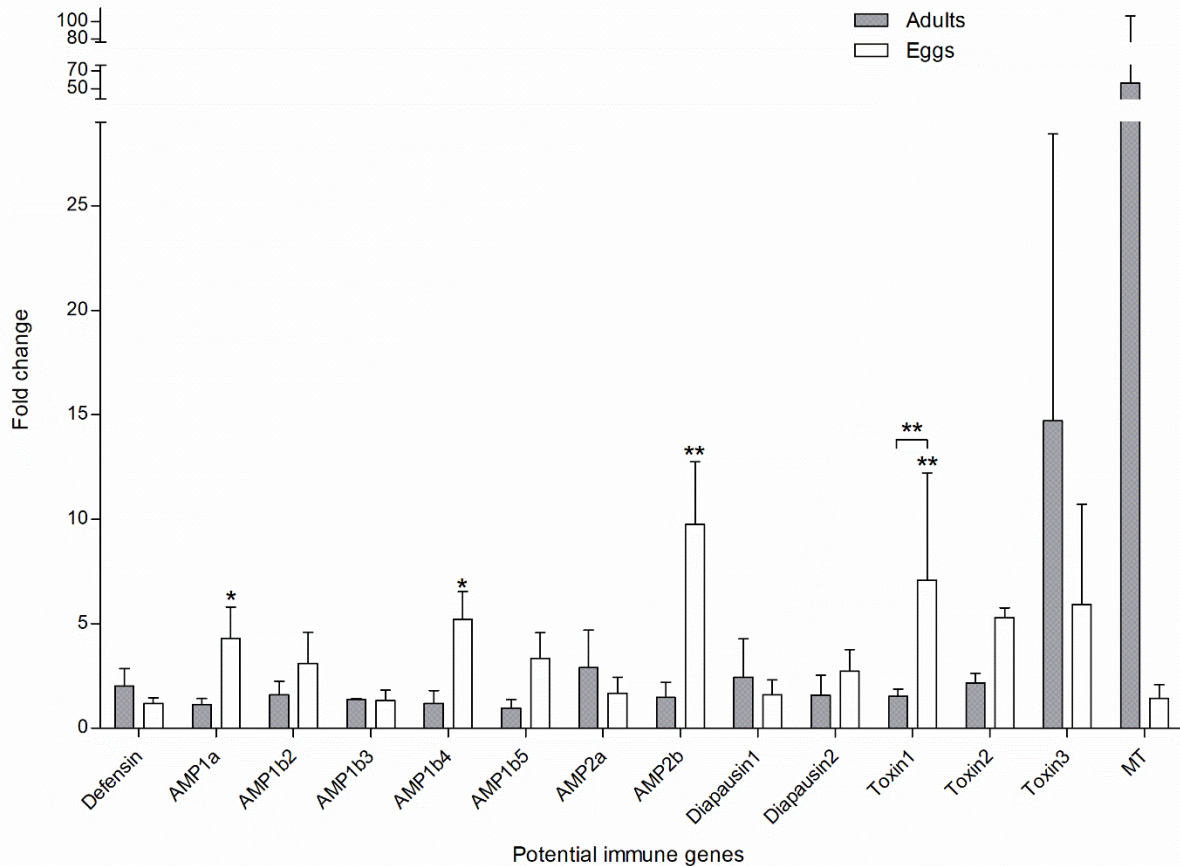


Figure 2-1. Temporal expression of 14 potential immune genes after bacterial challenge. Each vertical bar represented the mean  $\pm$  S.E (n = 3). Significant difference of fold change of these potential immune genes between adults and eggs was shown with the asterisk above the capped line (\* represented  $P < 0.05$ ). Statistical significance of delta Ct between septic injury and sterile injury of each gene in adults or eggs upon injections was indicated with the asterisk above the column (\* represented  $P < 0.05$ , \*\* represented  $P < 0.01$ , \*\*\* represented  $P < 0.001$ ), shown in Supplementary Figure 2-1. MT: Metallothionein.

### Maternally provided antimicrobial activity

To investigate if this immune response eggs is accompanied by standard absence of maternal protection, we investigated antimicrobial activity of eggs laid by unchallenged mothers in zone-of-inhibition assays. Neither water-extracts nor methanol-extracts of eggs prevented growth of the indicator strains *E. coli* or *M. luteus* (Figure 2-2) around discs, whereas clear halo's appeared around control discs with nalidixic acid. This shows that egg extracts of *O. cincta* did not possess antimicrobial activity against the indicator strains, and suggests that *Orchesella* mothers do not load their eggs with antimicrobials.

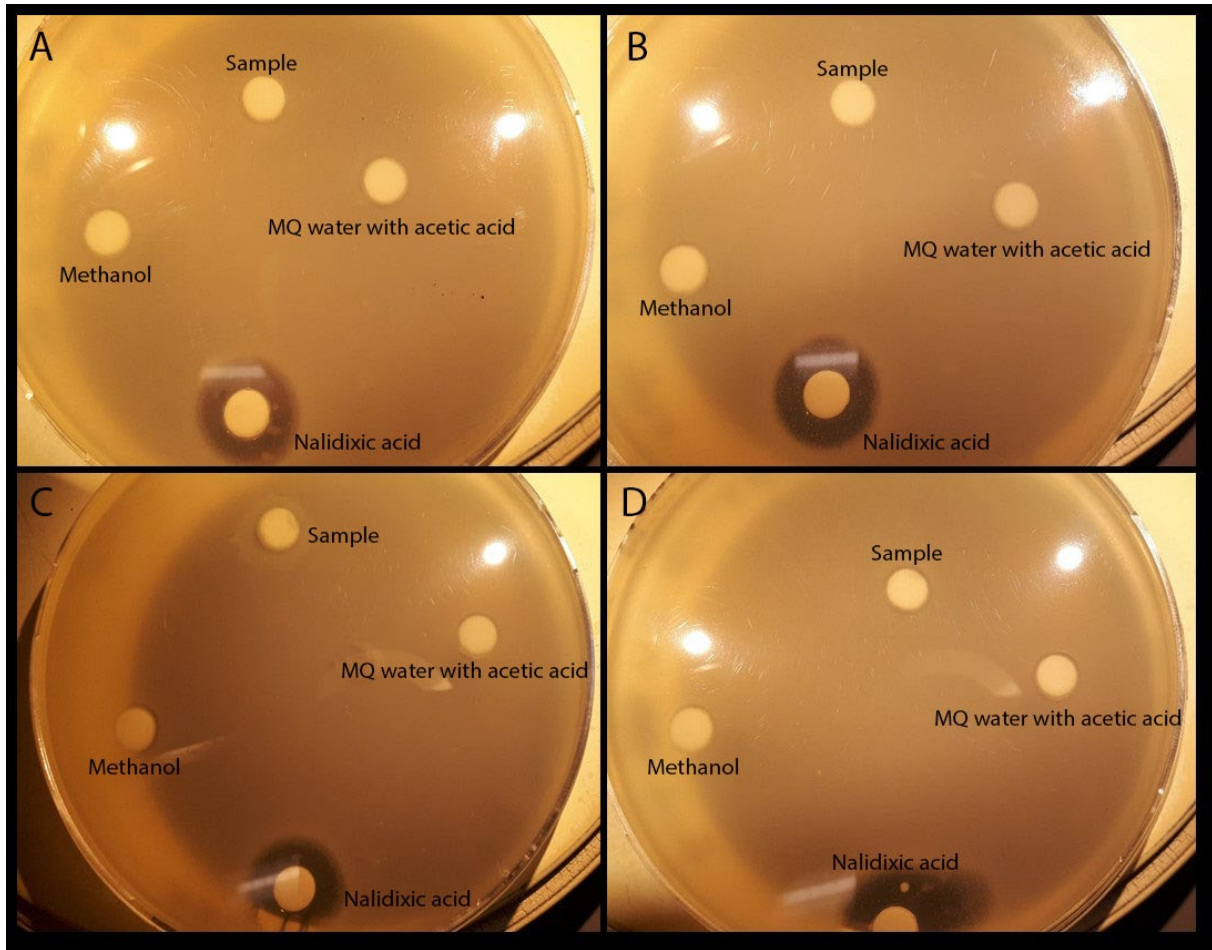


Figure 2-2. Antimicrobial activity of the springtails egg extracts. A: plate with *E. coli* as indicator, the sample was extracted with MQ water (0.05% acetic acid). B: plate with *M. luteus* as indicator, the sample was extracted with MQ water (0.05% acetic acid). C: plate with *E. coli* as indicator, the sample was extracted with methanol. D: plate with *M. luteus* as indicator, the sample was extracted with methanol.

## Discussion

Here, we report significant induction of four antimicrobial peptides in eggs of the springtail *Orchesella cincta*. In our study, we could not detect significant induction of AMPs upon infection in adults. As the average upregulation of some immune genes in adults is high (e.g. *Toxin 3* was on average upregulated 63.3-fold upon infection), the lack of significance in adults is due to the large variation among the biological replicates. This large experimental variation may have concealed a true immune response to some extent. In addition, our qPCR approach on candidate genes may be somewhat limited. The thirteen AMPs we tested are predicted AMPs lacking experimental confirmation of their antimicrobial activity. However, several AMP prediction tools, such as AMP\_Scanner (Veltri et al., 2018) do suggest antimicrobial activity of the predicted peptides. Finally, other springtails, such as *Folsomia candida* contain bacterial synthesis genes producing the beta-lactam antibiotic (Roelofs et al., 2013). Although beta-lactam genes seem to be absent in *Orchesella* (Suring et al., 2017), we cannot exclude that *Orchesella* adults upregulate other genes upon infection

than the candidate genes tested in this study. Taken together, RNAsequencing after infection may establish a less biased assessment of the immune response of *Orchesella* adults in future.

The most striking finding of our study is the presence of an inducible immune response in *Orchesella* eggs. We did not expect such response, as the immune response in insects is mounted by the extraembryonic serosa (Jacobs et al., 2014a; Jacobs et al., 2022), a structure that is not present in the hexapod subclass Collembola to which *Orchesella* belongs (Anderson, 1973; Jacobs et al., 2013). However, Jura (1972), Machida (2006), and Machida & Ando (1998) call the extraembryonic cells that never envelop the springtail embryo also a serosa (Jura, 1972; Machida, 2006; Machida and Ando, 1998). It is possible that these cells express our detected AMP transcripts, and provide the egg with an innate immune response. It is also possible that embryonic cells express AMPs in *Orchesella*, as immune gene expression has also been reported in late ectodermal cells of *Drosophila melanogaster* and *Oncopeltus fasciatus* embryos (Jacobs et al., 2022; Tan et al., 2014). Future *in situ* hybridizations should reveal the exact location of immune gene expression in *Orchesella cincta* eggs.

Lastly, we did not find any evidence for maternal provision of antibiotics to *Orchesella* eggs. We did, however, only investigate antimicrobial activity of eggs laid by unchallenged mothers. It is possible that mothers only provide antimicrobials to their eggs when challenged. In bumblebees and mealworm beetles, such maternal provision of antimicrobials upon infection has been demonstrated (Moreau et al., 2012; Tetreau et al., 2020). Future analysis of eggs laid by challenged mothers should resolve this issue, but our data demonstrate that *Orchesella* eggs are not standardly loaded with antimicrobials against *E. coli* or *M. luteus* by the mother.

In conclusion, our study shows that *Orchesella cincta* eggs can upregulate immune genes, and that the serosa is not a prerequisite for this. Within insects, the presence of a serosa is also not necessarily coupled to presence of immune competence. Eggs of the beetle *Nicrophorus vespilloides*, for instance, possess a serosa, but lack inducible immune gene expression (Jacobs et al., 2014b). Importantly, even in eggs of other arthropod groups without a serosa, such as the Crustacean *Litopenaeus vannamei*, an upregulation of immune genes has been reported (Alvarez-Lee et al., 2020). Thus, immune competence was probably present in arthropod eggs before the evolution of the serosa. The exact tissue expressing these immune genes in the egg remains to be determined.

## Acknowledgments

The author would like to thank Janine Mariën from the Animal Ecology Department of Vrije University Amsterdam for the protocol to take care of the springtails, and Kees Koops for care and maintenance of animals.

## References

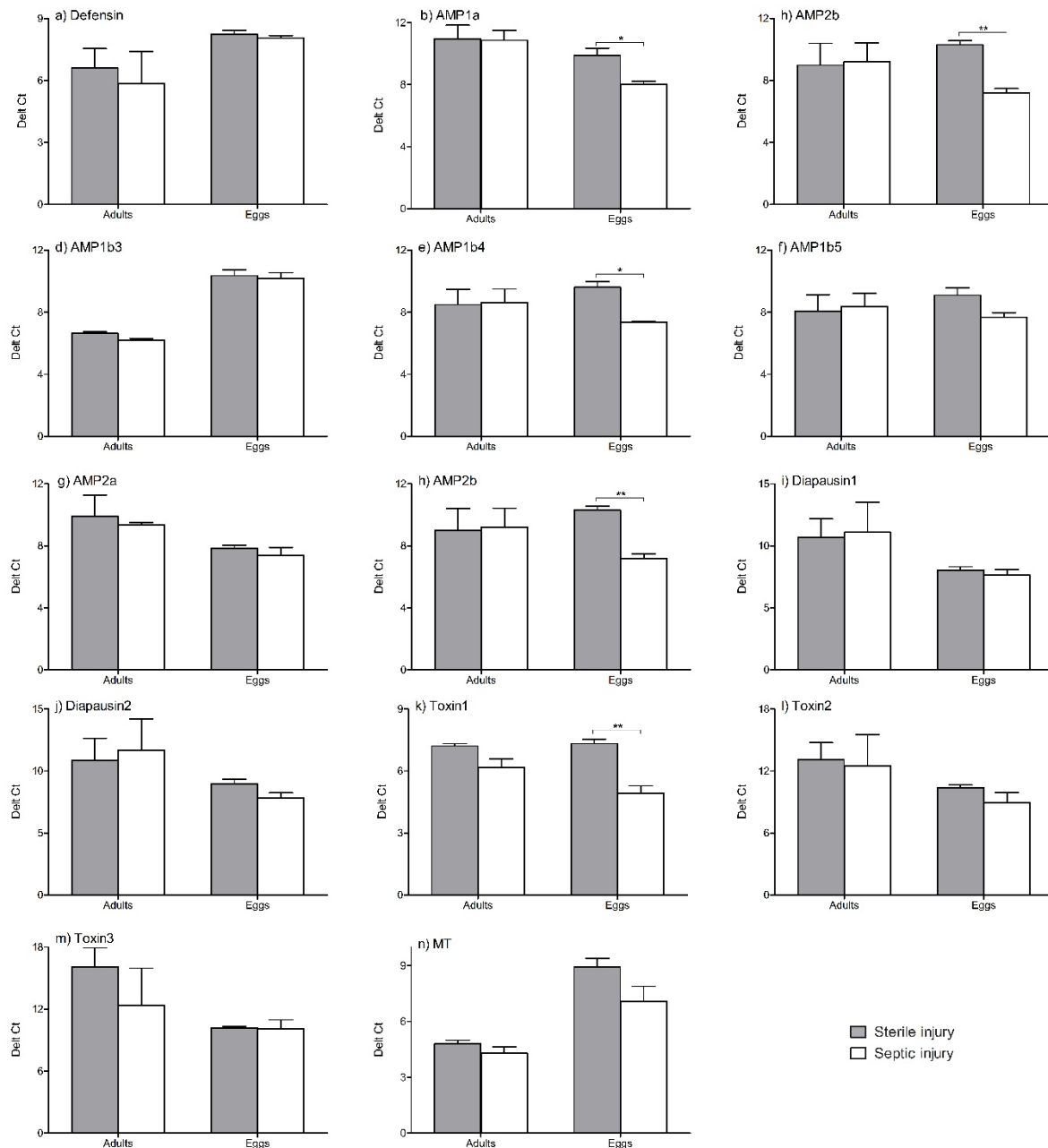
- Alvarez-Lee, A., Martínez-Díaz, S. F., Gutiérrez-Rivera, J. N. and Lanz-Mendoza, H. (2020). Induction of innate immune response in whiteleg shrimp (*Litopenaeus vannamei*) embryos. *Developmental & Comparative Immunology* **105**, 103577.
- Anderson, D. (1973). Embryology and phylogeny in annelids and arthropods. *Oxford, UK: Pergamon Press*.

- de Boer, M. E., de Boer, T. E., Mariën, J., Timmermans, M. J., Nota, B., van Straalen, N. M., Ellers, J. and Roelofs, D.** (2009). Reference genes for QRT-PCR tested under various stress conditions in *Folsomia candida* and *Orchesella cincta* (Insecta, Collembola). *BMC Molecular Biology* **10**, 54.
- Dubuffet, A., Zanchi, C., Boutet, G., Moreau, J., Teixeira, M. and Moret, Y.** (2015). Trans-generational immune priming protects the eggs only against gram-positive bacteria in the mealworm beetle. *PLoS pathogens* **11**, e1005178.
- Faddeeva-Vakhrusheva, A., Derks, M. F., Anvar, S. Y., Agamennone, V., Suring, W., Smit, S., van Straalen, N. M. and Roelofs, D.** (2016). Gene family evolution reflects adaptation to soil environmental stressors in the genome of the collembolan *Orchesella cincta*. *Genome biology and evolution* **8**, 2106-2117.
- Gorman, M., Kankanala, P. and Kanost, M.** (2004). Bacterial challenge stimulates innate immune responses in extra-embryonic tissues of tobacco hornworm eggs. *Insect molecular biology* **13**, 19-24.
- Hinton, H.** (1981). Biology of insect eggs. *Oxford, New York: Pergamon Press* Vols **1**, 1125.
- Jacobs, C. G., Rezende, G. L., Lamers, G. E. and van der Zee, M.** (2013). The extraembryonic serosa protects the insect egg against desiccation. *Proceedings of the Royal Society B: Biological Sciences* **280**, 20131082.
- Jacobs, C. G., Spaink, H. P. and van der Zee, M.** (2014a). The extraembryonic serosa is a frontier epithelium providing the insect egg with a full-range innate immune response. *elife* **3**, e04111.
- Jacobs, C. G., van der Hulst, R., Chen, Y.-T., Williamson, R. P., Roth, S. and van der Zee, M.** (2022). Immune function of the serosa in hemimetabolous insect eggs. *Philosophical Transactions of the Royal Society B* **377**, 20210266.
- Jacobs, C. G. and van der Zee, M.** (2013). Immune competence in insect eggs depends on the extraembryonic serosa. *Developmental & Comparative Immunology* **41**, 263-269.
- Jacobs, C. G., Wang, Y., Vogel, H., Vilcinskis, A., van Der Zee, M. and Rozen, D. E.** (2014b). Egg survival is reduced by grave-soil microbes in the carrion beetle, *Nicrophorus vespilloides*. *BMC Evolutionary Biology* **14**, 1-8.
- Jura, C.** (1972). Development of Apterygote insects. In S. J. Counce & C. H. Waddington (Eds.), *Developmental systems: insects* (pp. 49-94). *London, UK: Academic Press Inc.*
- Livak, K. J. and Schmittgen, T. D.** (2001). Analysis of relative gene expression data using real-time quantitative PCR and the 2<sup>-</sup>ΔΔCT method. *methods* **25**, 402-408.
- Machida, R.** (2006). Evidence from embryology for reconstructing the relationships of hexapod basal clades. *Arthropod Syst Phylogeny* **64**, 95-104.
- Machida, R. and Ando, H.** (1998). Evolutionary changes in developmental potentials of the embryo proper and embryonic membranes along with the derivative structures in Atelocerata, with special reference to Hexapoda (Arthropoda). In *Proc. Arthropod Embryol. Soc. Jpn*, pp. 1-13.
- Marchini, D., Marri, L., Rosetto, M., Manetti, A. G. and Dallai, R.** (1997). Presence of Antibacterial Peptides on the Laid Egg Chorion of the Medfly *Ceratitis capitata*. *Biochemical and Biophysical Research Communications* **240**, 657-663.
- Moreau, J., Martinaud, G., Troussard, J. P., Zanchi, C. and Moret, Y.** (2012). Trans-generational immune priming is constrained by the maternal immune response in an insect. *Oikos* **121**, 1828-1832.
- Moret, Y. and Schmid-Hempel, P.** (2000). Survival for immunity: the price of immune system activation for bumblebee workers. *Science* **290**, 1166-1168.
- Mylonakis, E., Podsiadlowski, L., Muhammed, M. and Vilcinskis, A.** (2016). Diversity, evolution and medical applications of insect antimicrobial peptides. *Philosophical Transactions of the Royal Society B: Biological Sciences* **371**, 20150290.
- Panfilio, K. A.** (2008). Extraembryonic development in insects and the acrobatics of blastokinesis. *Developmental biology* **313**, 471-491.
- Rafiqi, A. M., Lemke, S., Ferguson, S., Stauber, M. and Schmidt-Ott, U.** (2008). Evolutionary origin of the amnioserosa in cyclorrhaphan flies correlates with spatial and temporal expression changes of zen. *Proceedings of the National Academy of Sciences* **105**, 234-239.



- Rezende, G. L., Martins, A. J., Gentile, C., Farnesi, L. C., Pelajo-Machado, M., Peixoto, A. A. and Valle, D.** (2008). Embryonic desiccation resistance in *Aedes aegypti*: presumptive role of the chitinized serosal cuticle. *BMC developmental biology* **8**, 1-14.
- Roelofs, D., Timmermans, M. J., Hensbergen, P., van Leeuwen, H., Koopman, J., Faddeeva, A., Suring, W., de Boer, T. E., Mariën, J. and Boer, R.** (2013). A functional isopenicillin N synthase in an animal genome. *Molecular biology and evolution* **30**, 541-548.
- Roth, S.** (2004). Gastrulation in other insects. *Gastrulation: from cells to embryos* **105**, 121.
- Sastry, A., Vernberg, F. and Vernberg, W.** (1983). Ecological aspects of reproduction. *The biology of Crustacea* **8**, 179-270.
- Schmidt-Ott, U.** (2000). The amnioserosa is an apomorphic character of cyclorrhaphan flies. *Development genes and evolution* **210**, 373-376.
- Suring, W., Meusemann, K., Blanke, A., Mariën, J., Schol, T., Agamennone, V., Faddeeva-Vakhrusheva, A., Berg, M. P., consortium, K. B. H. and Brouwer, A.** (2017). Evolutionary ecology of beta-lactam gene clusters in animals. *Molecular ecology* **26**, 3217-3229.
- Tan, K. L., Vlisidou, I. and Wood, W.** (2014). Ecdysone mediates the development of immunity in the *Drosophila* embryo. *Current Biology* **24**, 1145-1152.
- Tetreau, G., Dhinaut, J., Galinier, R., Audant-Lacour, P., Voisin, S. N., Arafah, K., Chogne, M., Hilliou, F., Bordes, A. and Sabarly, C.** (2020). Deciphering the molecular mechanisms of mother-to-egg immune protection in the mealworm beetle *Tenebrio molitor*. *PLoS pathogens* **16**, e1008935.
- Timmermans, M. J., Ellers, J., Roelofs, D. and van Straalen, N. M.** (2005). Metallothionein mRNA expression and cadmium tolerance in metal-stressed and reference populations of the springtail *Orchesella cincta*. *Ecotoxicology* **14**, 727-739.
- Vargas, H. C., Panfilio, K. A., Roelofs, D. and Rezende, G. L.** (2021). Increase in egg resistance to desiccation in springtails correlates with blastodermal cuticle formation: Eco-evolutionary implications for insect terrestrialization. *Journal of Experimental Zoology Part B: Molecular and Developmental Evolution* **336**, 606-619.
- Vargas, H. C. M., Farnesi, L. C., Martins, A. J., Valle, D. and Rezende, G. L.** (2014). Serosal cuticle formation and distinct degrees of desiccation resistance in embryos of the mosquito vectors *Aedes aegypti*, *Anopheles aquasalis* and *Culex quinquefasciatus*. *Journal of insect physiology* **62**, 54-60.
- Veltri, D., Kamath, U. and Shehu, A.** (2018). Deep learning improves antimicrobial peptide recognition. *Bioinformatics* **34**, 2740-2747.
- Zeh, D. W., Zeh, J. A. and Smith, R. L.** (1989). Ovipositors, amnions and eggshell architecture in the diversification of terrestrial arthropods. *The Quarterly Review of Biology* **64**, 147-168.

## Supplementary information



Supplementary Figure 2-1. Statistical significance of delta Ct between septic injury and sterile injury in adults and eggs upon injections (\* represented  $P < 0.05$ , \*\* represented  $P < 0.01$ , \*\*\* represented  $P < 0.001$ ). Please notice that y-axis stands for delta Ct: a low delta Ct in septic injury means upregulation of the gene upon bacterial challenge. Each vertical bar represented the mean  $\pm$  S.E (n = 3). MT: Metallothionein.



# Chapter 3

## Correlated responses to selection for embryonic developmental time in *Tribolium castaneum*

Shixiong Cheng, Chris G.C. Jacobs, Kevin M. Bretscher, Femke Verweij, Sven Ungerer, Maurijn van der Zee

### Abstract

Life-history trade-offs have played a central role in theory and interpretation of life history studies. However, understanding fitness trade-offs remains a difficult task in evolutionary biology. Here, we test if developmental time trades off with (1) pupal weight, (2) fecundity and (3) immune response in the flour beetle *Tribolium castaneum*. To this end, we artificially selected *Tribolium* eggs for fast or slow embryonic development during 21 and 17 generations, respectively. This resulted in embryonic developmental times of 125 h in the fast lines, 136 h in the non-selected lines, and 155 h in the slow line. As correlated response, larval developmental time also differentiated significantly among the selection treatments. In these selection lines, we find that (1) pupae of the slow lines are significantly heavier than pupae of the other lines. We also find that (2) 50 mothers of the fast lines lay on average 123 eggs in 4 hours, whereas 50 mothers from the non-selected lines and slow lines lay significantly more eggs, i.e. 155 and 160 respectively. Finally, using qPCR, we find significant upregulation of antimicrobial peptides (AMPs) and prophenoloxidase upon bacterial infection in all eggs, but (3) upregulation of these immune genes did not differ consistently among the selection lines. In conclusion, we found that developmental time significantly trades off with pupal weight and fecundity in *Tribolium*, but found no evidence for a trade-off with immune defense.

### Introduction

The life history of an organism refers to the pattern of events that occur from birth to death related to survival and reproduction, along with the timing and occurrence of each of these events (Fox and Messina, 2013). Life-history traits (or fitness components) include egg production per brood, age-specific distribution of growth rates, size of young, the interaction of reproductive effort with adult mortality, the age distribution of reproductive effort, patterns of dormancy and dispersal, and so on (Stearns, 1976). Life-history traits are often correlated within a species. For instance, as a result of climate change, pied flycatchers optimize over a suite of different life-history traits including their laying date, clutch size and the onset of incubation. With the advance of the peak of caterpillars that act as their nestling food, the birds advanced their laying date, shortened their incubation time, and increased the clutch size to maximize their lifetime fitness (Both and Visser, 2005).

When one trait changes upon selection, correlated responses in other traits are widely observed in laboratory experiments and breeding programs as a consequence of selection (Rauw et al., 1998). For

example, a line of flies propagated by breeding old adults had longer development time from egg to adult, than fly lines in which only young flies were allowed to propagate (Partridge and Fowler, 1992). These changes in other traits than the trait under selection are called correlated responses. This change is necessarily dependent on a genetic covariance or correlation (Gromko, 1995).

Owing to finite resources in organisms, life-history traits are often negatively related to each other, resulting in trade-offs. Life-history trade-offs are associated with the strategies that organisms use for maximizing the sum of the costs and benefits (Roff, 2000). Competing requirements of growth, maintenance and reproduction prevent sole allocation of limited resources to a single trait, such as immune defense (Figure 1-8). No matter if the risk of infection is high or low, immune defense trades off with other life-history traits (Adamo et al., 2001; Schmid-Hempel, 2005). Trade-offs between immune function and growth have been demonstrated in birds and plants (Brommer, 2004; Lozano-Durán et al., 2013).

Insects are the most diverse and successful organisms and they inhabit almost all habitats and ecosystems (Grimaldi and Engel, 2005). The insect immune defense is an important component of fitness. In response to microbial infections, insects have evolved a strong and effective innate immune system consisting of interconnected cellular and humoral responses (Vilmos and Kurucz, 1998). The cellular immune response is carried out by many types of blood cells (hemocytes) which can phagocytose and kill pathogens. The humoral immune response of insects is based on the synthesis of various antimicrobial peptides (AMPs) activated by immune signaling pathways, i.e., Toll, IMD and JAK/STAT. These AMPs are released into hemolymph to eliminate pathogens. To date, 311 AMPs have been characterized in insects, such as defensins, cecropins, attacins and moricins (Manniello et al., 2021; Tsakas and Marmaras, 2010). Despite these responses, exposure to microbial pathogens still pose serious threats to developing insects, in particular during embryonic development.

In recent years, it has clearly been demonstrated that insect eggs are able to mount immune responses to protect the embryo (Cole et al., 2020; Gorman et al., 2004; Jacobs et al., 2014a; Jacobs et al., 2022). In addition, insects such as *Tenebrio molitor* (Moret, 2006) and *Tribolium castaneum* (Roth et al., 2009) can transfer specific immune protection to the offspring. Salmela et al. reported that the transfer of immunity is mediated via the egg-yolk protein vitellogenin (Salmela et al., 2015). Furthermore, other features of the insect egg, such as the complex chorion and the cuticle, can protect the embryo from adverse conditions, such as desiccation and drowning (Zeh et al., 1989). Developing insect embryos are well protected from pathogens and adverse environmental conditions.

As the most diverse organisms on Earth, insects can provide excellent models for addressing trade-offs between immune competence and other life-history traits. Trade-offs among immune reactions and other traits, such as growth and reproduction, have been observed in a diverse range of insect species, for instance the tobacco hornworm *Manduca sexta* (Diamond and Kingsolver, 2011; Mira and Bernays, 2002; Schwenke et al., 2016). In the host laboratory, it has been shown that eggs of the burying beetle *Nicrophorus vespilloides* lack an inducible innate immune response. At the same time, *N. vespilloides* eggs are extremely sensitive to desiccation (Jacobs et al., 2014b). Strikingly, its eggs develop extremely quickly and hatch in two days at 25°C. The model insect *D. melanogaster* eggs hatch within 24 hours at 25°C and develop extremely quickly as well. Its eggs have lost desiccation resistance and immune function too (Al-Saffar et al., 1995; Jacobs and van der Zee, 2013). Thus, it seems that egg immune competence trades off with embryonic developmental speed in insects.

In *T. castaneum*, Zou et al. reported 12 antimicrobial peptides (AMPs) involved in microbe immobilization or killing of which attacin2, cecropin3, coleopteracin1, defensin1, and defensin2 showed the most dramatic increase in transcript levels to participate in immune responses (Zou et al., 2007). As previously shown in the eggs of *T. castaneum*, all AMPs showed strong upregulation upon bacterial infection, such as attacin1, attacin2, cecropin3, coleopteracin1, defensin1 and defensin2 (Jacobs and van der Zee, 2013). Therefore, in this study, the induction profiles of mRNAs of *attacin1*, *attacin2*, *cecropin3*, *coleopteracin1* and *defensin2* will be compared in the selection lines of *Tribolium* eggs. We will also quantify the expression of *laccase2*, a prophenoloxidase involved in the melanisation reaction observed during insect immune defenses (González-Santoyo and Córdoba-Aguilar, 2012).

In this study, replicate outbred populations of *T. castaneum* had been selected for fast or slow embryonic development for over 21 or 17 generations, respectively. Correlated responses, namely correlated post-embryonic development time, were studied in these selected populations. Furthermore, we used these selection lines to explore trade-offs with the fitness components fecundity and pupal weight. We also used this emerging insect model *T. castaneum* to study a possible trade-off between immune defense and the duration of embryonic development. We quantified the expression of immune-related genes in the eggs of the selected populations upon simultaneous infection with gram-positive and gram-negative bacteria.

## Materials and methods

### Artificial selection for embryonic developmental time in *Tribolium* populations

An outbred population was created by individually crossing 250 beetles which came from a bakery in The Netherlands (collected by the Dutch pest control company Rentokil) with 250 beetles from the inbred *San Bernardino* laboratory strain. This outbred population could mix and reproduce for another seven generations. From this starting population, 2h egg lays were collected. Two of these egg lays were left unselected (Non-selectedA, Na; non-selectedB, Nb). From another egg lay, we continued to select the fastest developing half for the fast line (fastA, Fa), and the slowest developing half for the slow line (slowA, Sa), and, repeated this in a biological replicate (fastB, Fb; slowB, Sb) to check for consistent differences. The selection for embryonic developmental time was carried out in a semi-automated set-up, see Figure 3-1. A brief process diagram of the artificial selection experiment is shown in Figure 3-2. All populations were kept bigger than 500 individuals in every generation. Beetle cultures were kept as in (van der Zee et al., 2005), except for the temperature which was 25 °C.

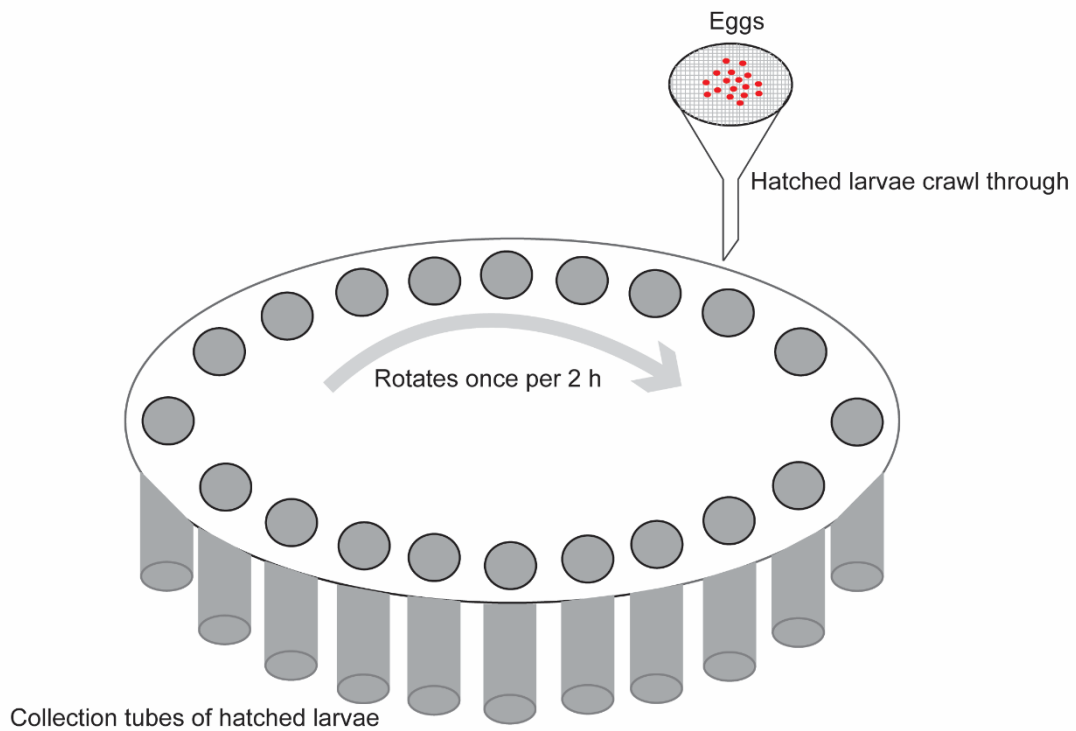


Figure 3-1. The fast or slow embryonic developmental time of *T. castaneum* were artificially selected on the rotary selection machine. The selection machine turns once per two hours in a clockwise pattern. *T. castaneum* eggs were maintained at 25°C until hatching. Once one egg hatched, it will crawl through into the below collection tube.

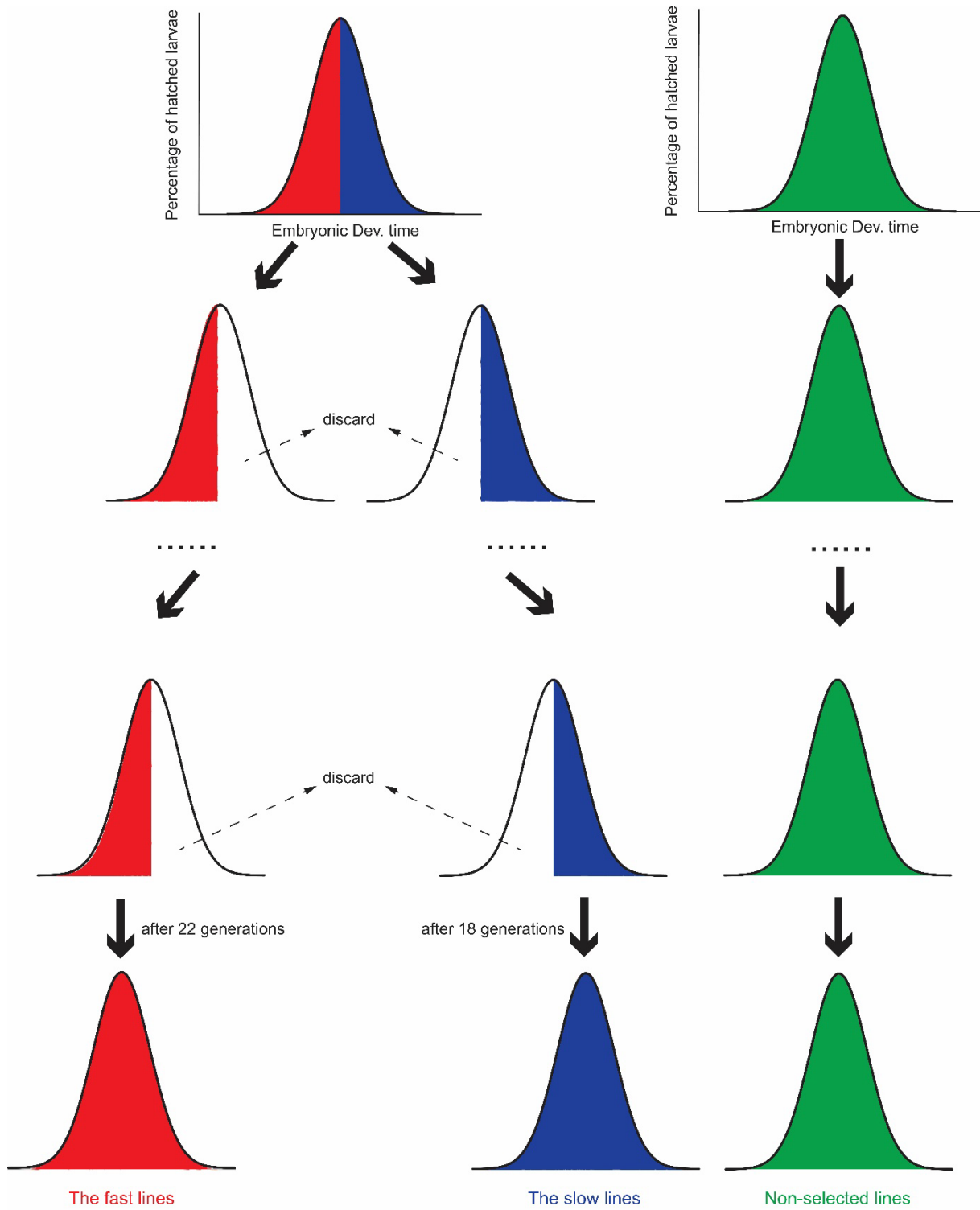


Figure 3-2. A brief process diagram of the artificial selection experiment in order to obtain our selection lines including the fast (red), non-selected (green) and slow lines (blue).

### Weight

The pupae of the selection lines were weighed using a high-precision analytical balance directly after moulting from the prepupal stage (XS 105, Mettler Toledo, Germany).



## **Fecundity assays**

To monitor fecundity among selection populations, we mixed 50 male and 50 female pupae of *T. castaneum*. After five days when they became fertile adults, we started to calculate the number of eggs laid within 4 h. Six biological replication were performed for selection lines including Fa, Fb, Na, Nb, Sa and Sb, respectively. Furthermore, we also summarize their eclosion rate when these eggs eclosed to adults.

## **Infection**

Infection experiments were carried out as described in (Jacobs and van der Zee, 2013). All infections were performed with a tungsten needle with a 1 micron tip (Fine Science Tools). *Tribolium* eggs (24 h old) of the fast, the non-selected and the slow lines were pricked with a tungsten needle dipped in a concentrated mixed suspension of *Micrococcus luteus* and *Escherichia coli*, as standardized in our laboratory (Jacobs et al., 2013; Jacobs and van der Zee, 2013). A sterile injection served as the control. In total of 300 eggs were injected in each treatment. Six hours later, eggs were used for RNA isolation.

## **RNA extraction and RT-qPCR**

The total RNA of 300 eggs was extracted using trizol extraction (Invitrogen) after which the RNA was purified using the RNeasy kit (Qiagen). The quality of isolated RNA was measured spectrophotometrically and on a 1.0% agarose gel. One microgram of total RNA was used for cDNA synthesis. First strand cDNA was made using the Promega Reverse Transcription system (Protocol, 2000), and 2  $\mu$ L of 1:10 diluted original cDNA was used in every RT-qPCR reaction. RT-qPCR reactions were done using the SsoAdvanced Universal SYBR Green Supermix (Bio-rad, Hercules, CA, USA) on a CFX96 thermocycler (Bio-rad, Hercules, CA, USA). The RT-qPCR parameters were as follows: an initial step at 95 °C for 30s; 40 cycles of 95 °C for 15 s, 60 °C for 30 s, 72 °C for 30 s. This was followed by dissociation analysis of a ramp from 65 °C to 95 °C with a read every 0.5 °C. The RPL13a gene was used as internal control to calculate  $\Delta C_T$  values (Lord et al., 2010). Fold upregulation was then calculated using the  $2^{-\Delta\Delta C_T}$  method (Livak and Schmittgen, 2001). Total RNA was isolated three times (biological replication) and each sample was measured by RT-qPCR twice (technical replication). The immune-related genes of *T. castaneum* studied here were: attacin1, attacin2, cecropin3, coleoptericin1, defensin2 and laccase 2. The primers were listed in Supplementary Table 3-1.

## **Statistical analysis**

All data were analyzed through one-way analysis of variance (ANOVA) by SPSS software (version 27). Statistical significance was set based on Duncan's multiple range test at the 5% probability level.

## **Results**

### **Developmental time of eggs of the fast lines is one day shorter than that of slow lines**

During artificial selection process, a selective pressure was created for embryonic development time by using fastest or slowest 50% of the hatchlings for fast and slow lines, respectively, while two

populations were left unselected. This selection during 21 generations in the fast lines, and 17 generations in the slow lines (Figure 3-3), resulted in embryonic developmental time of on average 125 hours for the two fast lines, 137 and 136 hours for the two non-selected lines (Na and Nb, respectively), and more than 154 hours for the two slow lines (Figure 3-4).

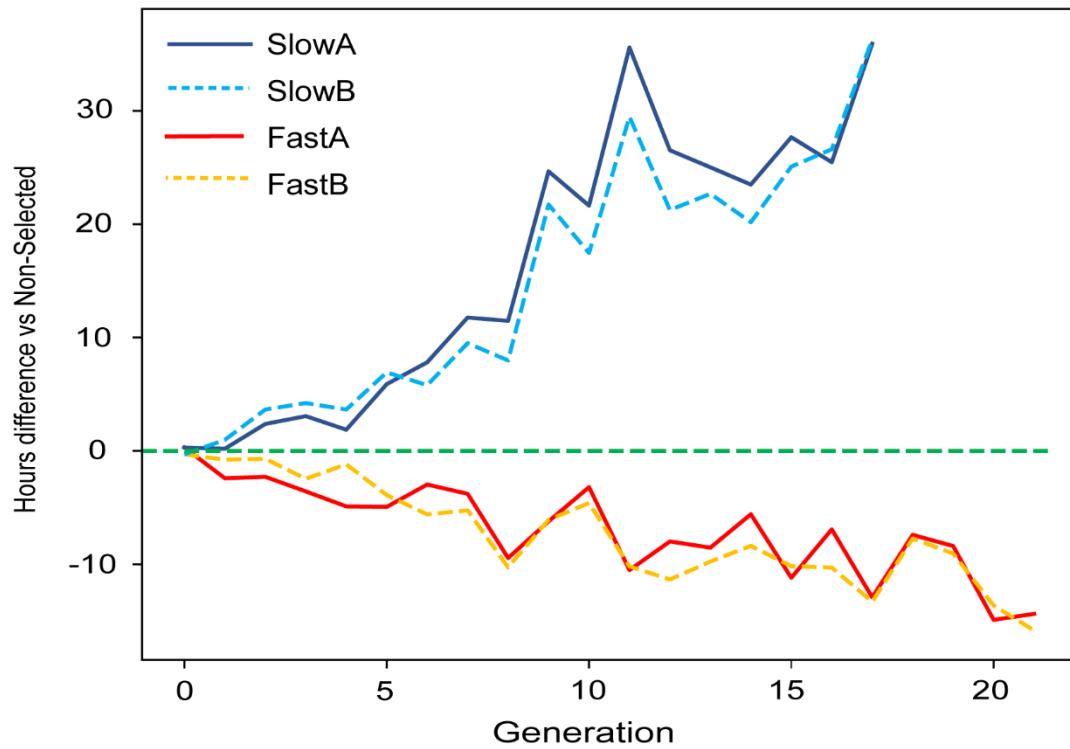


Figure 3-3. Time difference of fast and slow lines in every generation, compared to the non-selected lines. Red, orange, dark blue, and light blue lines stand for time difference of Fa, Fb, Sa and Sb respectively, compared to the non-selected lines (green).

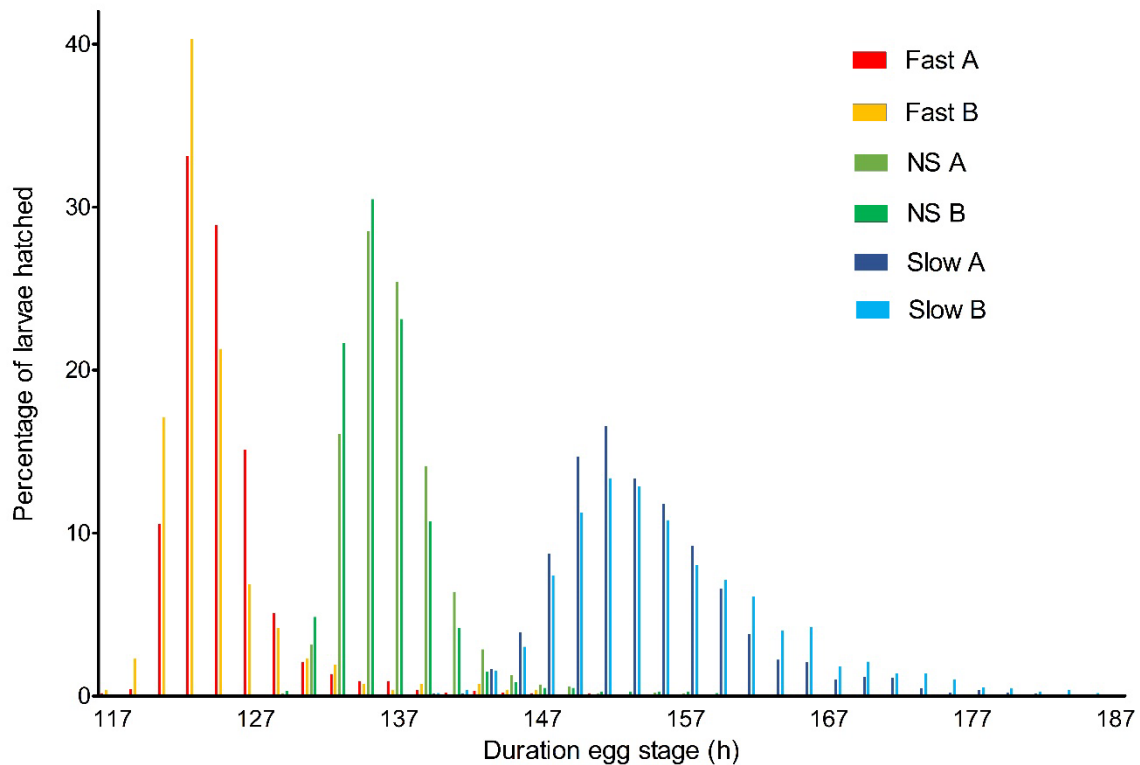


Figure 3-4. Hatching time of eggs of the selection lines. Fast, non-selected and slow lines showed the highest hatching rate at 123, 135 and 151 h post egg laying, respectively. Red, orange, green, light green, dark blue, and light blue lines stand for percentage of hatched larvae of Fa, Fb, Na, Nb, Sa, and Sb, respectively.

### Correlated responses to selection in post-embryonic developmental time

To check for correlated differences in post-embryonic development, we further measured larval and pupal developmental time in the selection lines at 25 °C. We found that newly hatched larvae of the Na and Nb lines spend on average 63.5 and 63.1 days during post-embryonic development before reaching the imago stage, while the Fa and Fb lines spend 49.88 and 50.73 days, and the Sa and Sb lines spend 68 and 64.6 days, respectively (Table 3-1). In conclusion, larval developmental time of fast lines is significantly shorter than non-selected and slow lines (Figure 3-5A). Although there is a trend towards shorter pupal time in the fast lines, there is no significance of pupal developmental time among the selection lines (Figure 3-5B). At the same time, growth rate (mg/day) did not differentiate between the fast and slow lines (Supplementary Figure 3-1).

Table 3-1. Post-embryonic development time from newly hatched larvae to emergence of imago. Significance of post-embryonic development time among six selection lines was confirmed by one-way analysis of variance (ANOVA). Different superscript letters display significant difference ( $P < 0.05$ ).

Selection lines	Days from newly hatched larvae to emergence of imago	
	Mean $\pm$ SD	N
Fa	49.88 $\pm$ 4.77 <sup>a</sup>	33
Fb	50.73 $\pm$ 4.03 <sup>a</sup>	33
Na	63.53 $\pm$ 6.58 <sup>b</sup>	36
Nb	63.13 $\pm$ 5.35 <sup>b</sup>	40
Sa	68.03 $\pm$ 5.69 <sup>c</sup>	33
Sb	64.61 $\pm$ 5.42 <sup>b</sup>	36

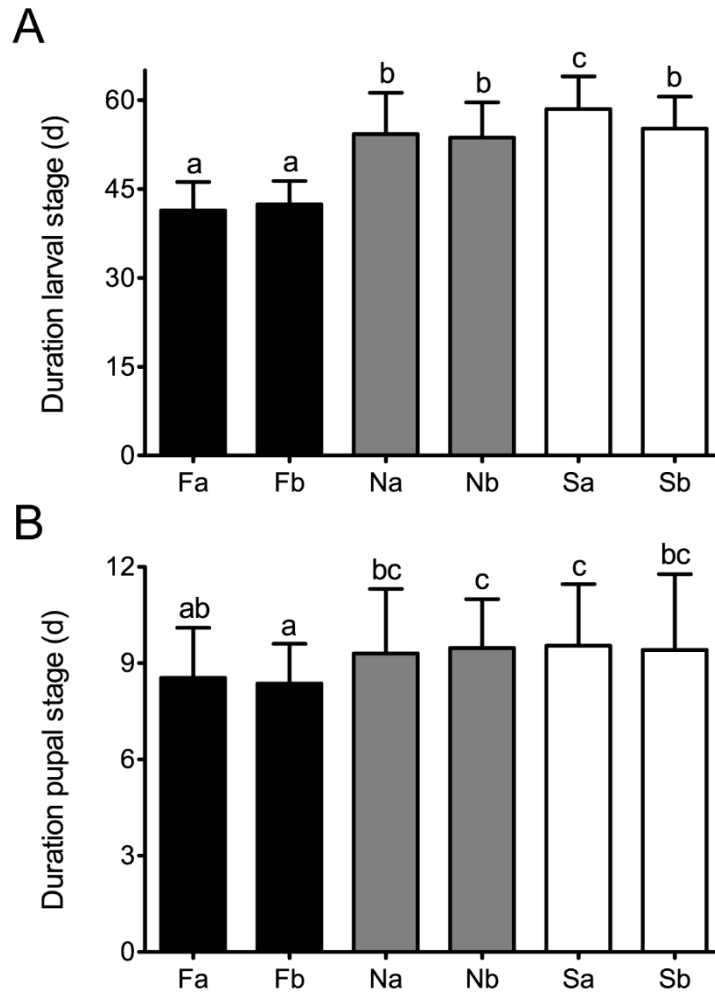


Figure 3-5. The duration of larval (A) and pupal (B) stages of the selection lines. Each vertical bar indicates Mean  $\pm$  SD (n = 33 of Fa, 33 of Fb, 36 of Na, 40 of Nb, 33 of Sa, and 36 of Sb, respectively). Different letters above the vertical bar display significant difference ( $P < 0.05$ ).

## Trade-offs

### *Heavier individuals of the slow lines*

The pupae of the slow lines were significantly heavier than the non-selected and fast lines, as shown in Figure 3-6A. The same is true for adult weight. The adults of the slow lines were significantly heavier than the non-selected and fast lines (Figure 3-6B). At the same time, the adults of the slow B line were

significantly heavier than the slow A line (Figure 3-6B). We found no significant difference in weight between female and male individuals considering all six selection lines together, as confirmed by a Welch two-samples t-test (Supplementary Table 3-2 and Supplementary Table 3-3). Within each selection line, females were significantly heavier than males only in the Sb line for both pupal and adult weight (Supplementary Table 3-2 and Supplementary Table 3-3).

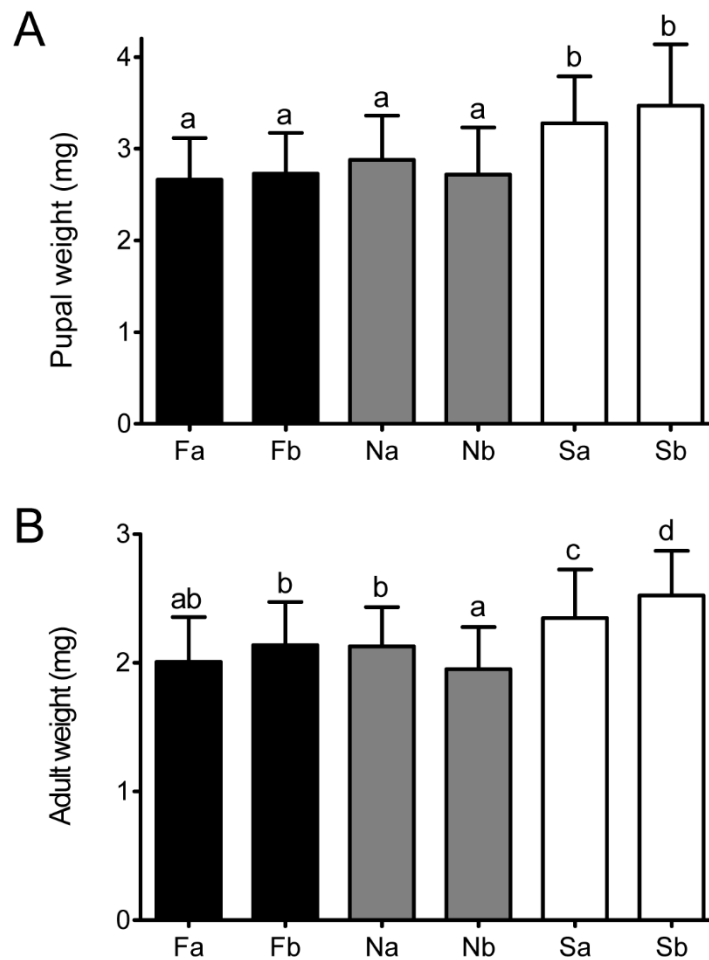


Figure 3-6. A, Weight of pupae directly after moulting from the prepupae stage. Each vertical bar indicates Mean  $\pm$  SD (n = 46 of Fa, 40 of Fb, 36 of Na, 41 of Nb, 38 of Sa, and 43 of Sb, respectively). B, Weight of adults of the selection lines. Each vertical bar indicates Mean  $\pm$  SD (n = 33 of Fa, 33 of Fb, 36 of Na, 40 of Nb, 33 of Sa, and 38 of Sb, respectively). Key: different letters above the vertical bar display significant difference ( $P < 0.05$ ).

### ***Low early fecundity of the fast lines***

To compare the egg production capacity, we counted the egg number from 50 mothers of the fast (Fa and Fb), the non-selected (Na and Nb) and the slow lines (Sa and Sb) laid within 4 h. The results showed that the fast line beetles laid significantly fewer eggs than the non-selected and the slow lines (Figure 3.7A). To be precise, Fa, Fb, Na, Nb, Sa and Sb-*T. castaneum* laid on average 124, 123, 156, 155, 153 and 166 eggs from 50 adult females within 4 hour, respectively (Figure 3-7A). Interestingly, the egg number of the Sb line beetles is significantly larger than that of the others. We did not find significant differences in final successful eclosion rate of the offspring that is counted from egg to adult among the selection lines, which was showed in Figure 3-7B.

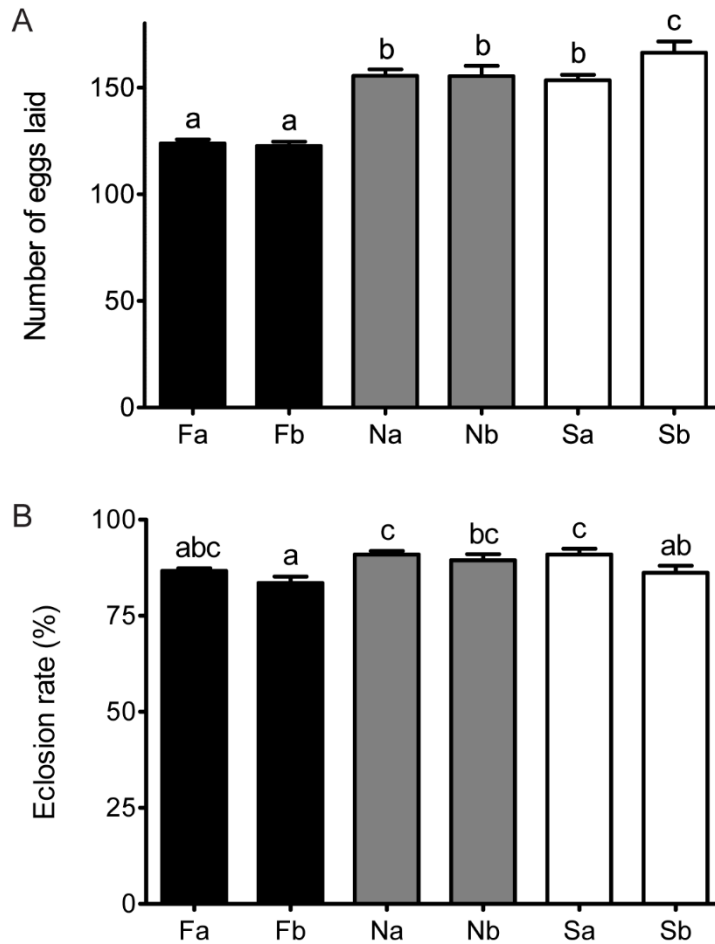


Figure 3-7. A, Fecundity of 50 *T. castaneum* females laid within 4 h among the selection lines. B, Eclosion rate (from eggs to adults) of *T. castaneum* among the selection lines. Each vertical bar indicates Mean  $\pm$  SE (n = 6). Different letters above the vertical bars display significant difference ( $P < 0.05$ ).

### Induction of immune genes in eggs of the selection lines

Finally, we measured changes in the expression of several antimicrobial peptides (AMPs) and *laccase2* at 6 h post bacterial challenge in septically injured eggs compared to sterilely injured eggs. In all selection lines, the six genes showed strong upregulation upon bacterial infection (Figure 3-8). However, no consistent differences were found between the fast and slow lines. The details of the induction of immune genes were as follows:

#### a) Attacins

Induction profiles of mRNAs of *attacin1* and *attacin2* are shown in Figure 3-8. There are no significant differences in the up-regulation of *attacin1* in the selection lines, except that upregulation is significantly higher in Sb than in Fa, Na and Sa (Figure 3-8A). Upregulation of *attacin2* was significantly higher in the Fb and Sb lines, compared with the Fa, Na and Sa lines (Figure 3-8B).

#### b) Cecropins

Upon bacterial infection, we examined gene expression of *cecropin3* in *Tribolium* eggs of the selection lines. The expression change of *cecropin3* is significantly higher in the Fb line than in the Fa line, but no consistent difference between the fast and slow lines was found (Figure 3-8C).

c) Coleoptericin

In all tested genes, *coleoptericin1* showed the strongest upregulation among the selection lines in response to bacterial challenge. At the same time, upregulation of *coleoptericin1* was significantly higher in the Sb line compared to all other lines, except the Fb line. Furthermore, a significantly higher upregulation of *coleoptericin1* was found in the Fb line compared with the Fa, Na, and Sa lines, but no consistent difference between the fast and slow lines was found (Figure 3-8D).

d) Defensins

Upon bacterial infection, upregulation of *defensin2* was significantly higher in the Fb and Sb lines compared to the other selection lines, but no consistent difference between the fast and slow lines was found (Figure 3-8E).

e) Laccase

*Laccase2* showed the relatively weak upregulation in response to bacterial infection compared with these AMPs. Significance in the expression changes of *laccase2* is similar to that of *cecropin3*. Upregulation in Fb is significantly higher than in Fa, but no consistent differences were found between the fast and slow lines (Figure 3-8F).

Thus, our expression data do not indicate a clear trade-off between developmental speed and immune competence.

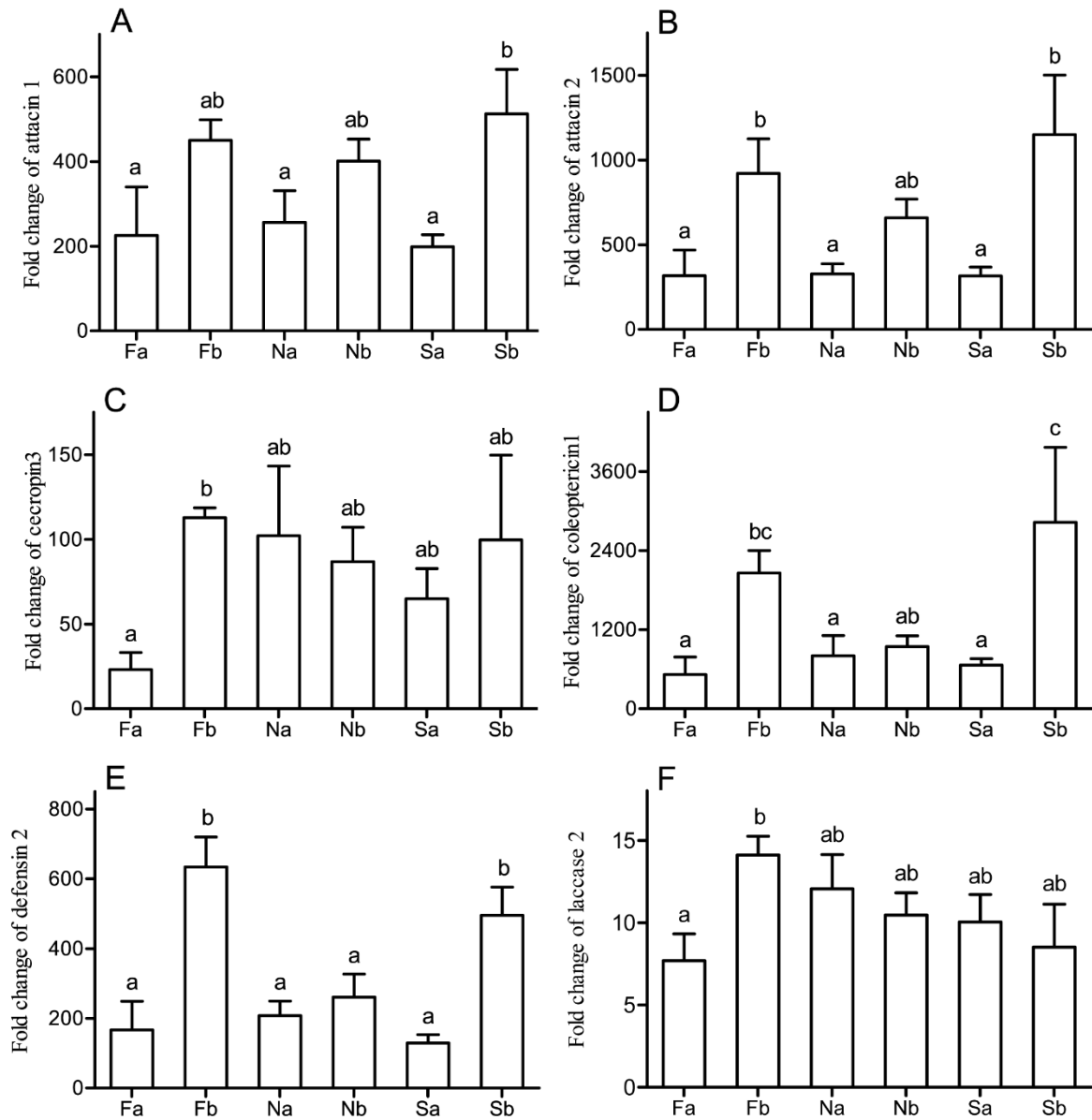


Figure 3-8. Upregulation of immune genes in the eggs of *T. castaneum* upon septic injury compared to sterile injury among the selection lines. Each vertical bar indicates mean fold change  $\pm$  SE ( $n = 3$ ). Different letters above the vertical bars display significant difference ( $P < 0.05$ ).

## Discussion

Artificial selection on developmental time has been carried out on *Tribolium castaneum* before (Englert and Bell, 1970; Garcia and Toro, 1990; Irwin and Carter, 2013; Roth and Kurtz, 2008; Soliman, 1982). For instance, three replicate populations of *T. castaneum* were selected for six generations, resulting in different lines with early or late pupation time (Englert and Bell, 1970). However, all these studies have been limited to larval and pupal stages. We report, for the first time, a successful response on selection for embryonic developmental time in *T. castaneum*. It is likely that such a response in life history is genetically correlated to other traits (Hill and Caballero, 1992). For instance, selection on early reproduction in *Drosophila* leads to fast larval development, whereas late



reproducing females develop slower (Zwaan et al., 1995a). We for the first time show correlated responses in larval and pupal developmental time to selection for embryonic developmental time in insects.

Trade-offs are a special category of correlated responses, as they defined as negatively correlated fitness components, for instance in size at birth, growth rate, age and size at maturity, fecundity and fertility, age- or size-specific rates of survival, and life span (Flatt, 2020). Stearns reported that there are at least 45 possible trade-offs focusing on 10 major life history traits (Stearns, 1992). Negative correlations between life-history traits are often caused by limited resources resulting in physiological trade-offs: the increment of resources allocated to one trait necessitates a decrement of resources to another trait (the traditional "Y" model of resource allocation) (Van Noordwijk and de Jong, 1986). In the red flour beetle *T. castaneum*, existence of a trade-off between life-history traits has been demonstrated before, for instance between predation avoidance and mating success in males. (Matsumura and Miyatake, 2015). Beetles of the established *Tribolium* strain with longer walking distances (L-strain) suffered higher predation risk than the strain with shorter walking distances (S-strain). At the same time, compared to S-strain males, L-strain males showed significantly increased mating success (Matsumura and Miyatake, 2015).

Artificial selection on life-history traits is regarded as one of the best empirical ways to understand the occurrence and consequences of their trade-offs (Brakefield, 2003; Hill and Caballero, 1992). Classical life-history theory predicts that developmental time trades off with weight (Flatt and Heyland, 2011; Stearns, 1992). In the model organism *D. melanogaster*, artificial selection on developmental time lead to lower adult weights in lines with fast larval development lines, and higher weights in the slow lines (Nunney, 1996; Zwaan et al., 1995a). White also found that *Drosophila* pupae of two slow developing laboratory strains (from oviposition to adult) were significantly heavier than seven field populations (White, 1984). We confirm the existence of a trade-off between developmental time and weight. Pupae and adults of the slow lines are significantly heavier than pupae and adults of the non-selected and slow lines. Given that the rate of weight increase is not different between the fast and slow lines (Supplementary Figure 3-1), the higher weight of the pupae of the slow lines is likely to be the simple consequence of the larvae having more time to accumulate biomass in the slow lines.

Trade-offs with fecundity are particularly prominent (Stearns, 1989). For instance, longevity trades off with fecundity in *Drosophila* (Djawdan et al., 2004; Leroi et al., 1994; Zwaan et al., 1995b). Long-lived flies, for example, start to lay only 0.24 eggs per female per 24 h and decrease quickly to 0 eggs after 7 days, whereas control females start to lay 1.8 eggs per 24h and slowly decrease to 0.32 after 20 day (Djawdan et al., 2004). Furthermore, it has been established that developmental speed trades off with fecundity. Adult females of fast developing lines show a 35% drop in fecundity after 15 generations of selection, compared to non-selected lines (Nunney, 1996). We confirm such trade-off between fast development and fecundity. Our fast developing lines lay 21% fewer eggs than the non-selected lines.

Surprisingly, we did not find evidence for a trade-off between developmental time and immune defense. Trade-offs between immune function and growth have been demonstrated in birds and plants (Brommer, 2004; Lozano-Durán et al., 2013). It could be that such trade-off between developmental time and immune defense does not exist in *Tribolium*. However, our qPCR approach on six immune genes is somewhat limited. It is also possible that some other immune genes or components associated

with the trade-off, such as the cellular response. Unexpectedly, relatively strong upregulation of all these tested genes occurred in the Fb line upon infection. This might be because the eggs of the Fb line put more resources into immune defense. Thus, the Fb beetles probably invest less resources on other life-history traits, for example, the longevity. This calls for in-depth investigation of fitness trade-offs in our selection lines, such as aging and longevity (Finch and Ruvkun, 2001; Flatt and Heyland, 2011).

It would be interesting to see if indications for a trade-off between immunity and developmental time in insect eggs can be found among insect species with different developmental time, instead of within species. The immune response in two relatively closely related insects with very different developmental times can be compared, for instance the moth midge *Clogmia albipunctata* that develops in 71 hours at 25°C (Jiménez-Guri et al., 2014), and the scuttle fly *Megaselia abdita* that develops in 27 hours at 25°C (Wotton et al., 2014). If a trade-off is present, we predict to find limited immune competence in the quickly developing *Megaselia* eggs. Furthermore, we can also compare immune competence in eggs of the mosquito pair *Culex pipiens* and *Aedes aegypti*, as *C. pipiens* develops within 46 hours at 25°C (Madder et al., 1983), while *A. aegypti* develops in 77 hours at 25°C (Vargas et al., 2014). Along the same line, a much weaker immune response in eggs of *Culex* than in *Aedes* would be indicative of a trade-off between immunity and developmental time.

Overall, we have artificially selected replicate outbred populations of *Tribolium* for fast and slow embryonic development, alongside a control. This resulted in a spectacular response, and lead to correlated responses in larval and pupal developmental time. We did not find evidence that developmental time trades off with immune defense. However, we did demonstrate that developmental time trades off with pupal and adult weight, and with fecundity. It would be interesting to know what the mechanistic and genetic mediators of these trade-offs would be. Likely, hormones such as juvenile hormone (JH), 20-hydroxyecdysone (20E), and insulin/insulin-like growth factor-like signaling (IIS) play a role as key switches for regulating life-history trade-offs (Flatt et al., 2005; Ketterson and Nolan, 1999; Stearns, 1989). These hormones regulate growth in *Drosophila melanogaster* (Nijhout et al., 2014). They could mediate the trade-off with fecundity as JH and insulin directly influence oogenesis (Abu-Hakima and Davey, 1975; LaFever and Drummond-Barbosa, 2005; Parthasarathy and Palli, 2011). In addition, such hormones could regulate potential trade-offs with immunity too, as 20E is a known potentiator of the immune response and required for embryonic immunity (Schwenke et al., 2016; Tan et al., 2014). Thus, we may expect alleles in genes involved in these pleiotropic hormone signalling pathways to underlie the observed trade-offs in our study. Our selection lines offer a great opportunity to start unravelling the genetic underpinnings of life-history trade-offs.

## References

- Abu-Hakima, R. and Davey, K.** (1975). Two actions of juvenile hormone on the follicle cells of *Rhodnius prolixus* Stål. *Canadian journal of zoology* **53**, 1187-1188.
- Adamo, S. A., Jensen, M. and Younger, M.** (2001). Changes in lifetime immunocompetence in male and female *Gryllus texensis* (formerly *G. integer*): trade-offs between immunity and reproduction. *Animal Behaviour* **62**, 417-425.
- Al-Saffar, Z., Grainger, J. and Aldrich, J.** (1995). The development rates of the egg and pupal stages of *Drosophila melanogaster* (Meigen) under changing conditions of temperature and humidity. *Journal of thermal biology* **20**, 399-404.

- Both, C. and Visser, M. E.** (2005). The effect of climate change on the correlation between avian life-history traits. *Global Change Biology* **11**, 1606-1613.
- Brakefield, P. M.** (2003). Artificial selection and the development of ecologically relevant phenotypes. *Ecology* **84**, 1661-1671.
- Brommer, J. E.** (2004). Immunocompetence and its costs during development: an experimental study in blue tit nestlings. *Proceedings of the Royal Society of London. Series B: Biological Sciences* **271**, S110-S113.
- Cole, E. L., Bayne, H. and Rosengaus, R. B.** (2020). Young but not defenceless: antifungal activity during embryonic development of a social insect. *Royal Society open science* **7**, 191418.
- Diamond, S. E. and Kingsolver, J. G.** (2011). Host plant quality, selection history and trade-offs shape the immune responses of *Manduca sexta*. *Proceedings of the Royal Society B: Biological Sciences* **278**, 289-297.
- Djawdan, M., Sugiyama, T. T., Schlaeger, L. K., Bradley, T. J. and Rose, M. R.** (2004). Metabolic aspects of the trade-off between fecundity and longevity in *Drosophila melanogaster*. In *Methuselah flies: A case study in the evolution of aging*, pp. 145-164: World Scientific.
- Englert, D. C. and Bell, A.** (1970). Selection for time of pupation in *Tribolium castaneum*. *Genetics* **64**, 541.
- Finch, C. E. and Ruvkun, G.** (2001). The genetics of aging. *Annual review of genomics and human genetics* **2**, 435-462.
- Flatt, T.** (2020). Life-history evolution and the genetics of fitness components in *Drosophila melanogaster*. *Genetics* **214**, 3-48.
- Flatt, T. and Heyland, A.** (2011). *Mechanisms of life history evolution: the genetics and physiology of life history traits and trade-offs*: Oxford university press.
- Flatt, T., Tu, M. P. and Tatar, M.** (2005). Hormonal pleiotropy and the juvenile hormone regulation of *Drosophila* development and life history. *Bioessays* **27**, 999-1010.
- Fox, C. W. and Messina, F. J.** (2013). *Life History*: Oxford University Press.
- Garcia, C. and Toro, M.** (1990). Individual and group selection for productivity in *Tribolium castaneum*. *Theoretical and Applied Genetics* **79**, 256-260.
- González-Santoyo, I. and Córdoba-Aguilar, A.** (2012). Phenoloxidase: a key component of the insect immune system. *Entomologia Experimentalis et Applicata* **142**, 1-16.
- Gorman, M., Kankanala, P. and Kanost, M.** (2004). Bacterial challenge stimulates innate immune responses in extra-embryonic tissues of tobacco hornworm eggs. *Insect molecular biology* **13**, 19-24.
- Grimaldi, D. and Engel, M. S.** (2005). *Evolution of the Insects*: Cambridge University Press.
- Gromko, M. H.** (1995). Unpredictability of correlated response to selection: pleiotropy and sampling interact. *Evolution* **49**, 685-693.
- Hill, W. G. and Caballero, A.** (1992). Artificial selection experiments. *Annual Review of Ecology and Systematics*, 287-310.
- Irwin, K. and Carter, P.** (2013). Constraints on the evolution of function-valued traits: A study of growth in *Tribolium castaneum*. *Journal of evolutionary biology* **26**, 2633-2643.
- Jacobs, C. G., Rezende, G. L., Lamers, G. E. and van der Zee, M.** (2013). The extraembryonic serosa protects the insect egg against desiccation. *Proceedings of the Royal Society B: Biological Sciences* **280**, 20131082.
- Jacobs, C. G., Spaink, H. P. and van der Zee, M.** (2014a). The extraembryonic serosa is a frontier epithelium providing the insect egg with a full-range innate immune response. *elife* **3**, e04111.
- Jacobs, C. G., van der Hulst, R., Chen, Y.-T., Williamson, R. P., Roth, S. and van der Zee, M.** (2022). Immune function of the serosa in hemimetabolous insect eggs. *Philosophical Transactions of the Royal Society B* **377**, 20210266.
- Jacobs, C. G. and van der Zee, M.** (2013). Immune competence in insect eggs depends on the extraembryonic serosa. *Developmental & Comparative Immunology* **41**, 263-269.
- Jacobs, C. G., Wang, Y., Vogel, H., Vilcinskis, A., van Der Zee, M. and Rozen, D. E.** (2014b). Egg survival is reduced by grave-soil microbes in the carrion beetle, *Nicrophorus vespilloides*. *BMC Evolutionary Biology* **14**, 1-8.
- Jiménez-Guri, E., Wotton, K. R., Gavilán, B. and Jaeger, J.** (2014). A staging scheme for the development of the moth midge *Clogmia albipunctata*. *PLoS One* **9**, e84422.

- Ketterson, E. D. and Nolan, J., Val** (1999). Adaptation, exaptation, and constraint: a hormonal perspective. *the american naturalist* **154**, S4-S25.
- LaFever, L. and Drummond-Barbosa, D.** (2005). Direct control of germline stem cell division and cyst growth by neural insulin in *Drosophila*. *Science* **309**, 1071-1073.
- Leroi, A. M., Chippindale, A. K. and Rose, M. R.** (1994). Long-term laboratory evolution of a genetic life-history trade-off in *Drosophila melanogaster*. 1. The role of genotype-by-environment interaction. *Evolution* **48**, 1244-1257.
- Livak, K. J. and Schmittgen, T. D.** (2001). Analysis of relative gene expression data using real-time quantitative PCR and the 2<sup>-</sup>  $\Delta\Delta$ CT method. *methods* **25**, 402-408.
- Lord, J. C., Hartzler, K., Toutges, M. and Oppert, B.** (2010). Evaluation of quantitative PCR reference genes for gene expression studies in *Tribolium castaneum* after fungal challenge. *Journal of microbiological methods* **80**, 219-221.
- Lozano-Durán, R., Macho, A. P., Boutrot, F., Segonzac, C., Somssich, I. E. and Zipfel, C.** (2013). The transcriptional regulator BZR1 mediates trade-off between plant innate immunity and growth. *elife* **2**, e00983.
- Madder, D., Surgeoner, G. and Helson, B.** (1983). Number of generations, egg production, and developmental time of *Culex pipiens* and *Culex restuans* (Diptera: Culicidae) in southern Ontario. *Journal of medical entomology* **20**, 275-287.
- Manniello, M., Moretta, A., Salvia, R., Scieuzo, C., Lucchetti, D., Vogel, H., Sgambato, A. and Falabella, P.** (2021). Insect antimicrobial peptides: potential weapons to counteract the antibiotic resistance. *Cellular and Molecular Life Sciences*, 1-24.
- Matsumura, K. and Miyatake, T.** (2015). Differences in attack avoidance and mating success between strains artificially selected for dispersal distance in *Tribolium castaneum*. *PLoS One* **10**, e0127042.
- Mira, A. and Bernays, E. A.** (2002). Trade-offs in host use by *Manduca sexta*: Plant characters vs natural enemies. *Oikos* **97**, 387-397.
- Moret, Y.** (2006). ‘Trans-generational immune priming’: specific enhancement of the antimicrobial immune response in the mealworm beetle, *Tenebrio molitor*. *Proceedings of the Royal Society B: Biological Sciences* **273**, 1399-1405.
- Nijhout, H. F., Riddiford, L. M., Mirth, C., Shingleton, A. W., Suzuki, Y. and Callier, V.** (2014). The developmental control of size in insects. *Wiley Interdisciplinary Reviews: Developmental Biology* **3**, 113-134.
- Nunney, L.** (1996). The response to selection for fast larval development in *Drosophila melanogaster* and its effect on adult weight: an example of a fitness trade-off. *Evolution* **50**, 1193-1204.
- Parthasarathy, R. and Palli, S. R.** (2011). Molecular analysis of nutritional and hormonal regulation of female reproduction in the red flour beetle, *Tribolium castaneum*. *Insect biochemistry and molecular biology* **41**, 294-305.
- Partridge, L. and Fowler, K.** (1992). Direct and correlated responses to selection on age at reproduction in *Drosophila melanogaster*. *Evolution* **46**, 76-91.
- Protocol, R. T.** (2000). Reverse Transcription System.
- Rauw, W., Kanis, E., Noordhuizen-Stassen, E. and Grommers, F.** (1998). Undesirable side effects of selection for high production efficiency in farm animals: a review. *Livestock production science* **56**, 15-33.
- Roff, D.** (2000). Trade-offs between growth and reproduction: an analysis of the quantitative genetic evidence. *Journal of Evolutionary Biology* **13**, 434-445.
- Roth, O. and Kurtz, J.** (2008). The stimulation of immune defence accelerates development in the red flour beetle (*Tribolium castaneum*). *Journal of Evolutionary Biology* **21**, 1703-1710.
- Roth, O., Sadd, B. M., Schmid-Hempel, P. and Kurtz, J.** (2009). Strain-specific priming of resistance in the red flour beetle, *Tribolium castaneum*. *Proceedings of the Royal Society B: Biological Sciences* **276**, 145-151.
- Salmela, H., Amdam, G. V. and Freitak, D.** (2015). Transfer of immunity from mother to offspring is mediated via egg-yolk protein vitellogenin. *PLoS pathogens* **11**, e1005015.
- Schmid-Hempel, P.** (2005). Evolutionary ecology of insect immune defenses. *Annu. Rev. Entomol.* **50**, 529-551.

- Schwenke, R. A., Lazzaro, B. P. and Wolfner, M. F.** (2016). Reproduction–immunity trade-offs in insects. *Annual review of entomology* **61**, 239.
- Soliman, M.** (1982). Directional and stabilizing selection for developmental time and correlated response in reproductive fitness in *Tribolium castaneum*. *Theoretical and Applied Genetics* **63**, 111-116.
- Stearns, S. C.** (1976). Life-history tactics: a review of the ideas. *The Quarterly review of biology* **51**, 3-47.
- Stearns, S. C.** (1989). Trade-offs in life-history evolution. *Functional ecology* **3**, 259-268.
- (1992). *The evolution of life histories*: Oxford university press Oxford.
- Tan, K. L., Vlisidou, I. and Wood, W.** (2014). Ecdysone mediates the development of immunity in the *Drosophila* embryo. *Current Biology* **24**, 1145-1152.
- Tsakas, S. and Marmaras, V.** (2010). Insect immunity and its signalling: an overview. *Invertebrate Survival Journal* **7**, 228-238.
- van der Zee, M., Berns, N. and Roth, S.** (2005). Distinct functions of the *Tribolium* *zerknu llt* genes in serosa specification and dorsal closure. *Current Biology* **15**, 624-636.
- Van Noordwijk, A. J. and de Jong, G.** (1986). Acquisition and allocation of resources: their influence on variation in life history tactics. *The American Naturalist* **128**, 137-142.
- Vargas, H. C. M., Farnesi, L. C., Martins, A. J., Valle, D. and Rezende, G. L.** (2014). Serosal cuticle formation and distinct degrees of desiccation resistance in embryos of the mosquito vectors *Aedes aegypti*, *Anopheles aquasalis* and *Culex quinquefasciatus*. *Journal of insect physiology* **62**, 54-60.
- Vilmos, P. and Kurucz, E.** (1998). Insect immunity: evolutionary roots of the mammalian innate immune system. *Immunology letters* **62**, 59-66.
- White, G.** (1984). Variation between field and laboratory populations of *Tribolium castaneum* (Herbst)(Coleoptera: Tenebrionidae). *Australian journal of ecology* **9**, 153-155.
- Wotton, K. R., Jimenez-Guri, E., Garcia Matheu, B. and Jaeger, J.** (2014). A staging scheme for the development of the scuttle fly *Megaselia abdita*. *PLoS One* **9**, e84421.
- Zeh, D. W., Zeh, J. A. and Smith, R. L.** (1989). Ovipositors, amnions and eggshell architecture in the diversification of terrestrial arthropods. *The Quarterly Review of Biology* **64**, 147-168.
- Zou, Z., Evans, J. D., Lu, Z., Zhao, P., Williams, M., Sumathipala, N., Hetru, C., Hultmark, D. and Jiang, H.** (2007). Comparative genomic analysis of the *Tribolium* immune system. *Genome biology* **8**, 1-16.
- Zwaan, B., Bijlsma, R. and Hoekstra, R.** (1995a). Artificial selection for developmental time in *Drosophila melanogaster* in relation to the evolution of aging: direct and correlated responses. *Evolution* **49**, 635-648.
- (1995b). Direct selection on life span in *Drosophila melanogaster*. *Evolution* **49**, 649-659.

## Supplementary information

Supplementary Table 3-1. Primers for immune sequences of *Tribolium castaneum*.

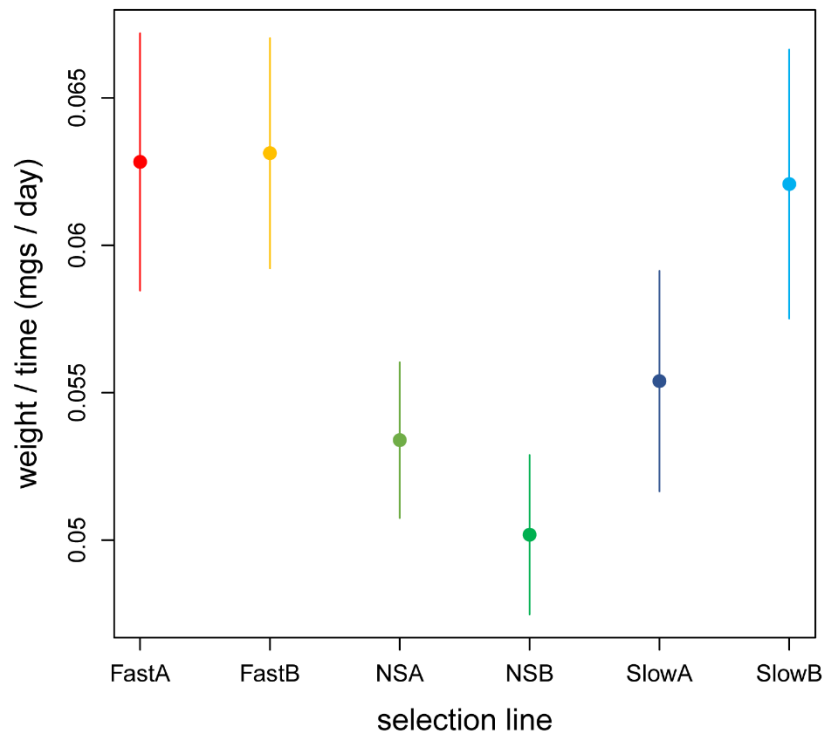
Gene name	TC number	Forward primer (5'-3')	Reverse primer (5'-3')
<i>Tribolium castaneum</i>			
<i>Attacin1</i>	TC007737	TTTTGCCTCCAAACAATTCC	CACCGACGTTTtaggTTCGAT
<i>Attacin2</i>	TC007738	CCCGGAATCCTCAAActACA	GGGGCATCTTTATTGACGAA
<i>Cecropin3</i>	TC000500	GCTGTTCCCGTGGTTAAAAA	ACTGGAGGCGCATACTGAAT
<i>Coleoptericin1</i>	TC005093	TTTGGCACTTTTTGCACTTG	GGGATGTCCTGTTCTACGGA
<i>Defensin2</i>	TC010517	TCACTTGTGACGTCCTCAGC	CGCGTTTCTTCAAAAAGAGG
<i>Laccase 2</i>	TC010489	TACAACAGACATTTAGTTGCACCA	AGGTGGGGCCATGTAGGAAA

Supplementary Table 3-2. Pupal weight of female and male of the selection lines.

Selection line	Female weight (mg)		Male weight (mg)		Welch two-samples t-test	
	Mean $\pm$ SD	N	Mean $\pm$ SD	N	T value	P value
Fa	2.64 $\pm$ 0.39	27	2.69 $\pm$ 0.55	19	-0.3134	0.7562
Fb	2.82 $\pm$ 0.53	20	2.64 $\pm$ 0.33	20	1.2529	0.2195
Na	2.90 $\pm$ 0.44	22	2.84 $\pm$ 0.56	14	0.3582	0.7234
Nb	2.75 $\pm$ 0.59	21	2.68 $\pm$ 0.43	20	0.4251	0.6733
Sa	3.34 $\pm$ 0.64	16	3.23 $\pm$ 0.41	22	0.6120	0.5464
Sb	3.64 $\pm$ 0.79	24	3.26 $\pm$ 0.41	19	2.052	0.0475
All lines	3.00 $\pm$ 0.67	130	2.90 $\pm$ 0.51	114	1.3700	0.1720

Supplementary Table 3-3. Adult weight of female and male of the selection lines.

Selection line	Female weight (mg)		Male weight (mg)		Welch two-samples t-test	
	Mean $\pm$ SD	N	Mean $\pm$ SD	N	T value	P value
Fa	2.05 $\pm$ 0.32	19	1.95 $\pm$ 0.39	14	0.7759	0.4451
Fb	2.17 $\pm$ 0.39	17	2.10 $\pm$ 0.27	16	0.6099	0.5468
Na	2.17 $\pm$ 0.31	22	2.07 $\pm$ 0.31	14	0.9363	0.3572
Nb	2.00 $\pm$ 0.33	20	1.90 $\pm$ 0.32	20	0.8894	0.3794
Sa	2.35 $\pm$ 0.39	14	2.35 $\pm$ 0.38	19	0.0102	0.9919
Sb	2.63 $\pm$ 0.36	22	2.37 $\pm$ 0.27	16	2.5621	0.0148
All lines	2.23 $\pm$ 0.41	114	2.13 $\pm$ 0.37	99	1.9609	0.0512



Supplementary Figure 3-1. Growth rate defined as adult weight divided by total postembryonic time (larval development time and pupal development time) of an individual (mg/day; means  $\pm$  2 x s.e.m.). Selection regime had an effect ( $\chi^2=11.099$ ;  $df=2$ ;  $p=0.0039$ ), but the fast lines are not significantly different from the slow lines ( $\chi^2= 2.34$ ;  $df=1$ ;  $p= 0.127$ ).

# Chapter 4

## A novel allele of large effect that alters developmental time and mediates trade-offs

Shixiong Cheng, Elisa A. Mogollón Pérez, Daipeng Chen, Joep van de Sanden, Amke Hackmann, Roeland M. H. Merks, Joost van den Heuvel, Maurijn van der Zee

### Abstract

During current climate change, insect developmental time can adapt quickly to match shifted host plant or prey availability. However, the genetic basis of such adaptation in developmental timing is hardly studied. Here, we show that ecdysone signaling starts dorsal closure and is the main target of long-term artificial selection for fast embryonic development in replicate, outbred populations of the beetle *Tribolium castaneum*. Pooled whole genome resequencing (Pool-seq), RNAseq, qPCR, and a small RNAi screen pinpoint a 222 bp deletion upstream of the ecdysone degrading enzyme *Cyp18a1*. This allele contains Tramtrack and Broad binding sites which are responsible for chromatin architectural alterations, and may act as an enhancer regulating expression of *Cyp18a1*. Using CRISPR-Cas9 technology, we recreated this deletion in the homogeneous genetic background of the Georgia lab strain, and demonstrate that this single allele advances the ecdysone peak inducing dorsal closure, accelerates larval development and causes a trade-off with fecundity. Our study demonstrates the relevance of ecdysone during embryonic development, and reveals the presence of large-effect life-history alleles in natural populations.

### Introduction

When global warming affects species differently, ecological mismatches in seasonal timing occur (Kharouba et al., 2018; Samplonius et al., 2021; Thackeray et al., 2016). Mismatches with host plant or prey availability exert strong selection on developmental time in insects (Singer and Parmesan, 2010; Visser and Gienapp, 2019). Eggs of the winter moth *Operopthera brumata*, for instance, decreased their temperature sensitivity to synchronize larval hatching with the budburst of their primary food source, the oak *Quercus robur* (Brinkman, 2017). Failure to adapt to changes in seasonal timing can lead to population extinction (McLaughlin et al., 2002; Singer and Parmesan, 2010). It is thus of great importance to understand to what extent insects can respond to such selective pressures on developmental time (Franks and Hoffmann, 2012; Renner and Zohner, 2018).

New phenotypes are thought to generally arise from selection on standing genetic variation, but the ultimate source of new alleles is mutation. These mutations eventually affect protein networks, and manifest themselves through development and physiology as phenotypic variation (Gissis et al., 2011; Shapiro, 2011). Such alleles can increase in frequency by natural selection, but fluctuating environments, trade-offs, balancing selection and drift in small populations can make natural selection complicated (Brakefield, 2003). Such problems are avoided in artificial selection experiments (Brakefield, 2003).

Artificial selection has long been practiced by humans to produce animals and crops with desirable phenotypic traits in their offspring. This strong selection has led to innovations in both animals and plants and has affected human evolution and the biosphere as a whole (Larson and Fuller, 2014; Xiang



et al., 2018). Artificial selection is a useful tool for evolutionary geneticists too. The underlying genetics of rapidly changed phenotypic traits can be investigated (Brakefield, 2003; Franks et al., 2018). Most importantly, constant environments and large populations can facilitate the study of evolution compared to natural selection in field populations. Finally, using replicate populations increases statistical power of artificial selection experiments (Brakefield, 2003).

Insects provide excellent models for experimental evolution, as they can be kept in large numbers and are the most diverse animal group (Grimaldi and Engel, 2005). Most artificial selection studies have been performed in *D. melanogaster*, such as on egg-to-adult developmental time (Chippindale et al., 1997; Nunney, 1996; Prasad et al., 2000; Sharma et al., 2020; Yadav and Sharma, 2013; Zwaan et al., 1995), fitness components (Rose, 1984), mating speed (Manning, 1961), or a courtship signal (Ritchie and Kyriacou, 1996). Finding the genetic targets of selection is a current challenge for biology.

Evolve-and-resequence (E&R) studies combine experimental evolution with next-generation sequencing of pools of individuals (Pool-seq). E&R can thus examine SNP frequency differences to identify causative alleles or genes (Schlötterer et al., 2014) and the loci underlying complex traits (Vlachos and Kofler, 2019). E&R studies have not only been successfully applied in bacteria and yeast, but also in *Drosophila* (Long et al., 2015). These experiments in *Drosophila* have focused on genome-wide responses to selection for generation time or time of reproduction (Burke et al., 2010; Graves et al., 2017; Teotonio et al., 2009). Also in the silkworm *Bombyx mori*, targets of artificial selection during domestication have been revealed (Yukuhiro et al., 2012; Zhu et al., 2019), for instance by resequencing genomes of 29 domesticated and 11 wild *B. mori* lines (Xia et al., 2009).

The red flour beetle *Tribolium castaneum* has become the second most important emerging model insect species after *Drosophila*, and is a ubiquitous Coleopteran pest of stored grain, flour, and other cereal products (Campbell et al., 2022; Klingler and Bucher, 2022; Pointer et al., 2021). Its embryos exhibit many ancestral features shared with most insects, such as short-germ development, embryonic leg development and an extensive extraembryonic serosa (Klingler, 2004; Panfilio, 2008; Schröder et al., 2008). This serosa protects the egg against desiccation and can mount a full-range immune response (Jacobs et al., 2013; Jacobs et al., 2014; Jacobs and van der Zee, 2013; Rafiqi et al., 2008). Since the genome of *T. castaneum* was published, plenty of available resources and technologies had been further developed for *Tribolium* researchers, such as CRISPR-Cas9 and systematic RNA interference (RNAi) (Bucher et al., 2002; Gilles et al., 2015). Knockdown phenotypes can be induced at all life stages and functionally transferred to the offspring through parental RNAi (pRNAi) (Consortium, 2008; Dönitz et al., 2015; Linz et al., 2014). In addition, long-term live imaging data of *T. castaneum* embryos can display the complete, continuous embryogenesis and did expand our knowledge of morphogenetic concepts beyond the *Drosophila* paradigm (Strobl and Stelzer, 2014).

Here, we have performed an E&R study on *T. castaneum*, artificially selecting for fast and slow embryonic development. During current climate change, it is important to understand to what extent insects can respond to selection on developmental time (Franks and Hoffmann, 2012; Renner and Zohner, 2018), as ecological mismatches in seasonal timing occur when global warming affects species differently (Kharouba et al., 2018; Samplonius et al., 2021; Thackeray et al., 2016). A striking example is the selective pressure on developmental time of the winter moth *O. brumata* to match shifted oak tree leaf-out (Van Asch et al., 2013). Until now, selection experiments have mainly been restricted to egg-to-adult developmental time in *Drosophila* (Chippindale et al., 1997; Nunney, 1996; Prasad et al., 2000; Sharma et al., 2020; Yadav and Sharma, 2013; Zwaan et al., 1995) and a few other insects (Fischer et al., 2007; Seslija and Tucic, 2003). Selection experiments on embryonic developmental time in have been scarce or reported as unsuccessful (Marinkovic, 1986; Neyfakh and Hartl, 1993). In chapter 3, I have reported the response to this selection in our six selection lines: fast A (Fa), fast B (Fb), non-selected A (Na), non-selected B (Nb), slow A (Sa) and slow B (Sb).

Here, we performed pooled resequencing on these lines in order to unravel the genetics underlying embryonic developmental time. We identify the cytochrome P450 *Cyp18a1* as a main target of selection. This enzyme catabolizes active ecdysone (E20) by 26-hydroxylation (Guittard et al., 2011; Rewitz et al., 2010). The steroid hormone 20E is crucial in controlling developmental timing such as molting and metamorphosis, and is synthesized by other cytochrome P450 enzymes collectively called the Halloween genes. In this chapter, we also study the function of the Halloween genes and other cytochromes in larval, pupal and embryonic development. We report an ecdysone peak during embryonic development that initiates dorsal closure, one of the last stages of embryonic development during which the lateral ectodermal sides of the embryo dorsally meet to include the yolk (Panfilio, 2008). We find an allele, a 222 base pairs (bp) deletion upstream of *Cyp18a1*, that increased in frequency in the fast lines over the course of the selection. We demonstrate with CRISPR-Cas9 technology that this single deletion advances the embryonic ecdysone peak, advances dorsal closure, accelerates embryonic development, and trades off with fecundity, by regulating expression of *Cyp18a1* and accumulation of ecdysone.

## Materials and methods

### Selection lines of *Tribolium castaneum* beetles

The fast A (Fa), fast B (Fb), non-selected A (Na), non-selected B (Nb), slow A (Sa) and slow B (Sb) selection lines of *T. castaneum* are described in Chapter 3 (see materials and methods section, outbred populations of *Tribolium castaneum* beetles). After selection, they were kept as in (van der Zee et al., 2005).

### Pooling genomic resequencing

Around 100 eggs of every selection line were dechlorinated in commercial bleach (5% NaClO) and washed well with tap water. DNA was extracted using a standard phenol-chloroform extraction (phenol:chloroform:isoamyl-alcohol 25:24:1). The pooled DNA was sequenced on an Illumina HiSeq4000 machine with a paired-end 150 basepair layout. Reads have been deposited as NCBI BioProject PRJNA942224.

### SNP analysis

The raw reads were trimmed using TRIMMOMATIC (v 0.27, LEADING:3, TRAILING:3, SLIDINGWINDOW:4:15, MINLENGTH:70) (Bolger et al., 2014). The trimmed reads were aligned on the Tcas 5.2 (GCF\_000002335.3) genome using bwa mem (v 0-7-15, default parameters, <http://arxiv.org/abs/1303.3997>). After mapping reads were filtered for quality (20) and sorted using samtools (v 0.1.19) (Li et al., 2009). We then removed duplicate using picard tools (v.2.8.2, <http://picard.sourceforge.net>) and performed realignment around indels with GATK (v .3.7-0) (McKenna et al., 2010).

The resulting BAM files were combined in mpileup format (samtools, mpileup, default parameters, v 0.1.19) (Li et al., 2009), after which SNPs and indels were separately called using varscan (v 2.3.9, using mpileup2snps and mpileup2indel resp., --output-vcf 1, --min-var-freq 0.05) (Koboldt et al., 2009) for which we only kept those variants that differed between the samples. The resulting raw vcf files was then annotated with snpEff (v 4.3)(Cingolani et al., 2012) using the Tcas 5.2 GCF\_000002335.3 annotation file (GFF) (Herndon et al., 2020) as input. The resulting vcf files were further filtered using vcfR (v 1.8.0) (Knaus and Grunwald, 2017).

For the contrast between the fast and non-selected, as well as the slow and non-selected a similar approach was used. Only biallelic SNPs were analyzed that had a minimum coverage between the 0.05 and 0.98 quantiles (using `quantile()` function) of total depth for all samples. Furthermore, SNPs were

removed if they lay near indels (<10 bp) and if they were not present on the major chromosome scaffolds. A generalized linear model (GLM) was fitted with binomial error structure testing for treatments against non-selected, which was previously shown to be a powerful test for an evolve and re-sequence experiment (Hoedjes et al., 2019).

To create a  $H_0$  permuted p value distribution, the two other possible sample configurations were used, and a GLM was run as well. For instance, for fast against non-selected, we tested FastA and FastB against NSA and NSB as the observed GLM. Then FastA and NSA were tested against FastB and NSB as the first permutation and FastA and NSB were tested against FastB and NSA as a second permutation. These two permuted distributions were then used to calculate the permuted p value distribution (`empPvals(observed,c(H0_1,H0_2),pool=TRUE)`) and the resulting permuted p values were transformed into qvalues using the `qvalue` function (`qvalue` package). Loci were called significant when this qvalue was below 0.01.

### **Embryo fixation and DAPI staining**

Fifty embryos of the selection lines were collected every 8 h at 25°C until more than 50% of all eggs hatched. Eggs were fixed in a 1:1 mix of 3.7% formaldehyde in PBS (PBS, pH 7.4) and heptane for 20 min, and devitellinized using a methanol shock. They were brought back to PBST (PBS with 0.2% Tween 20), and, stained with 4'-6-diamidino-2-phenylindole (DAPI) for 15 min, and finally mounted on microscope slides to take pictures. Embryos were photographed under a Zeiss Axioplan 2 imaging microscope (Zeiss, Mannheim, Germany) equipped with a DAPI filter (XF-06, excitation 330–390 nm, emission 410–490 nm). Images were processed using Adobe Photoshop (version 23.5). The embryonic stage values were attributed to each embryo according to the staging scheme in Supplementary Figure 4-1). The average stage values are reported in Figure 4-2.

### **Sample collection for transcriptional analysis**

Embryonic development of the selection lines for transcriptional analysis was decided according to fluorescent microscopic analysis. For RT-qPCR and RNAseq, total RNA of approximately 200-300 eggs was isolated by Trizol extraction (Invitrogen) after which the RNA was purified and DNA digested on column with the RNeasy kit (Qiagen). The quality of isolated RNA was measured spectrophotometrically and on a 1.0% agarose gel. We collected three biological samples for the fast (Fa and Fb) and the non-selected lines (Na and Nb) at 76 h post-oviposition according to *T. castaneum* embryos live imaging results (Figure 4-2), giving a total of 12 biological samples. For RNAseq, cDNA library synthesis and sequencing was performed by ZF-screens (Leiden, the Netherlands) sequencing company on an Illumina HiSeq2500 sequencer. For qPCR analysis, we collected four biological samples for the fast (2 samples of Fa and 2 of Fb) and the non-selected lines (2 samples of Na and 2 of Nb), at 76, 92 and 108 h post-oviposition.

### **RNA sequencing analysis**

The raw reads were checked for quality using FastQC version 0.11.9 (<https://www.bioinformatics.babraham.ac.uk/projects/fastqc/>). Reads were trimmed by eliminating any ambiguous or low-grade reads and the adaptor sequences using Trimmomatic (v0.39; HEADCROP:10 MINLEN:50 TRAILING:20). The trimmed paired end reads were aligned and mapped to the *Tribolium* genome 5.2 using STAR (2.7.10a). Read counts per gene were quantified using htseq-count (Anders et al., 2015). Differential expression analysis was performed using DESeq2 version 1.34.0 (Love et al., 2014). The significant difference is represented in gene expression by more than 1.25-fold upregulation and 0.8-repression both with a threshold adjusted  $P < 0.05$ . The false discovery rate (FDR) was performed as described as in (Jacobs et al., 2014).

## **cDNA synthesis and qPCR**

The experimental RNA was collected as described under ‘Sample collection for transcriptional analysis’. One microgram of total RNA was performed for cDNA synthesis (Promega Reverse Transcription system). 2  $\mu$ L of 1:10 diluted original cDNA was used in every RT-qPCR reaction. qPCR reactions were done using the SsoAdvanced Universal SYBR Green Supermix (Bio-rad) on a CFX96 thermocycler (Bio-rad). Thermal conditions were as follow: an initial step at 95 °C for 30s; 40 cycles of 95°C for 15 s, 60°C for 30 s, 72°C for 30 s; this was followed by dissociation analysis of a ramp from 65°C to 95°C with a read every 0.5°C. RPL13a gene was used as internal control to calculate  $\Delta$ CT values (Lord et al., 2010). Relative expression was calculated with regard to the average of the non-selected lines (Figure 4-5) or a defined time point (Figure 4-13, Figure 4-14, Figure 4-15) using the  $2^{-\Delta\Delta CT}$  method (Livak and Schmittgen, 2001), or presented as fraction of RPL13a expression (Figure 4-33). Total RNA for each treatment was isolated two times (biological replication) and each sample was measured by RT-qPCR twice (technical replication). All candidate genes and their acronyms are listed in Supplementary Table 4-1. All of primers used for qPCR were in Supplementary Table 4-2. Significance of fold change differences was estimated by a student’s t-test, shown in Figure 4-5.

## **Molecular cloning and RNAi**

The *Tribolium* stock used for RNAi was the other common wild-type strain of *Tribolium*, Georgia-1 (GA-1). RNAi for all of candidate genes were performed as described in (van der Zee et al., 2005; Zee et al., 2006). All target genes were searched from GenBank and showed in Supplementary Table 4-3 and Supplementary Table 4-4. Gene fragments were cloned into the pCR<sup>TM</sup>II-TOPO<sup>TM</sup> TA vector (Invitrogen), and inserts were confirmed by Sanger sequencing. The plasmids were linearized with an appropriate restriction enzyme to generate DNA templates for in vitro transcription with SP6 and T7 polymerases, and resulting dsRNA was purified using the Ambion MEGAscript RNAi kit. The control dsRNA was synthesized as a 500 bp the pCR<sup>TM</sup>II-TOPO<sup>TM</sup> TA vector sequence (Invitrogen) (Jacobs et al., 2013; Jacobs et al., 2014).

For parental RNAi (pRNAi), a mixture of 0.4  $\mu$ L of 0.5-1.0  $\mu$ g/ $\mu$ L dsRNA was also performed according to (Bucher et al., 2002; Zee et al., 2006). 2h egg lays were put in on the selection machine (see in Chapter 3) to measure developmental time next to a control RNAi with dsRNA from the 500 bp bacterial vector sequence without target in the *Tribolium* genome (Jacobs et al., 2013; Jacobs et al., 2014). Measurements were performed in triplicate and significance of the difference with control developmental time was determined by a student’s t-test.

For larvae RNAi, a mixture of 0.4  $\mu$ L of 0.5-1.0  $\mu$ g/ $\mu$ L dsRNA was injected into the dorsal segments of the penultimate-instar or last-instar larvae. For pupae RNAi, a mixture of 0.2  $\mu$ L of 0.5-1.0  $\mu$ g/ $\mu$ L dsRNA was injected into the abdomen of both female and male pupae (Linz et al., 2014). For embryonic RNAi, 4-6 h old eggs of LifeAct-nGFP line (van Drongelen et al., 2018) were injected as much as possible but avoiding leaking much yolk (Berghammer et al., 2009).

## **Ecdysone detection**

At the desired timepoint after a 2h egg lay, 50 eggs were dechorionated in 0.5% bleach for 2 min, homogenized in 300  $\mu$ l of methanol, and centrifuged for 10 min at 12,000rcf. The supernatant was collected into a new 1.5 mL tube, dried completely in a vacuum centrifuge, and the precipitate was redissolved in 120  $\mu$ l EIA buffer provided by a competitive enzyme immune assay (EIA) kit for 20-hydroxyecdysone (20E, Bertin Pharma). After 2h incubation at room temperature, the samples were diluted 4 times in EIA buffer and applied to the detection plate according to the manufacturers protocol. The plate was developed with 200  $\mu$ l of Ellman's reagent and incubated with an orbital shaker at in the dark at RT. After 90 min, the plate was measured at a wavelength of 410 nm on a

Tecan Spark microplate reader. The concentrations were determined by a four parameter logistic fitting.

### ***In situ* hybridization**

An 1124 bp fragment of *Cyp18a1* and a 837 bp fragment of *Spo* were cloned into the pCR<sup>TM</sup>II-TOPO<sup>TM</sup> TA vector (Invitrogen). The fragments of *Cyp18a1* and *spook* (*Spo*) used here was same with that used for RNAi (Supplementary Table 4-3 and Supplementary Table 4-4). Templates were generated using M13 primers. DIG-labeled antisense probes were synthesized using SP6 polymerase for *Cyp18a1* and T7 polymerase for *Spo* (Ambion) with Roche RNA labeling mix (Roche). Sense probes were synthesized as control. *In situ* hybridizations on whole mount fixed eggs (see embryo fixation and dapi staining) were essentially performed as described in (Tautz and Pfeifle, 1989), but without the ProteinaseK step. To manually dissect eggs containing the serosa from the vitelline membrane, we used Tc-CHS1 RNAi eggs, as the serosa tightly associates with the vitelline membrane (Jacobs et al., 2014).

### **PCR genotyping**

DNA from individual beetles was extracted using the phenol-chloroform extraction (phenol:chloroform:isoamyl-alcohol 25:24:1), after 1.5 µg/µl proteinaseK incubation overnight at 55°C. PCRs with Bio SeqAMP polymerase (Takara) using the primers 5'-AAGGGGCCCTCTCAAACATC-3' and 5'-CAGGCACCTCTGCGTTATCC-3' generated a 942 bp band for homozygotes containing both repeats, a 720 bp band for homozygotes for the deletion, and both bands plus a hybrid band running slower because of the formed loop for the heterozygotes.

### **Population genetic modeling**

Using the genotyping data from generations 0, 3, 7, and 21, we fitted a model with and without fitness differences for the three genotypes. For each generation, the initial allele frequency for F was fitted. For each of the parameter settings, the model was calculated forward and the multinomial probability of finding the actual genotype counts was calculated and denoted as the likelihood of the model. The two models, with or without selection were then tested for significant difference using the likelihood ratio test, which was tested against the  $\chi^2$  distribution using

$$\chi^2 = -2(L_{WFF==WFS==WSS} - L_{WFF!=WFS!=WSS}) \quad (1)$$

where L is the log likelihood. The models were fitted starting from the estimated initial frequency for F, using the count data at generation 0 and equal fitness values for the genotypes FF, FS and SS. Then the likelihood of the model was calculated, and the parameters updated using a change randomly drawn from a normal distribution (mean 0, std of 0.01). The new parameters for allele frequency were limited such that they would not be smaller than 0 or larger than 1. For fitness, the changes were not allowed to become lower than 0. At each iteration, the maximum fitness was set to 1. When the likelihood of the model was higher than the previous best fit, the parameters were updated using the new best fit parameters.

### **CRISPR/Cas9 constructions and *Tribolium* injection**

The oligonucleotides 5'-AGTGAAATATAGGGTGTTCATT-3' and 5'-AAACAATGGAACACCCTATATTT-3' were ligated into the BsaI-digested p(U6a-BsaI-gRNA) vector (Addgene) (Gilles et al., 2015) for in vivo expression of the desired gRNA. This construct and the TrueCut Cas9 Protein v2 (Invitrogen) were co-injected each at a concentration of 500 ng/µl into 2h old embryos of the Georgia laboratory strain according to (Berghammer et al., 2009). A brief process diagram of Crispr/Cas experiment for a repeated region is shown in Figure 4-1. Single crosses of virgin G0 animals were set up, and their G1 offspring was collected. A PCR (as described above for

genotyping) on the mosaic G0 parents was performed to get an impression of excision efficiency. Offspring from G0 parents that still showed the repeat containing 942 bp band was rejected, leaving G1 offspring from 6 G0 pairs. Among the remaining G1 offspring, 22 single virgin crosses were set-up, and their G2 offspring was collected. G1 parents were genotyped by PCR in order to choose a pair to set up the stock. PCR products were cloned to determine the sequence of all 4 alleles present in the stock (Figure 4-30).

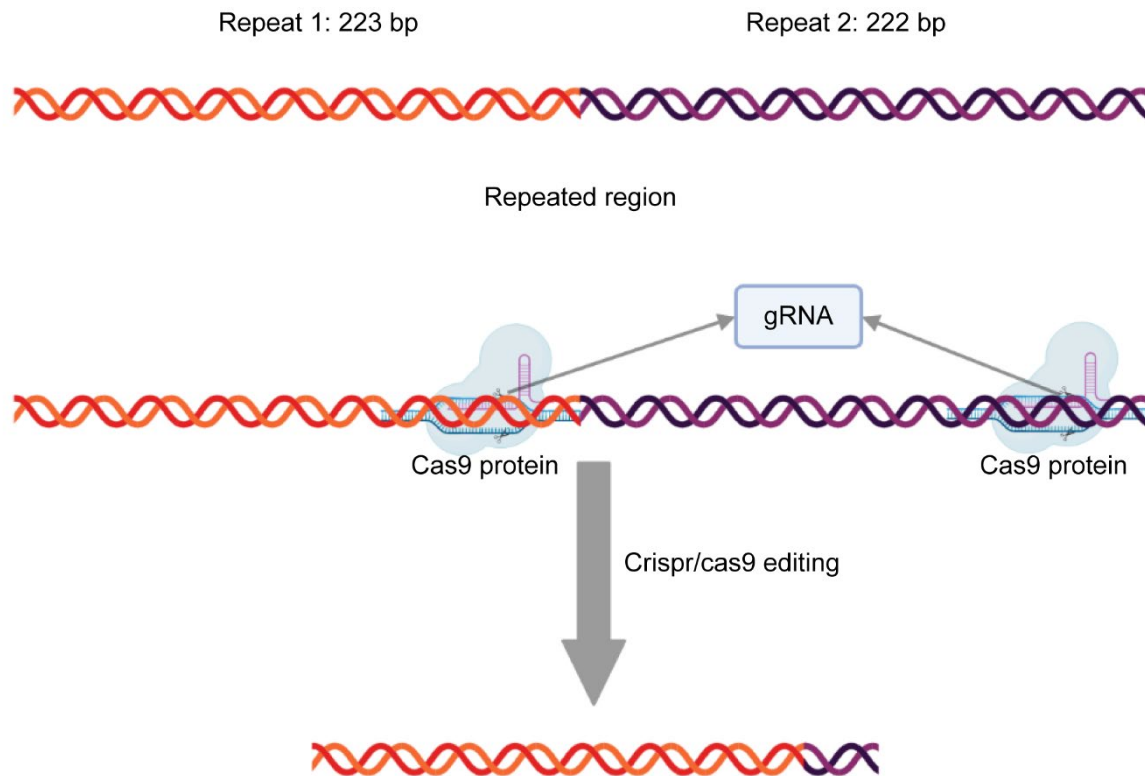


Figure 4-1. A brief process diagram of Crispr/Cas experiment to obtain the CRISPR-induced deletion strain of *Tribolium castaneum*.

### Live imaging

200 females of the nGFP line (Sarrazin et al., 2012) were selected at the pupal stage, and 100 of these females were crossed with 100 males of GA-1, and the other 100 females were crossed with 100 males of the CRISPR line (see above). These two groups of 200 parents were allowed to lay eggs for 20 minutes, and 10-15 of their eggs were imaged under a Nikon AX confocal laser scanning microscope (Nikon Europe B.V., Amsterdam, Netherlands) taking full scans every 26 minutes.

### Binding site analysis

Binding matrices for Br (var.4), Ttk, and EcR::usp, we downloaded from JASAPAR (Castro-Mondragon et al., 2022), and used to search motifs in the whole intergenic region upstream of Cyp18a1 (chromosome 9: NC\_007424.3[1611573..1619999]) with FIMO (Grant et al., 2011).

## Results

### Variation under artificial selection is in the timing at start of dorsal closure

To investigate whether the different embryonic developmental times (see in Chapter 3) were caused by overall acceleration or deceleration, or whether specific developmental processes sped up or slowed down, we defined a numerical staging table (Supplementary Figure 4-1). We fixed and DAPI stained around 50 eggs of selection lines every 8 h until hatching. By fluorescent microscopic analysis, we found that embryonic development among selection lines do not show any difference before germband extension, of which the judgement value is defined as 8. After 72 h post-oviposition, the eggs of the fast lines directly start to develop into next stage which is called “start of dorsal closure” and is characterized by formation of the dorsal organ, the retracting serosa (Supplementary Figure 4-1j). However, embryonic development of both non-selected and slow lines continued in the retracted germband stage for another 8 and 16 h, respectively, while eggs of fast lines are already in the hatching stage after these 16h. Thus, the average stage values demonstrate that the start of dorsal closure differs among the lines, and that the start of dorsal closure occurs earlier in the fast lines (Figure 4-2).

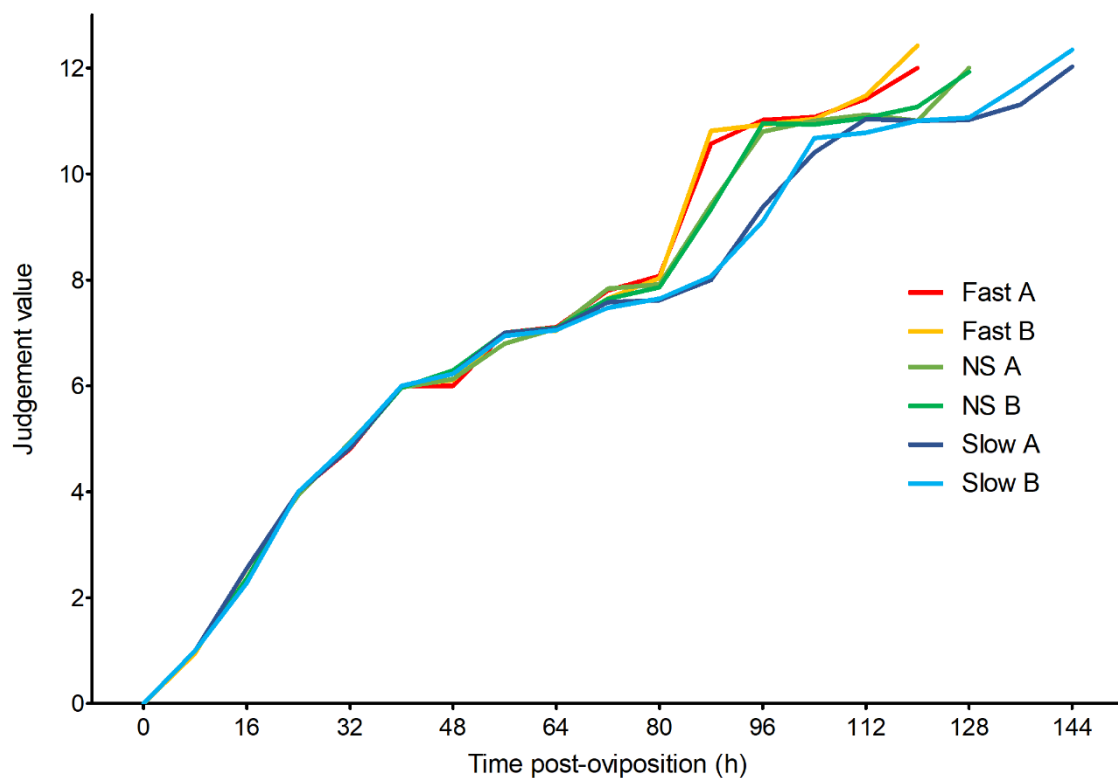


Figure 4-2. Developmental stage during embryonic developmental time (hours after egg lay) of the selection lines (stage values defined in Supplementary Figure 4-1). Start of dorsal closure is the first stage at which a difference in timing can be detected among the selection lines. Judgement values given to fourteen embryonic stages are used to score embryonic development of the selection lines. 0=no nuclei at surface; 1=undifferentiated blastoderm; 2=differentiated blastoderm; 3=gastrulation; 4=extending germband; 5=extended germband; 6=limbs growing and extending; 7=retracting germband; 8=completely retracted germband; 9=start of dorsal closure (dorsal organ formation); 10=dorsal closure in progress; 11=dorsal closure completed; 12=hatching; and 13=hatched. See more details in Supplementary Figure 4-1. Fast A, fast B, non-selected A (NS A), non-selected B (NS B), slow A and slow B are shown with red, orange, green, light green, dark blue, and light blue lines.

## Pooled whole-genome resequencing reveals 45 candidate genes under selection

Manhattan plots show that SNP frequency differences between the slow lines and the non-selected lines are hardly ever below  $q=0.01$  (i.e.  $-\log(p)$  is above 33.0538; red line in Supplementary Figure 4-2). Only 1258 SNPs differed significantly in frequency between the slow and non-selected lines (Supplementary Figure 4-2). However, 8469 SNPs differed significantly in frequency between the fast and non-selected lines (Figure 4-3A). Two areas, on chromosome 3 and on chromosome 9, contain a high number of these very significant SNPs and appear to have been under strong selection in the fast lines (Figure 4-3A). We focus on these two genomic regions in the remainder of this study.

In these regions (position 13.8-15.8 MB on chromosome 3 and position 0.5-4 MB on chromosome 9), we identified 48 principal SNPs based on significance of allele frequency differences (Supplementary Table 4-1). In detail (Supplementary Table 4-1), principal SNPs have an allele frequency difference  $>0.6$  and do not have a higher SNP within 10kb. On chromosome 3, principal SNPs have a  $-\log p$  value  $> 58.5$ . On chromosome 9, principal SNPs have a  $-\log p > 60$ . All principal SNPs are indicated in red (Figure 4-3B, C). In addition, we also selected 9 very significant SNPs ( $-\log p$  value  $> 40$ , Supplementary Table 4-1) neighboring these principal SNPs. We defined these principal and significant SNPs together as our lead SNPs in this study. We associated these 57 lead SNPs with 45 candidate genes in total (numbered in Figure 4-3B, C). See all lead SNPs, genes and their annotations in Supplementary Table 4-1. For instance, a gene called Cytochrome P450 18A1 was identified by the most significant SNP on chromosome 9 at position 1,613,665 (Cyp18a1, gene 32, Figure 4-3C, Supplementary Table 4-1). Melted was identified by the principal SNP 6 that has the highest frequency difference of all these lead SNPs (at position 14,086,409, gene 5, Figure 4-3B, Supplementary Table 4-1).

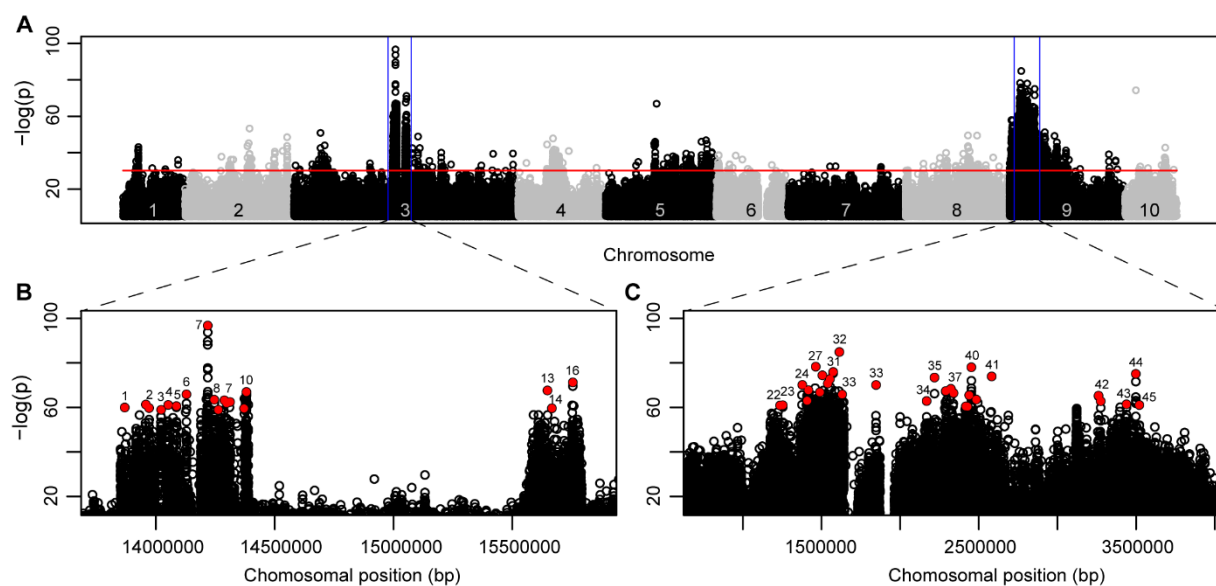


Figure 4-3. SNP analysis on whole genome of *Tribolium castaneum* between the fast lines and the non-selected lines (A). of which, red line represents  $q = 0.01$  or  $-\log(p) > 30.2275$ . The significance of allele frequency differences zoomed in on chromosome 3 (B) and 9 (C), respectively. Principal SNPs are indicated in red. Numbers refer to the associated genes with 48 principal SNPs. See all SNPs and their associated genes in Supplementary Table 4-1.

## Expression analysis restricts the number of candidate genes to 15

As none of our 57 lead SNPs leads to alternative proteins, we first investigated differential gene expression between the fast and the non-selected lines using RNAseq. We isolated RNA at 76h, just



before the differences among the selection lines become apparent during embryonic development (Figure 4-3).

A total of 739 genes were upregulated ( $FC > 1.25$  and  $padj < 0.05$ ) and 258 genes were downregulated ( $FC < 0.8$  and  $padj < 0.05$ ) in the embryos of the fast lines compared to the samples of the non-selected lines (all dots in Figure 4-4). However, only 7 of these overlapped with the 45 genes that were identified as targets of selection in the SNP analysis. These are *mGluR*, *Cyp18a1*, *Lac2*, *LOC657682*, *Lipase*, *Cyp306a1* and *Sec61a* that were significantly upregulated in the fast lines. And *Deadpan* and *LOC103314169* that were significantly down-regulated in the fast embryos compared to the non-selected samples. If the more stringent fold-change cut-off of  $>2$  and  $<0.5$  was applied, the number of differentially expressed genes was restricted to 122 (red and green dots Figure 4-4), and reduced the candidate genes to *mGluR* and *Cyp18a1*.

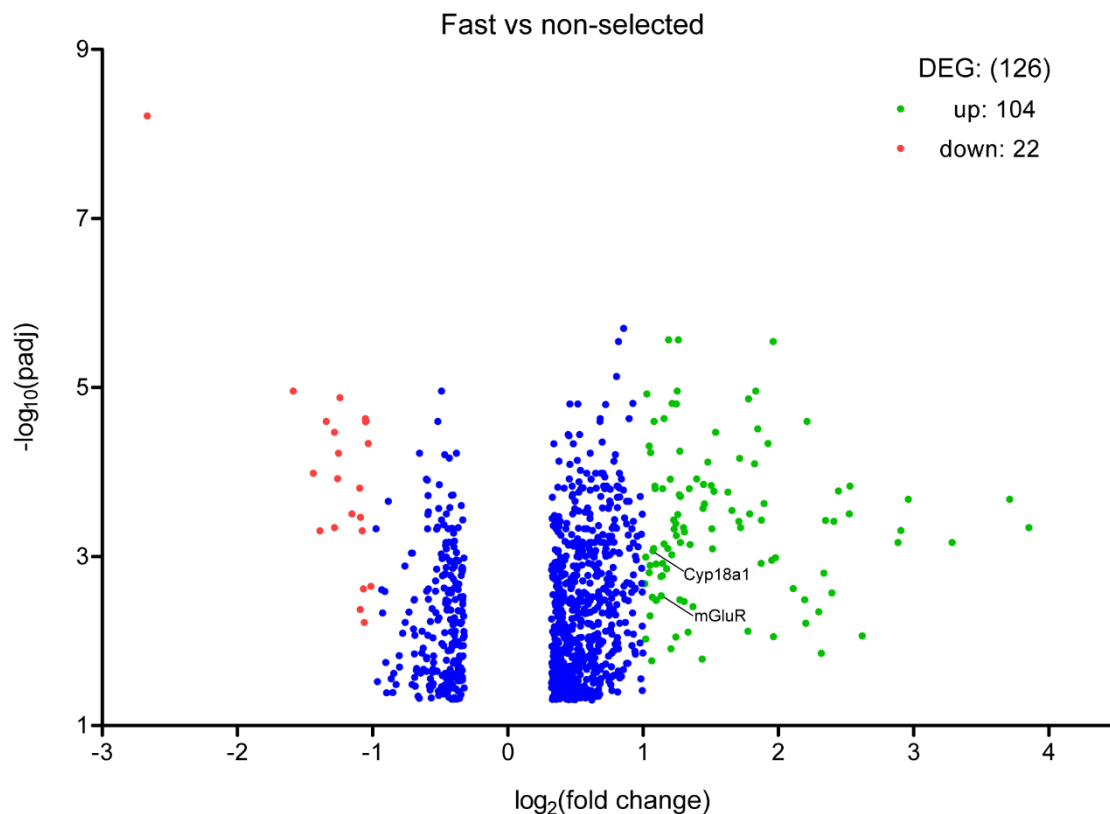


Figure 4-4. Volcano plot of differentially expressed genes in the fast and non-selected lines, with *Cyp18a1* labeled. Differentially expressed genes were selected by  $|\log_2(\text{fold change})| > 1$  and  $padj < 0.05$ . X-axis, the fold change in gene expression between fast and non-selected lines; y-axis, statistical significance of the differences. Dots represent different genes. Green dots represent significantly up-regulated genes  $>2$  fold. Red dots represent significantly down-regulated genes  $<0.5$  fold. Blue dots stand for genes with  $padj < 0.05$  but  $1.25 < FC < 2$ , or  $0.5 < FC < 0.8$ .

To get more precise insight in the differential expression over time of the 45 candidate genes identified in the Pool-seq SNP analysis, we performed qPCR on all of these 45 genes before (76 h post-oviposition), during (92 h) and after (108 h) dorsal closure. Of two polycystin-related genes (genes 22 and 23), we could not detect any expression, but of the remaining 43 genes, 27 showed significant differential expression at one of the three timepoints at least (Figure 4-5).

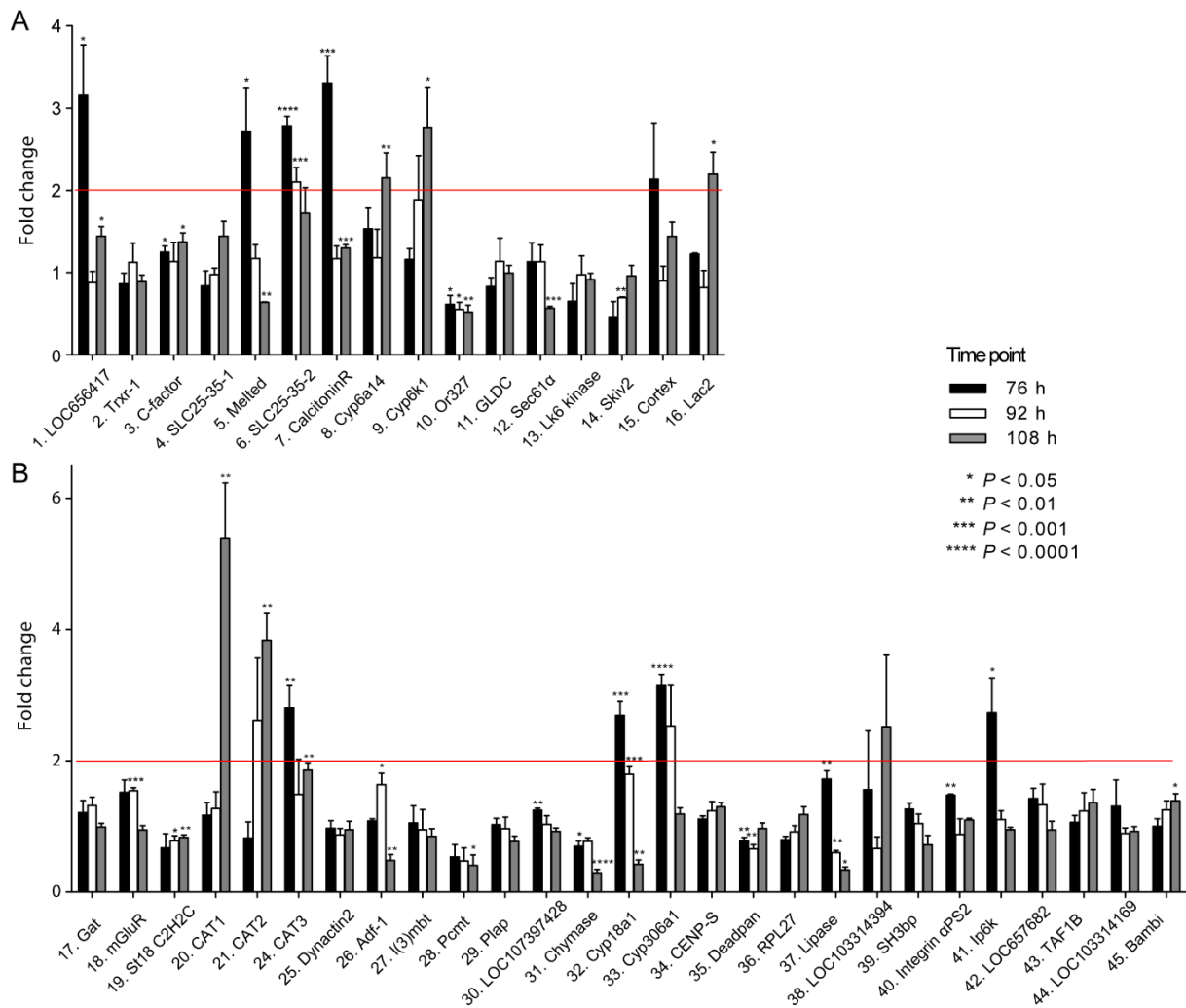


Figure 4-5. Fold change (FC) in the expression of candidate genes. A, FC on chromosome 3, and B, FC on chromosome 9 when we compared between fast and non-selected lines at 76, 92 and 108 hours post-oviposition. Each vertical bar represents the mean fold change plus standard error based on four biological replicates (each replicate is the mean of two technical replicates), of which 2 biological replicates from A line, and 2 from B line. The student t-test was performed to compare the control and treatments. Asterisks, significant difference between fast and non-selected lines. P-values are shown in the figure and indicated with \*,  $P < 0.05$ ; \*\*,  $P < 0.01$ ; \*\*\*,  $P < 0.001$ ; \*\*\*\*,  $P < 0.0001$ .

In particular, before dorsal closure, fast developing embryos showed significantly higher expression of 12 genes ( $P < 0.05$ ), of which 5 genes were located on chromosome 3, and 7 genes on chromosome 9. We also observed significantly lower expression ( $P < 0.05$ ) of 1 gene on chromosome 3, and 2 on chromosome 9. During dorsal closure, 3 genes on chromosome 3 and 6 on chromosome 9 were differentially expressed ( $P < 0.05$ ). After dorsal closure, 10 genes were significantly upregulated ( $P < 0.05$ ), including 6 on chromosome 3, and 4 on chromosome 9. At this last timepoint, 9 genes were significantly downregulated ( $P < 0.05$ ); comprising 3 genes on chromosome 3, and 6 on chromosome 9 (Figure 4-5).

We then applied a more stringent rule: fold change of a gene is greater than 2 or less than 0.4 times. This resulted in 15 selected genes shown in Table 4-1, including *Cyp18a1*, *Lac2*, *lipase* and *Cyp306a1* that were also found in the RNAseq analysis, but not *mGluR*, *Sec61a* and *deadpan*.

Table 4-1. All genes on chromosome 3 and 9 that show a higher than 2 or smaller than 0.4 fold change in qPCRs at 76, 92 or 108 h post-oviposition.

Time point	Chromosome	Genes acronym	Mean of fold change
76 h	3	1. <i>LOC656417</i>	3.16
		5. <i>Melted</i>	2.72
		6. <i>SLC25-35-2</i>	2.78
		7. <i>CalcitoninR</i>	3.30
	9	24. <i>CAT3</i>	2.81
		32. <i>Cyp18a1</i>	2.69
		33. <i>Cyp306a1</i>	3.15
92 h	3	41. <i>Ipk1</i>	2.73
		6. <i>SLC25-35-2</i>	2.10
108 h	3	8. <i>Cyp6a14</i>	2.15
		9. <i>Cyp6k1</i>	2.77
		16. <i>Lac2</i>	2.20
	9	20. <i>CAT1</i>	5.39
		21. <i>CAT2</i>	3.83
		31. <i>Chymase</i>	0.29
		37. <i>Lipase</i>	0.34

### A pRNAi screen identifies four genes under selection that are involved in developmental timing

We performed parental RNAi (pRNAi) screening on these 15 identified candidate genes from Table 4-1 to identify those genes functionally involved in the timing of embryonic development. The primers to generate templates for dsRNA synthesis are shown in Supplementary Table 4-3.

The results showed that the embryos from the mothers injected with *Cyp18a1* dsRNA developed significantly slower (167 h) than those from the mothers injected with the control dsRNA (152 h), as confirmed by a student's t-test ( $P < 0.0001$ ). While two thirds of the eggs hatched to larvae in the control pRNAi, only one third of the *Cyp18a1* RNAi eggs hatched to larvae. Of these larvae, a quarter displayed normal hatching times, whereas three quarters hatched with a strong delay compared to control pRNAi larvae (Figure 4-6). Furthermore, there was no difference in embryonic development between the control pRNAi and blank control (Supplementary Figure 4-3), where we did not inject any mothers but collected the eggs from the same number of females.

We also found slower developmental time upon *Melted* (160 h) and *SLC25-35-2* (161 h) pRNAi, and slightly delayed development upon *CAT1* dsRNA injections (155 h) into *Tribolium* mothers. pRNAi against other candidate genes did not show a significant effect on the time of embryonic development compared to the control (Figure 4-6).

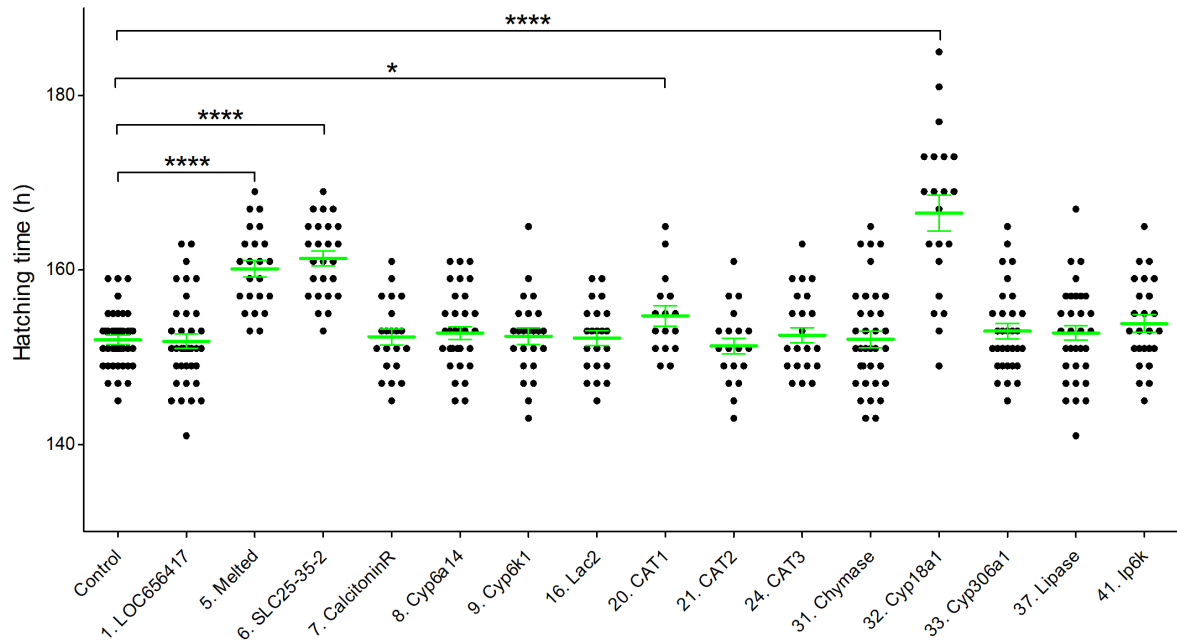


Figure 4-6. The embryonic developmental time of offspring embryos upon a pRNAi screen. It was significantly delayed upon *Melted*, *SLC25-35-2*, *CAT1* and *Cyp18a1* dsRNA injections into 50 *Tribolium* mothers, compared to injections of non-targeting control dsRNA. Key: Green lines, mean of embryonic developmental time plus standard error. Black dot, the time of every hatched embryo. The student t-test was performed to compare the control and treatments. Asterisks, significant difference in hatching time (\*,  $P < 0.05$ ; \*\*\*\*,  $P < 0.0001$ ).

Hatching rate upon *Melted*, *SLC25-35-2* and *Cyp18a1* pRNAi is 56, 63 and 33%, respectively, compared to a 67% hatching rate upon control RNAi. These hatching rates are also reflected in the number of adults observed. When we collected all eggs laid within 2 days from 50 injected mothers, 132, 120, 128 and 11 adults were found upon control, *Melted*, *SLC25-35-2* and *Cyp18a1* pRNAi, respectively (Figure 4-6).

In conclusion, the pRNAi screen has identified four interesting target genes involved in developmental timing: *Melted*, *SLC25-35-2*, *CAT1* and *Cyp18a1*, of which knockdown of *Cyp18a1* caused the largest developmental delay.

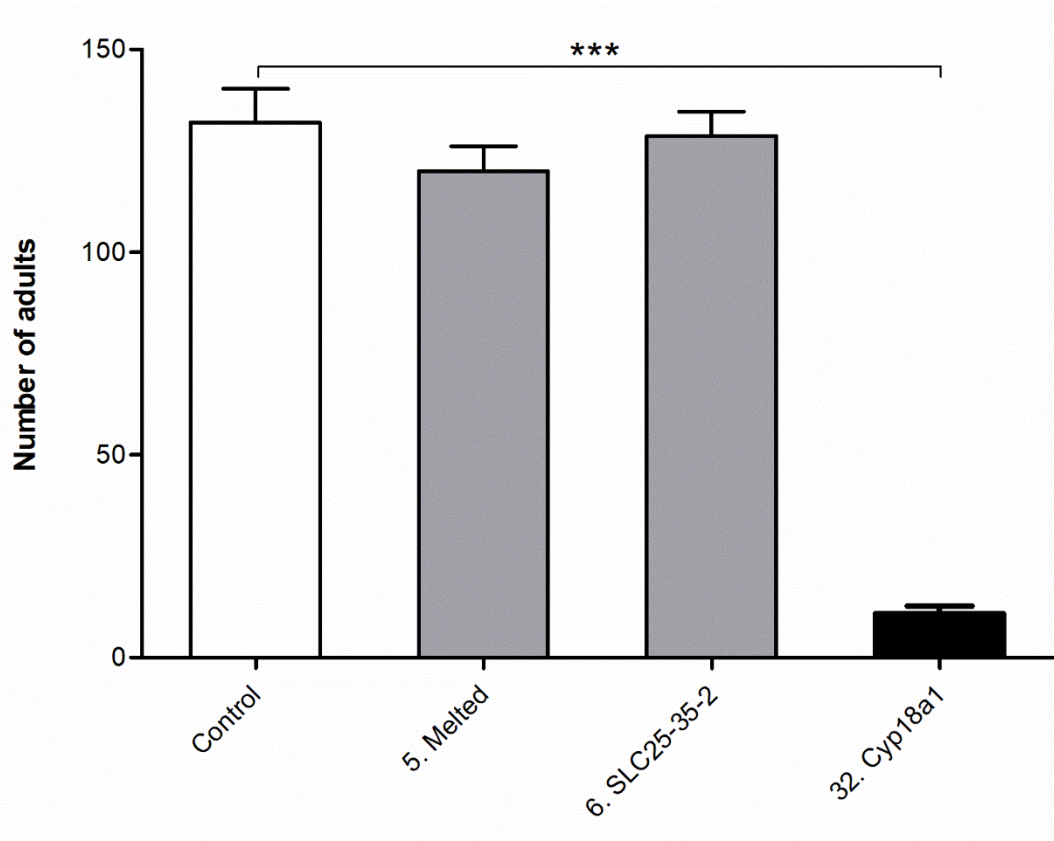


Figure 4-7. Number of adults upon pRNAi, when we collected eggs within 2 days upon control, *Melted*, *SLC25-35-2* and *Cyp18a1* pRNAi, respectively. Measurements were performed in triplicate. Each vertical bar represents the mean fold change plus standard error. The student t-test was performed to compare the control and treatments. Asterisks, significant difference in number of adults (\*\*\*,  $P < 0.001$ ).

### Cyp18a1 is required for pupation and eclosion

*Cyp18a1* is a Cytochrome P450 enzyme that catabolizes active ecdysone (20E) by 26-hydroxylation (Guittard et al., 2011; Rewitz et al., 2010). The steroid hormone 20E is crucial in regulating developmental timing events such as larval moulting, pupation and eclosion (Nijhout et al., 2014). 20E is synthesized by other Cytochrome P450 enzymes, such as Phantom (*Cyp306a1*), Spook (*CYP307A1*), Shadow (*CYP315A1*) and Shade (*Cyp314A1*), collectively called the Halloween genes (Niwa and Niwa, 2016). Besides *Cyp18a1*, three other Cytochrome P450 enzymes are differentially expressed among our selection lines, including one known Halloween gene (*Phantom*, *Cyp306a1*), and two others: *Cyp6a14* and *Cyp6k1*.

As ecdysone regulates tractable developmental events such as pupation and eclosion, we first analyzed the role of these four cytochromes (*Cyp6a14*, *Cyp6k1*, *Cyp18a1*, and *Cyp306a1*) in these timing events. We did this by RNAi with a high concentration of dsRNA (0.8 mg/ml), alongside a combined RNAi against the ecdysone receptors *EcR* and *Ultraspiracle* (*Usp*) in similar concentration as positive control. The results showed that *Cyp18a1* RNAi had caused the highest mortality in both larvae (97%,  $n = 30$ ) and pupae (100%,  $n=30$ ) (Figure 4-8). All the pupae injected with 0.2  $\mu$ L of the highly concentrated (0.8  $\mu$ g/ $\mu$ L) *Cyp18a1* dsRNA arrested their development within 3 d post-injection and then died owing to the melanization reaction (Figure 4-9). The second higher mortality was found in the positive control group in larvae (87%) and pupae (40%) (Figure 4-8). At the same time, no obvious increase in mortality was observed upon *Cyp6a14*, *Cyp6k1* and *Cyp306a1* RNAi in larvae and pupae

compared to non-targeting control dsRNA injections (Figure 4-8). All of primers of the Halloween genes to clone templates for RNAi are listed in Supplementary Table 4-5.

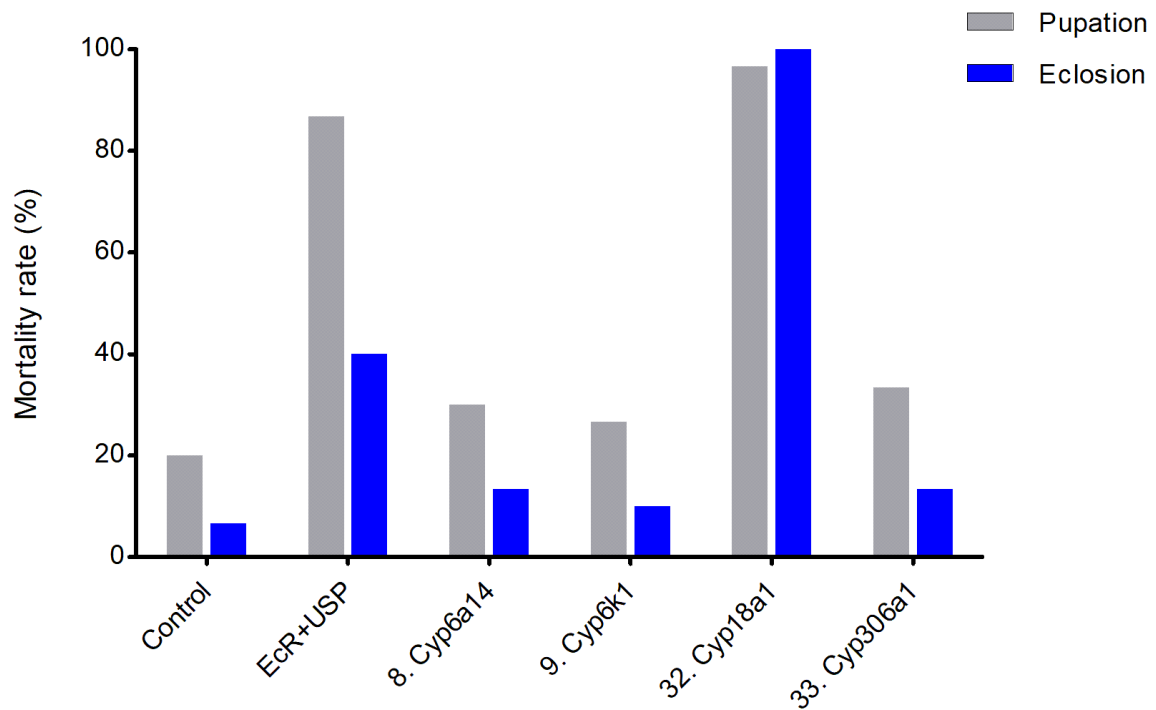


Figure 4-8. Mortality of *Tribolium* larvae and pupae after injections of non-targeting control, the positive control (*Ecr* and *USP*), or the four cytochrome P450s (*Cyp18a1*, *Cyp306a1*, *Cyp6k1* & *Cyp6a14*) dsRNA during pupation (grey columns) and eclosion (blue columns), respectively. n = 30 per treatment.

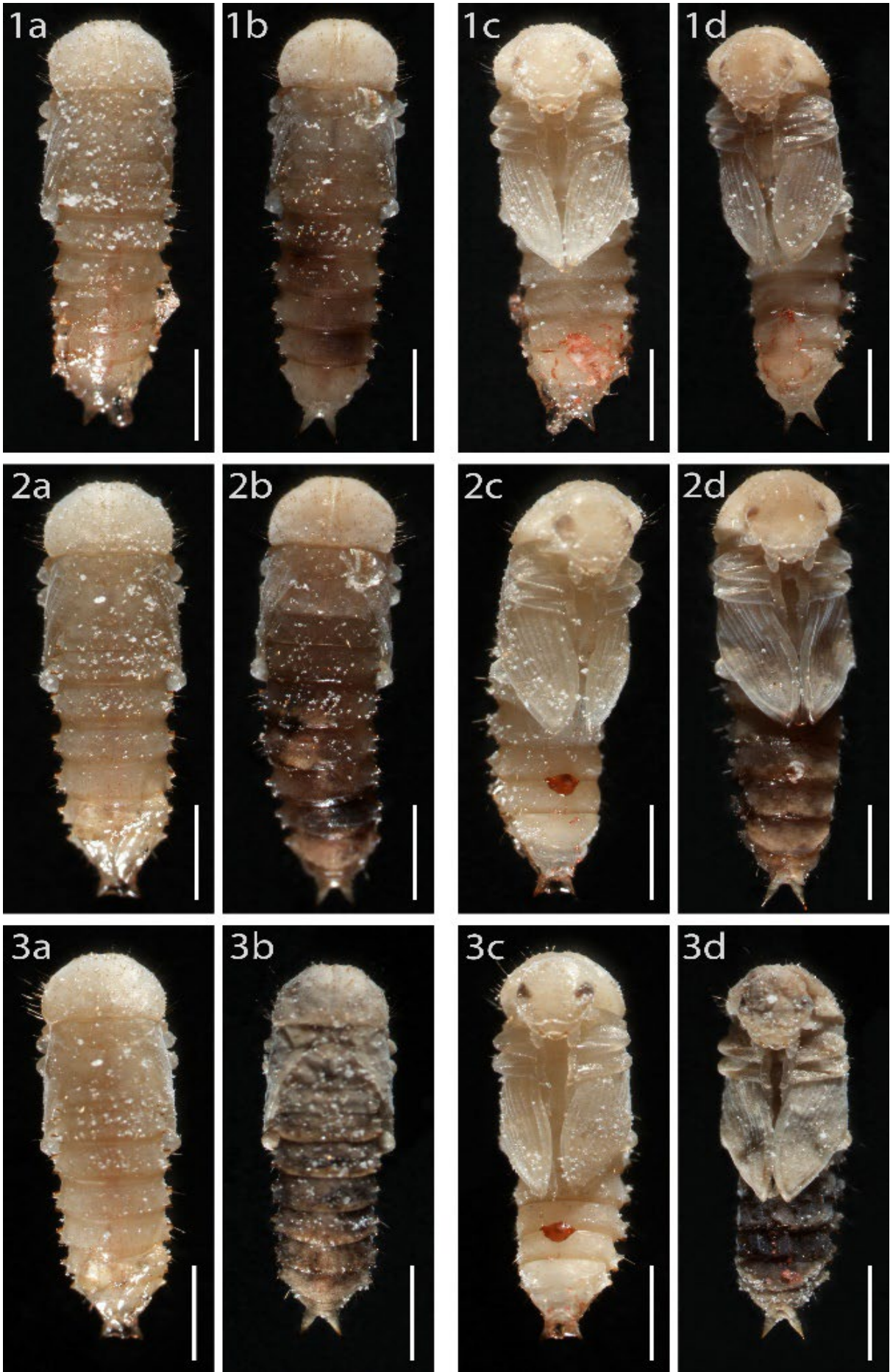


Figure 4-9. *Cyp18a1* RNAi phenotypes in pupae. All the pupae injected with *Cyp18a1* dsRNA arrested their development within 3 days post-injection. Letters "a" and "c" represent the dorsal and ventral side of pupae upon the control gene RNAi, respectively. While "b" and "d" are from the *Cyp18a1* RNAi. "1", "2" and "3" indicate 1 day, 2 days and 3 days post-injection, respectively. Scale bar: 1 mm.

Of the surviving RNAi larvae, the *EcR/USP* RNAi and *Cyp6a14* RNAi (0.8 ug/ul) delayed development to some extent, but the strongest delay was observed upon the strong *Cyp18a1* RNAi (0.8 ug/ul) (Figure 4-10). Surprisingly, no effect on developmental timing was observed upon RNAi against the known Halloween gene *Cyp306a1*. Taken together, *Cyp18a1* RNAi arrested development (Figure 4-9) or led to strong developmental delay (Figure 4-10), whereas no strong indication for involvement of *Cyp6a14*, *Cyp6k1* or *Cyp306a1* was found.

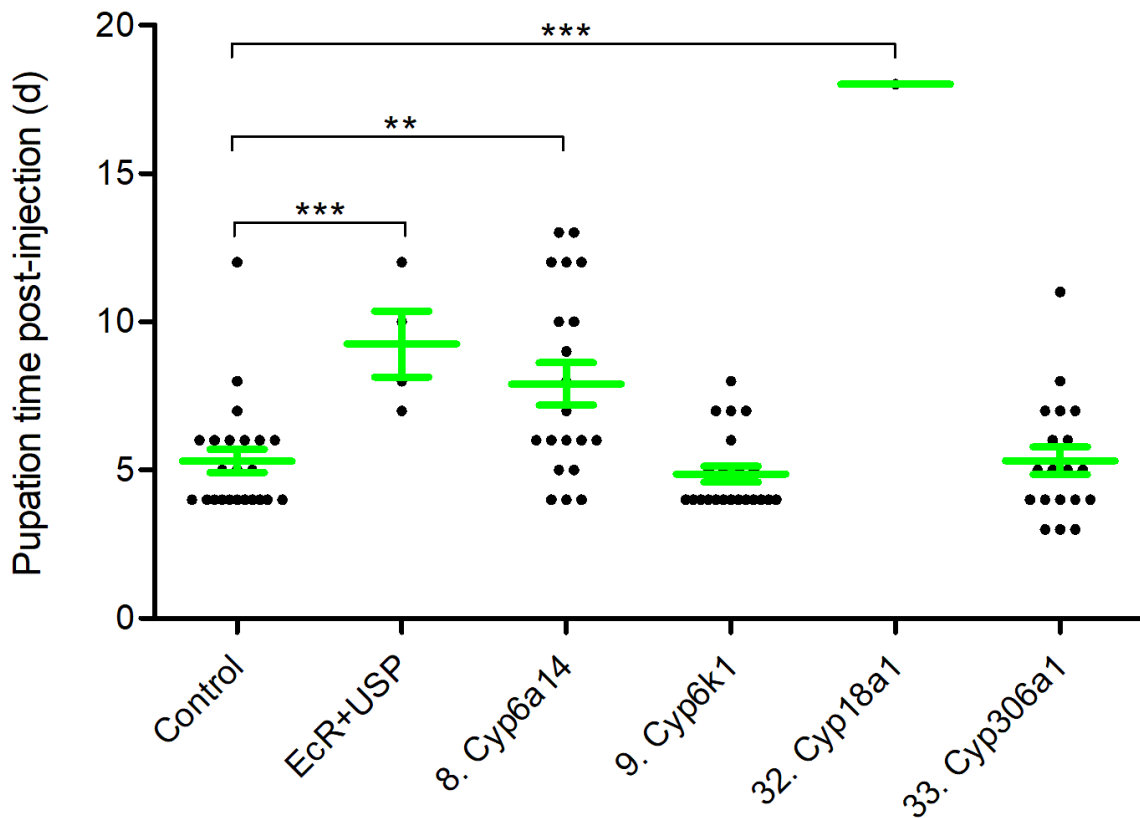


Figure 4-10. Pupation time post-injection with non-targeting control, the positive control or the four cytochrome P450s (*Cyp18a1*, *Cyp306a1*, *Cyp6k1* & *Cyp6a14*) dsRNAs in 15 day old larvae. Key: Green lines, mean of developmental pupation time plus standard error. Black dot, the pupation time of every surviving beetle. The student t-test was performed to compare the control and treatments. Asterisks, significant difference in pupation time post-injection (\*\*,  $P < 0.01$ ; \*\*\*,  $P < 0.001$ ).

To reduce the high mortality upon *Cyp18a1* RNAi (Figure 4-8), and in order to study a developmental phenotype in more detail, we reduced volume and concentration of the dsRNA injections by half (to a 0.1 ul injection of 0.4 ug/ul dsRNA). All the quiescent larvae (prepupae) (n=22) never pupated upon the injections of *Cyp18a1* dsRNA and showed abnormal body color and melanization (Figure 4-11). While 55% (12/22) quiescent larvae can hatch to pupae upon non-targeting control RNAi. This shows that that *Cyp18a1* is required for pupation.



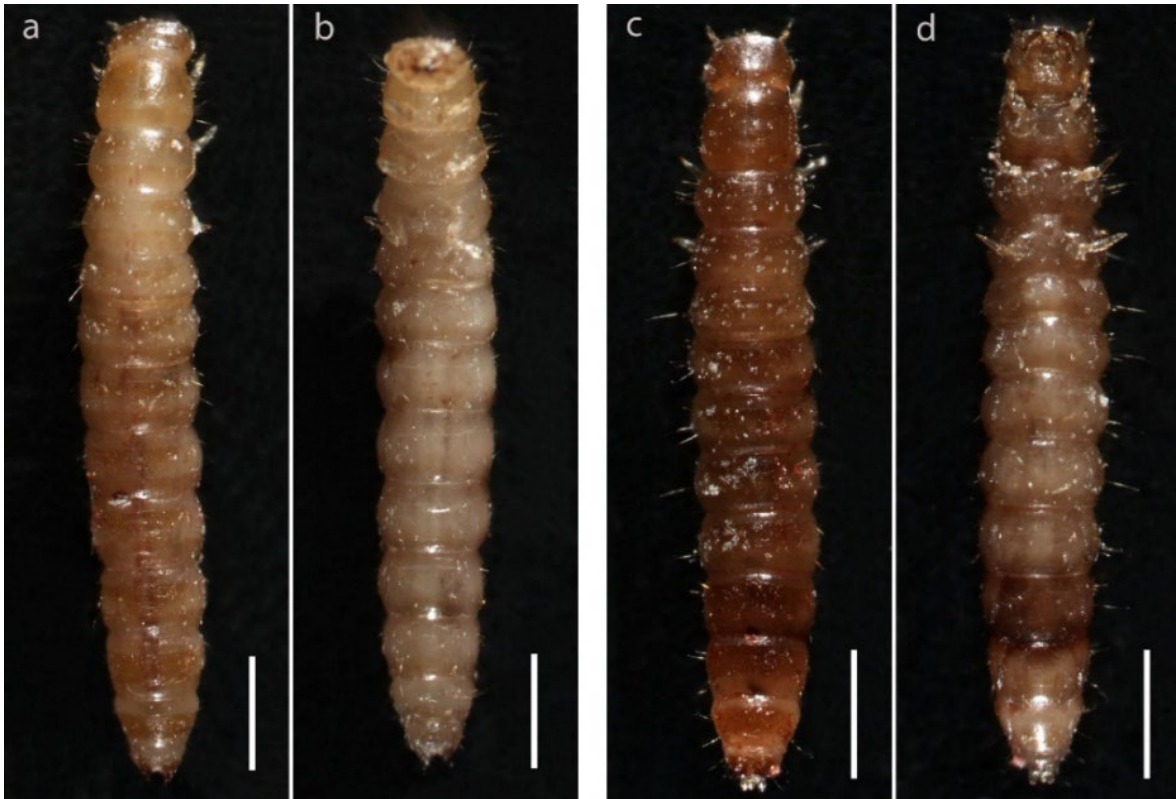


Figure 4-11. *Cyp18al* RNAi phenotypes in prepupae at 30 hours post-injection. Letters "a" and "b" represent the dorsal and ventral sides, respectively, of prepupae after injections of the control dsRNA; "c" and "d" are results upon *Cyp18al* RNAi. Scale bar: 1 mm.

For pupae injections, a mixture of 0.1  $\mu\text{l}$  of 0.4  $\mu\text{g}/\mu\text{l}$  dsRNA was injected into the abdomen of 0-day pupae. All of the control injected pupae ( $n = 20$ ) eclosed as adults (Figure 4-12a-c). However, 85% of the *Cyp18al* dsRNA injected pupae ( $n = 17/20$ ) never eclosed (Figure 4-12dg,eh,fi). These pupae sclerotized, but did never develop typical adult features, such as the folding of wings and elytra over the abdomen (Figure 4-12dg,eh,fi). In conclusion, *Cyp18al* is also required for eclosion.

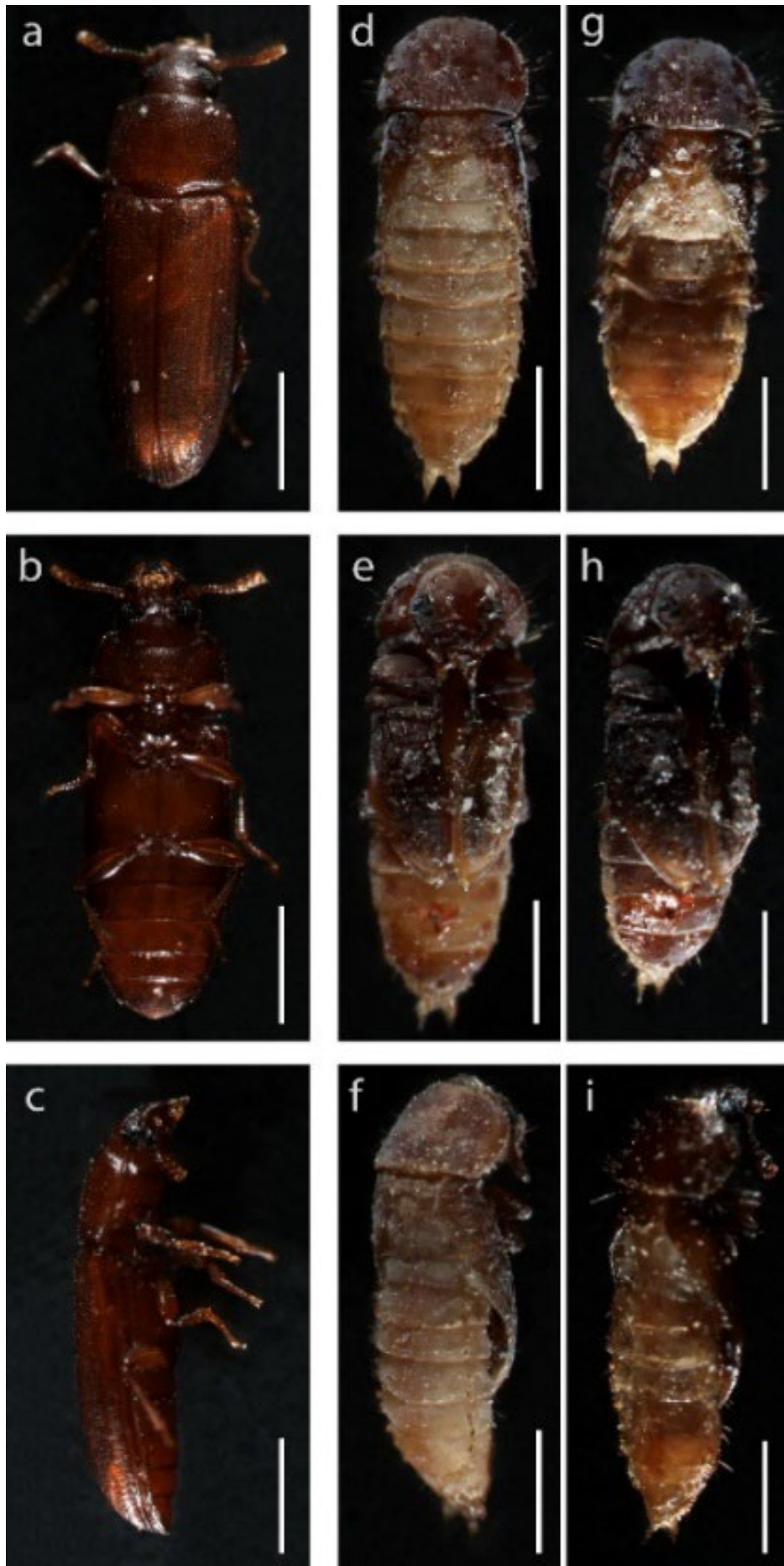


Figure 4-12. Low concentration (0.4  $\mu\text{g}/\text{ul}$ ) of *Cyp18a1* dsRNA injected beetles resulted in abnormal phenotypes in the folding of wings and elytra over the abdomen. The abnormal wing could not cover the dorsal side of the pupae and these pupae subsequently died due to dehydration (d, g, f, i). Sclerotization of the abdomen was incomplete (d, g, e, h, f, j). Letters "a", "b" and "c" represent the dorsal, ventral and lateral side of adult, respectively upon injections of the control dsRNA; "d", "e" and "f" are from pupae that failed to eclose after *Cyp18a1* dsRNA injections; "g", "h" and "i" are from older pupae which failed to eclose and died of dehydration after the *Cyp18a1* dsRNA injections. Scale bar: 1 mm.

Taken together, our RNAi data demonstrate that *Cyp18a1* is required for pupation and eclosion. We wondered whether *Cyp18a1* expression peaks during these developmental events. Therefore, we measured *Cyp18a1* expression in the lab-strain Georgia line using qPCR. Indeed, *Cyp18a1* expression increases in prepupae towards pupation (Figure 4-13), and increases in pupae towards eclosion (Figure 4-13B).

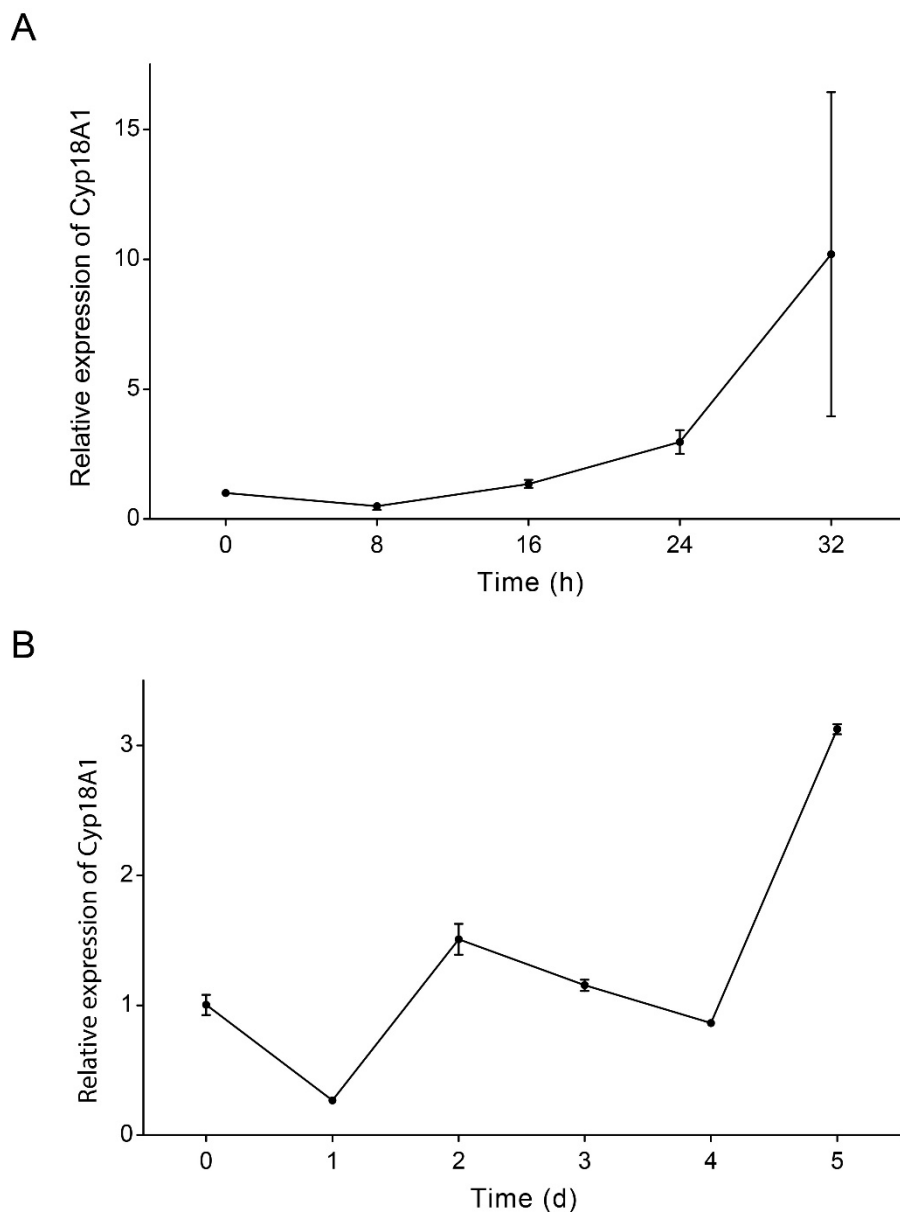


Figure 4-13. Relative expression of *Cyp18a1* in prepupa (A) and pupa (B) during their development. Each point represents the mean *Cyp18a1* expression based on two biological replicates (each replicate is the mean of two technical replicates).

## Ecdysone titers and *Cyp18a1* expression levels rise during dorsal closure

Although Ecdysone is well known to regulate events such as molting or metamorphosis, an ecdysone peak has also been detected during embryogenesis in *Drosophila* (Kozlova and Thummel, 2003; Maróy et al., 1988). This peak has recently been shown to regulate dorsal closure (Yoo et al., 2021). We first investigated ecdysone levels, *Cyp18a1* expression, expression of the Halloween gene *Spook* (*Cyp307a1*) and of the ecdysone target gene *Broad* (Niwa and Niwa, 2016).

We found two peaks of 20E titers during GA-1 embryonic development: a weak peak (248.40 pg/mL) at 40 h and a strong peak (3711.34 pg/mL) at 120 h post-oviposition (Figure 4-14). Titers of 20E kept a relatively lower level between 40 h and 96 h post-oviposition. However, it started to gradually increase at 96 h and reached the peak level at 120 h post-oviposition. The following 20E levels dropped dramatically and then stayed at a relatively lower level until hatching. The peak at 120 h post-oviposition is preceded by high gene expression of the early Halloween gene *spook* (*Cyp307a1*, *Spo*) involved in the ecdysone biosynthesis (blue, Figure 4-14). The ecdysone-inactivating enzyme *Cyp18a1* starts to increase at 112-120 h, and remains high until hatching. The early ecdysone response gene *broad* (*Br*) follows the ecdysone peak with some delay (Figure 4-14). All of primers of the Halloween genes and *Br* for qPCR are listed in Supplementary Table 4-5.

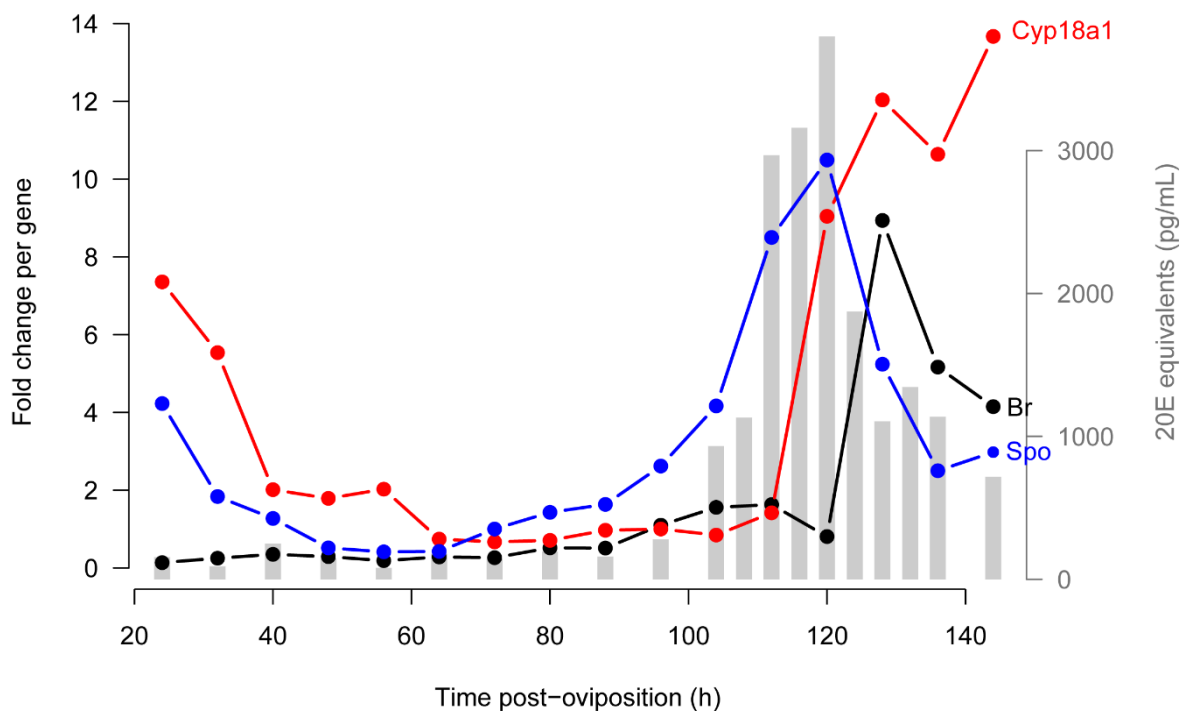


Figure 4-14. Ecdysone titers (grey columns) and the related gene expression (lines) during embryonic development of the wild-type Georgia strain of *Tribolium castaneum*. Black line stands for relative expression of *broad* (*Br*) over time, red line is *Cyp18a1*, and blue line is *spook* (*Cyp307A1*, *Spo*). The transcript level of *Br*, *Cyp18a1* and *Spo* was taken as 1 at 96 h, 96 h and 72 h post-egg laying, respectively. Each column stands for the mean of ecdysone level based on two technical replicates. Each point represents the mean fold change plus standard error based on two biological replicates (each replicate is the mean of two technical replicates according to the protocol of the kit).

In addition, we also quantified other Halloween genes involved in the ecdysone biosynthesis during embryonic development of *T. castaneum*, including *phantom* (*Cyp306A1*, *Phm*), *disembodied*

(*Cyp302A1*, *Dib*), *shadow* (*Cyp315A1*, *Sad*) and *shade* (*Cyp314A1*, *Shd*). *Phm* shows the highest expression level at 128 h post-egg laying. *Dib* is highly expressed at 32 h and shows the same expression pattern with *Phm* between 96 h and 136 h. *Sad* is highly expressed at both 24 h and 48 h. *Shd* shows two dramatic expression peaks at 48 h and 96 h, respectively (Figure 4-15).

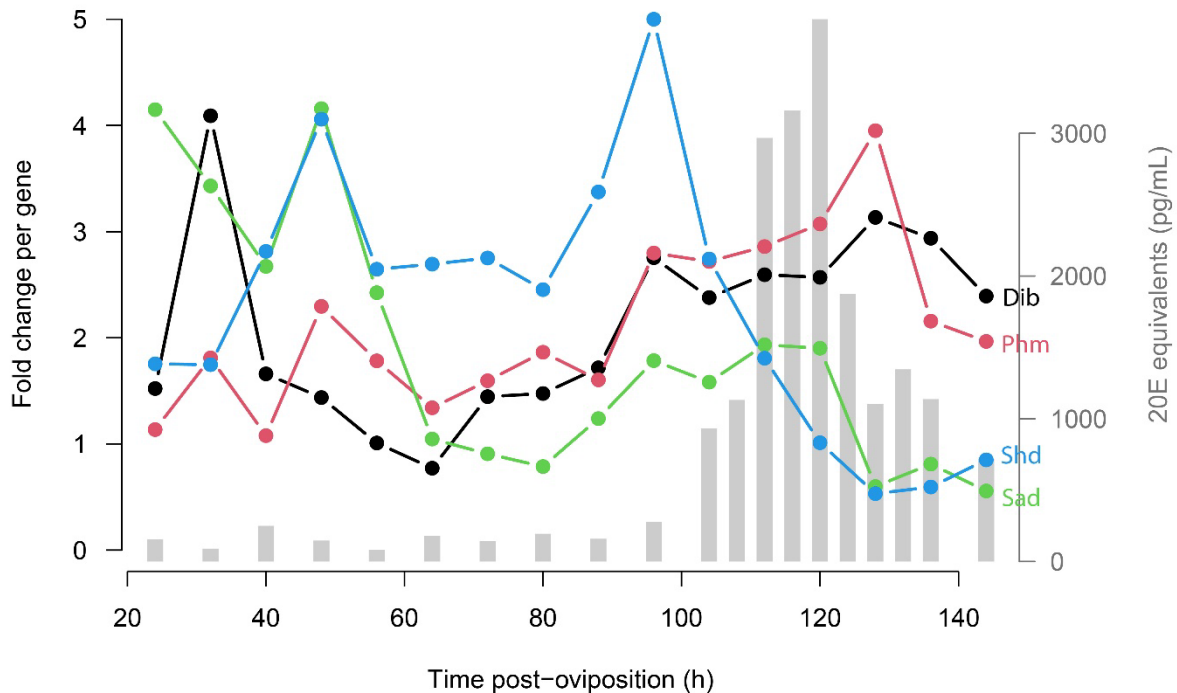


Figure 4-15. Ecdysone titers (grey columns) and some Halloween gene expression (lines) during embryonic development of the wild-type Georgia strain of *Tribolium castaneum*. Black line stands for relative expression of *disembodied* (*Cyp302A1*, *Dib*) over time, red line is *phantom* (*Cyp306A1*, *Phm*), blue line is *shade* (*Cyp314A1*, *Shd*), and green line is *shadow* (*Cyp315A1*, *Sad*). The transcript level of *Phm*, *Dib*, *Sad* and *Shd* was taken as 1 at 40 h, 56 h, 64 h and 120 h post-egg laying, respectively. Each column stands for the mean of ecdysone level based on two technical replicates. Each point represents the mean fold change plus standard error based on two biological replicates (each replicate is the mean of two technical replicates according to the protocol of the kit).

At the same time, around 50 GA-1 eggs were fixed and stained (DAPI) to assess the specific embryonic developmental stage at each time point of testing 20E titers. Judgement values were described under 'Variation under artificial selection is in the timing after germband extension, before dorsal closure' (Supplementary Figure 4-21). According to fluorescent microscopic results for GA-1 eggs, 40 h is at the stage of extended limbs, and 120 h post-oviposition is at the complete dorsal closure. Interestingly, 96 h is around the stage of start of dorsal closure (Figure 4-16).

In summary, a high ecdysone peak, and increasing *Cyp18a1* levels are found during dorsal closure, suggesting a role for ecdysone during dorsal closure.

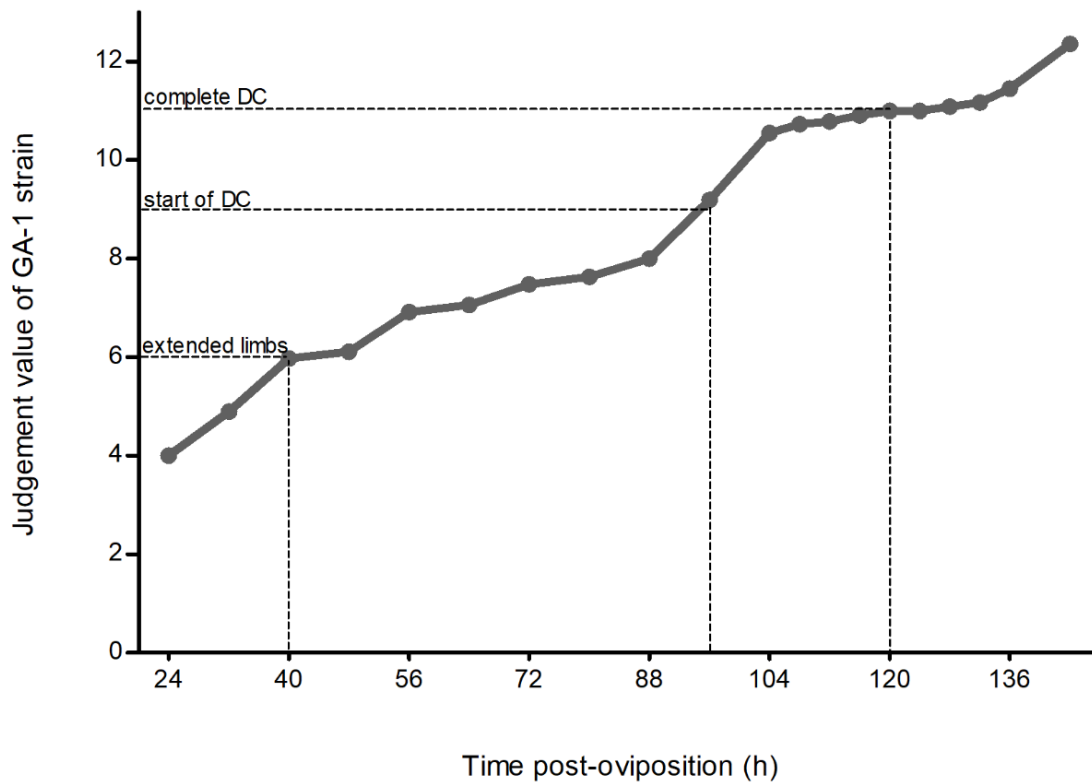


Figure 4-16. Judgement values given to fourteen embryonic stages are used to score embryonic development of wild-type Georgia strain. 0=no nuclei at surface; 1=undifferentiated blastoderm; 2=differentiated blastoderm; 3=gastrulation; 4=extending germband; 5=extended germband; 6=limbs growing and extending; 7=retracting germband; 8=completely retracted germband; 9=start of dorsal closure (dorsal organ formation); 10=dorsal closure in progress; 11=dorsal closure completed; 12=hatching; and 13=hatched. See more details in Supplementary Figure 4-1. Fast A, fast B, non-selected A (NS A), non-selected B (NS B), slow A and slow B are shown with red, orange, green, light green, dark blue, and light blue lines.

### ***Cyp18a1* is expressed in the dorsal organ**

To reveal what tissue is involved in ecdysone synthesis and degradation during dorsal closure, we performed *in situ* hybridization for *Spook* and *Cyp18a1*. We found that *Spo* is expressed in the dorsal ectoderm already before dorsal closure (Figure 4-17A), and continues this expression pattern during dorsal closure (Figure 4-17B). The dorsal closure process is shown schematically in Figure 1-6B (Chapter 1) and Supplementary Figure 4-4. In contrast, we could not detect expression of *Cyp18a1* during germband retraction (Figure 4-17C). At the beginning of dorsal closure, *Cyp18a1* starts to be expressed in the dorsal organ, the contracting serosa (Panfilio, 2008) (Figure 4-17D).

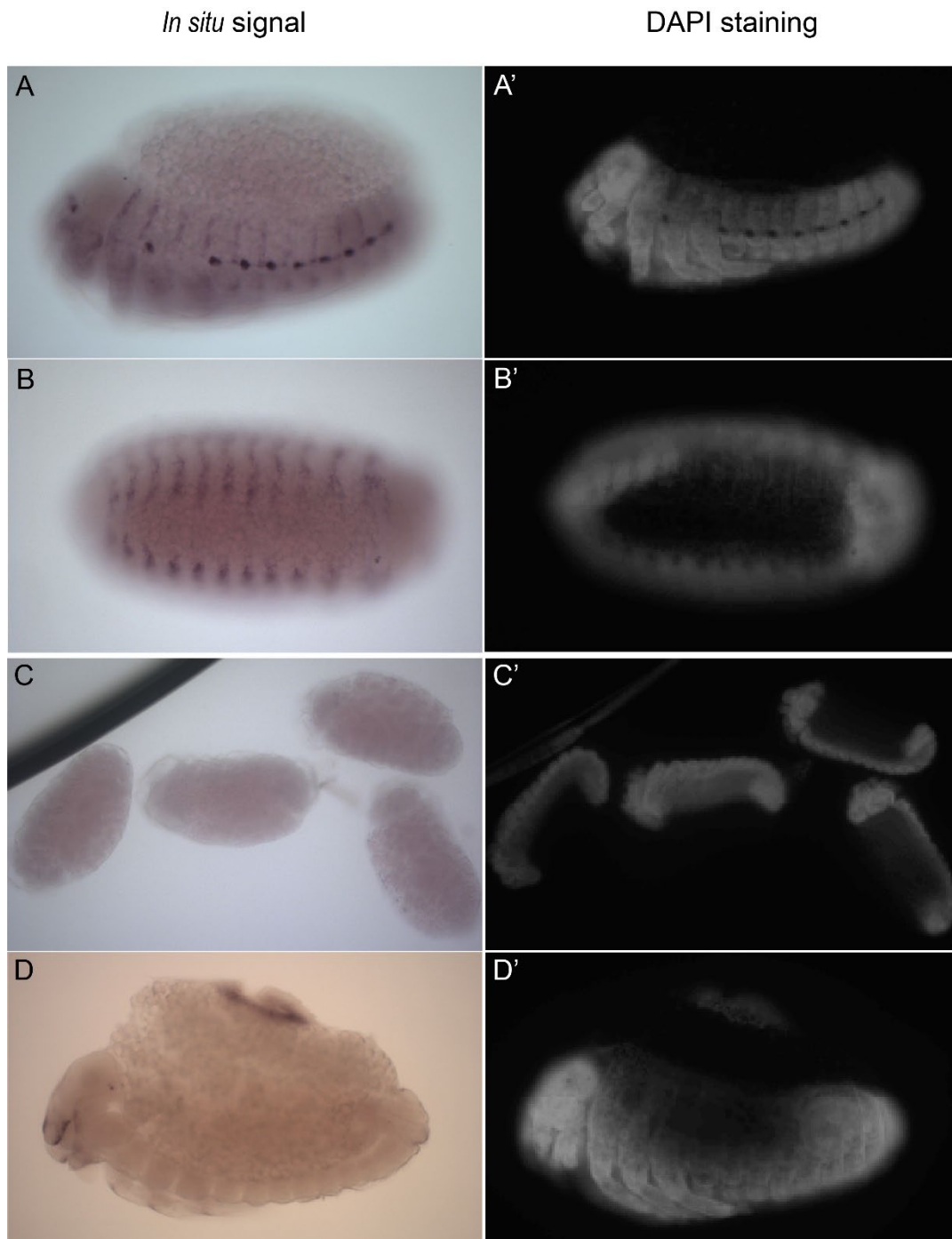


Figure 4-17. *In situ* hybridization for *spook* and *Cyp18a1*. A, *Spook in situ* hybridization at the retracted germband stage. B, *Spook in situ* hybridization during dorsal closure. C, *Cyp18a1 in situ* hybridization at the retracting or retracted germband stage. D, *Cyp18a1 in situ* hybridization at the stage of start of dorsal closure. A', B', C', and D', the corresponding embryos stained by DAPI, respectively.

## Cyp18a1 degrades active ecdysone and is required for dorsal closure

To understand the role of Cyp18a1 during embryonic development, we injected 200 female beetles with *Cyp18a1* dsRNA. When they started to lay eggs, we fixed and stained (DAPI) these eggs every day before they hatch to larvae. When we observe the stage still after more than 24h, we define this as a developmental arrest. When we find a developmental stage later, but less than 24 h after this stage was observed in the control pRNAi, we categorize this as a developmental delay. For example, the formation of the blastoderm occurs in the 0-1 d old eggs. If we observed this stage in 1-2 d old eggs, we define this kind of eggs as a developmental delay. If we observed this stage at later stages (2-7 d old), we define this kind of eggs as a developmental arrest. As the stage of no nuclei at surface occurs at the very beginning of development, we define 1-7 d old eggs at this stage as “No start of development”.

Fluorescent microscopic analysis showed that 20% of the *Cyp18a1* RNAi eggs (out of 147) showed no start of development, compared to only 8% in the control (out of 248 eggs). During blastoderm, germband extension and dorsal closure, a total of 43% eggs showed a developmental arrest upon *Cyp18a1* RNAi (Table 4-2). The eggs arrested during germband extension remained a short germband during further development (Figure 4-18A), suggesting a role for Cyp18a1 in segmentation or germ band extension. Most importantly, the embryos that were arrested during dorsal closure were left dorsally open (Figure 4-18B, Figure 4-19). This demonstrates that Cyp18a1 is required for dorsal closure.

Table 4-2. Summary of phenotypic percentage of the eggs upon the control and *Cyp18a1* pRNAi. No start of development stands for the stage of no nuclei at surface.

Development of the eggs		Control (%)	Cyp18a1 (%)
Normal development		88	33
No start of development		8	20
Developmental delay		4	4
	during blastoderm	0	5
Developmental arrest	during germband extension	0	13
	during dorsal closure	0	25



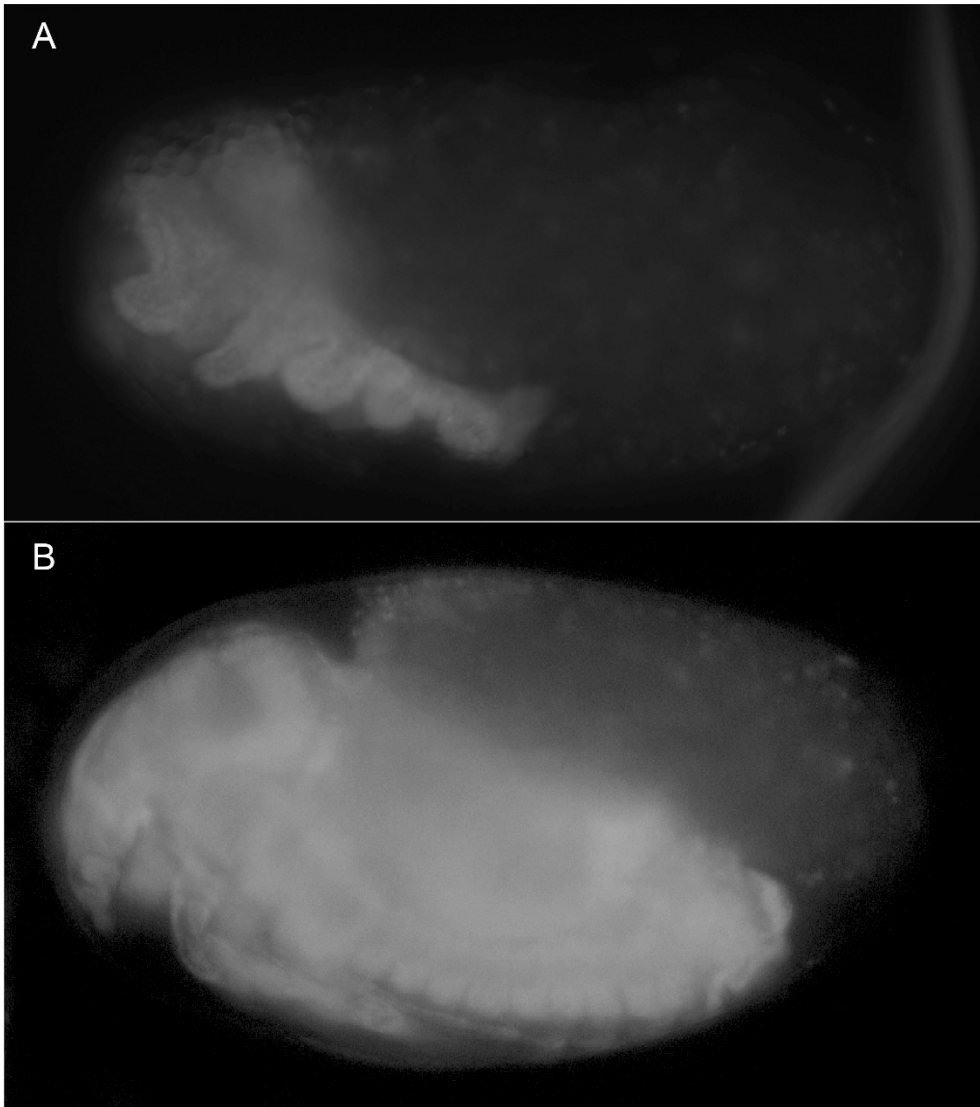


Figure 4-18. Phenotypes upon *Cyp18a1* pRNAi during germband extension, showing a short germband (A) and a dorsally open embryo at dorsal closure (B).

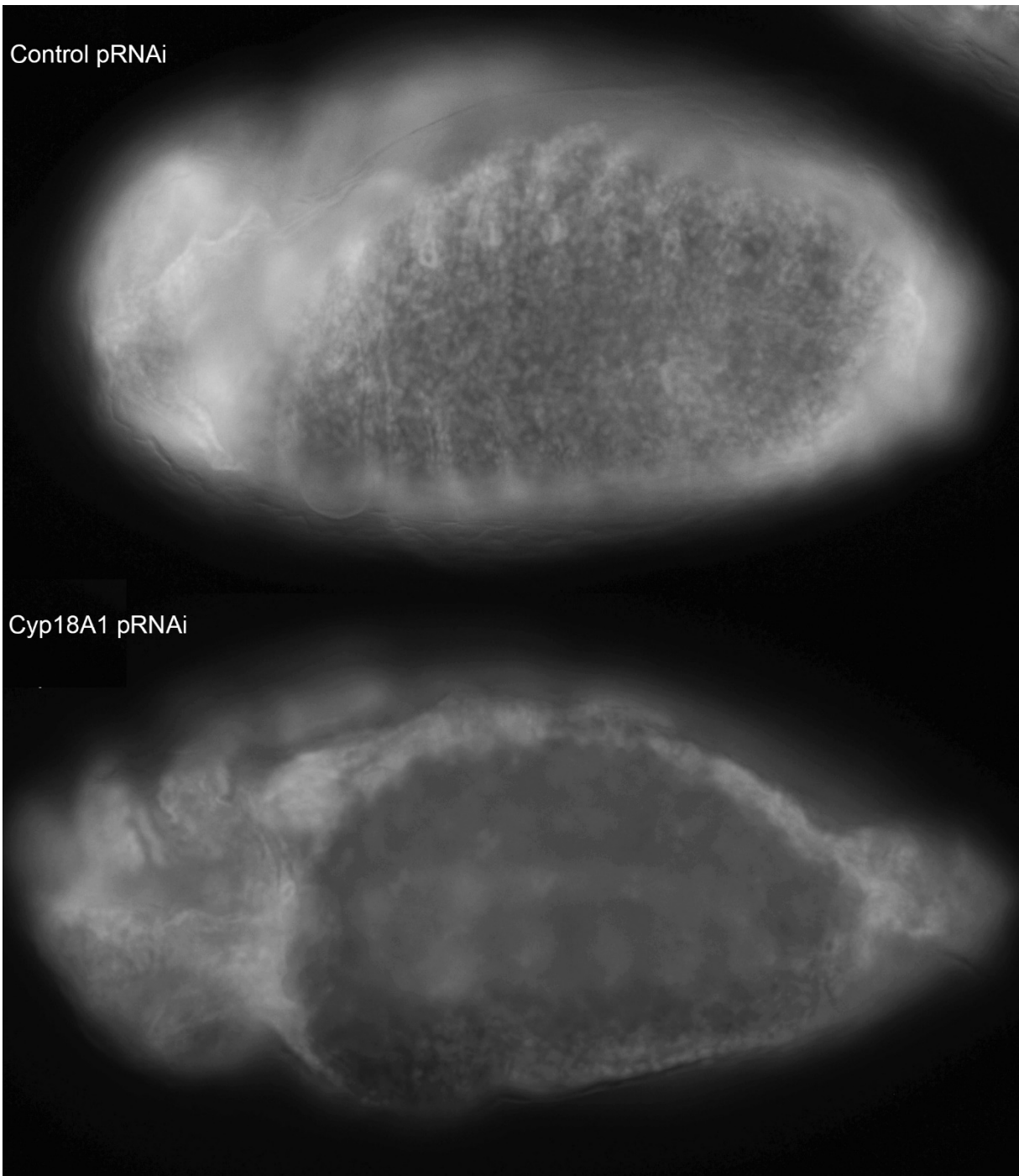


Figure 4-19. Phenotypes of the embryos upon control and *Cyp18a1* pRNAi, respectively. Upon control pRNAi, the dorsal side of the embryo is well-closed, while the dorsal side of the embryo is still open upon *Cyp18a1* pRNAi.

By combining *Cyp18a1* pRNAi results from the pRNAi screen (Figure 4-6) and fluorescent microscopic analysis (Table 4-2), we assessed embryonic development of the eggs upon *Cyp18a1* pRNAi (Figure 4-20). It is estimated that 20% eggs are not fertilized or do not start development (see first line in Figure 4-20). In addition, 5%, 13% and 25% eggs are arrested during blastoderm, germband extension and dorsal closure, respectively (Figure 4-20). Of the eggs that hatch, 8% eggs hatch with a normal developmental time, whereas 25% eggs delay their development, as we observed in Figure 4-6.

### Summary of Cyp18a1 pRNAi

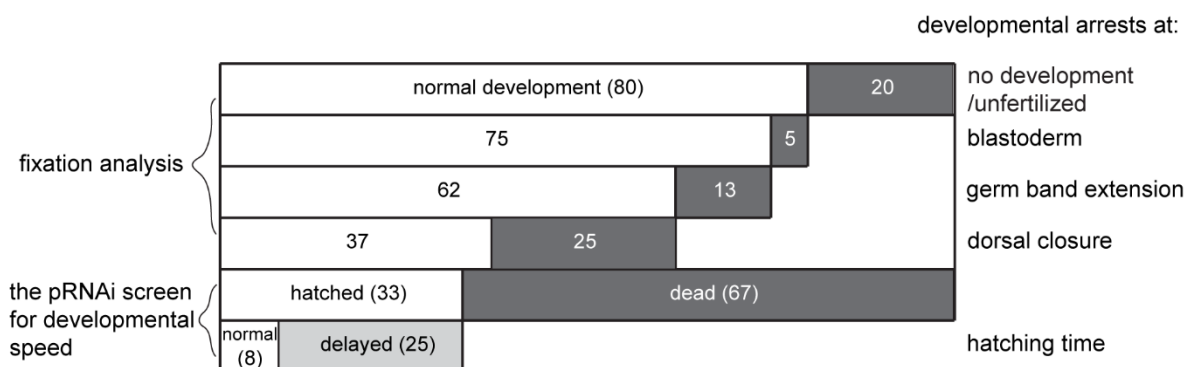


Figure 4-20. The assessment for embryonic development of the eggs upon *Cyp18a1* pRNAi. Normal development of the eggs is in white boxes. The death or failure of development are indicated with a certain percentage in dark grey boxes. Of one third hatched eggs, the developmental delay is indicated with a certain percentage in a light grey box.

As *Cyp18a1* degrades active ecdysone (Guittard et al., 2011; Rewitz et al., 2010), the 20E levels of the eggs upon *Cyp18a1* pRNAi were measured focusing on the dorsal closure stage. For measuring 20E titer, we collected the precipitate from 20 eggs for each time point and did not dilute it with EIA buffer. We collected 96 to 160 h old eggs post-oviposition upon *Cyp18a1 pRNAi*. The results showed that 20E titers gradually reached the relatively higher level at 128 h and gave rise to the highest titer at 160 h post-oviposition (Figure 4-21). This confirms that, also in *Tribolium*, *Cyp18a1* degrades active ecdysone. Together with the morphological analysis, it also shows that a pulse of ecdysone is required for dorsal closure and that mere high levels are not sufficient.

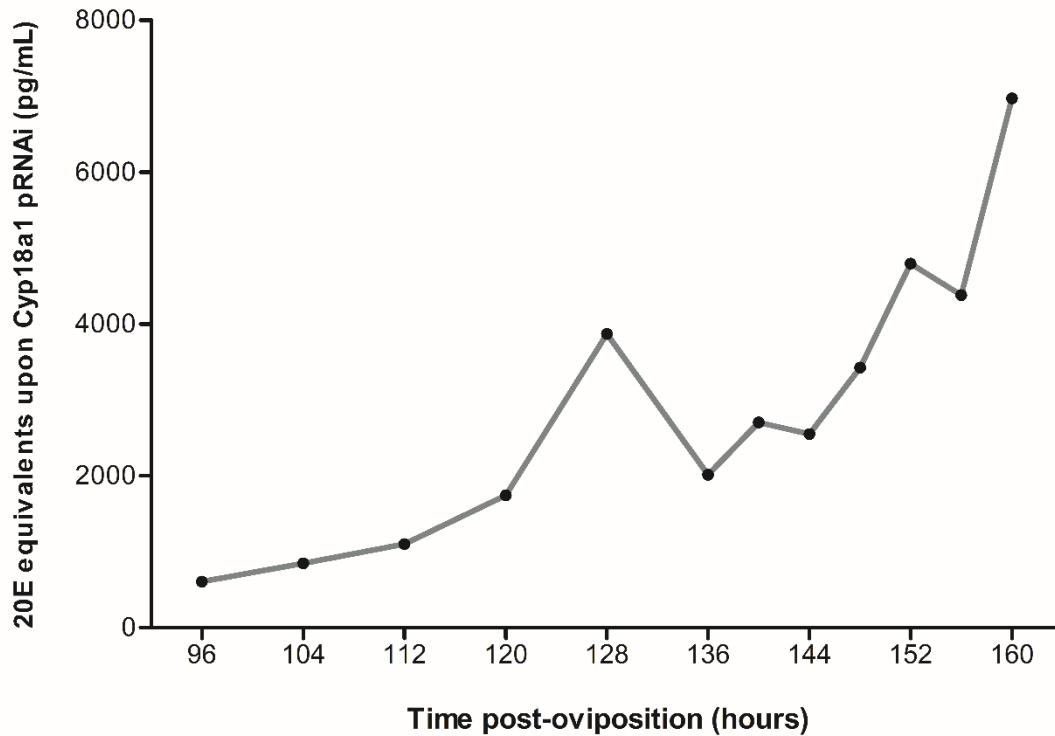


Figure 4-21. Ecdysone titers of the eggs upon *Cyp18a1* pRNAi. Black dots stand for ecdysone levels measured in duplicate according to the manufacturer's instruction.

In summary, when *Cyp18a1* is knocked down, ecdysone levels continue to increase, and a significant fraction of the embryos remain dorsally open and do no complete dorsal closure.

### **Spook may be involved in segmentation or germband extension**

We also attempted to investigate the role of the other Halloween genes during embryonic development. However, using parental RNAi, we found that no eggs were laid within a month post-injection against *Cyp307a1* (*spook*, *Spo*), *Cyp315a1* (*shadow*, *Sad*), *Cyp314a1* (*shade*, *Shd*), and the mix of *EcR* and *USP*. The beetles did lay eggs upon *Cyp306a1* (Figure 4-6) and *Cyp302a1* (*disembodied*, *Dib*) pRNAi. As reported before (Figure 4-6), pRNAi against *Cyp306a1* did not alter developmental time. In addition, we did not find significant difference of the embryonic developmental time upon *Cyp302a1* RNAi, compared to the control pRNAi (Figure 4-22).

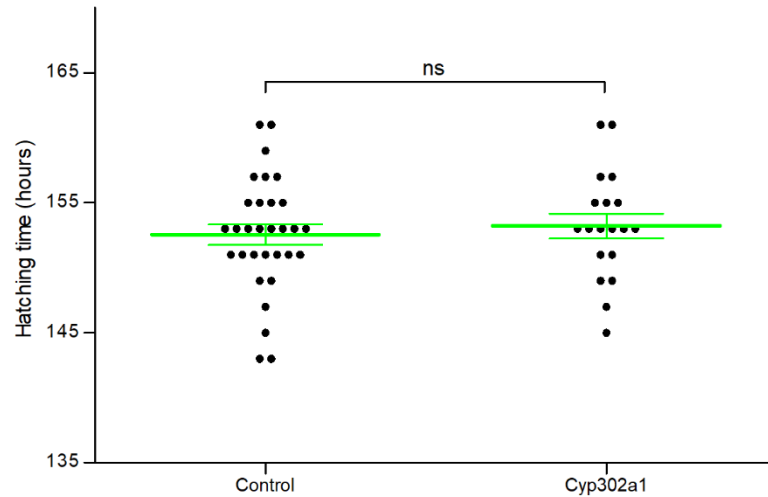


Figure 4-22. The embryonic developmental time of offspring embryos upon *Cyp302a1* dsRNA injections into 50 *Tribolium* mothers, compared to injections of non-targeting control dsRNA. Key: Green lines, mean of embryonic developmental time plus standard error. Black dot, the time of every hatched embryo. The student t-test was performed to compare the control and *Cyp302a1* pRNAi. Key: ns, no significant difference observed in hatching time.

To circumvent adult sterility upon pRNAi, we studied the role of *Spo*, *Sad* and *Shd* during embryonic development, using embryonic RNAi (eRNAi) on 4-6 h old eggs of the LifeAct-nGFP line (van Drongelen et al., 2018). In total, 140 eggs were injected per gene. Embryos were checked under a Zeiss Axioplan 2 microscope once a day post-injection. Fluorescent microscopic analysis showed that all eggs could hatch to larvae upon *Sad* and *Shd* RNAi. The percentage of hatched eggs were 15.7% and 21.4% upon *Sad* and *Shd* eRNAi, respectively, compared to 29.3 percent hatching upon the control RNAi. However, no eggs hatched upon injections of *Spo* dsRNA. The vast majority of *Spo* RNAi eggs died during germband extension, suggesting a role for *Spo* during germband extension or segmentation (Figure 4-23).

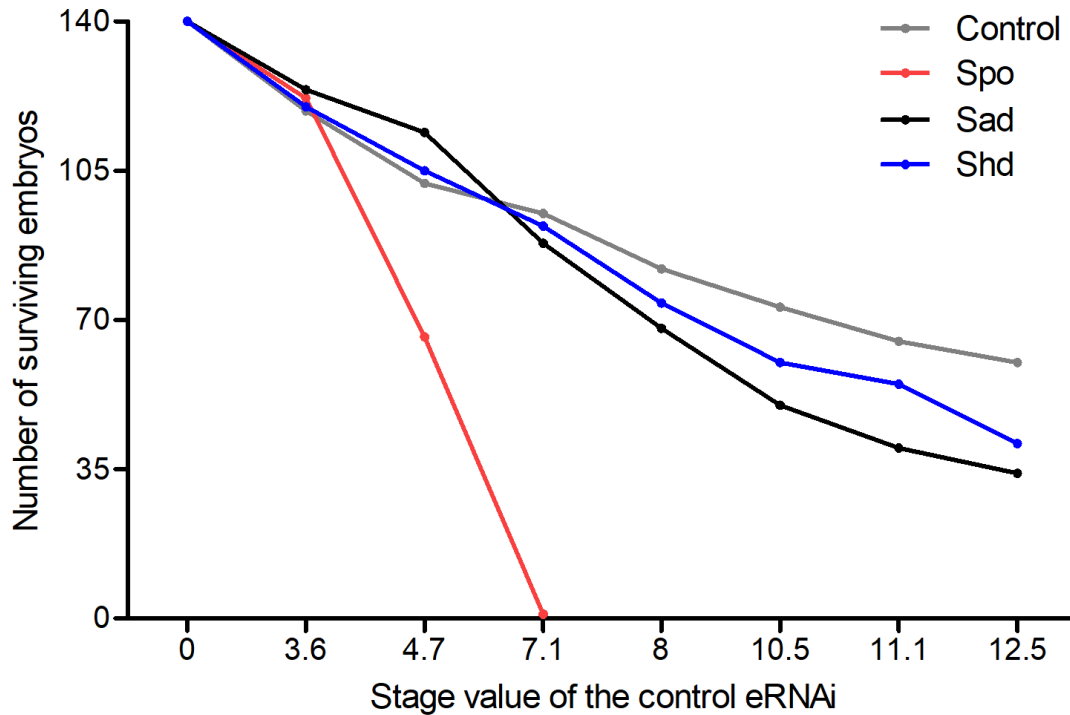


Figure 4-23. The number of surviving embryos upon the control (grey line), *Spo* (*Cyp307a1*, *spook*, red line), *Sad* (*Cyp315a1*, *shadow*, black line) and *Shd* (*Cyp314a1*, *shade*, blue line) eRNAi. 0=no nuclei at surface; 3=gastrulation; 4=extending germband; 5=extended germband; 6=limbs growing and extending; 7=retracting germband; 8=completely retracted germband; 10=dorsal closure in progress; 11=dorsal closure completed; 12=hatching; and 13=hatched. See more details in Supplementary Figure 4-1.

### Embryonic ecdysone peaks differ in timing and height among the selection lines

To investigate if the ecdysone levels vary among the selection lines, ecdysteroid titers during embryonic development were determined (Figure 4-24). The results showed that 20E equivalents of fast, non-selected and slow lines remained at low concentrations during the first 80, 88 and 96 h post-oviposition, respectively. Ecdysteroid titers reached their peaks at 96, 104, and 120 h post-oviposition, respectively. After these peaks, ecdysteroid titers gradually dropped back to the relatively lower levels among the selection lines. Thus, like the start of dorsal closure, the ecdysone peaks also differ consistently in timing among the selection lines.

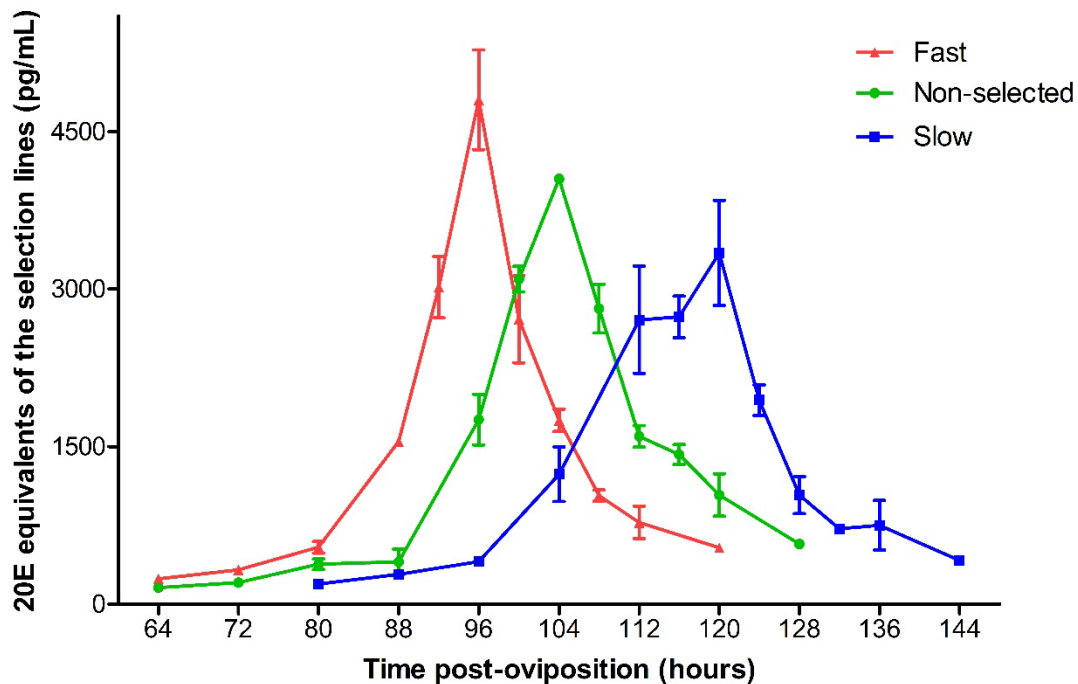


Figure 4-24. Ecdysteroid levels of the eggs of the selection lines of *Tribolium castaneum*. Each time point represents the mean ecdysteroid levels of two biological replicates (each biological replicate is based on two technical replicates according to the protocol of the kit).

### High frequency of a 222 bp deletion upstream of *Cyp18a1* in the fast lines

As *Cyp18a1* was identified as the main candidate gene, we inspected the pooled resequencing data around this gene in more detail. At position 1,613,941 on chromosome 9, less than 300 bp downstream of the *Cyp18a1* lead SNP (the highest SNP on chromosome 9, Supplementary Table 4-1), and around 6kb upstream of the *Cyp18a1* transcription start site (TSS), a conspicuous 445 bp sequence starts consisting of two 222 bp repeats. We named the two 222 bp repeats repeat 1 and repeat 2 (Figure 4-25). The alignment of two 222 bp repeats is in Supplementary Figure 4-5. Surprisingly, the pooled resequencing data suggest that one of these repeats is deleted in the fast lines, and that the frequency of this 222 bp deletion is 1 in the fast lines, 0 in the slow lines, and 0.15 and 0.16 in the two non-selected lines (Table 4-3). So, we also called this 222 bp deletion the fast allele (F in Figure 4-25), and the 445 bp repeated region the slow allele (S in Figure 4-25) in this study.

Table 4-3. Number of reads discovered that carry the specific 1 or 2 repeat sequence (Fast or Slow allele, respectively).. These sequences are “AATTTTTTTTAAATTCATTATTTCAATTTTTTATCCTTCCC” for the fast allele and “AATTTTTTTTAAATTTATTATTTCAAATTTTTTATCCTTCCC” for the slow allele. The forward and reverse complement added summed (totals first two columns: ‘All reads’). We corrected for doubles (overlap of the paired ends), and duplicates (identical sequencing PCR duplications close in position on the flow cell) in the last two columns.

	All reads		Doubles and Duplications removed	
	F allele	S allele	F allele	S allele
FastA	41	0	35	0
FastB	30	0	24	0
SlowA	0	37	0	25
SlowB	0	27	0	17
NSA	3	23	3	17
NSB	7	36	5	26

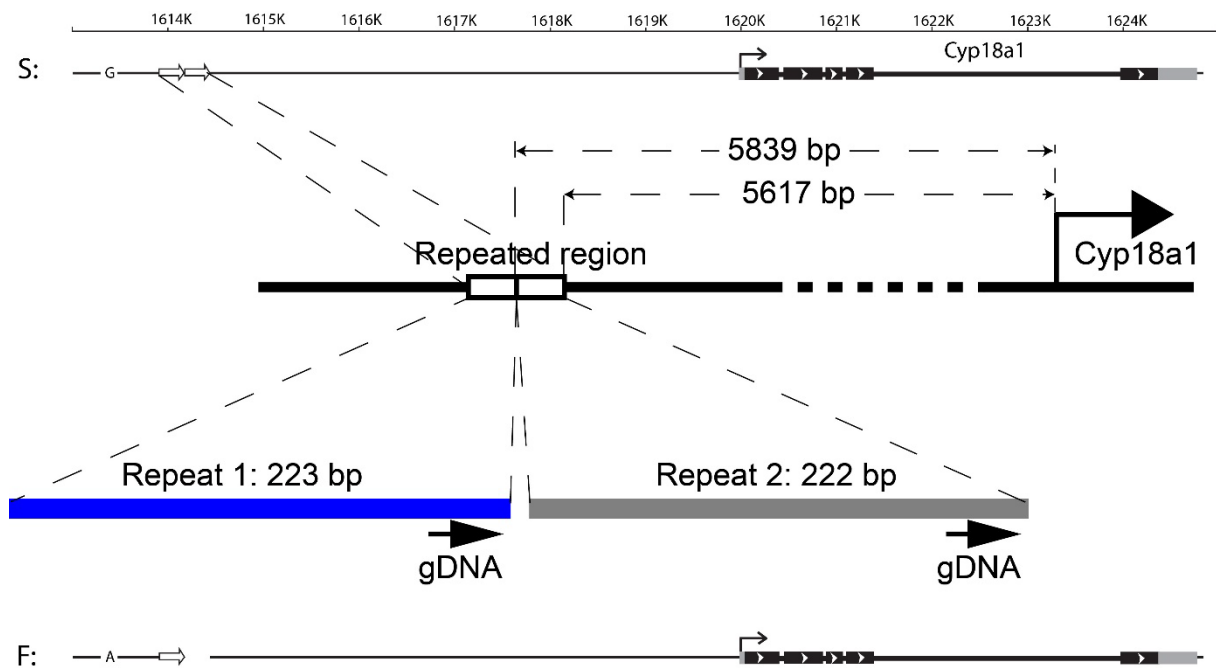


Figure 4-25. Schematic overview of the repeated region in the upstream of *Cyp18a1* comprising 223 bp repeat 1 and 222 bp repeat 2. S: It contains the repeated region with 445 bp close to the lead SNP of *Cyp18a1*. F: It has the deleted region with 223 bp. The distance from the *Cyp18a1* transcription start site to repeat 1 and repeat 2 is 5839 and 5617 bp, respectively.

The presence of such F and S alleles was supported by Sanger sequenced cloned PCR products obtained from fast, non-selected and slow beetles. In total, we sequenced one clone from 19 different individuals: from 4 from Fast A, Non-selected A and Non-selected B each, 3 from Fast B, and 2 beetles from Slow A and Slow B each. Alignments of these cloned Sanger-sequenced PCR products are shown in Supplementary File 4-1. The unique sequences used to distinguish the fast and slow allele in the pooled resequencing data (Table 4-3) is shaded in grey. The results show that all sequences from fast individuals contain the 222 bp deletion (F allele). Only one of the 8 sequences from the non-selected lines contains the deletion. All other sequences, including all sequences from the slow lines, contain the 445 bp repeat (S allele). These numbers correspond well with the pooled resequencing counts (Table 4-3).

When aligning 445 bp repeated region comprising repeat 1 and repeat 2 from the 445 bp repeated region, with the fast allele, we found some single-nucleotide variants of the fast allele are identical to repeat 1, some of them are identical to repeat 2, but still some are unique (Figure 4-26).





Table 4-5. Pearson's Chi-squared test was performed to compare fast allele and slow allele between the fast and non-selected lines in generation 0, 3, 7, 10 and 21.

	X-squared	Degree of freedom	P-value
Gen. 0	2.1223	1	0.1452
Gen. 3	2.4027	1	0.1211
Gen. 7	10.691	1	0.001077
Gen. 10	34.114	1	5.196e-09
Gen. 21	40.682	1	1.791e-10

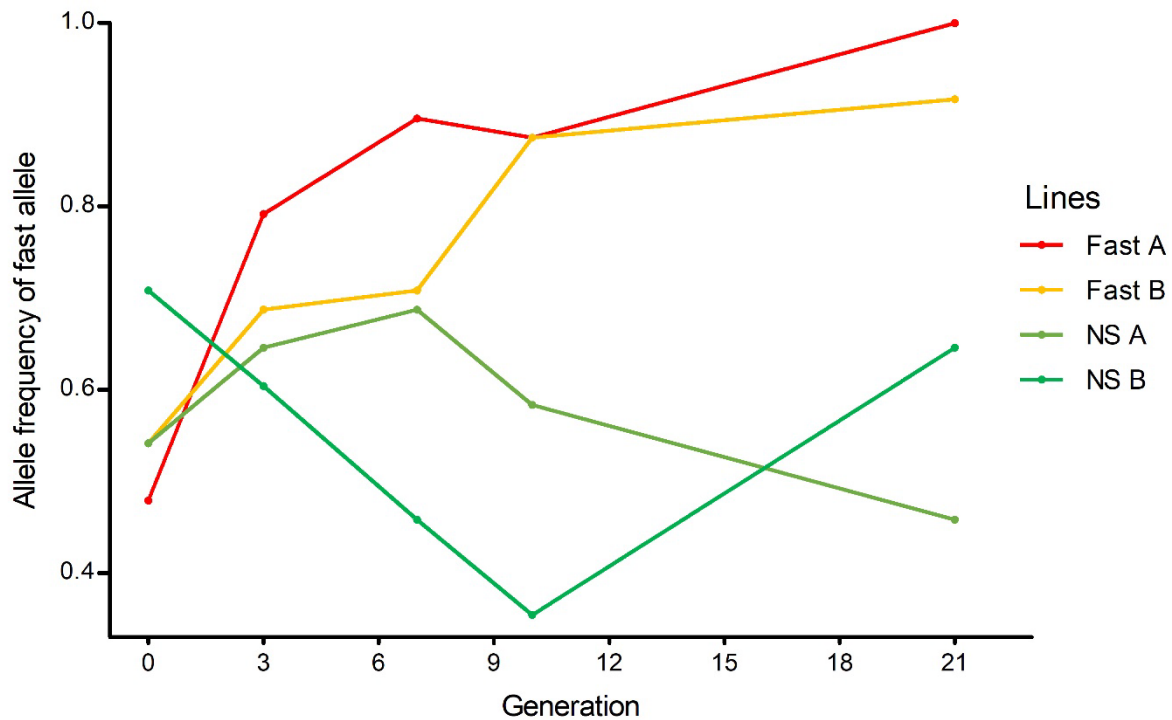


Figure 4-27. Change of allele frequency of fast allele (the 222 bp deleted region) in the upstream of *Cyp18a1* in the fast and non-selected lines over the course of the selection.

Using these data, we fitted a population genetics model with and without fitness differences for these three genotypes. For both Fast A and Fast B the model with different fitness values of the three genotypes was highly significantly different from the model without fitness differences ( $P < 0.001$ ), while for NSA this was not the case ( $P = 0.148$ ), and for NSB this was only significant at a level of  $P < 0.05$ . Furthermore, while for Fast A and Fast B the fitness for FF was higher compared to FS, which had higher estimated fitness than SS, for NSB the fitness was highest for the heterozygote, so that selection is non-directional. The fit for the three difference fitness values of Fast A, Fast B and NSB can be found in Figure 4-28, while for NSA the null-hypothesis without fitness differences was accepted. Thus, the F allele has been under strong positive selection in the fast lines.

Table 4-6. Best fit estimates for the fitness values of the genotypes FF, FS and SS combined with the best starting allele frequency at generation 0. The columns with L, indicate the likelihoods of the models. Chi indicates the test statistic as calculated by equation (1). Key: \*,  $P < 0.05$ ; \*\*\*,  $P < 0.0001$ .

	Model with fitness differences				Model without fitness differences			
Line	WFF	WFS	WSS	pP(FF)	L	p(FF)	L	Chi
FastA	<b>1</b>	<b>0,888</b>	<b>0,291</b>	<b>0,489</b>	-15,99	0,808	-39,47	<b>46,96****</b>
FastB	<b>1</b>	<b>0,950</b>	<b>0,650</b>	<b>0,545</b>	-16,23	0,746	-27,48	<b>22,5****</b>
NSA	0,787	0,437	1	0,617	-18,90	<b>0,583</b>	-20,81	3,82
NSB	<b>0,474</b>	<b>1</b>	<b>0,488</b>	<b>0,717</b>	-21,38	0,554	-24,98	<b>7,20*</b>

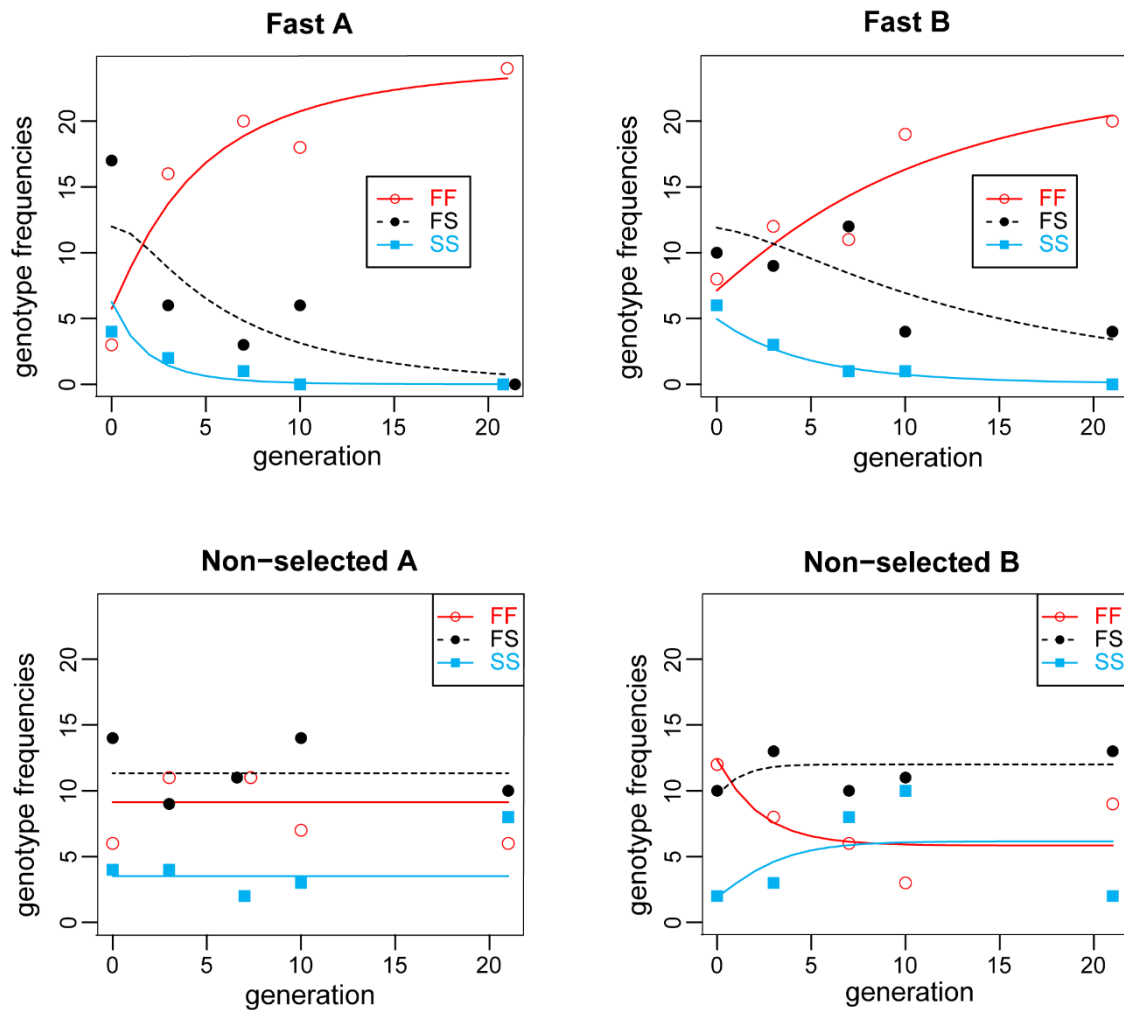


Figure 4-28. Counts of the three genotypes for generation 0, 3, 7, 10 and 21. For each subpanel counts for each genotype is indicated by the different symbols and the estimates change from the models are indicated by the different lines (see legend). Key: FF, homozygotes with the 222 bp deleted region; SS, homozygotes with the 445 bp repeated region; and FS, heterozygotes with both of the deleted region and the repeated region.

In the end, we genotyped 48 beetles from the original wild population that was used to set up our outbred starting population. We found both alleles (F and S alleles) are present in this original wild population (Figure 4-29). Of which, 31 show only a 720 bp band (homozygous F allele), 2 show only a 942 bp band (homozygous S allele), and 14 are heterozygote (both bands + a hybrid band present). Thus, the allele frequency of F is 0.81, and S is 0.19 in this natural population.

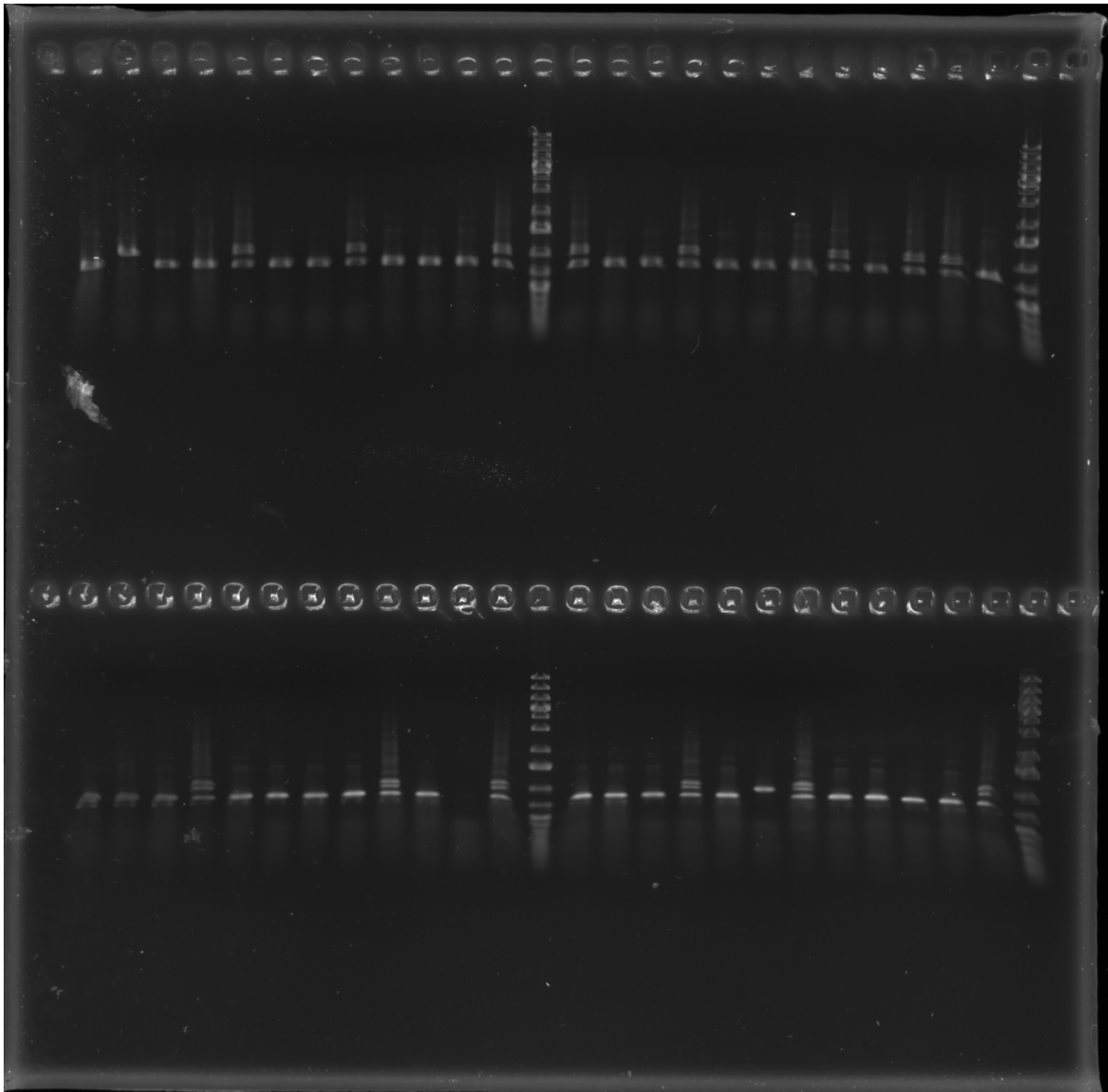


Figure 4-29. Allele frequency of F in a natural population is 0.81. Genotyping PCR (Ethidium bromide staining shown on a 1.0% agarose gel) of 48 beetles from the wild population collected by Rentokil from a bakery in The Netherlands (see Materials and methods). Ladder is GeneRuler 1kb plus DNA ladder (Invitrogen).

Together, these data show that the F allele is a natural allele that was present in the outbred population, but dramatically increased in frequency during selection for fast development.

### **The F allele is associated with fast development in a non-selected line**

To see if there is a relation between the F allele and fast development, we genotyped the 64 larvae that had the fastest embryonic development, and the 64 larvae that had the slowest embryonic development out of more than 2000 larvae for both the non-selected A and non-selected B line. This extreme genotyping within the non-selected lines shows that the frequency of the 222 bp (F allele) is significantly associated with fast development in the NS B line. However, this was not the case in the NSA line (Table 4-7). This suggests that the F allele has a role in fast development, but that genetic background and other alleles are also important.

Table 4-7. Extreme genotyping. Beetles from the non-selected A (NS A) and from the non-selected B (NS B) lines were allowed to lay eggs for 2h, and hatching was recorded in 2h intervals on the selection machine (see methods). In total, more than 2000 eggs were analyzed for each non-selected line. The fastest and slowest 64 beetles were genotyped.  $\chi^2$  -tests show that FF beetles are only significantly overrepresented (and SS beetles significantly underrepresented) among the fastest beetles of the NSB line, but not significantly in the NSA lines.

Selection line		Genotype			Chi-squared test		
		FF	FS	SS	X-squared	Degree of freedom	P-value
NS A	fastest	11	35	18	1.4652	2	0.4807
	slowest	8	32	24			
NS B	fastest	12	33	19	6.1722	2	0.04568
	slowest	5	28	31			

### **The CRISPR deletion strain of *T. castaneum* develops faster, but has reduced fecundity**

In order to study the role of the F allele in isolation, we recreated this deletion in the homogenous genetic background of the GA-1 (Georgia) lab strain (that is homozygous for the repeat) by applying CRISPR-Cas9 technology using a single guide (Figure 4-1). We set up a stock homozygous for the deletion. Sanger sequencing data shows that the recovered 4 alleles present in the stock are more or less an exact reproduction of the Fast allele, with a maximum indel of 9 bp around the PAM site (Figure 4-30). We called them Allele1, Allele2, Allele3 and Allele4. The length of the deletion is 230, 217, 218 and 214 bp, respectively. The alleles present in this stock are aligned in Figure 4-30. Interestingly, the remaining first repeat in Allele1 and Allele2 also contains some SNPs characteristic for the second repeat (Figure 4-30), possibly caused by DNA repair from this sequence.



First, we compared embryonic developmental time of the CRISPR-induced deletion strain and the wild type GA-1 strain of *T. castaneum*. The average time of embryonic development of Crispr line is significantly smaller than that of GA-1. The difference between GA-1 and Crispr lines is 5 h (Figure 4-31). Thus, this allele has a large effect on developmental time.

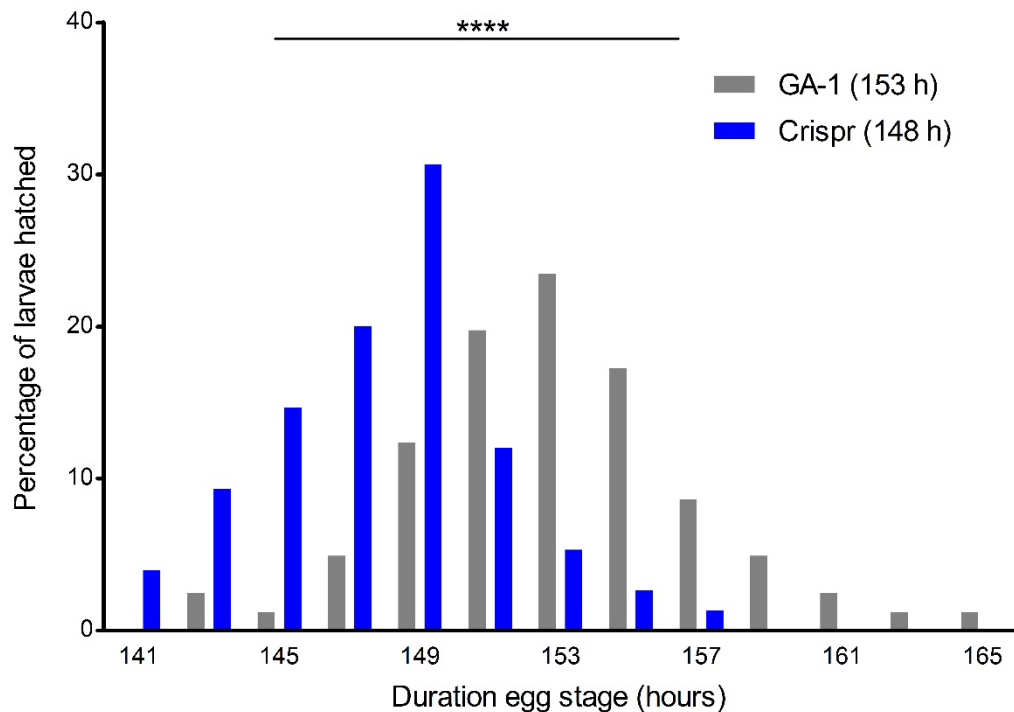


Figure 4-31. Hatching time of eggs of the Georgia 1 (GA-1) line and its Crispr line. Hatching time of eggs of the Georgia 1 line (GA-1, grey) and its Crispr line (blue). The average hatching time of GA-1 and Crispr lines is 153 h and 148 h post-oviposition, respectively. The student t-test was performed to compare GA-1 and its Crispr. Asterisks, significant difference in hatching time (\*\*\*\*,  $P < 0.0001$ ).

Second, we measured pupal weight and early fecundity of GA-1 strain and the Crispr line. The methods are described in Chapter 3 under 'Pupal weight' and 'Fecundity assays'. We did not find significant difference of pupal weight between GA-1 strain and the Crispr line (Figure 4-32A), but there was also no significant difference in pupal weight between the fast selection lines and the non-selected lines (Chapter 3, Figure 3-7). However, the number of eggs laid by 50 Crispr female adults was significant smaller than GA-1 strain (Figure 4-32B), just like the fecundity of the fast lines is reduced compared to the non-selected lines (Chapter 3, Figure 3-8). Thus, this single deletion speeds up development, and causes a trade-off with fecundity.

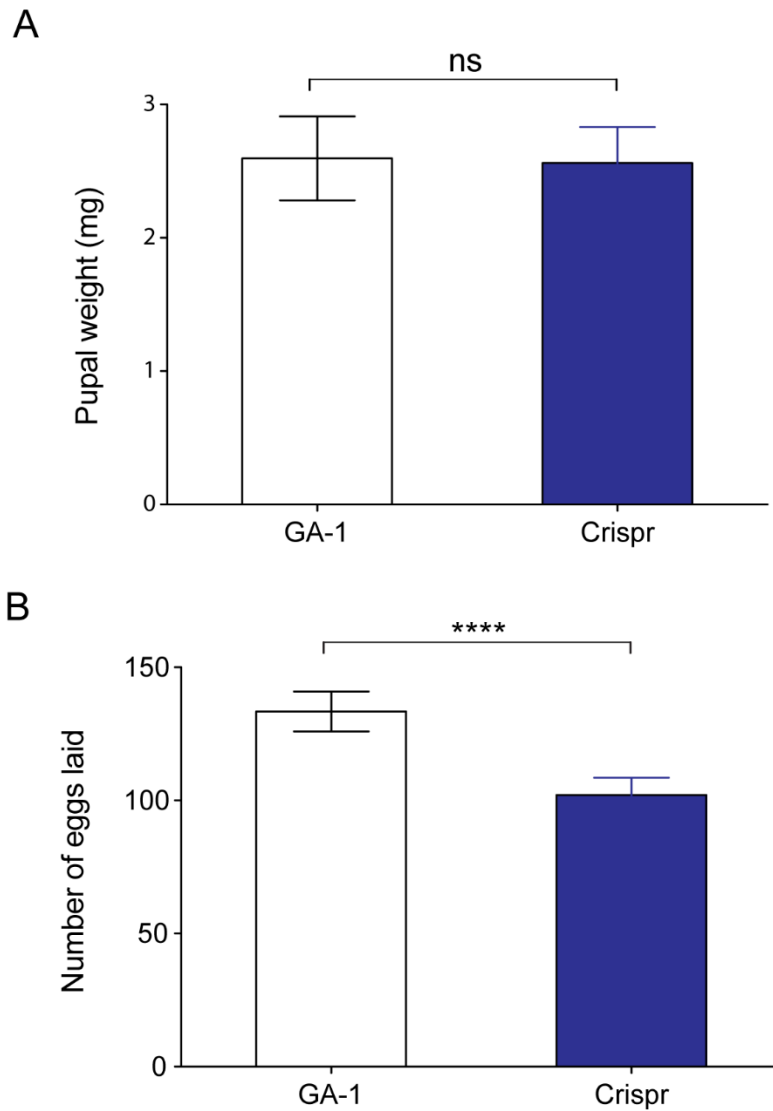


Figure 4-32. Life-history trade-offs of Crispr experiments. A, weight of the newly-hatched pupae of GA-1 strain and its Crispr line. Each vertical bar indicates Mean  $\pm$  SD (n=60). Key: ns, no significant difference observed in hatching time. B, Fecundity of 50 *Tribolium castaneum* females laid within 4 h of GA-1 strain and its Crispr line. Each vertical bar indicates Mean  $\pm$  SD (n=9). Asterisks, significant difference in fecundity (\*\*\*\*,  $P < 0.0001$ ).

### The deletion advances the embryonic ecdysone peak

Further, we analyzed *Cyp18a1* expression and ecdysone dynamics in the CRISPR strain. Transcript levels of *Cyp18a1* were normalized to the reference gene ribosomal protein 13a (RPL13a) (TC013477). The results showed that *Cyp18a1* mRNA reached the peaks at 120 h and then kept in the relative higher level in both Crispr and GA-1 strain. However, the increase of *Cyp18a1* expression in GA-1 strain started much earlier than Crispr strain. Namely, GA-1 strain started to induce *Cyp18a1* mRNA at 104 h, while Crispr strain was at 112 h post-oviposition (Figure 4-33).



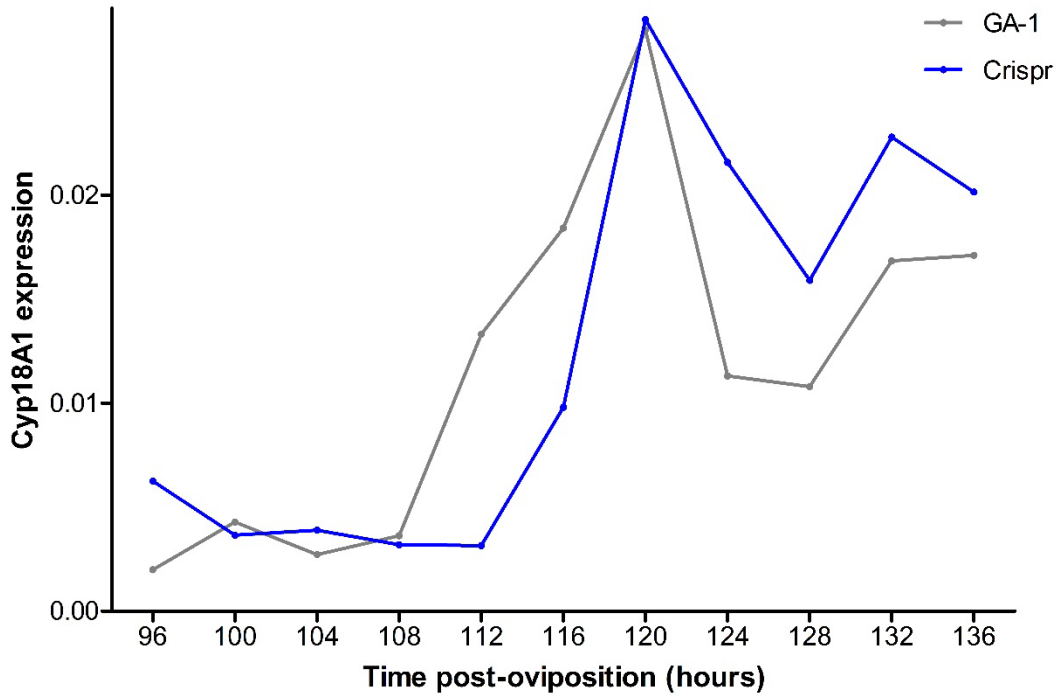


Figure 4-33. Relative expression of *Cyp18A1* in the Georgia 1 (GA-1) line and its Crispr line during later embryonic development. Each point represents the mean *Cyp18A1* expression based on two biological replicates (each replicate is the mean of two technical replicates).

At the same time, we measured 20E titers during dorsal closure. The Crispr and GA-1 lines reached their peaks at 114 and 120 h post-oviposition, respectively. Meanwhile, 20E peak of Crispr line is earlier and stronger than that of GA-1 line (Figure 4-34).

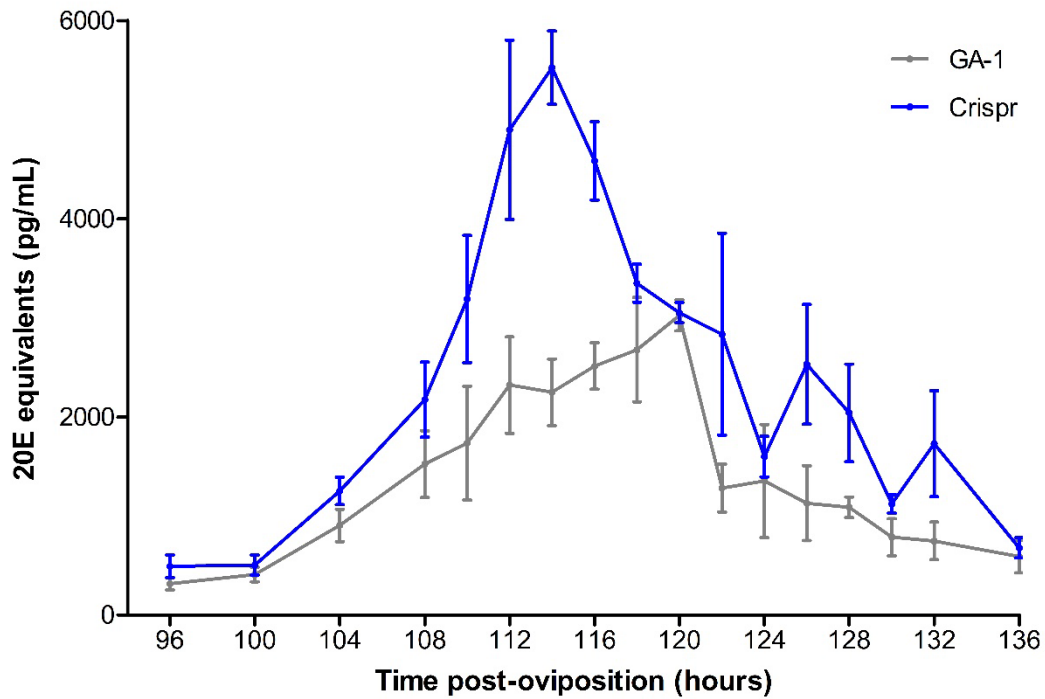


Figure 4-34. Ecdysteroid titer in the Georgia 1 (GA-1) line and its Crispr line during later embryonic development. Each point represents the mean ecdysteroid titer plus standard error based on three biological replicates (each replicate is the mean of two technical replicates according to the protocol of the kit).

Thus, the F allele delays *Cyp18a1* expression, but advances the embryonic ecdysone peak.

### Live imaging shows that the deletion advances dorsal closure

In order to establish whether the F allele drives earlier dorsal closure, we crossed our CRISPR line to the nGFP line (Sarrazin et al., 2012) for confocal live imaging of their heterozygous offspring. The nGFP line is homozygous for the 445 bp S allele (confirmed by PCR in Supplementary Figure 4-8). As control, we crossed GA-1 to the nGFP line. Imaging analysis shows that the completely retracted germband stage in the heterozygous CRISPR/nGFP embryos occurs at the same time as in the heterozygous GA-1/nGFP embryos. However, the start of dorsal closure stage of nGFP-CRISPR embryos occurs earlier than in heterozygous nGFP-GA-1 offspring ( $P < 0.05$ , Figure 4-35). As a consequence, completion of dorsal closure is also earlier in CRISPR-nGFP offspring (Figure 4-35). However, this acceleration is not caused by the duration dorsal closure, as no significant difference found between nGFP-GA-1 and nGFP-Crispr offspring (Figure 4-36B); it is only the consequence of dorsal closure starting earlier. Thus, the 222 bp deletion shortens the interval between completely retracted germband and the start of dorsal closure during embryonic development of *Tribolium* (Figure 4-36A, see stills of representative movies in Supplementary Figure 4-9 and Supplementary Figure 4-10).

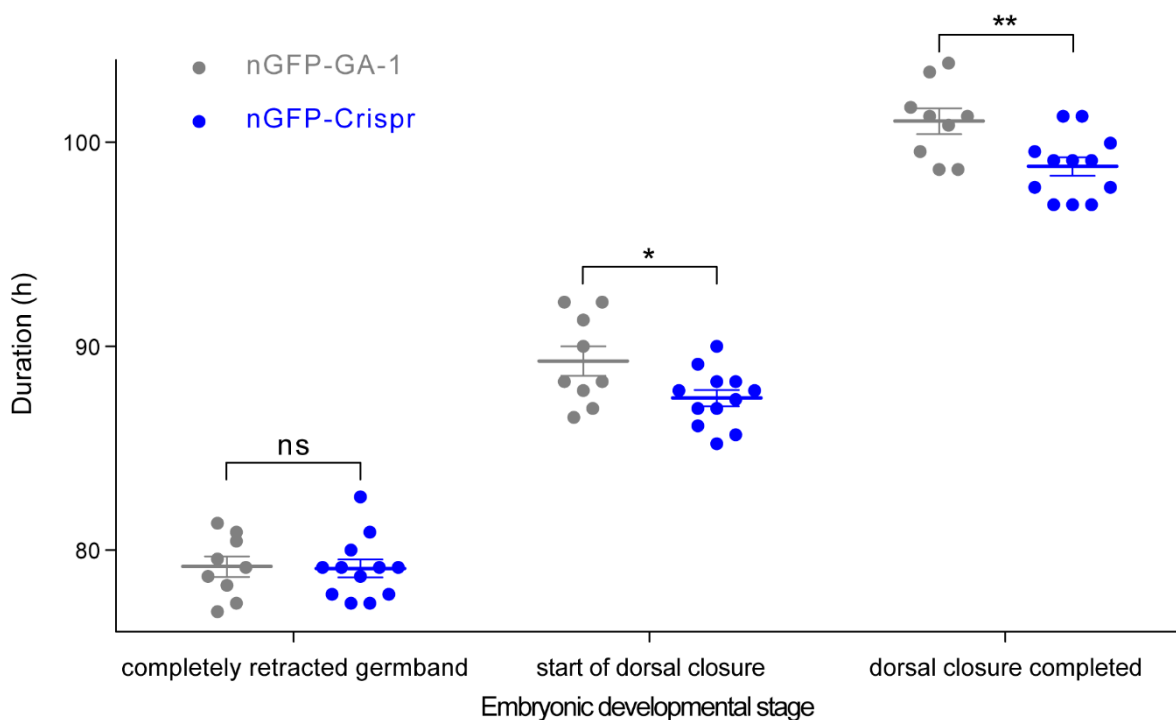


Figure 4-35. Duration embryonic developmental stages, including completely retracted germband, start of dorsal closure and dorsal closure completed. To the stage of completely retracted germband, there is no significant difference of duration between nGFP-GA-1 and nGFP-Crispr offspring. To the stage of start of dorsal closure or dorsal closure completed, nGFP-Crispr develops significantly faster than nGFP-GA-1 offspring. P-values are shown in the figure and indicated with ns, no significance; \*,  $P < 0.05$ ; \*\*,  $P < 0.01$ .

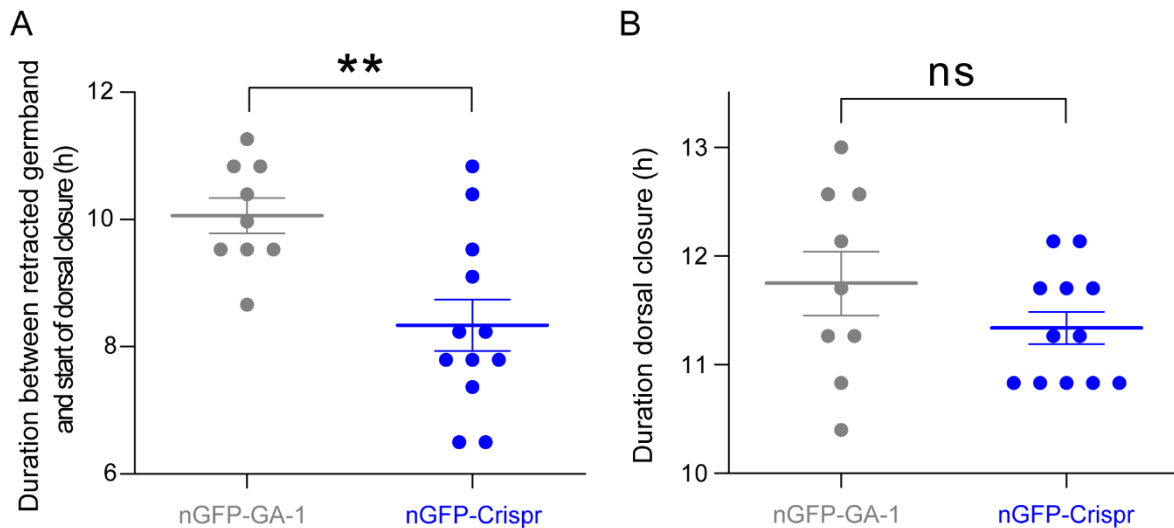


Figure 4-36. Duration between two embryonic developmental stages. A, Duration between completely retracted germband and start of dorsal closure. B, Duration between start of dorsal closure and dorsal closure completed. P-values are shown in the figure and indicated with \*\*,  $P < 0.01$ ; ns, no significance.

In conclusion, this recreated deletion advances the embryonic ecdysone peak inducing dorsal closure, shortens development, and causes a trade-off with fecundity. This single deletion may thus be considered a major life-history allele.

## Discussion

### Identification of candidate genes on chromosome 3 and 9

Whole-genome sequencing of pools of individual DNAs (Pool-seq) represents an attractive and cost-effective approach. In *Drosophila melanogaster*, for instance, Pool-seq identified two cis-regulatory regions near *tan* and *bric-à-brac 1*, associating with light and dark abdominal pigmentation of females (Kofler et al., 2012). Pool-seq has been proven to be accurate and reliable to estimate the allele frequency differences in evolve and resequence (E&R) studies (Schlötterer et al., 2014; Vlachos and Kofler, 2019). In our study, sequencing pools of eggs of four selection lines with fast and non-selected embryonic development revealed two genomic regions on chromosome 3 and 9 with alleles under strong selection (Figure 4-3).

In these two regions, we identified 57 lead SNPs. However, it is likely that not all of them play a role in fast development, due to linkage disequilibrium (LD). LD is the non-random association of alleles at two or more loci, and can be caused by many factors including genetic drift and reduced recombination because of small physical distance on the chromosome. The effect of genetic drift is probably low in our study, as we used large population (>500 beetles). However, reduced recombination could well play a role. This effect is known as the hitchhiking. As a result, hundreds of surrogate SNPs can be yielded for each linked group of the actual SNPs. These hitchhiking mutations can achieve a high frequency due to close physical linkage with the driver allele on the same chromosome (Lang et al., 2013; Papadopoulos et al., 1999; Tenaillon et al., 2012). For example, 92 of 116 mutations have no obvious benefit on fitness (adaptation in asexual populations) in 11 yeast evolved populations adapted to high glucose medium (Buskirk et al., 2017). In the end, additional assays are always needed to distinguish a driver allele from neutral hitchhiking mutations.

As none of our lead SNPs leads to alternative proteins, our first additional assay was a gene expression analysis. In genome-wide association experiments, most SNPs are found in non-coding regions of the DNA (Tak and Farnham, 2015). For example, in *D. melanogaster*, the majority of SNPs (84.4%) affecting sleep are located in non-coding regions (Harbison et al., 2013). In 25 human colon cancer risk SNPs, only one is located in the third exon of the *MYNN* gene, while the others are located in non-coding regions (Yao et al., 2014). These non-coding regions are introns and intergenic regions that contain cis-regulatory elements (CREs), such as silencers, promoters, and enhancers (Barrett et al., 2012). These CREs contain multiple 4–30 bp DNA motifs that function as binding sites for sequence-specific transcription factors (TFs) (Marand and Schmitz, 2022; Wittkopp and Kalay, 2012). Sequence variation in these binding sites can thus alter gene expression. Mutations in cis-regulatory elements and resulting variation in gene regulation is considered to be crucial for evolution (Carroll, 2008), which has been confirmed over and over again (Mazo-Vargas et al., 2022; Siepel and Arbiza, 2014; Verta and Jones, 2019).

In general, our transcriptional analysis did not reduce the number of candidate genes drastically. In our RNAseq analysis, 997 genes were differentially expressed between the fast and non-selected lines, of which 9 were also genes with our lead SNPs. In our qPCR analysis, 27 of the 45 genes with these 57 lead SNPs showed differential expression on at least one timepoint. Thus, many genes are differentially expressed between the fast- and non-selected lines. In Supplementary File 4-2, information about each of the 27 genes detected by qPCR is given. The RNAseq at 76 hrs is more reliable than the qPCR data, as it is based on three biological replicates, instead of two. However, the qPCR data involve two extra later timepoints during (92 hrs) and after dorsal closure (108 hrs), providing a better temporal resolution. Thus, our transcriptional analysis was not very effective in distinguishing driver alleles from hitchhikers, as quite a number of candidate genes remained. Likely, many of them display differential expression as a consequence of fast development, and are not causative. A functional RNAi screen was needed to distinguish the driving genes from neutral ones.

RNA interference (RNAi) has been well established in *Tribolium* for functional analysis (Horn et al., 2022; Tomoyasu et al., 2008). RNAi was first found in *Caenorhabditis elegans* in 1998. By introducing a double-stranded RNA (dsRNA) of a specific gene into cells, the endonuclease protein Dicer which is conserved in fungi, plants, worms, flies, and mammals, cuts the dsRNA into 21–23 nucleotide guide sequences. These small interfering RNA (siRNA), are incorporated into a protein complex, forming the RNA-induced silencing complex (RISC). Subsequently, the sense (non-guide) strand (or passenger strand) of the siRNA is removed, and leaves the guide RNA single stranded. This guide RNA directs the RISC complex to the specific target messenger RNA (mRNA), and cleaves this mRNA, achieving mRNA degradation and gene silencing (Bernstein et al., 2001; Bumcrot et al., 2006; Fire et al., 1998). Robust, systemic RNAi is observed across every life-history stage of many insects, including *T. castaneum* (Miller et al., 2012; Tomoyasu et al., 2008). A genome-wide RNAi project has been undertaken in *T. castaneum*, and a growing database for RNAi phenotypes is available. A database for RNAi phenotypes from a large-scale RNAi screen, iBeetle-Base, is available for *Tribolium* (Dönitz et al., 2015). Parental RNAi in *Tribolium* has the advantage of knockdown responses achieved in offspring embryos upon RNAi in mothers. Parental RNAi efficacy in offspring can persist for weeks (Bucher et al., 2002; Horn et al., 2022).

Our pRNAi screen did drastically reduce the number of candidate genes to four. Two genes, *melted* and *SLC25-35-2* are located adjacently to each other on chromosome 3. *Melted* is a likely candidate. By interacting with tuberous sclerosis 1 (Tsc1) and FOXO, Melted enhances insulin/TOR (target of rapamycin) activity (Teleman et al., 2005), a pivotal pathway enhancing growth rate (Baker and Thummel, 2007; Nijhout et al., 2014). It is unclear, however, how solute carrier family 25 member 35-2 (SLC25-35-2) can affect developmental time. It may be possible that RNAi against *SLC25-35-2* reduces transcription of the adjacent *melted* gene, similar to the observed spreading of RNAi-induced transcriptional silencing in pericentromeric repeats of yeast (Noma et al., 2004). Thus, *melted* seems

the driving gene here. The causative allele is likely located in the intergenic region between *melted* and *SLC25-35-2*. However, mapping of the Illumina reads to this area of chromosome 3 suggests major rearrangements such as large insertions or inversions that are impossible to reconstruct using these short reads. Future long-read nanopore sequencing may resolve this issue.

The two high peaks on chromosome 3 (Figure 4-3A, B, D), are located on either side of the centromere. The centromere is a the eukaryotic chromosomal site where the two chromatids are joined at mitosis and meiosis. Recombination rates are reduced around the centromere (Blair et al., 2018; Nachman, 2002; Sardell et al., 2018). Thus, it is even possible that the only allele under selection on chromosome 3 was the chromosomal rearrangement affecting *melted*, and that the peak at the other side of the centromere was dragged along during selection.

The two other genes, *CAT1* and *Cyp18a1* are located on chromosome 9. *CAT1* is a likely candidate, as it is orthologous to slimfast, an amino acid sensor in the fat body that can overrule peripheral insulin/TOR activity by PI3K modulation affecting developmental time (Baker and Thummel, 2007; Colombani et al., 2003). However, the effect of its knockdown on embryonic developmental time is small (2.75h) and minimally significant (Figure 4-6). This does not mean that the allele affecting slimfast has no effect. On the contrary, small-effect alleles help reach genotypes closer to a fitness optimum. If the populations are near their optimum, large-effect alleles are often deleterious. However, large-effect alleles are more likely to be favored when populations are far from the adaptive peak (Dittmar et al., 2016), and possibly during strong artificial selection such as in our experiment. The knockdown with the largest effect on embryonic developmental time is that of Cytochrome P450 18A1 (*Cyp18a1*, gene 32, Figure 4-6).

In conclusion, our pooled resequencing, expression analysis, and RNAi screen identify two main alleles under selection. One chromosomal rearrangement affecting *melted* on chromosome 3. And an allele affecting *Cyp18a1* on chromosome 9. The broad high peak on chromosome 9, and the two narrow peaks on each side of the centromere on chromosome 3 may all be the consequence of selection on these two alleles only.

## **The function of the Halloween orthologs in larvae, pupae and adults of *Tribolium***

*Cyp18a1* is a cytochrome P450 enzyme that catabolizes active ecdysone (20-hydroxyecdysone, 20E) by 26-hydroxylation (Guittard et al., 2011; Rewitz et al., 2010). The steroid hormone 20E is crucial in controlling developmental timing such as molting and metamorphosis, and is synthesized by other Cytochrome P450 enzymes collectively called the Halloween genes (Gilbert, 2004; Niwa and Niwa, 2016; Yamanaka et al., 2013). The initial step of ecdysone biosynthesis is the dehydrogenation of cholesterol to 7-dehydrocholesterol in the prothoracic gland by the Rieske oxygenase neverland (Nvd) (Figure 4-37). It is worth noting that Nvd is not present in the genome of *T. castaneum*. Surprisingly, Nvd seems to be absent in all holometabolous insects, except the Diptera. All hemimetabolous insect genomes do contain a Nvd ortholog. Using the Halloween genes *spook* (*Spo*, *Cyp307A1*), *spookier* (*Spok*, *Cyp307A2*), *phantom* (*Phm*, *Cyp306A1*), *disembodied* (*Dib*, *Cyp302A1*) and *shadow* (*Sad*, *Cyp315A1*), insects can convert cholesterol and/or plant sterols to ecdysone. The uncharacterized conversion steps, "BLACK BOX", have not been identified so far as the precise intermediates between 7dC and 5 $\beta$ -ketodiol are chemically unstable (Figure 4-37). The small and fat-soluble steroidal prohormone ecdysone can easily pass through the cell membrane. When it enters the cytoplasm, it is converted to the active form 20E by the Halloween gene *shade* (*Shd*, *Cyp314A1*) (Gilbert, 2004).

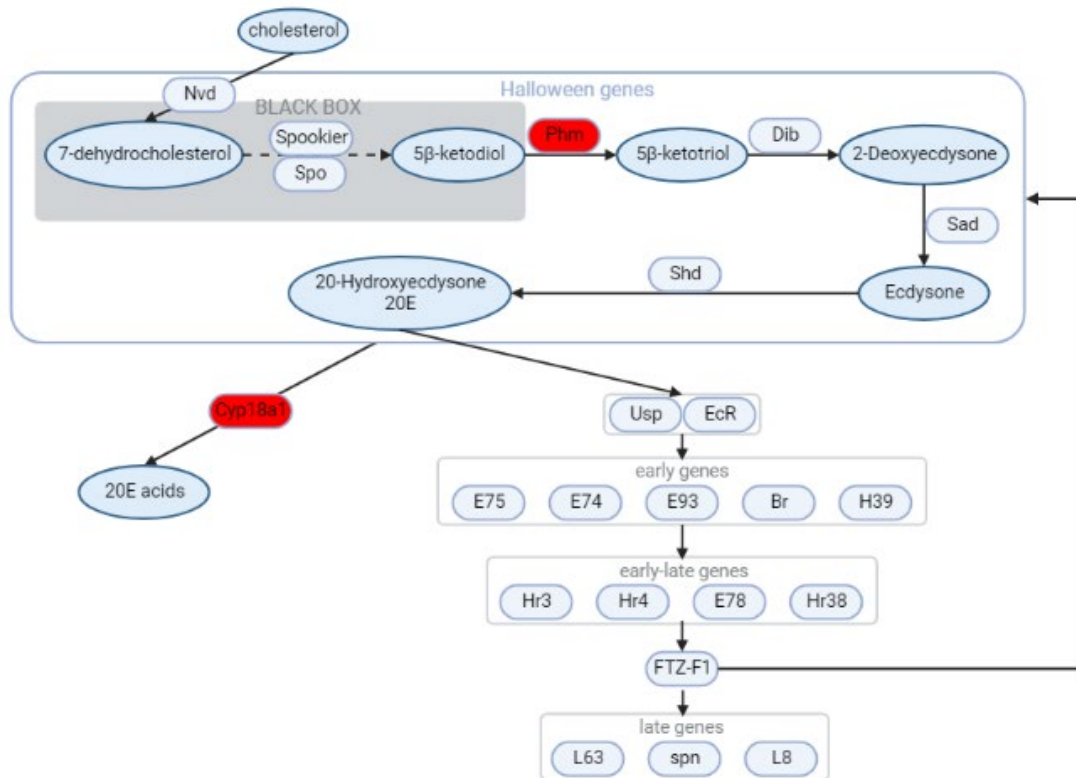


Figure 4-37. Ecdysone biosynthesis and 20E signaling pathway in insects. Modified from (Luan et al., 2013; Niwa and Niwa, 2014). Candidate genes identified in this study are shown in red boxes. The Halloween genes including *neverland* (*Nvd*), *spook* (*Spo*), *phantom* (*Phm*), *disembodied* (*Dib*), *shadow* (*Sad*) and *shade* (*Shd*) are responsible for biosynthesis of ecdysone and 20E, and *Cyp18a1* is used for 20E inactivation. The 20E/EcR/USP complex initiates 20E signaling with the expression of the early genes, early-late genes and late genes. USP, Ultraspiracle; EcR, ecdysone receptor; E75, ecdysone-inducible gene 75; E74, ecdysone-inducible gene 74; E93, ecdysone-induced protein 93F; Br, broad; HR39, hormone receptor-like in 39; HR3, hormone receptor 3; HR4, hormone receptor 4; E78, ecdysone-inducible gene 78; HR38, hormone receptor-like in 38; FTZ-F1, Fushi-tarazu transcription factor 1; L63, Ecdysone-induced protein 63E; Spn, D-spinophilin; L82, mustard.

The active 20E goes on to bind a heterodimeric complex of nuclear receptors comprising ecdysone receptor (EcR) and ultraspiracle (USP). The 20E/EcR/USP complex initiates various gene expression cascades by attaching to the DNA of the early target genes (Niwa and Niwa, 2014; Schumann et al., 2018). These early genes, such as ecdysone-inducible gene 74 (*E74*), ecdysone-inducible gene 75 (*E75*) and *Br*, further induce the “early-late” and “late” genes which directly control biological responses (Luan et al., 2013; Thummel, 2002). Ecdysone also induces expression of *Cyp18a1* encoding an ecdysteroid 26-hydroxylase that catabolizes active ecdysone.

RNAi silencing of the Halloween genes has been performed in many insects. However, the knockdown phenotypes are distinct in different insects with dose-dependent effects. For example, *Phm* RNAi resulted in lethality in *D. melanogaster* (Chung et al., 2009). In the small brown planthopper *Laodelphax striatellus*, *Phm* silencing decreased *EcR* expression levels, caused a higher nymphal mortality rate, and delayed development (Jia et al., 2015). From other arthropods, *Phm* RNAi has been reported to affect the molting of *Macrobrachium nipponense* and inhibit its growth (Pan et al., 2022). However, larval and pupal RNAi against *Phm* in our study did not affect mortality rate or post-embryonic development of *Tribolium* (Figure 4-8). As we did not confirm knockdown of the transcript by qPCR, it is possible that our RNAi against *Phm* was not efficient.

RNAi depletion of the Halloween genes and *Cyp18a1* delayed the molting process of *Bemisia tabaci* by 1–3 days (in total of 9 days in the control treatment) at the 4th nymphal stage (Liu et al., 2020). In

our study, pRNAi silencing of *Spo*, *Sad* and *Shd* rendered beetles permanently sterile and therefore no eggs were produced by the injected mothers. However, mothers injected with *Dib* and *Phm* dsRNA can normally lay eggs and the embryonic development of their offspring was not disrupted. This is very similar to knockdown experiments in the desert locust *Schistocerca gregaria*. Depleting the expression of *Spo*, *Sad* and *Shd* in *S. gregaria* significantly affected oogenesis and oviposition, and drastically altered the shapes of the growing oocytes, while silencing *Phm* and *Dib* did not have any effect (Schellens et al., 2022). In the cabbage beetle *Colaphellus bowringi*, knocking down *Spo*, *Sad*, *Shd* and *EcR* in the females inhibited yolk deposition and ovarian growth and development (Guo et al., 2021), confirming a general role for ecdysone in oogenesis.

In *Drosophila*, silencing of *Cyp18a1* caused a high lethality in the larval or pupal stage (Guittard et al., 2011). We found a dramatic increase of *Cyp18a1* expression in prepupae and pupae, already indicating that *Cyp18a1* is required for metamorphosis and eclosion of *Tribolium*, as reported in *Drosophila* (Rewitz et al., 2010). Indeed, *Cyp18a1* inactivation in these post embryonic stages caused a high lethality, and prevented pupation and eclosion (Figure 4-12). Taken together, our data suggest that the requirement of ecdysone degradation for pupation and eclosion is conserved between *Drosophila* and *Tribolium*. Surprisingly, *Cyp18a1* pRNAi did not lead to sterility, providing us with the chance to study its function during embryonic development.

## **Ecdysone during embryonic development of *Tribolium***

Here, we systemically studied gene expression profiles of the Halloween genes, *Cyp18a1* and *Br* during embryogenesis of *T. castaneum*. We found two expression peaks of them at early and later embryonic development, but not in the middle stage. The same is true for ecdysone itself with two peaks at 40 h and 120 h post-oviposition (Figure 4-14). In *Drosophila*, only a late peak was found and was recently shown to regulate dorsal closure during embryogenesis (Yoo et al., 2021). In our study, we focused on the late peak.

We showed that these late peaks in the selection lines and Georgia strain all occurred at the complete dorsal closure stage. We also demonstrated that the high ecdysteroid titer was closely followed by high *Cyp18a1* expression after dorsal closure (Figure 4-14). In our selection lines, the fast lines started and finished dorsal closure earlier than the non-selected lines (Figure 4-2). As a result, relative expression of *Cyp18a1* in the fast lines compared to the non-selected lines was higher before dorsal closure but lower after dorsal closure (Figure 4-5).

Interestingly, the expression peak of *Shd*, the last Halloween gene expression seemed to largely precede the ecdysone peak (Figure 4-15). This pattern of ecdysone levels and *Shd* expression suggests that *Shd* is a long-lived protein that can continue to modify ecdysone in an efficient and effective way, and that more precise rise of the ecdysone peak is regulated by earlier Halloween genes, such as *Spook* whose expression exactly overlaps with the ecdysone peak (Figure 4-14).

Strikingly, silencing of *Cyp18a1* by pRNAi resulted in continuously rising ecdysteroid levels (Figure 4-21), and failure to start dorsal closure (Figure 4-19). This demonstrates that a pulse of ecdysone is required to start dorsal closure. Continuous high levels of ecdysone are not sufficient, as also shown for the juvenile-adult transition (Rewitz et al., 2010).

In early-stage eggs, we also observed the conspicuous earlier phenotype of incomplete germband extension and shortened germbands (Figure 4-18). This may be caused by disrupted segmentation, as Cruz *et al.* recently found that 20E signaling is essential for germband formation and segmentation in hemimetabolous insect *Blattella germanica* (Cruz et al., 2022). When using embryonic RNAi (eRNAi) against *Spo*, we also found that the injected eggs cannot survive to germband retraction and were arrested during segmentation and germband elongation. Together, these results suggest that the first

lower peak of ecdysone around 40h is required for segmentation, while the second high peak of ecdysone at 120h is required for dorsal closure. However, duration of segmentation and germband extension did not differ among our selection lines, only dorsal closure (Figure 4-2).

Further work needed to fully understand the role of *Cyp18a1* or even ecdysone in early embryonic development. Although a third of *Cyp18a1* RNAi embryos hatched (Figure 4-20), most of them did not survive to larvae (Figure 4-7), mainly as a consequence of disrupted segmentation and dorsal closure.

## The role of the deletion

We have identified a 222 bp deletion that increased in frequency during selection in the fast lines, and has a frequency of 0 in the slow lines (Table 4-3). We tested the function of this deletion by applying a CRISPR/Cas9 strategy in which we used a single guide targeting the repeated sequence to exactly recreate this deletion in the homogenous genetic background of the Georgia lab astrain. The effectivity of CRISPR-Cas9 has been demonstrated in *Tribolium* before (Gilles et al., 2015), and we could also efficiently generate the desired excision. Sequencing of the alleles present in our stock show that a maximum indel of 9 bp was present around the PAM (Figure 4-30). In two alleles, the remaining first repeat contained some SNPs typical for the second repeat (Figure 4-30). Possibly, these SNPs were introduced into the first repeat by DNA repair using the excised second repeat as template.

We assume that the deletion is located in a cis-regulatory element (CRE/enhancer) that regulates *Cyp18a1* expression. Using the JASPAR database and FIMO, we indeed find a binding site for Tramtrack (Ttk), and a high-affinity binding site for Broad (Br) in the deletion, immediately followed by a binding site for the Ecdysone Receptor (Figure 4-39). The Ttk and Br binding sites are thus duplicated when the repeat is present (the slow allele, Supplementary Figure 4-7), but only single Ttk and Br binding sites exist in the fast allele.

Both Ttk and Br encode *Cys<sub>2</sub>/His<sub>2</sub>* zinc-finger proteins (DiBello et al., 1991; Fairall et al., 1993), and belong to the Broad-complex/Tramtrack/Bric-à-brac or poxvirus and zinc finger (BTB/POZ) family. BTB/POZ proteins not only play a critical role in transcriptional regulation but also in chromatin remodeling or modification (Chaharbakhshi and Jemc, 2016). Br has four protein isoforms (Br-Z1 to Br-Z4) and is an early ecdysone target gene (Bayer et al., 1996; Mugat et al., 2000). Crucially, Broad has been shown to regulate Ecdysone target genes, for instance during metamorphosis (Huang et al., 2013; Karim et al., 1993; Mugat et al., 2000; Truman, 2019; Uhlirova et al., 2003). Ttk usually acts as a transcriptional repressor during development (Badenhorst et al., 2002; Li et al., 1997; Pagans et al., 2002; Xiong and Montell, 1993). The transcriptional repression of *fushi tarazu* (*FTZ*) by Ttk, for instance, is probably caused by alterations of chromatin structure (Harrison and Travers, 1990; Li et al., 1997). However, Ttk has also been shown to be a strong activator of gene expression (Yu et al., 1999), and required for the ecdysone-induced upregulation of *Cut* in *Drosophila* (Sun et al., 2008).

In the 20E signaling pathway, the formation of chromatin loops establishing contacts between enhancers and basal promoters is required to start transcriptional regulation of early ecdysone-induced genes, such as *Br*, *E74* and *E75* (Bernardo et al., 2014). Recent studies established that the steroid hormone ecdysone can stimulate the activation of chromatin architectural alterations in *Drosophila*, activating genes (Cheng et al., 2022; Gutierrez-Perez et al., 2019; Hitrik et al., 2016; Kreher et al., 2017). For example, Gutierrez-Perez et al. revealed that ecdysone induces dramatic changes in three-dimensional chromatin architecture by connecting enhancers bound by Polycomb and Pipsqueak to their promoters, thus forming a chromatin loop to start target gene transcription (Gutierrez-Perez et al., 2019).



In conclusion, it is highly likely that our deletion is located in an ecdysone-inducible enhancer that regulates *Cyp18a1* expression. We wondered if the shifted ecdysone peak could be caused by altered *Cyp18a1* expression. To test this hypothesis, we developed a mathematical model.

We model *Cyp18a1* as a sigmoidal function of ecdysone levels, in which we can vary the sensitivity to ecdysone by changing  $s$  (Figure 4-38A equation (I); Figure 4-38B). Total levels of *Cyp18a1* are then its production rate in response to ecdysone, minus a degradation  $\lambda$  (Figure 4-38A equation (II)). We model that ecdysone levels ( $E$ ) are dependent on a self-regulated positive feedback loop ( $b$ ) minus its degradation by *Cyp18a1* ( $C$ ) (Figure 4-38A equation (III)). This model shows that lower sensitivity to ecdysone (larger  $s$ ) induces *Cyp18a1* expression later (Figure 4-38C), resulting in a higher and earlier ecdysone peak (Figure 4-38D). Thus, an earlier ecdysone peak is caused by later induction of *Cyp18a1* by ecdysone. This is exactly what we measured in the CRISPR line: delayed induction of *Cyp18a1* (Figure 4-33), but an earlier ecdysone peak (Figure 4-34). Thus, the deletion makes the *Cyp18a1* enhancer less sensitive to ecdysone.

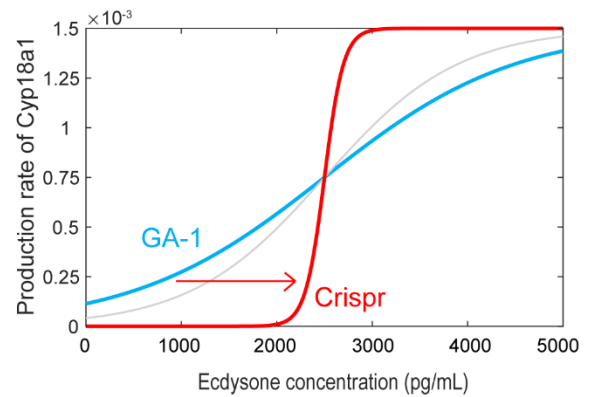
A

$$(I) \quad f(E) = \frac{V_{max}}{1 + \exp(\frac{\theta - E}{s})}$$

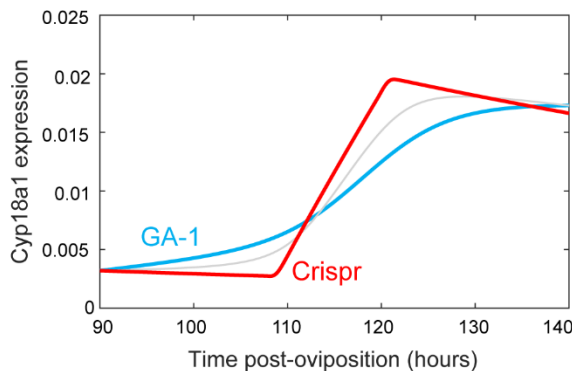
$$(II) \quad \frac{dC}{dt} = f(E) - \lambda C$$

$$(III) \quad \frac{dE}{dt} = bE - kCE$$

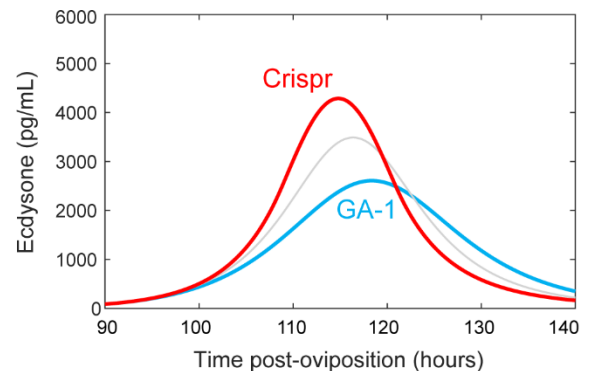
B



C



D



E

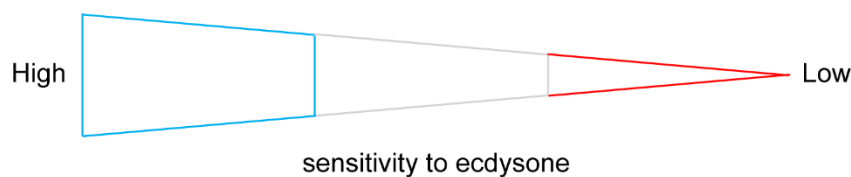


Figure 4-38. The mathematical model used for the dynamics of *Cyp18a1* expression and ecdysone levels. A, We model *Cyp18a1* levels (C) as a sigmoidal function of Ecdysone ( $f(E)$ ) in which we can vary sensitivity to ecdysone ( $s$ ) (formula i) minus a degradation rate ( $\lambda$ ) (formula ii). We assume Ecdysone levels (E) are dependent on a self-regulated positive feedback loop (b) minus its degradation by *Cyp18a1* (C) (formula iii). See details in Supplementary File 4-3. B, Proposed production of *Cyp18a1* as function of Ecdysone concentration ( $f(E)$ ) at different sensitivities for ecdysone ( $s=1000$  for GA-1, blue;  $s=100$  for Crispr, red). C, Resulting *Cyp18a1* expression over time, taking the assumptions from B. C, In Crispr (F allele, red), *Cyp18a1* expression starts to rise later and steeper than in GA-1 (S allele, blue). D, Resulting Ecdysone levels over time, taking the assumptions from B. In the CRISPR line, the Ecdysone peak is higher and earlier (F allele, red), as observed in the fast lines. E, Schematic overview of sensitivity to ecdysone by changing  $s$ .

In other words, the 445 bp repeated region or 222 bp deleted region act as an enhancer. To start *Cyp18a1* transcription, the formation of a chromatin loop is required to connect the enhancer with the basal promoter. This looping requires a certain amount of ecdysone. As the BTB/POZ architectural binding sites are doubled in the GA strain, low levels of ecdysone are already sufficient to form the chromatin loop, turning on *Cyp18a1* transcription. But with only half of the BTB/POZ architectural binding sites, higher levels of ecdysone are required to form this chromatin loop in the Crispr line with the deletion (Figure 4-39B).

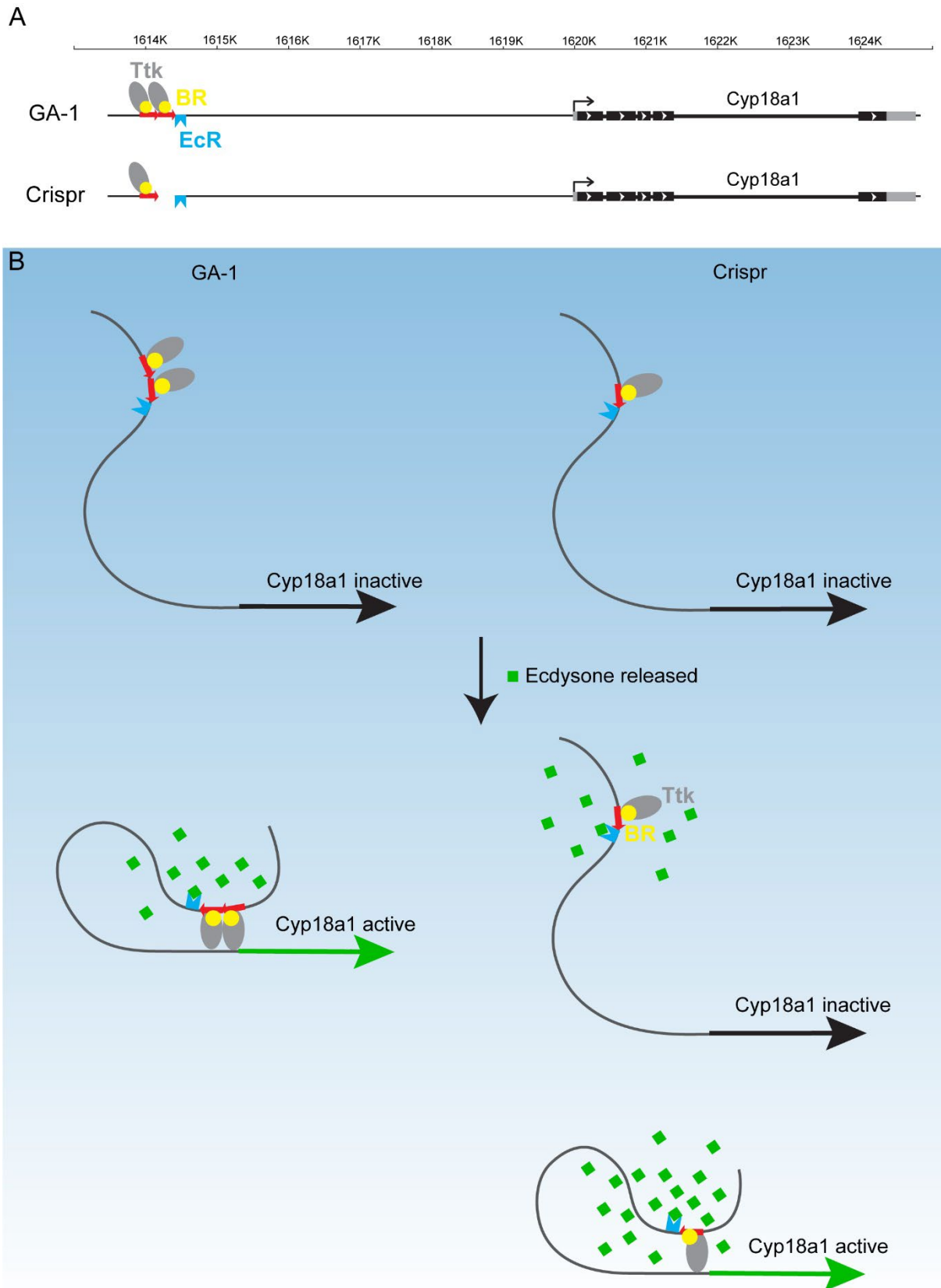


Figure 4-39. Control of *Cyp18a1* transcription through an enhancer–promoter loop. A, motifs of transcription factor binding sites (Supplementary Table 4-6) including Tramtrack (grey oval), Broad (yellow circle), and ecdysone receptor (cyan polygon) in the upstream of *Cyp18a1*. The repeated region in the Georgia strain (GA-1) and its Crispr result in the genome are indicated with red arrows. In addition, GA-1 has doubled binding sites in

this repeated region, compared to its Crispr line. B, when ecdysone (green square) released into the cytoplasm, it will bind to ecdysone receptor, driving the formation of the loop. Further, high levels of ecdysone are required to form the enhancer–promoter loop in the Crispr line, as it has deleted region with half ecdysone-related transcription factor binding sites. Once forming the enhancer–promoter loop, *Cyp18a1* transcription can be activated.

The inconsistent aspect of this model, is that multiple binding sites for transcription factor in an enhancer, usually lead to a steeper response in transcription of the cis-regulated gene (Giorgetti et al., 2010; Jens and Rajewsky, 2015). This phenomenon is caused by cooperative binding (Stefan and Le Novere, 2013). In our case, however, we would have to assume that deleting binding sites (as in the CRISPR) causes a steeper response of *Cyp18a1*. It could be that the supposed enhancer is affecting *Cyp18a1* expression in another way. The supposed enhancer may be the enhancer of another gene, for instance of *Cyp306a1*, *Phantom*, that is oriented tail to tail with *Cyp18a1* in *Tribolium*. This is not only the case in *Tribolium* but in all insects (Figure 4-40), including *Drosophila*, *Apis*, *Bombyx*, *Aedes aegypti*, *Aphis gossypii*, *Bactrocera latifrons*, *Cryptotermes secundus*, *Helicoverpa armigera*, *Leptinotarsa decemlineata*, *Melanaphis sacchari*, *Nasonia vitripennis*, *Nilaparvata lugens*, *Plutella xylostella*, *Sipha flava* and *Zeugodacus cucurbitae*, and crustaceans *Daphnia magna* in the NCBI database. This pattern in genomic order might suggest a regulatory switch either enabling transcription of *phantom* making ecdysone or enabling transcription of *Cyp18a1* degrading ecdysone. Future chromosome conformation capture technologies would be required to experimentally prove this hypothesis (McCord et al., 2020).

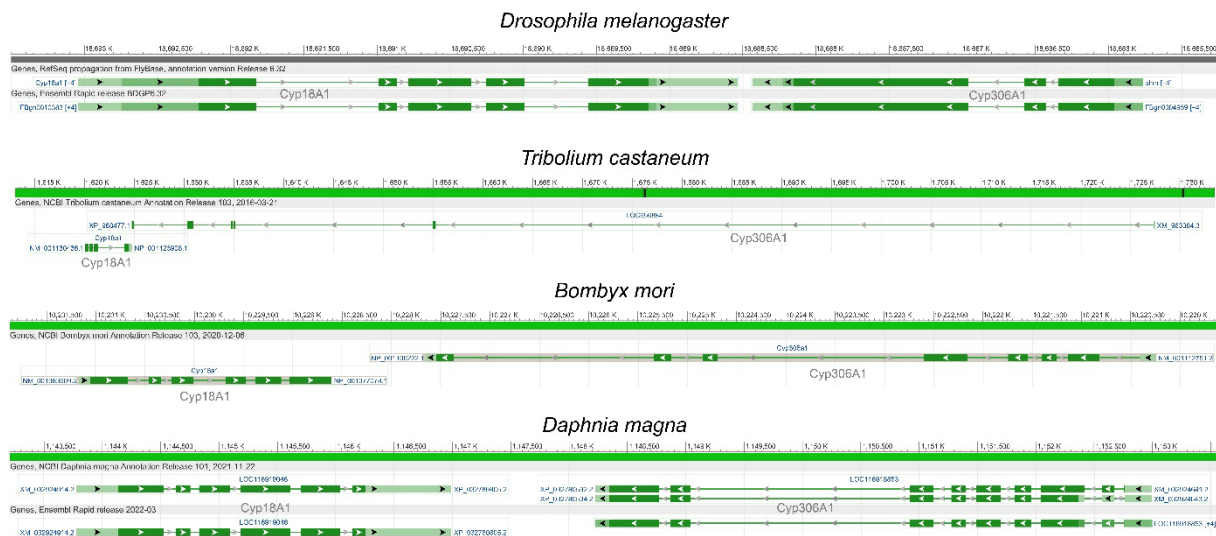


Figure 4-40. A schematic representation of *Cyp18a1* and *Cyp306a1* in genomic order of insects, including *D. melanogaster*, *T. castaneum*, *B. mori* and *D. magna*. *Cyp18a1* and *Cyp306a1* are shown in grey.

## The role of the fast and slow allele in nature

We have identified two alternative, pleiotropic life-history alleles affecting ecdysone dynamics. Both alleles, the fast and slow allele, are present in the original wild population that was used to set up our outbred starting population (Figure 4-29). The maintenance of this polymorphism may be explained by balancing selection (Charlesworth, 2015). For instance, when food sources are temporary, rapid adult dispersal may be required, resulting in selection for fast development. Thus, in such environments, the

fast allele may be favored. In more stable conditions, however, the slow allele having a higher fecundity may be favored.

Classically, quantitative traits are thought to be determined by many alleles of small effect (Charlesworth and Edwards, 2018). Our study, however, demonstrates the existence of large effect life history alleles in natural populations. Such alleles must be crucial when climate change requires rapid adaptation of insect developmental time.

Insects respond to higher temperatures by faster development (Gilbert and Raworth, 1996; Ratte, 1985). Overall temperature of our planet has been ongoingly increasing since the pre-industrial period, namely global warming (Masson-Delmotte et al., 2018). Classically, fast development of insects trades off with small size or low weight, whereas slow development trades off with big size or high weight (Flatt and Heyland, 2011; Stearns, 1992). These trade-offs were also found in our selection lines in *T. castaneum* in Chapter 3, where we also showed that fast development trades off with high fecundity. In this chapter, we provide molecular underpinnings for such corrected responses to selection for fast or slow embryonic development of *Tribolium*. This also means that climate change is not only expected to cause responses in developmental time of insects, but also in other life history traits including fecundity.

## References

- Anders, S., Pyl, P. T. and Huber, W. (2015). HTSeq—a Python framework to work with high-throughput sequencing data. *bioinformatics* **31**, 166-169.
- Badenhorst, P., Finch, J. T. and Travers, A. A. (2002). Tramtrack co-operates to prevent inappropriate neural development in *Drosophila*. *Mechanisms of development* **117**, 87-101.
- Baker, K. D. and Thummel, C. S. (2007). Diabetic larvae and obese flies—emerging studies of metabolism in *Drosophila*. *Cell metabolism* **6**, 257-266.
- Barrett, L. W., Fletcher, S. and Wilton, S. D. (2012). Regulation of eukaryotic gene expression by the untranslated gene regions and other non-coding elements. *Cellular and molecular life sciences* **69**, 3613-3634.
- Bayer, C. A., Holley, B. and Fristrom, J. W. (1996). A Switch in Broad-Complex Zinc-Finger Isoform Expression Is Regulated Posttranscriptionally during the Metamorphosis of *Drosophila* Imaginal Discs. *Developmental biology* **177**, 1-14.
- Berghammer, A. J., Weber, M., Trauner, J. and Klingler, M. (2009). Red flour beetle (*Tribolium*) germline transformation and insertional mutagenesis. *Cold Spring Harb Protoc* **2009**, pdb prot5259.
- Bernardo, T. J., Dubrovskaya, V. A., Xie, X. and Dubrovsky, E. B. (2014). A view through a chromatin loop: insights into the ecdysone activation of early genes in *Drosophila*. *Nucleic acids research* **42**, 10409-10424.
- Bernstein, E., Caudy, A. A., Hammond, S. M. and Hannon, G. J. (2001). Role for a bidentate ribonuclease in the initiation step of RNA interference. *Nature* **409**, 363-366.
- Blair, M. W., Cortés, A. J., Farmer, A. D., Huang, W., Ambachew, D., Penmetsa, R. V., Carrasquilla-Garcia, N., Assefa, T. and Cannon, S. B. (2018). Uneven recombination rate and linkage disequilibrium across a reference SNP map for common bean (*Phaseolus vulgaris* L.). *PLoS one* **13**, e0189597.
- Bolger, A. M., Lohse, M. and Usadel, B. (2014). Trimmomatic: a flexible trimmer for Illumina sequence data. *Bioinformatics* **30**, 2114-2120.
- Brakefield, P. M. (2003). Artificial selection and the development of ecologically relevant phenotypes. *Ecology* **84**, 1661-1671.
- Brinkman, R. (2017). Synchrony of Winter Moth (*Operophtera Brumata*) Larval Eclosion With Bud-Break of Different Tree Species in New England and Its Effect on Defoliation.
- Bucher, G., Scholten, J. and Klingler, M. (2002). Parental RNAi in *tribolium* (coleoptera). *Current Biology* **12**, R85-R86.

- Bumcrot, D., Manoharan, M., Koteliensky, V. and Sah, D. W.** (2006). RNAi therapeutics: a potential new class of pharmaceutical drugs. *Nature chemical biology* **2**, 711-719.
- Burke, M. K., Dunham, J. P., Shahrestani, P., Thornton, K. R., Rose, M. R. and Long, A. D.** (2010). Genome-wide analysis of a long-term evolution experiment with *Drosophila*. *Nature* **467**, 587-U111.
- Buskirk, S. W., Peace, R. E. and Lang, G. I.** (2017). Hitchhiking and epistasis give rise to cohort dynamics in adapting populations. *Proceedings of the National Academy of Sciences* **114**, 8330-8335.
- Campbell, J. F., Athanassiou, C. G., Hagstrum, D. W. and Zhu, K. Y.** (2022). *Tribolium castaneum*: A model insect for fundamental and applied research. *Annual Review of Entomology* **67**, 347-365.
- Carroll, S. B.** (2008). Evo-devo and an expanding evolutionary synthesis: a genetic theory of morphological evolution. *Cell* **134**, 25-36.
- Castro-Mondragon, J. A., Riudavets-Puig, R., Rauluseviciute, I., Lemma, R. B., Turchi, L., Blanc-Mathieu, R., Lucas, J., Boddie, P., Khan, A., Manosalva Perez, N., et al.** (2022). JASPAR 2022: the 9th release of the open-access database of transcription factor binding profiles. *Nucleic Acids Res* **50**, D165-D173.
- Chaharbakhshi, E. and Jemc, J. C.** (2016). Broad-complex, tramtrack, and bric-à-brac (BTB) proteins: Critical regulators of development. *Genesis* **54**, 505-518.
- Charlesworth, B.** (2015). Causes of natural variation in fitness: evidence from studies of *Drosophila* populations. *Proceedings of the National Academy of Sciences* **112**, 1662-1669.
- Charlesworth, B. and Edwards, A. W.** (2018). A century of variance. *Significance* **15**, 20-25.
- Cheng, D., Dong, Z., Lin, P., Shen, G. and Xia, Q.** (2022). Transcriptional Activation of Ecdysone-Responsive Genes Requires H3K27 Acetylation at Enhancers. *International Journal of Molecular Sciences* **23**, 10791.
- Chippindale, A. K., Alipaz, J. A., Chen, H. W. and Rose, M. R.** (1997). Experimental evolution of accelerated development in *Drosophila*. 1. Developmental speed and larval survival. *Evolution* **51**, 1536-1551.
- Chung, H., Sztal, T., Pasricha, S., Sridhar, M., Batterham, P. and Daborn, P. J.** (2009). Characterization of *Drosophila melanogaster* cytochrome P450 genes. *Proceedings of the National Academy of Sciences* **106**, 5731-5736.
- Cingolani, P., Platts, A., Wang, L. L., Coon, M., Nguyen, T., Wang, L., Land, S. J., Lu, X. Y. and Ruden, D. M.** (2012). A program for annotating and predicting the effects of single nucleotide polymorphisms, SnpEff: SNPs in the genome of *Drosophila melanogaster* strain w(1118); iso-2; iso-3. *Fly* **6**, 80-92.
- Colombani, J., Raisin, S., Pantalacci, S., Radimerski, T., Montagne, J. and Léopold, P.** (2003). A nutrient sensor mechanism controls *Drosophila* growth. *Cell* **114**, 739-749.
- Consortium, T. G. S.** (2008). The genome of the model beetle and pest *Tribolium castaneum*. *Nature* **452**, 949.
- Cruz, J., Maestro, O., Franch-Marro, X. and Martín, D.** (2022). Ecdysone signaling controls early embryogenesis in the short-germ hemimetabolous insect *Blattella germanica*. *bioRxiv*.
- DiBello, P., Withers, D., Bayer, C., Fristrom, J. and Guild, G.** (1991). The *Drosophila* Broad-Complex encodes a family of related proteins containing zinc fingers. *Genetics* **129**, 385-397.
- Dittmar, E. L., Oakley, C. G., Conner, J. K., Gould, B. A. and Schemske, D. W.** (2016). Factors influencing the effect size distribution of adaptive substitutions. *Proceedings of the Royal Society B: Biological Sciences* **283**, 20153065.
- Dönitz, J., Schmitt-Engel, C., Grossmann, D., Gerischer, L., Tech, M., Schoppmeier, M., Klingler, M. and Bucher, G.** (2015). iBeetle-Base: a database for RNAi phenotypes in the red flour beetle *Tribolium castaneum*. *Nucleic acids research* **43**, D720-D725.
- Fairall, L., Schwabe, J. W., Chapman, L., Finch, J. T. and Rhodes, D.** (1993). The crystal structure of a two zinc-finger peptide reveals an extension to the rules for zinc-finger/DNA recognition. *Nature* **366**, 483-487.
- Fire, A., Xu, S., Montgomery, M. K., Kostas, S. A., Driver, S. E. and Mello, C. C.** (1998). Potent and specific genetic interference by double-stranded RNA in *Caenorhabditis elegans*. *nature* **391**, 806-811.

- Fischer, K., Zwaan, B. J. and Brakefield, P. M.** (2007). Realized correlated responses to artificial selection on pre-adult life-history traits in a butterfly. *Heredity* **98**, 157-164.
- Flatt, T. and Heyland, A.** (2011). *Mechanisms of life history evolution: the genetics and physiology of life history traits and trade-offs*: Oxford university press.
- Franks, S. J., Genovese, N., Stockdale, M., Weber, J. J., Ansaldi, B. H. and van Wilgenburg, E.** (2018). The Effects of Artificial Selection for Rapid Cycling in Brassica rapa on Herbivore Preference and Performance. *International Journal of Plant Sciences* **179**, 175-181.
- Franks, S. J. and Hoffmann, A. A.** (2012). Genetics of climate change adaptation. *Annual review of genetics* **46**, 185-208.
- Gilbert, L. I.** (2004). Halloween genes encode P450 enzymes that mediate steroid hormone biosynthesis in *Drosophila melanogaster*. *Molecular and cellular endocrinology* **215**, 1-10.
- Gilbert, N. and Raworth, D.** (1996). Insects and temperature—a general theory. *The Canadian Entomologist* **128**, 1-13.
- Gilles, A. F., Schinko, J. B. and Averof, M.** (2015). Efficient CRISPR-mediated gene targeting and transgene replacement in the beetle *Tribolium castaneum*. *Development* **142**, 2832-2839.
- Giorgetti, L., Siggers, T., Tiana, G., Caprara, G., Notarbartolo, S., Corona, T., Pasparakis, M., Milani, P., Bulyk, M. L. and Natoli, G.** (2010). Noncooperative interactions between transcription factors and clustered DNA binding sites enable graded transcriptional responses to environmental inputs. *Molecular cell* **37**, 418-428.
- Gissis, S. B., Gissis, S., Jablonka, E. and Zeligowski, A.** (2011). *Transformations of Lamarckism: from subtle fluids to molecular biology*: MIT press.
- Grant, C. E., Bailey, T. L. and Noble, W. S.** (2011). FIMO: scanning for occurrences of a given motif. *Bioinformatics* **27**, 1017-1018.
- Graves, J. L., Hertweck, K. L., Phillips, M. A., Han, M. V., Cabral, L. G., Barter, T. T., Greer, L. F., Burke, M. K., Mueller, L. D. and Rose, M. R.** (2017). Genomics of Parallel Experimental Evolution in *Drosophila*. *Molecular Biology and Evolution* **34**, 831-842.
- Grimaldi, D. and Engel, M. S.** (2005). *Evolution of the Insects*: Cambridge University Press.
- Guittard, E., Blais, C., Maria, A., Parvy, J.-P., Pasricha, S., Lumb, C., Lafont, R., Daborn, P. J. and Dauphin-Villemant, C.** (2011). CYP18A1, a key enzyme of *Drosophila* steroid hormone inactivation, is essential for metamorphosis. *Developmental biology* **349**, 35-45.
- Guo, S., Tian, Z., Wu, Q.-W., King-Jones, K., Liu, W., Zhu, F. and Wang, X.-P.** (2021). Steroid hormone ecdysone deficiency stimulates preparation for photoperiodic reproductive diapause. *PLoS genetics* **17**, e1009352.
- Gutierrez-Perez, I., Rowley, M. J., Lyu, X., Valadez-Graham, V., Vallejo, D. M., Ballesta-Illan, E., Lopez-Atalaya, J. P., Kremisky, I., Caparros, E. and Corces, V. G.** (2019). Ecdysone-Induced 3D chromatin reorganization involves active enhancers bound by pipsqueak and polycomb. *Cell reports* **28**, 2715-2727. e2715.
- Harbison, S. T., McCoy, L. J. and Mackay, T. F.** (2013). Genome-wide association study of sleep in *Drosophila melanogaster*. *BMC genomics* **14**, 1-18.
- Harrison, S. D. and Travers, A. A.** (1990). The tramtrack gene encodes a *Drosophila* finger protein that interacts with the ftz transcriptional regulatory region and shows a novel embryonic expression pattern. *The EMBO journal* **9**, 207-216.
- Herndon, N., Shelton, J., Gerischer, L., Ioannidis, P., Ninova, M., Donitz, J., Waterhouse, R. M., Liang, C., Damm, C., Siemanowski, J., et al.** (2020). Enhanced genome assembly and a new official gene set for *Tribolium castaneum*. *BMC Genomics* **21**, 47.
- Hitrik, A., Popliker, M., Gancz, D., Mukamel, Z., Lifshitz, A., Schwartzman, O., Tanay, A. and Gilboa, L.** (2016). Combgap promotes ovarian niche development and chromatin association of EcR-binding regions in BR-C. *PLoS Genetics* **12**, e1006330.
- Hoedjes, K. M., van den Heuvel, J., Kapun, M., Keller, L., Flatt, T. and Zwaan, B. J.** (2019). Distinct genomic signals of lifespan and life history evolution in response to postponed reproduction and larval diet in *Drosophila*. *Evolution Letters* **3**, 598-609.
- Horn, T., Narov, K. D. and Panfilio, K. A.** (2022). Persistent parental RNAi in the beetle *Tribolium castaneum* involves maternal transmission of long double-stranded RNA. *Advanced Genetics* **3**, 2100064.

- Huang, J.-H., Lozano, J. and Belles, X.** (2013). Broad-complex functions in postembryonic development of the cockroach *Blattella germanica* shed new light on the evolution of insect metamorphosis. *Biochimica et Biophysica Acta (BBA)-General Subjects* **1830**, 2178-2187.
- Jacobs, C. G., Rezende, G. L., Lamers, G. E. and van der Zee, M.** (2013). The extraembryonic serosa protects the insect egg against desiccation. *Proceedings of the Royal Society B: Biological Sciences* **280**, 20131082.
- Jacobs, C. G., Spaink, H. P. and van der Zee, M.** (2014). The extraembryonic serosa is a frontier epithelium providing the insect egg with a full-range innate immune response. *elife* **3**, e04111.
- Jacobs, C. G. and van der Zee, M.** (2013). Immune competence in insect eggs depends on the extraembryonic serosa. *Developmental & Comparative Immunology* **41**, 263-269.
- Jens, M. and Rajewsky, N.** (2015). Competition between target sites of regulators shapes post-transcriptional gene regulation. *Nature Reviews Genetics* **16**, 113-126.
- Jia, S., Wan, P. J. and Li, G. Q.** (2015). Molecular cloning and characterization of the putative Halloween gene Phantom from the small brown planthopper *Laodelphax striatellus*. *Insect Science* **22**, 707-718.
- Karim, F. D., Guild, G. M. and Thummel, C. S.** (1993). The *Drosophila* Broad-Complex plays a key role in controlling ecdysone-regulated gene expression at the onset of metamorphosis. *Development* **118**, 977-988.
- Kharouba, H. M., Ehrlen, J., Gelman, A., Bolmgren, K., Allen, J. M., Travers, S. E. and Wolkovich, E. M.** (2018). Global shifts in the phenological synchrony of species interactions over recent decades. *Proceedings of the National Academy of Sciences of the United States of America* **115**, 5211-5216.
- Klingler, M.** (2004). *Tribolium*. *Current Biology* **14**, R639-R640.
- Klingler, M. and Bucher, G.** (2022). The red flour beetle *T. castaneum*: elaborate genetic toolkit and unbiased large scale RNAi screening to study insect biology and evolution. *EvoDevo* **13**, 1-11.
- Knaus, B. J. and Grunwald, N. J.** (2017). VCFR: a package to manipulate and visualize variant call format data in R. *Mol Ecol Resour* **17**, 44-53.
- Koboldt, D. C., Chen, K., Wylie, T., Larson, D. E., McLellan, M. D., Mardis, E. R., Weinstock, G. M., Wilson, R. K. and Ding, L.** (2009). VarScan: variant detection in massively parallel sequencing of individual and pooled samples. *Bioinformatics* **25**, 2283-2285.
- Kofler, R., Betancourt, A. J. and Schlötterer, C.** (2012). Sequencing of pooled DNA samples (Pool-Seq) uncovers complex dynamics of transposable element insertions in *Drosophila melanogaster*. *PLoS genetics* **8**, e1002487.
- Kozlova, T. and Thummel, C. S.** (2003). Essential roles for ecdysone signaling during *Drosophila* mid-embryonic development. *Science* **301**, 1911-1914.
- Kreher, J., Kovač, K., Bouazoune, K., Mačinković, I., Ernst, A. L., Engelen, E., Pahl, R., Finkernagel, F., Murawska, M. and Ullah, I.** (2017). EcR recruits dMi-2 and increases efficiency of dMi-2-mediated remodelling to constrain transcription of hormone-regulated genes. *Nature communications* **8**, 1-13.
- Lang, G. I., Rice, D. P., Hickman, M. J., Sodergren, E., Weinstock, G. M., Botstein, D. and Desai, M. M.** (2013). Pervasive genetic hitchhiking and clonal interference in forty evolving yeast populations. *Nature* **500**, 571-574.
- Larson, G. and Fuller, D. Q.** (2014). The evolution of animal domestication. *Annual Review of Ecology, Evolution, and Systematics* **45**, 115-136.
- Li, H., Handsaker, B., Wysoker, A., Fennell, T., Ruan, J., Homer, N., Marth, G., Abecasis, G., Durbin, R. and Proc, G. P. D.** (2009). The Sequence Alignment/Map format and SAMtools. *Bioinformatics* **25**, 2078-2079.
- Li, S., Li, Y., Carthew, R. W. and Lai, Z.-C.** (1997). Photoreceptor cell differentiation requires regulated proteolysis of the transcriptional repressor Tramtrack. *Cell* **90**, 469-478.
- Linz, D. M., Clark-Hachtel, C. M., Borràs-Castells, F. and Tomoyasu, Y.** (2014). Larval RNA interference in the red flour beetle, *Tribolium castaneum*. *JoVE (Journal of Visualized Experiments)*, e52059.
- Liu, S., He, C., Liang, J., Su, Q., Hua, D., Wang, S., Wu, Q., Xie, W. and Zhang, Y.** (2020). Molecular characterization and functional analysis of the Halloween genes and CYP18A1 in *Bemisia tabaci* MED. *Pesticide Biochemistry and Physiology* **167**, 104602.



- Livak, K. J. and Schmittgen, T. D.** (2001). Analysis of relative gene expression data using real-time quantitative PCR and the 2(-Delta Delta C(T)) Method. *Methods* **25**, 402-408.
- Long, A., Liti, G., Luptak, A. and Tenailon, O.** (2015). Elucidating the molecular architecture of adaptation via evolve and resequence experiments. *Nature Reviews Genetics* **16**, 567-582.
- Lord, J. C., Hartzler, K., Toutges, M. and Oppert, B.** (2010). Evaluation of quantitative PCR reference genes for gene expression studies in *Tribolium castaneum* after fungal challenge. *Journal of microbiological methods* **80**, 219-221.
- Love, M. I., Huber, W. and Anders, S.** (2014). Moderated estimation of fold change and dispersion for RNA-seq data with DESeq2. *Genome biology* **15**, 1-21.
- Luan, J.-B., Ghanim, M., Liu, S.-S. and Czosnek, H.** (2013). Silencing the ecdysone synthesis and signaling pathway genes disrupts nymphal development in the whitefly. *Insect Biochemistry and Molecular Biology* **43**, 740-746.
- Manning, A.** (1961). The effects of artificial selection for mating speed in *Drosophila melanogaster*. *Animal Behaviour* **9**, 82-92.
- Marand, A. P. and Schmitz, R. J.** (2022). Single-cell analysis of cis-regulatory elements. *Current Opinion in Plant Biology* **65**, 102094.
- Marinkovic, D. A., F.J.** (1986). Selection for different rates of embryonic development in *Drosophila melanogaster* and *Drosophila simulans*. *Genetika* **18**, 205-219.
- Maróy, P., Kaufmann, G. and Dübendorfer, A.** (1988). Embryonic ecdysteroids of *Drosophila melanogaster*. *Journal of Insect Physiology* **34**, 633-637.
- Masson-Delmotte, V., Zhai, P., Pörtner, H.-O., Roberts, D., Skea, J., Shukla, P. R., Pirani, A., Moufouma-Okia, W., Péan, C. and Pidcock, R.** (2018). Global warming of 1.5 C. *An IPCC Special Report on the impacts of global warming of 1*, 43-50.
- Mazo-Vargas, A., Langmüller, A. M., Wilder, A., van der Burg, K. R., Lewis, J. J., Messer, P. W., Zhang, L., Martin, A. and Reed, R. D.** (2022). Deep cis-regulatory homology of the butterfly wing pattern ground plan. *Science* **378**, 304-308.
- McCord, R. P., Kaplan, N. and Giorgetti, L.** (2020). Chromosome conformation capture and beyond: toward an integrative view of chromosome structure and function. *Molecular cell* **77**, 688-708.
- McKenna, A., Hanna, M., Banks, E., Sivachenko, A., Cibulskis, K., Kernytsky, A., Garimella, K., Altshuler, D., Gabriel, S., Daly, M., et al.** (2010). The Genome Analysis Toolkit: A MapReduce framework for analyzing next-generation DNA sequencing data. *Genome Research* **20**, 1297-1303.
- McLaughlin, J. F., Hellmann, J. J., Boggs, C. L. and Ehrlich, P. R.** (2002). Climate change hastens population extinctions. *Proceedings of the National Academy of Sciences of the United States of America* **99**, 6070-6074.
- Miller, S. C., Miyata, K., Brown, S. J. and Tomoyasu, Y.** (2012). Dissecting systemic RNA interference in the red flour beetle *Tribolium castaneum*: parameters affecting the efficiency of RNAi. *PloS one* **7**, e47431.
- Mugat, B., Brodu, V., Kejzlarova-Lepesant, J., Antoniewski, C., Bayer, C. A., Fristrom, J. W. and Lepesant, J.-A.** (2000). Dynamic expression of broad-complex isoforms mediates temporal control of an ecdysteroid target gene at the onset of *Drosophila* metamorphosis. *Developmental biology* **227**, 104-117.
- Nachman, M. W.** (2002). Variation in recombination rate across the genome: evidence and implications. *Current opinion in genetics & development* **12**, 657-663.
- Neyfakh, A. A. and Hartl, D. L.** (1993). Genetic-Control of the Rate of Embryonic-Development - Selection for Faster Development at Elevated-Temperatures. *Evolution* **47**, 1625-1631.
- Nijhout, H. F., Riddiford, L. M., Mirth, C., Shingleton, A. W., Suzuki, Y. and Callier, V.** (2014). The developmental control of size in insects. *Wiley Interdisciplinary Reviews: Developmental Biology* **3**, 113-134.
- Niwa, R. and Niwa, Y. S.** (2014). Enzymes for ecdysteroid biosynthesis: their biological functions in insects and beyond. *Bioscience, biotechnology, and biochemistry* **78**, 1283-1292.
- Niwa, Y. S. and Niwa, R.** (2016). Transcriptional regulation of insect steroid hormone biosynthesis and its role in controlling timing of molting and metamorphosis. *Development, growth & differentiation* **58**, 94-105.

- Noma, K.-i., Sugiyama, T., Cam, H., Verdel, A., Zofall, M., Jia, S., Moazed, D. and Grewal, S. I.** (2004). RITS acts in cis to promote RNA interference-mediated transcriptional and post-transcriptional silencing. *Nature genetics* **36**, 1174-1180.
- Nunney, L.** (1996). The response to selection for fast larval development in *Drosophila melanogaster* and its effect on adult weight: An example of a fitness trade-off. *Evolution* **50**, 1193-1204.
- Pagans, S., Ortiz-Lombardía, M., Espinás, M. L., Bernués, J. and Azorín, F.** (2002). The *Drosophila* transcription factor tramtrack (TTK) interacts with Trithorax-like (GAGA) and represses GAGA-mediated activation. *Nucleic acids research* **30**, 4406-4413.
- Pan, F., Fu, Y., Zhang, W., Jiang, S., Xiong, Y., Yan, Y., Gong, Y., Qiao, H. and Fu, H.** (2022). Characterization, expression and functional analysis of CYP306a1 in the oriental river prawn, *Macrobrachium nipponense*. *Aquaculture Reports* **22**, 101009.
- Panfilio, K. A.** (2008). Extraembryonic development in insects and the acrobatics of blastokinesis. *Developmental biology* **313**, 471-491.
- Papadopoulos, D., Schneider, D., Meier-Eiss, J., Arber, W., Lenski, R. E. and Blot, M.** (1999). Genomic evolution during a 10,000-generation experiment with bacteria. *Proceedings of the National Academy of Sciences* **96**, 3807-3812.
- Pointer, M. D., Gage, M. J. and Spurgin, L. G.** (2021). Tribolium beetles as a model system in evolution and ecology. *Heredity* **126**, 869-883.
- Prasad, N. G., Shakarad, M., Gohil, V. M., Sheeba, V., Rajamani, M. and Joshi, A.** (2000). Evolution of reduced pre-adult viability and larval growth rate in laboratory populations of *Drosophila melanogaster* selected for shorter development time. *Genet Res* **76**, 249-259.
- Rafiqi, A. M., Lemke, S., Ferguson, S., Stauber, M. and Schmidt-Ott, U.** (2008). Evolutionary origin of the amnioserosa in cyclorrhaphan flies correlates with spatial and temporal expression changes of zen. *Proceedings of the National Academy of Sciences* **105**, 234-239.
- Ratte, H. T.** (1985). Temperature and insect development. *Environmental physiology and biochemistry of insects*, 33-66.
- Renner, S. S. and Zohner, C. M.** (2018). Climate change and phenological mismatch in trophic interactions among plants, insects, and vertebrates. *Annual review of ecology, evolution, and systematics* **49**, 165-182.
- Rewitz, K. F., Yamanaka, N. and O'Connor, M. B.** (2010). Steroid hormone inactivation is required during the juvenile-adult transition in *Drosophila*. *Developmental cell* **19**, 895-902.
- Ritchie, M. G. and Kyriacou, C. P.** (1996). Artificial selection for a courtship signal in *Drosophila melanogaster*. *Animal Behaviour* **52**, 603-611.
- Rose, M. R.** (1984). Artificial selection on a fitness-component in *Drosophila melanogaster*. *Evolution*, 516-526.
- Samplonius, J. M., Atkinson, A., Hassall, C., Keogan, K., Thackeray, S. J., Assmann, J. J., Burgess, M. D., Johansson, J., Macphie, K. H., Pearce-Higgins, J. W., et al.** (2021). Strengthening the evidence base for temperature-mediated phenological asynchrony and its impacts. *Nat Ecol Evol* **5**, 155-+.
- Sardell, J. M., Cheng, C., Dagilis, A. J., Ishikawa, A., Kitano, J., Peichel, C. L. and Kirkpatrick, M.** (2018). Sex differences in recombination in sticklebacks. *G3: Genes, Genomes, Genetics* **8**, 1971-1983.
- Sarrazin, A. F., Peel, A. D. and Averof, M.** (2012). A segmentation clock with two-segment periodicity in insects. *Science* **336**, 338-341.
- Schellens, S., Lenaerts, C., Pérez Baca, M. d. R., Cools, D., Peeters, P., Marchal, E. and Vanden Broeck, J.** (2022). Knockdown of the Halloween Genes spook, shadow and shade Influences Oocyte Development, Egg Shape, Oviposition and Hatching in the Desert Locust. *International journal of molecular sciences* **23**, 9232.
- Schlötterer, C., Tobler, R., Kofler, R. and Nolte, V.** (2014). Sequencing pools of individuals—mining genome-wide polymorphism data without big funding. *Nature Reviews Genetics* **15**, 749-763.
- Schröder, R., Beermann, A., Wittkopp, N. and Lutz, R.** (2008). From development to biodiversity—*Tribolium castaneum*, an insect model organism for short germband development. *Development genes and evolution* **218**, 119-126.

- Schumann, I., Kenny, N., Hui, J., Hering, L. and Mayer, G.** (2018). Halloween genes in panarthropods and the evolution of the early moulting pathway in Ecdysozoa. *Royal Society Open Science* **5**, 180888.
- Seslija, D. and Tucic, N.** (2003). Selection for developmental time in bean weevil (*Acanthoscelides obtectus*): correlated responses for other life history traits and genetic architecture of line differentiation. *Entomol Exp Appl* **106**, 19-35.
- Shapiro, J. A.** (2011). *Evolution: a view from the 21st century*: Pearson education.
- Sharma, K., Mishra, N. and Shakarad, M. N.** (2020). Evolution of reduced minimum critical size as a response to selection for rapid pre-adult development in *Drosophila melanogaster*. *Roy Soc Open Sci* **7**.
- Siepel, A. and Arbiza, L.** (2014). Cis-regulatory elements and human evolution. *Current opinion in genetics & development* **29**, 81-89.
- Singer, M. C. and Parmesan, C.** (2010). Phenological asynchrony between herbivorous insects and their hosts: signal of climate change or pre-existing adaptive strategy? *Philos T R Soc B* **365**, 3161-3176.
- Stearns, S. C.** (1992). *The evolution of life histories*: Oxford university press Oxford.
- Stefan, M. I. and Le Novere, N.** (2013). Cooperative binding. *PLoS computational biology* **9**, e1003106.
- Strobl, F. and Stelzer, E. H.** (2014). Non-invasive long-term fluorescence live imaging of *Tribolium castaneum* embryos. *Development* **141**, 2331-2338.
- Sun, J., Smith, L., Armento, A. and Deng, W.-M.** (2008). Regulation of the endocycle/gene amplification switch by Notch and ecdysone signaling. *The Journal of cell biology* **182**, 885-896.
- Tak, Y. G. and Farnham, P. J.** (2015). Making sense of GWAS: using epigenomics and genome engineering to understand the functional relevance of SNPs in non-coding regions of the human genome. *Epigenetics & chromatin* **8**, 1-18.
- Tautz, D. and Pfeifle, C.** (1989). A non-radioactive in situ hybridization method for the localization of specific RNAs in *Drosophila* embryos reveals translational control of the segmentation gene hunchback. *Chromosoma* **98**, 81-85.
- Teleman, A. A., Chen, Y.-W. and Cohen, S. M.** (2005). *Drosophila* Melted modulates FOXO and TOR activity. *Developmental cell* **9**, 271-281.
- Tenaillon, O., Rodríguez-Verdugo, A., Gaut, R. L., McDonald, P., Bennett, A. F., Long, A. D. and Gaut, B. S.** (2012). The molecular diversity of adaptive convergence. *science* **335**, 457-461.
- Teotonio, H., Chelo, I. M., Bradic, M., Rose, M. R. and Long, A. D.** (2009). Experimental evolution reveals natural selection on standing genetic variation. *Nature Genetics* **41**, 251-257.
- Thackeray, S. J., Henrys, P. A., Hemming, D., Bell, J. R., Botham, M. S., Burthe, S., Helaouet, P., Johns, D. G., Jones, I. D., Leech, D. I., et al.** (2016). Phenological sensitivity to climate across taxa and trophic levels. *Nature* **535**, 241-U294.
- Thummel, C.** (2002). Ecdysone-regulated puff genes 2000. *Insect biochemistry and molecular biology* **32**, 113-120.
- Tomoyasu, Y., Miller, S. C., Tomita, S., Schoppmeier, M., Grossmann, D. and Bucher, G.** (2008). Exploring systemic RNA interference in insects: a genome-wide survey for RNAi genes in *Tribolium*. *Genome biology* **9**, 1-22.
- Truman, J. W.** (2019). The evolution of insect metamorphosis. *Current Biology* **29**, R1252-R1268.
- Uhlirova, M., Foy, B. D., Beaty, B. J., Olson, K. E., Riddiford, L. M. and Jindra, M.** (2003). Use of Sindbis virus-mediated RNA interference to demonstrate a conserved role of Broad-Complex in insect metamorphosis. *Proceedings of the National Academy of Sciences* **100**, 15607-15612.
- Van Asch, M., Salis, L., Holleman, L. J., Van Lith, B. and Visser, M. E.** (2013). Evolutionary response of the egg hatching date of a herbivorous insect under climate change. *Nature Climate Change* **3**, 244-248.
- van der Zee, M., Berns, N. and Roth, S.** (2005). Distinct functions of the *Tribolium* *zerknu llt* genes in serosa specification and dorsal closure. *Current Biology* **15**, 624-636.

- van Drongelen, R., Vazquez-Faci, T., Huijben, T. A., van der Zee, M. and Idema, T.** (2018). Mechanics of epithelial tissue formation. *Journal of Theoretical Biology* **454**, 182-189.
- Verta, J.-P. and Jones, F. C.** (2019). Predominance of cis-regulatory changes in parallel expression divergence of sticklebacks. *Elife* **8**, e43785.
- Visser, M. E. and Gienapp, P.** (2019). Evolutionary and demographic consequences of phenological mismatches. *Nat Ecol Evol* **3**, 879-885.
- Vlachos, C. and Kofler, R.** (2019). Optimizing the power to identify the genetic basis of complex traits with evolve and resequence studies. *Molecular biology and evolution* **36**, 2890-2905.
- Wittkopp, P. J. and Kalay, G.** (2012). Cis-regulatory elements: molecular mechanisms and evolutionary processes underlying divergence. *Nature Reviews Genetics* **13**, 59-69.
- Xia, Q., Guo, Y., Zhang, Z., Li, D., Xuan, Z., Li, Z., Dai, F., Li, Y., Cheng, D. and Li, R.** (2009). Complete resequencing of 40 genomes reveals domestication events and genes in silkworm (*Bombyx*). *Science* **326**, 433-436.
- Xiang, H., Liu, X., Li, M., Zhu, Y. n., Wang, L., Cui, Y., Liu, L., Fang, G., Qian, H. and Xu, A.** (2018). The evolutionary road from wild moth to domestic silkworm. *Nature ecology & evolution* **2**, 1268-1279.
- Xiong, W. C. and Montell, C.** (1993). tramtrack is a transcriptional repressor required for cell fate determination in the *Drosophila* eye. *Genes & development* **7**, 1085-1096.
- Yadav, P. and Sharma, V. K.** (2013). Correlated changes in circadian clocks in response to selection for faster pre-adult development in fruit flies *Drosophila melanogaster*. *Journal of Comparative Physiology B-Biochemical Systems and Environmental Physiology* **183**, 333-343.
- Yamanaka, N., Rewitz, K. F. and O'Connor, M. B.** (2013). Ecdysone control of developmental transitions: lessons from *Drosophila* research. *Annual review of entomology* **58**, 497-516.
- Yao, L., Tak, Y. G., Berman, B. P. and Farnham, P. J.** (2014). Functional annotation of colon cancer risk SNPs. *Nature communications* **5**, 1-13.
- Yoo, B., Kim, H.-y., Chen, X., Shen, W., Jang, J. S., Stein, S. N., Cormier, O., Pereira, L., Shih, C. R. and Krieger, C.** (2021). 20-hydroxyecdysone (20E) signaling regulates amnioserosa morphogenesis during *Drosophila* dorsal closure: EcR modulates gene expression in a complex with the AP-1 subunit, Jun. *Biology open* **10**, bio058605.
- Yu, Y., Yussa, M., Song, J., Hirsch, J. and Pick, L.** (1999). A double interaction screen identifies positive and negative ftz gene regulators and ftz-interacting proteins. *Mechanisms of development* **83**, 95-105.
- Yukuhiro, K., Sezutsu, H., Tamura, T., Kosegawa, E., Iwata, K., Ajimura, M., Gu, S.-H., Wang, M., Xia, Q. and Mita, K.** (2012). Little gene flow between domestic silkworm *Bombyx mori* and its wild relative *Bombyx mandarina* in Japan, and possible artificial selection on the CAD gene of *B. mori*. *Genes & genetic systems* **87**, 331-340.
- Zee, M. v. d., Stockhammer, O., Levetzow, C. v., Fonseca, R. N. d. and Roth, S.** (2006). Sog/Chordin is required for ventral-to-dorsal Dpp/BMP transport and head formation in a short germ insect. *Proceedings of the National Academy of Sciences* **103**, 16307-16312.
- Zhu, Y.-N., Wang, L.-Z., Li, C.-C., Cui, Y., Wang, M., Lin, Y.-J., Zhao, R.-P., Wang, W. and Xiang, H.** (2019). Artificial selection on storage protein 1 possibly contributes to increase of hatchability during silkworm domestication. *PLoS genetics* **15**, e1007616.
- Zwaan, B., Bijlsma, R. and Hoekstra, R. F.** (1995). Artificial Selection for Developmental Time in *Drosophila-Melanogaster* in Relation to the Evolution of Aging - Direct and Correlated Responses. *Evolution* **49**, 635-648.

## Supplementary information

Supplementary Table 4-1. List of candidate genes. Candidate genes 1-16 are in chromosome 3, and 17-45 are on chromosome 9.

Candidate genes (NCBI's annotation)	Gene symbol	Acronym	Lead SNP type	SNP position and Ref/Alt	-logP-value	AF divergence
1. uncharacterized LOC656417	LOC656417	1. LOC656417	Principal SNP	13868791, T/A	59.93	0.661
2. thioredoxin reductase 1, mitochondrial	LOC103314616	2. Trxr-1	Principal SNP	13957908, A/G	61.27	0.663
		2. Trxr-1	Principal SNP	13971318, C/T	59.7	0.786
3. C-factor	LOC656669	3. C-factor	Principal SNP	14022139, T/C	58.89	0.681
4. solute carrier family 25 member 35	LOC656748	4. SLC25-35-1	Principal SNP	14051912, T/A	61.09	0.733
5. Protein melted	LOC656839	5. Melted	Principal SNP	14086409, G/T	60.56	0.879
6. solute carrier family 25 member 35, transcript variant X3	LOC657090	6. SLC25-35-2	Principal SNP	14128581, T/C	65.84	0.781
7. calcitonin gene-related peptide type 1 receptor	LOC657479	7. CalcitoninR	Principal SNP	14218183, T/C	96.72	0.803
8. probable cytochrome P450 6A14	LOC657560	8. Cyp6a14	Principal SNP	14245723, T/A	63.43	0.662
7. calcitonin gene-related peptide type 1 receptor	LOC657479	7. CalcitoninR	Principal SNP	14262745, T/C	58.89	0.724
		7. CalcitoninR	Principal SNP	14288001, A/G	63.18	0.750
		7. CalcitoninR	Principal SNP	14298023, A/T	61.91	0.756
		7. CalcitoninR	Principal SNP	14312131, C/G	62.43	0.698
9. cytochrom P450 6K1	LOC658029	9. Cyp6k1	Principal SNP	14370963, G/A	59.51	0.731
10. Uncharacterized Loc103312175	LOC103312175	10. Or327	Principal SNP	14381004, C/T	66.91	0.674
11. glycine dehydrogenase (decarboxylating), mitochondrial	LOC658613	11. GLDC	Significant SNP	15582940, G/C	40.08	0.438
12. protein transport protein Sec61 subunit alpha isoform 2	LOC658693	12. Sec61 $\alpha$	Significant SNP	15609700, A/C	53.41	0.852
13. MAP kinase-interacting serine/threonine-protein kinase 1	LOC658754	13. Lk6 kinase	Principal SNP	15648008, G/T	67.59	0.700
14. superkiller viralicidic activity 2-like 2	LOC658969	14. Skiv2	Principal SNP	15666693, G/C	59.59	0.668
15. cell division cycle protein 20 homolog	LOC659043	15. Cortex	Significant SNP	15717468, T/C	51.84	0.820
16. laccase-2	Lac2	16. Lac2	Principal SNP	15754769, T/C	71.21	0.738
17. sodium- and chloride-dependent GABA transporter 1	LOC655406	17. Gat	Significant SNP	412499, A/G	57.82	0.600
18. metabotropic glutamate receptor 2-like	LOC656715	18. mGluR	Significant SNP	414797, T/A	40.98	0.830
19. suppression of tumorigenicity 18 protein	LOC656465	19. St18 C2H2C	Significant SNP	966489, C/G	50.88	0.482
20. high affinity cationic amino acid transporter 1	LOC655390	20. CAT1	Significant SNP	1176055, G/A	53.19	0.497
21. cationic amino acid transporter 2	LOC655468	21. CAT2	Significant SNP	1199876, T/A	53.01	0.554
22. polycystic kidney disease 1-related protein-like	LOC107398588	22. Pkd1	Principal SNP	1236554, G/T	60.85	0.749

23. Polycystin-2-like	LOC107398589	23. Polycystin2	Principal SNP	1253862, A/G	60.95	0.669
24. high affinity cationic amino acid transporter 1	LOC655801	24. CAT3	Principal SNP	1378218, C/A	70.07	0.686
25. dynactin subunit 2	LOC655964	25. Dynactin2	Principal SNP	1409012, A/G	62.97	0.848
26. transcription factor Adf-1	LOC103314616	26. Adf-1	Principal SNP	1416931, A/T	67.72	0.751
27. lethal(3)malignant brain tumor-like protein 4	LOC656299	27. l(3)mbt	Principal SNP	1463470, A/G	78.27	0.810
28. protein-L-isoaspartate O-methyltransferase domain-containing protein 1	LOC656461	28. Pemt	Significant SNP	1453282, G/A	63.12	0.831
29. phospholipase A-2-activating protein	LOC656630	29. Plap	Principal SNP	1489792, A/T	66.79	0.772
		29. Plap	Principal SNP	1505606, T/G	74.39	0.705
30. uncharacterized LOC107397428	LOC107397428	30. LOC107397428	Principal SNP	1540084, A/G	70.70	0.780
		30. LOC107397428	Principal SNP	1553652, T/C	72.68	0.875
31. chymase	LOC103314618	31. Chymase	Principal SNP	1574195, G/A	75.88	0.821
32. cytochrome P450 CYP18A1	Cyp18a1	32. Cyp18a1	Principal SNP	1613665, G/A	84.85	0.797
33. cytochrome P450 306A1	LOC656884	33. Cyp306a1	Principal SNP	1631265, T/C	65.80	0.759
		33. Cyp306a1	Principal SNP	1846872, A/T	70.05	0.603
34. centromere protein S	LOC103315036	34. CENP-S	Principal SNP	2168201, G/C	62.86	0.809
35. protein deadpan	LOC656046	35. Deadpan	Principal SNP	2218287, T/A	73.39	0.723
36. 60S ribosomal protein L27	LOC657523	36. RPL27	Principal SNP	2289810, C/A	67.32	0.742
37. pancreatic triacylglycerol lipase	LOC657679	37. Lipase	Principal SNP	2322171, T/C	68.34	0.716
		37. Lipase	Principal SNP	2339313, A/G	66.40	0.756
38. hypothetical protein	LOC103314394	38. LOC103314394	Principal SNP	2417247, G/A	60.44	0.729
39. SH3 domain-binding protein 5 homolog	LOC657915	39. SH3bp	Principal SNP	2427805, T/A	60.31	0.810
40. integrin alpha-PS2	LOC657993	40. Integrin $\alpha$ PS2	Principal SNP	2438730, T/G	65.45	0.717
		40. Integrin $\alpha$ PS2	Principal SNP	2452502, C/T	78.01	0.701
		40. Integrin $\alpha$ PS2	Principal SNP	2483912, A/G	63.49	0.771
41. inositol hexakisphosphate kinase 1	LOC658073	41. Ip6k	Principal SNP	2581813, T/G	73.88	0.795
42. uncharacterized LOC657682	LOC657682	42. LOC657682	Principal SNP	3260859, T/C	65.26	0.788
		42. LOC657682	Principal SNP	3274854, A/G	62.77	0.683
43. TATA box-binding protein-associated factor RNA polymerase I subunit B	LOC103314719	43. TAF1B	Principal SNP	3438606, C/T	61.37	0.734
44. putative uncharacterized protein DDB G0271606	LOC103314169	44. LOC103314169	Principal SNP	3497871, A/G	75.03	0.722

45. BMP and activin membrane-bound inhibitor homolog	LOC103314 170	45. Bambi	Principal SNP	3519980, T/C	61.05	0.645
--	------------------	-----------	---------------	--------------	-------	-------

Supplementary Table 4-2. Primers of candidate genes used for qPCR.

Gene acronym	Forward primer (5'-3')	Reverse primer (5'-3')
<b><i>Tribolium castaneum</i></b>		
1. <i>LOC656417</i>	CAGCAGAGGTGCCGTCTTTA	CCACTTGCCACCGGGATAATA
2. <i>Trxr-1</i>	GTTCATACGGTGACCAAACAG	ACGGCACCCGGTATATTAG
3. <i>C-factor</i>	AAATGCGCCACTGGATGTTG	ACCTCCATTGTGGCTTTCGT
4. <i>SLC25-35-1</i>	TTTAACTGCATTTGCTGCCAG	GCGTCGTAACAATATCAAACG
5. <i>Meltd</i>	GGTGATGTGATTTGTAGCGGTG	CACCTCCAAGGATGCAAAGG
6. <i>SLC25-35-2</i>	GCGGTGGGACATCAGCATAA	GCTGAAGCCCCAACTACTGTC
7. <i>CalcitoninR</i>	GCACCAACTGAACCTTTGTGCG	GTTATTCGCGCGTTTTTCGTGC
8. <i>Cyp6a14</i>	TGTAGCCCTCCTGGTCATCA	GACTGTGGGTGGGAGGAATG
9. <i>Cyp6k1</i>	GATGTGAAAATGGCAGCACAAAG	CCAGTTCGTAGAGAGCGAAAAG
10. <i>Or327</i>	TGGCAACAATAACATCTGGC	AGATACCAAGGGATCGAAGAC
11. <i>GLDC</i>	TAACTCTTCTCCGACCACC	CGCACCAAGGACTGATTAC
12. <i>Sec61a</i>	AACAGAGGAACCCTGATGG	AAAGCTCGGTCTTTCGGTG
13. <i>Lk6 kinase</i>	TGGCATGACCCGGTACCTTA	TGGCGAAATCTTGGGTGAGG
14. <i>Skiv2</i>	AATCAGACGGCCATTCCTGG	TGGTACGATGCAATCTGTGGT
15. <i>Cortex</i>	TGAAACGGACACAATTAGCC	TTCCTTTGACCTACTCTACTG
16. <i>Lac2</i>	TACAACAGACATTTAGTTGCACCA	AGGTGGGGCCATGTAGGAAA
17. <i>Gat</i>	GATCCTTGTTGTAACCCTGA	GGTCCAGGAACTATACTTGAG
18. <i>mGluR</i>	GCTTTATTTACCCAGATCCC	GAAATCACCATCCCACTCC
19. <i>St18 C2H2C</i>	GGAACAGCACAAAGCAGCAG	AGGACAGCCGCTCAAAGAAC
20. <i>CAT1</i>	ATGGAAGGCGCAGCTCAATG	GGGAAATGACGATGGCTAGAGG
21. <i>CAT2</i>	TCGAAGCGGGAGGAGAACTA	CGCTCCTAATGCTATGGCAA
22. <i>Pkd1</i>	GAGAACGCTGCATGTTTCAGT	CCGTTGCCAAAATCGTCCAT
23. <i>Polycystin2</i>	GCGGTGCCTTTGTGTTTTCT	AGCAGGAAGGCCATTTCCT
24. <i>CAT3</i>	GCCCTCAGTTGTCTTGTCGT	CGCAGACGTAGCTGTAGATGT
25. <i>Dynactin2</i>	ACCCACAAGGGACGCAAATC	CGTGCTTGTCCGGTTCGATA
26. <i>Adf-1</i>	GTAAAGCCAGCACTAGCAACC	AACGATTTCGTGATAACTCACGTC
27. <i>l(3)mbt</i>	GCAGCTTGCTGGAAGTGATT	AGGCCGTAACAGCCACATTC
28. <i>Pcmt</i>	TGAAGAGCGAGCCGAAAAC	AGCAGCTCATCTCCTAAGCC
29. <i>Plap</i>	ACGCTTCCTTACCTGGCAA	GACGCGACAAAGCACTCAAG
30. <i>LOC107397428</i>	TCCACACATGGCCCGAAAAC	CCAAAGTACCACGGTAGCAAC
31. <i>Chymase</i>	GCAGTAACAAGTGGACGACAAC	TCGGCAATCCAAGGAAAATAGG
32. <i>Cyp18a1</i>	TCCTCTTCATGCTGCATCACC	CGCAACACTTCCAACATCGTC
33. <i>Cyp306a1</i>	ACGGATTACCGAGGCTTTT	AAGTGAGTCCAAACCGACCC
34. <i>CENP-S</i>	CACTTCTCGAAAAATGTCACGC	GAAAGCTTCTAAATCCGACGC
35. <i>Deadpan</i>	GGGAAATCGCCTTGCTTTTAC	GGAGGACTTACCGAAGTTGATG
36. <i>RPL27</i>	CATAAACGCATGGGCAAGGG	ACCGAATAACGTGTGGGCAT
37. <i>Lipase</i>	GATATTGATGCCAGCGATTTCC	ATCCAGTCCAGTGATCCTCC
38. <i>LOC103314394</i>	TGGTCTCTGCTCCTTACTC	ACAAAGCTCACCCAAGTTGTC

39. <i>SH3bp</i>	AACTCGAGAAGCTCAACACCA	TCGGAAAGTGGTGTGGCTT
40. <i>Integrin αPS2</i>	GTTATTCACGCCAGTTCGTC	AGTTCGTCCGCCGTTTTTC
41. <i>Ip6k</i>	GACCTCCTCAGACGTGACCA	CTTACAGATCGTGCTCGGGT
42. <i>LOC657682</i>	TCGCATCGTTTATTACCCACC	CAGTCACTTTGTACCCAGCC
43. <i>TAF1B</i>	GATAAGACAGCGAAGACTGAG	TCCACAAGAGACGAACGAC
44. <i>LOC103314169</i>	TGGTCTCTGCTCCTTACTC	ACAAAGCTCACCCAAGTTGTC
45. <i>Bambi</i>	ACCATCGGCAACTTACAAC	AGAATGACTGCTCCACAAAC

Supplementary Table 4-3. Primers used for pRNAi.

Gene acronym	Forward primer (5'-3')	Reverse primer (5'-3')	Product length (bp)
<b><i>Tribolium castaneum</i></b>			
1. <i>LOC656417</i>	TCAGTGCACGGACTTGTGT	GCTCACACGAGAACTCCTCG	658
5. <i>Meltd</i>	CAAGGGCTGGAGACCTGTTT	AGTGTGACCACCACCTTGG	1977
6. <i>SLC25-35-2</i>	TGGAGCTGCACTTCTGATGC	CCAGCACCTTTGTACAAGCC	615
7. <i>CalcitoninR</i>	TTCAGTTGGTGC GCGT TTTGT	TCCCAAGACGCTCCTCACAG	910
8. <i>Cyp6a14</i>	TCGACATTCTGGGCGTGTCT	TGTGTCCTTCCTGCTACCCG	1384
9. <i>Cyp6k1</i>	GACAACTGGCGCAATCTCCG	TATAGCCCCCGGGTCCAAC	1068
16. <i>Lac2</i>	CCAGCTCAGTTGACGATTCA	TCAACTTTGTGGGTGCACAT	650
20. <i>CAT1</i>	TGCTCGAGTCCCTAAGGCAG	GCATCGAAGGCAGCTGTGAA	1185
21. <i>CAT2</i>	ATGGGTCTGCGCACTATCAC	TGCCAGGGATCCAAGGAACT	1594
24. <i>CAT3</i>	GGTGTGGAGGGTGTGACGA	TTCCCGTTCGGTTTGACGGA	1827
31. <i>Chymase</i>	GCTGCTTTTCTTTGCCTCTGA	CCGGGTGTCTATGATGTGGG	722
32. <i>Cyp18a1</i>	TGCACCTGCACTTCAGGGAT	TTCAGCGTTGATGAACCGGC	1124
33. <i>Cyp306a1</i>	ACACTTCAGTTTCGTCCCAA	GAATCCGAGACACCCACCAA	492
37. <i>Lipase</i>	CGCCTTCGGTGCTGTTTAGT	ACTCTCGTCCCGTGGTAAGG	1344
41. <i>Ip6k</i>	GAGATACTGAAACCCGCAAC	CGTCGTAGCAACAGGGGACT	954

Supplementary Table 4-4. Primers used for RNAi in ecdysone biosynthesis and 20E signaling pathway.

Gene acronym	Forward primer (5'-3')	Reverse primer (5'-3')	Product length (bp)
<b><i>Tribolium castaneum</i></b>			
<i>Spo</i>	GCTCAAGTCCTTCCTCCACC	GTCTCTTTCCCGTGCTGAA	837
<i>Phm</i>	ACACTTCAGTTTCGTCCCAA	GAATCCGAGACACCCACCAA	492
<i>Dib</i>	CTACTGCTGTTGATCCGCCA	CTGTAGTTAGAGGGGCCGCA	1005
<i>Sad</i>	TTCATGGATGGGGCCAAC	TGGTTCCCCAGCTCAACTTC	962
<i>Shd</i>	ACTCATAACCGGACCCTTGG	GCGTCCGAAAATTGCGTTC	1083
<i>Ecr</i>	TCCGGTTACCACTACAACGC	TTCGAAAATCCGCCCTCCAAA	1122
<i>USP</i>	ATCTCTCGATGGGCAGCTTG	TGCCCACACACTAAACCCT	1217

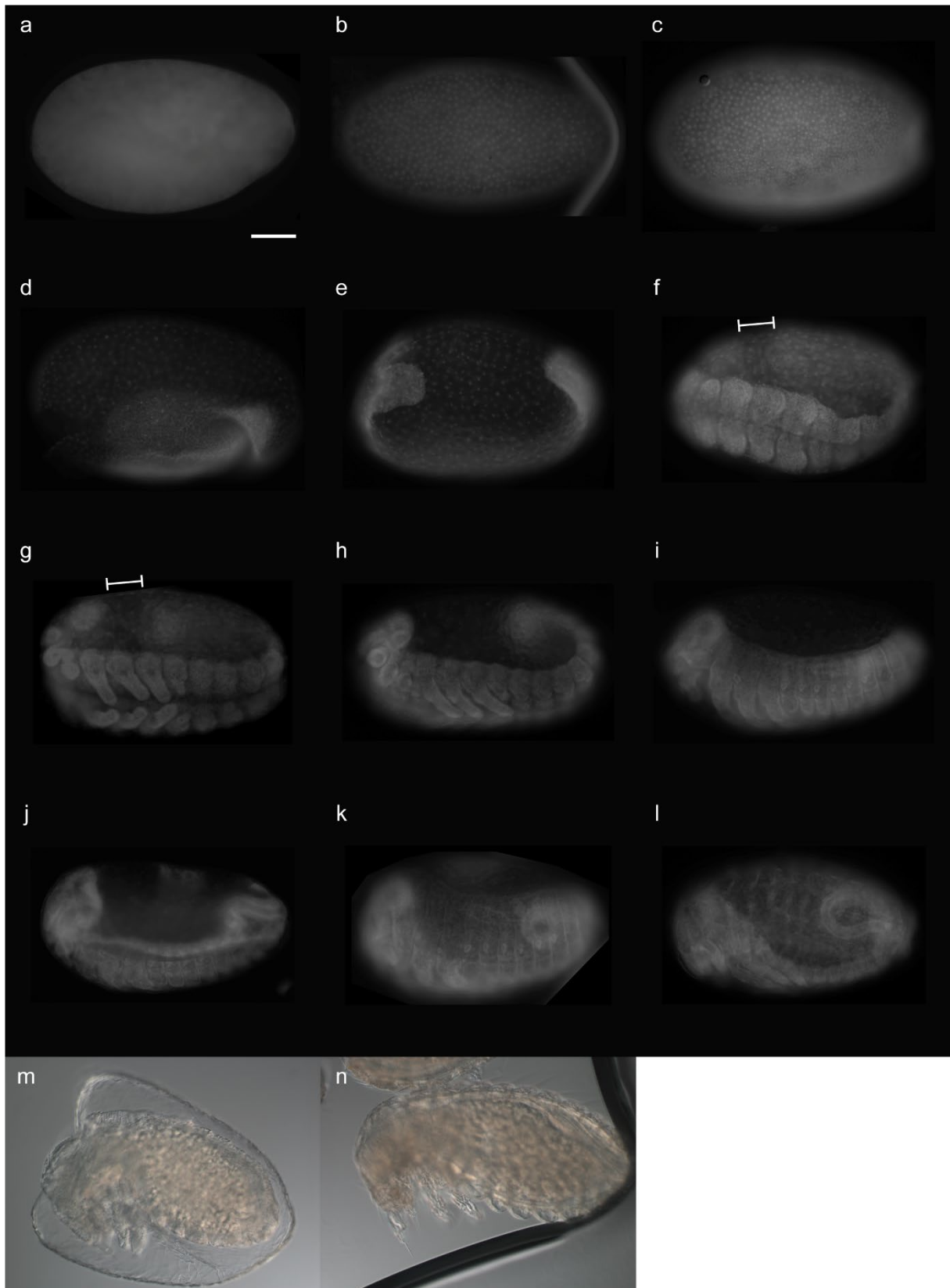


Supplementary Table 4-5. Primers used for qPCR in ecdysone biosynthesis and 20E signaling pathway.

Gene acronym	Forward primer (5'-3')	Reverse primer (5'-3')
<b><i>Tribolium castaneum</i></b>		
<i>Spo</i>	GGGACGAGCCTGGACTGTT	CCCGTGCTGAAAGGAATGA
<i>Phm</i>	ACGGATTCACCGAGGCTTTT	AAGTGAGTCCAAACCGACCC
<i>Dib</i>	ACAGGAAGAGCCACCTCACC	ACCATTCGGGTCCATTTGTT
<i>Sad</i>	GCTAAGAGCCCGCAAATCC	GGTAAAGCCGCAAAGTCTCCT
<i>Shd</i>	GGTCAACGAACAAGGTGAGG	GAGTCGGTCTGCGATGTAGTTT
<i>Br</i>	CACAACACTTCTGTCTGCGGTG	CACAGGGTGTTTGCAAGGAG

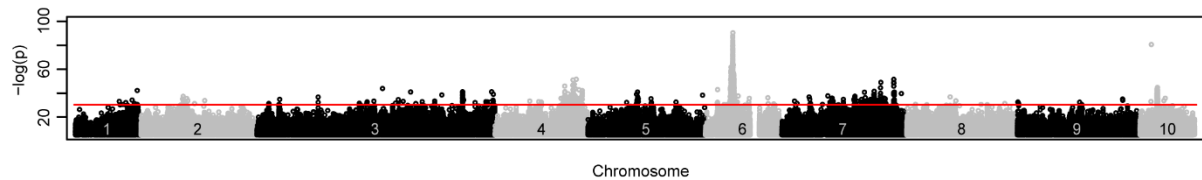
Supplementary Table 4-6. Motifs of transcription factor binding sites found significantly enriched in sequences between Chymase and Cyp18a1 in Find Individual Motif Occurrences (FIMO) database.

Matrix ID	Name	<i>Drosophila</i> sequence	<i>Tribolium</i> sequence	p-value	Detailed class information
MA0460.1	Ttk	AAGGATAAT	AAGGATAAA	8.13e-05	C2H2 zinc finger factors
MA0013.1	Br	TAGTAAACAAA	TAGTAAAAAAA	6.36e-06	C2H2 zinc finger factors
MA0534.1	EcR::usp	GAGTTCATTGACCTT	AAATTCAGTGAAATA	7.95e-05	Nuclear receptors with C4 zinc fingers

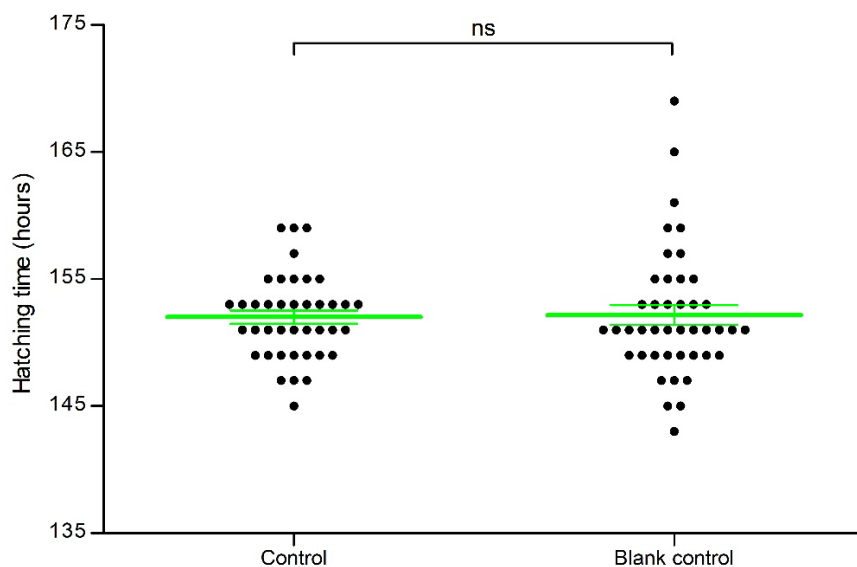


Supplementary Figure 4-1. Numerical staging table for *Tribolium castaneum*. Largely based on (Handel et al., 2000; Hilbrant et al., 2016). **(a)** 0=no nuclei at surface; **(b)** 1=undifferentiated blastoderm (equal nuclei at the surface). **(c)** 2=differentiated blastoderm (the large polyploid nuclei of the serosa can be distinguished from the more dense, smaller nuclei of the germ rudiment). **(d)** 3=gastrulation (amnion and serosa fold over the embryo; serosal window not yet closed). **(e)** 4=extending germband (serosa closed). **(f)** 5=extended germ band (distance between posterior end and head is small, size bar; limbs are buds). **(g)** 6=limbs growing and extending (head and

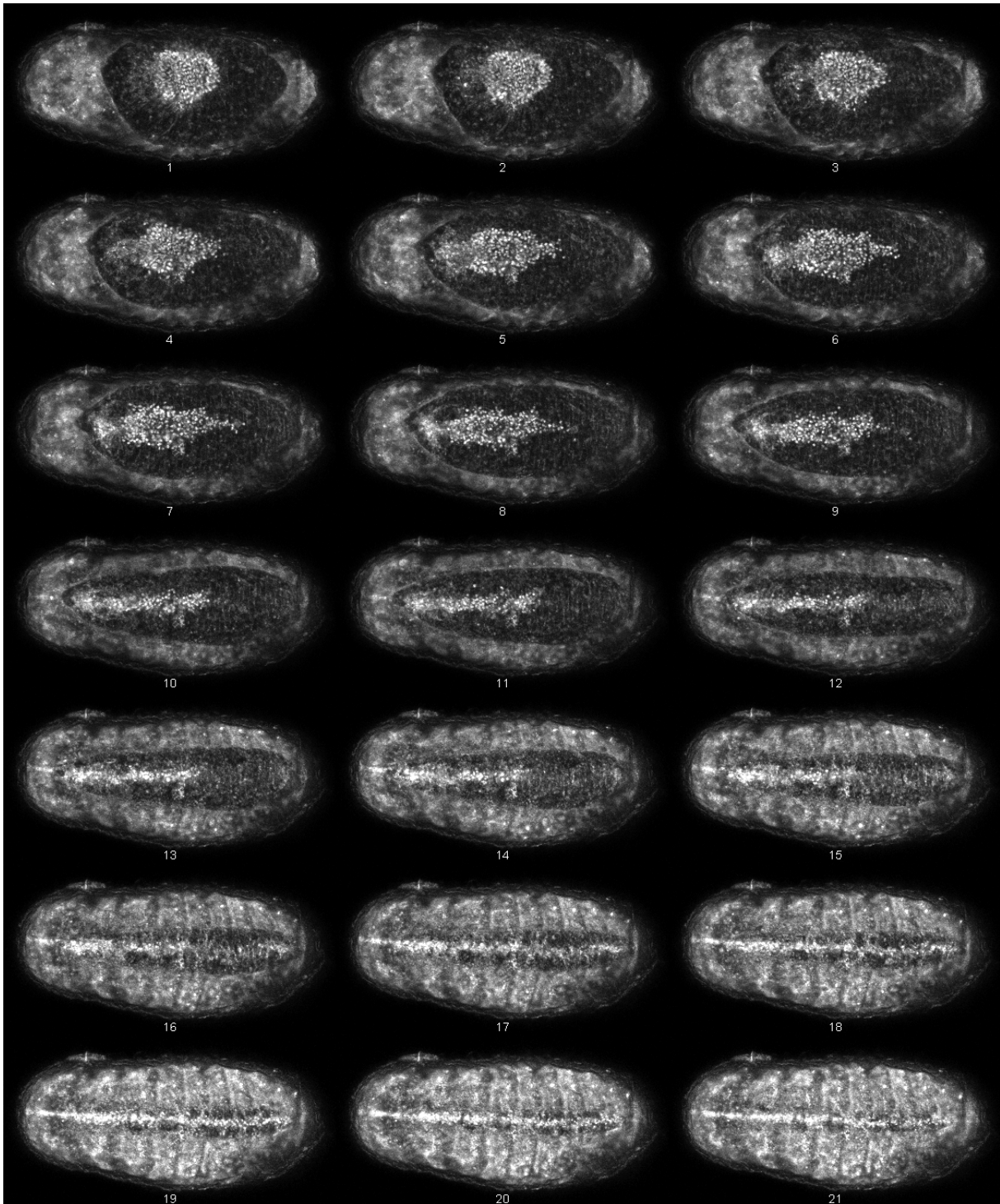
posterior of the germband still close, see size bar; limbs well developing and extending). **(h)** 7=retracting germband (dorsal distance between head and posterior end of the embryo increases again). **(i)** 8=completely retracted germband. **(j)** 9=start of dorsal closure (dorsal organ formation). **(k)** 10=dorsal closure in progress (dorsal organ flatter, lateral sides of the embryo have moved towards dorsal). **(l)** 11=dorsal closure completed (lateral sides of the embryo dorsally fused). **(m)** 12=hatching (still in vitelline membrane). **(n)** 13=hatched (out of vitelline membrane). Scalebar = 200  $\mu\text{m}$ .



Supplementary Figure 4-2. SNP analysis on whole genome of *T. castaneum* between the slow lines and the non-selected lines. The red line indicates  $q = 0.01$  or  $-\log_{10}P$  value equal to 33.0538. In total, 1258 SNPs differ in frequency significantly.



Supplementary Figure 4-3. The embryonic developmental time of offspring embryos in the blank control group, compared to injections of non-targeting control dsRNA into 50 *Tribolium* mothers. Key: Green lines, mean of embryonic developmental time plus standard error. Black dot, the time of every hatched embryo. The student t-test was performed to compare the control and blank control. Key: ns, no significant difference observed in hatching time.

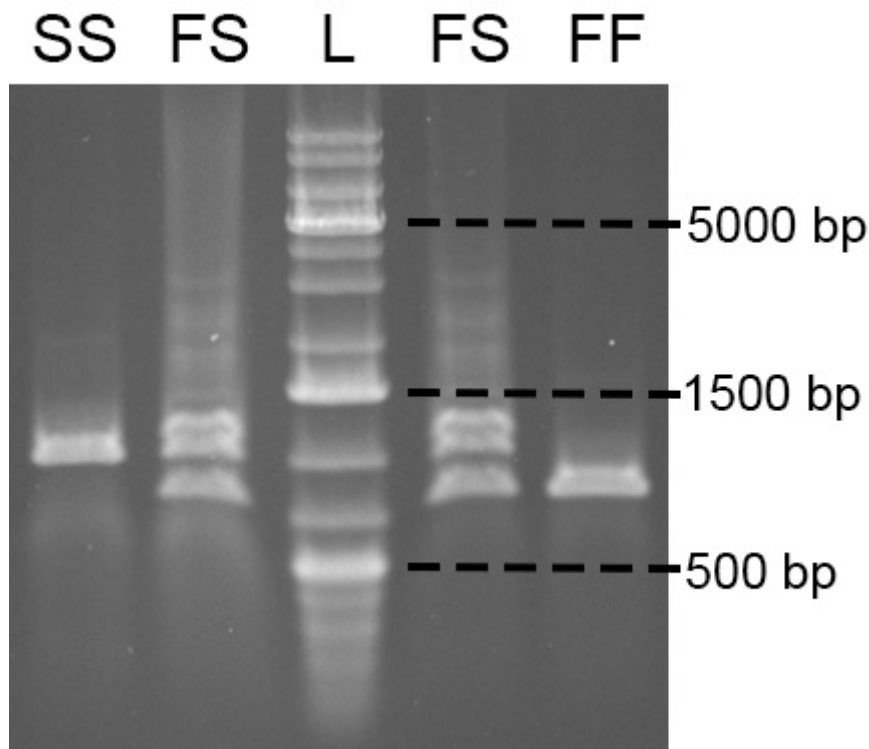


Supplementary Figure 4-4. Overview of dorsal closure process from the dorsal organ (Num. 1) to dorsal closure completely (Num. 21). The *Tribolium castaneum* LifeAct-nGFP line was used for live imaging at 27°C under a confocal microscopy. Numbers indicate 20 min intervals during development.

The 445 bp repeated region

Repeat 1	CTGGGAAGGATAAAAAAATTGAAATAATAAATTTAAAAAATTTATAAAAAAAGAAAATA	60
Repeat 2	CAAGGAAGGATAAAAAAATTGAAATAATAAATTTAAAAAATTTATAAAAAAAGAAAATA *.:*****.*****	60
Repeat 1	TAGTAAAAAAGCGGACAAATGTATTGATACTAATTACAATGAAAGATTCAAATTTTGTG	120
Repeat 2	TAGTAAAAAAGCGGACAAATGTATTGATACTAATTACAATGAAAGATTCAAATTTTGTG *****.*****	120
Repeat 1	TTTTTGCCTTATTTTATAAAGGCGATTGTTTTTTGCTTATTTTAAAATCACTCTGTA	180
Repeat 2	TTTTTGCCTT-ATTTTATAAAGGCGATTGTTTTTTGCTTATTTTAAAATCACTCTGTA *****.*****	179
Repeat 1	TGTCAAAAAATGCATAAAATATAGGGTGTTCATTTGGAAGAT	223
Repeat 2	TGTCAAAAAAGCATAAAATATAGGGTGTTCATTTGGAAGAT *****.*****	222

Supplementary Figure 4-5. Alignment of repeat 1 and repeat 2 in the repeated region of Georgia strain.

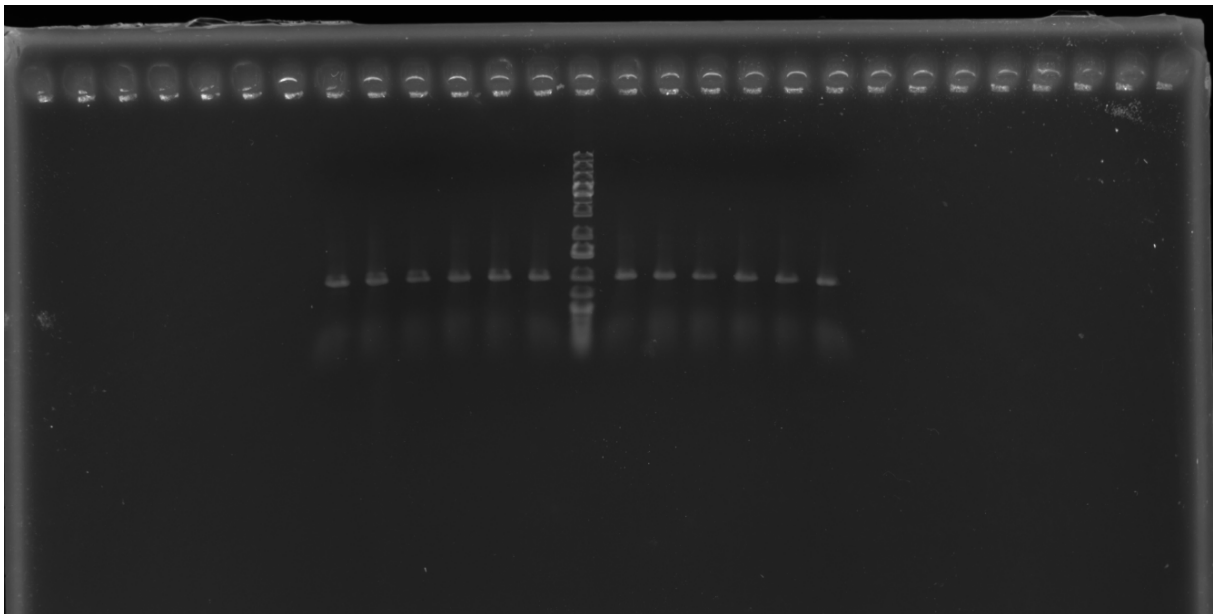


Supplementary Figure 4-6. PCR products including three types of genotypes. SS (Lane 1): homozygotes of the slow allele with the 445 bp repeated region. FS (Lane 2, 4): heterozygotes of the slow allele and the fast allele. L (Lane 3): DNA ladder, GeneRuler 1kb plus DNA ladder (Invitrogen). FF (Lane 5): homozygotes of the fast allele with the 222 bp deleted region.

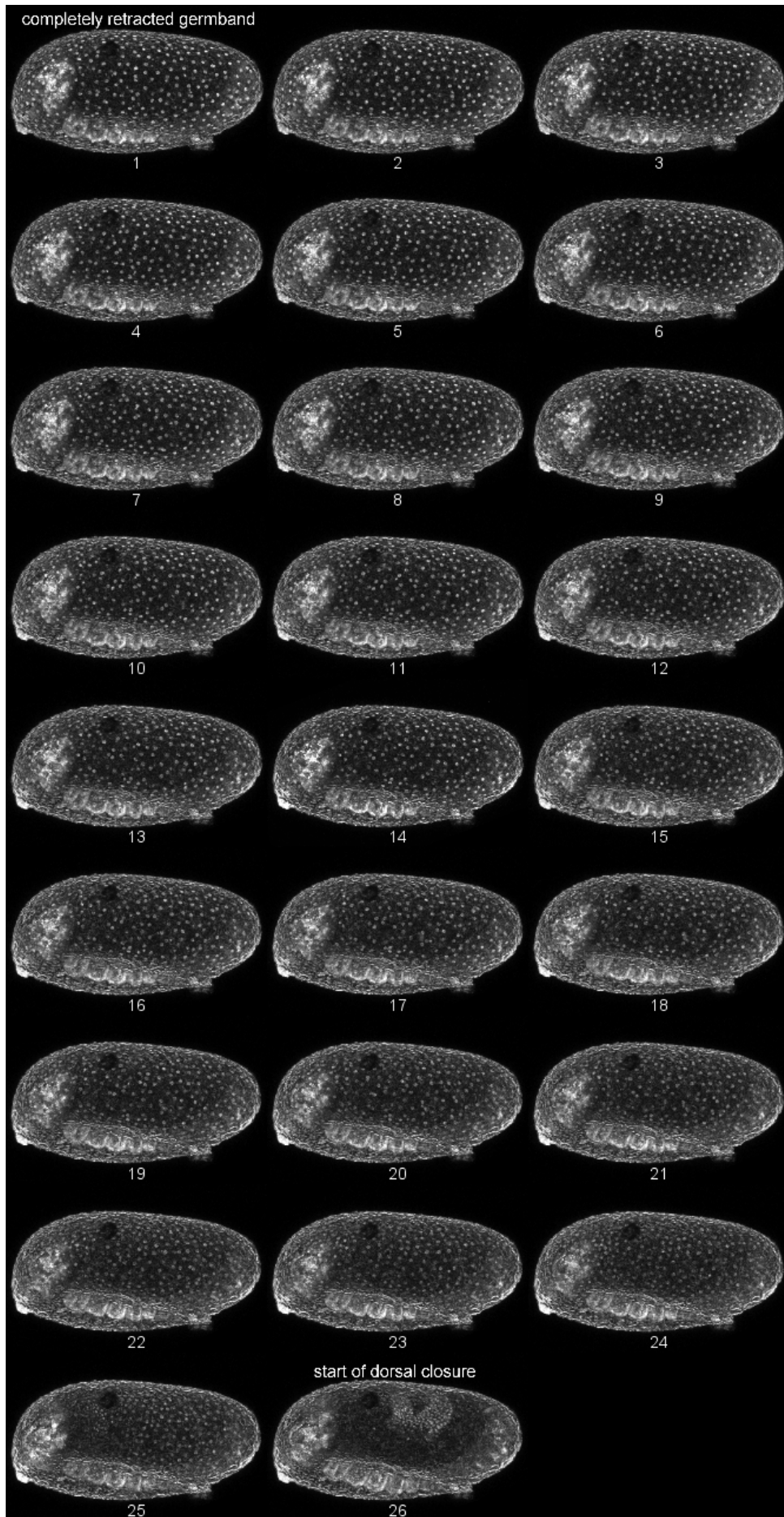
Repeated region

	Tramtrack	
CTGGG	AAGGATAAA	AAATTTGAAATAATAAATTTAAAAAATTTATAAAAAAGAAAATA 60
	Broad	
	TAGTAAAAAA	GGCGGACAAATGTATTGATACTAATTACAATGAAAGATTCAAATTTTGTG 120
TTTTTGCTTTATTTTATAAAGGCGATTGTTTTTTTGCTTATTTTAAAATCACTCTGTA 180		
TGTCAAAAAATGCATAAAATATAGGGTGTTCCATTTGGAAGATCAAGG	Tramtrack	
	AAGGATAAA	AAA 240
	Broad	
ATTGAAATAATAAATTTAAAAAATTTATAAAAAAGAAAATA	TAGTAAAAAA	GCGGAC 300
AAATGTATTGATACTAATTACAATGAAAGATTCAAATTTGTGTTTTGCCTTATTTTAT 360		
AAAAGGCGATTGTTTTTTTGCTTATTTTAAAATCACTCTGTATGTCAAAAAAGCATAAA 420		
ATATAGGGTGTTCCATTTGGAAGAT 445		

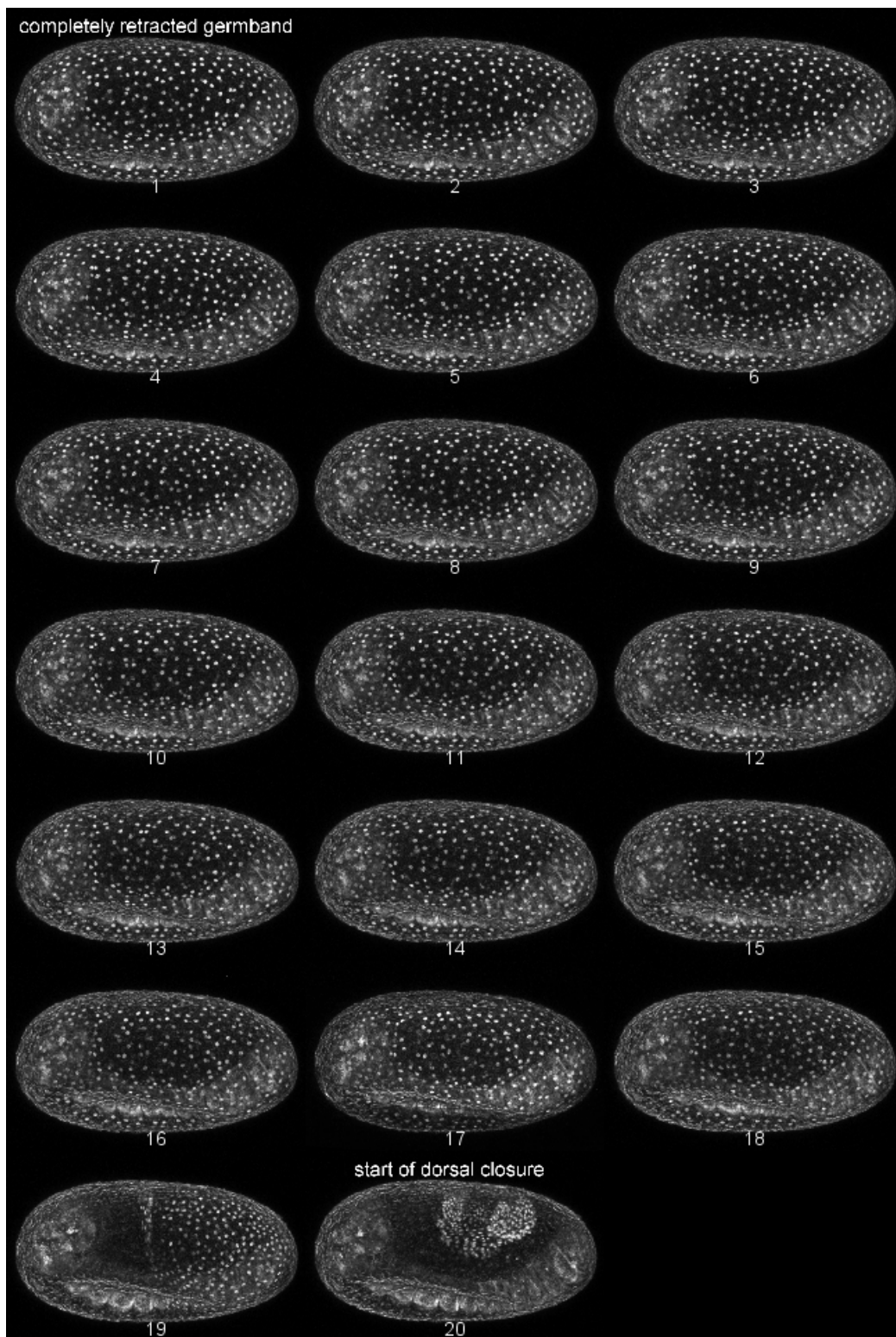
Supplementary Figure 4-7. The transcription factor binding sites Tramtrack (red) and Broad (yellow) in the repeated region.



Supplementary Figure 4-8. Allele frequency of F in the nGFP line is 1. Genotyping PCR (Ethidium bromide staining shown on a 1.0% agarose gel) of 10 beetles from the nGFP line. Ladder is GeneRuler 1kb plus DNA ladder (Invitrogen).



Supplementary Figure 4-9. Duration between completely retracted germband (Num. 1) and start of dorsal closure (Num. 26) of heterozygous nGFP-GA-1 offspring. The developmental progression of the offspring was visualized for live imaging at 25°C under a confocal microscopy. Numbers stand for 26 min intervals during embryonic development.



Supplementary Figure 4-10. Duration between completely retracted germband (Num. 1) and start of dorsal closure (Num. 20) of heterozygous nGFP-Crispr offspring. The developmental progression of the offspring was visualized for live imaging at 25°C under a confocal microscopy. Numbers indicate 26 min intervals during embryonic development.



### Supplementary figure references

- Handel, K., Grunfelder, C. G., Roth, S. and Sander, K.** (2000). Tribolium embryogenesis: a SEM study of cell shapes and movements from blastoderm to serosal closure. *Dev Genes Evol* **210**, 167-179.
- Hilbrant, M., Horn, T., Koelzer, S. and Panfilio, K. A.** (2016). The beetle amnion and serosa functionally interact as apposed epithelia. *eLife* **5**.

**Supplementary File 4-1. Alignments of cloned Sanger-sequenced PCR products from the beetles of the selection lines.**

Fa1	AATTTTGATATTTTAAATAAATAATATAAAAAGCCTAATAAACAAAAGTTTTTTAAATAATA	60
Fa2	AATTTTGATATTTTAAATAAATAATATAAAAAGCCTAATAAACAAAAGTTTTTTAAATAATA	60
Fa3	AATTTTGATATTTTAAATAAATAATATAAAAAGCCTAATAAACAAAAGTTTTTTAAATAATA	60
Fa4	AATTTTGATATTTTAAATAAATAATATAAAAAGCCTAATAAACAAAAGTTTTTTAAATAATA	60
Fb1	AATTTTGATATTTTAAATAAATAATATAAAAAGCCTAATAAACAAAAGTTTTTTAAATAATA	60
Fb2	AATTTTGATATTTTAAATAAATAATATAAAAAGCCTAATAAACAAAAGTTTTTTAAATAATA	60
Fb3	AATTTTGATATTTTAAATAAATAATATAAAAAGCCTAATAAACAAAAGTTTTTTAAATAATA	60
Nb4	AATTTTGATATTTTAAATAAATAATATAAAAAGCCTAATAAACAAAAGTTTTTTAAATAATA	60
Na1	AATTTTGATATTTTAAATAAATAATATAAAAAGCCTAATAAACAAAAGTTTTTTAAATAATA	60
Na2	AATTT-GATA-TTTAATAAATAATATAAAAAGC-TAATGAACAAAAGTTTTTTAAATAATA	57
Na3	AATTTTGATA-TTTAATAAATAATATAAAAAGCCTAATGAACAAAAGTTTTTTAAATAATA	59
Na4	AATTTTGATATTTTAAATAAATAATATAAAAAGCCTAATGAACAAAAGTTTTTTAAATAATA	60
Nb1	AATTTTGATATTTTAAATAAATAATATAAAAAGCCTAATGAACAAAAGTTTTTTAAATAATA	60
Nb2	AATTTTGATATTTTAAATAAATAATATAAAAAGCCTAATGAACAAAAGTTTTTTAAATAATA	60
Nb3	AATTTTGATATTTTAAATAAATAATATAAAAAGCCTAATGAACAAAAGTTTTTTAAATAATA	60
Sa1	AATTT-GATA-TTTAATAAATAATATAAAAAGC-TAATGAACAAAAGTTTTTTAAATAATA	57
Sa2	AATTTTGATATTTTAAATAAATAATATAAAAAGCCTAATGAACAAAAGTTTTTTAAATAATA	60
Sb1	AATTTTGATATTTTAAATAAATAATATAAAAAGCGTAATGAACAAAAGTTTTTTAAATAATA	60
Sb2	AATTT-GATATTTTAAATAAATAATATAAAAAGCCTAATGAACAAAAGTTTTTTAAATAATA	59
	***** .*****	

Fa1	ATCAAAGAAATCTTTTTAATGCACATTTTAAATAAATTAATAAATTGTTATTATGTACTA	120
Fa2	ATCAAAGAAATCTTTTTAATGCACATTTTAAATAAATTAATAAATTGTTATTATGTACTA	120
Fa3	ATCAAAGAAATCTTTTTAATGCACATTTTAAATAAATTAATAAATTGTTATTATGTACTA	120
Fa4	ATCAAAGAAATCTTTTTAATGCACATTTTAAATAAATTAATAAATTGTTATTATGTACTA	120
Fb1	ATCAAAGAAATCTTTTTAATGCACATTTTAAATAAATTAATAAATTGTTATTATGTACTA	120
Fb2	ATCAAAGAAATCTTTTTAATGCACATTTTAAATAAATTAATAAATTGTTATTATGTACTA	120
Fb3	ATCAAAGAAATCTTTTTAATGCACATTTTAAATAAATTAATAAATTGTTATTATGTACTA	120
Nb4	ATCAAAGAAATCTTTTTAATGCACATTTTAAATAAATTAATAAATTGTTATTATGTACTA	120
Na1	ATCAAAGAAATCTTTTTAATGCTCATTTTAAATAAATTAATAAATTGTTATTATGTACTA	120
Na2	ATCAAAGAAATCTTTTTAATGCTCATTTTAAATAAATTAATAAATTGTTATTATGTACTA	117
Na3	ATCAAAGAAATCTTTTTAATGCTCATTTTAAATAAATTAATAAATTGTTATTATGTACTA	119
Na4	ATCAAAGAAATCTTTTTAATGCTCATTTTAAATAAATTAATAAATTGTTATTATGTACTA	120
Nb1	ATCAAAGAAATCTTTTTAATGCTCATTTTAAATAAATTAATAAATTGTTATTATGTACTA	120
Nb2	ATCAAAGAAATCTTTTTAATGCTCATTTTAAATAAATTAATAAATTGTTATTATGTACTA	120
Nb3	ATCAAAGAAATCTTTTTAATGCTCATTTTAAATAAATTAATAAATTGTTATTATGTACTA	120
Sa1	ATCAAAGAAATCTTTTTAATGCTCATTTTAAATAAATTAATAAATTGTTATTATGTACTA	117
Sa2	ATCAAAGAAATCTTTTTAATGCTCATTTTAAATAAATTAATAAATTGTTATTATGTACTA	120
Sb1	ATCAAAGAAATCTTTTTAATGCTCATTTTAAATAAATTAATAAATTGTTATTATGTACTA	120
Sb2	ATCAAAGAAATCTTTTTAATGCTCATTTTAAATAAATTAATAAATTGTTATTATGTACTA	119
	*****:*****	

Fa1	CGTTTAGGGTAAGTTTAAAGCAATAAAAAAGTTTATATTTCTGTTGTGGGTCATTTTTTG	180
Fa2	CGTTTAGGGTAAGTTTAAAGCAATAAAAAAGTTTATATTTCTGTTGTGGGTCATTTTTTG	180
Fa3	CGTTTAGGGTAAGTTTAAAGCAATAAAAAAGTTTATATTTCTGTTGTGGGTCATTTTTTG	180
Fa4	CGTTTAGGGTAAGTTTAAAGCAATAAAAAAGTTTATATTTCTGTTGTGGGTCATTTTTTG	180
Fb1	CGTTTAGGGTAAGTTTAAAGCAATAAAAAAGTTTATATTTCTGTTGTGGGTCATTTTTTG	180
Fb2	CGTTTAGGGTAAGTTTAAAGCAATAAAAAAGTTTATATTTCTGTTGTGGGTCATTTTTTG	180
Fb3	CGTTTAGGGTAAGTTTAAAGCAATAAAAAAGTTTATATTTCTGTTGTGGGTCATTTTTTG	180
Nb4	CGTTTAGGGTAAGTTTAAAGCAATAAAAAAGTTTATATTTCTGTTGTGGGTCATTTTTTG	180
Na1	CGTTTAGGGTAAGTTTAAAGCAATAAAAAAGTTTATATTTCTGTTGTGGGTCATTTTTTG	180
Na2	CGTTTAGGGTAAGTTTAAAGCAATAAAAAAGTTTATATTTCTGTTGTGGGTCATTTTTTG	177
Na3	CGTTTAGGGTAAGTTTAAAGCAATAAAAAAGTTTATATTTCTGTTGTGGGTCATTTTTTG	179
Na4	CGTTTAGGGTAAGTTTAAAGCAATAAAAAAGTTTATATTTCTGTTGTGGGTCATTTTTTG	180
Nb1	CGTTTAGGGTAAGTTTAAAGCAATAAAAAAGTTTATATTTCTGTTGTGGGTCATTTTTTG	180
Nb2	CGTTTAGGGTAAGTTTAAAGCAATAAAAAAGTTTATATTTCTGTTGTGGGTCATTTTTTG	180
Nb3	CGTTTAGGGTAAGTTTAAAGCAATAAAAAAGTTTATATTTCTGTTGTGGGTCATTTTTTG	180
Sa1	CGTTTAGGGTAAGTTTAAAGCAATAAAAAAGTTTATATTTCTGTTGTGGGTCATTTTTTG	177
Sa2	CGTTTAGGGTAAGTTTAAAGCAATAAAAAAGTTTATATTTCTGTTGTGGGTCATTTTTTG	180
Sb1	CGTTTAGGGTAAGTTTAAAGCAATAAAAAAGTTTATATTTCTGTTGTGGGTCATTTTTTG	180
Sb2	CGTT-AGGGTAAGTTTAAAGCAATAAAAAAGTTTATATTTCTGTTGTGGGTCATTTTTTG	178



Fa1	-----	360
Fa2	-----	360
Fa3	-----	360
Fa4	-----	360
Fb1	-----	360
Fb2	-----	360
Fb3	-----	360
Nb4	-----	360
Na1	AAAGAAAATATAGTAAAAAAGGCGGACAAATGTATTGATACTAATTACAATGAAAGATTC	420
Na2	AAAGAAAATATAGTAAAAAAGGCGGACAAATGTATTGATACTAATTACAATGAAAGATTC	417
Na3	AAAGAAAATATAGTAAAAAAGGCGGACAAATGTATTGATACTAATTACAATGAAAGATTC	419
Na4	AAAGAAAATATAGTAAAAAAGGCGGACAAATGTATTGATACTAATTACAATGAAAGATTC	420
Nb1	AAAGAAAATATAGTAAAAAAGGCGGACAAATGTATTGATACTAATTACAATGAAAGATTC	420
Nb2	AAAGAAAATATAGTAAAAAAGGCGGACAAATGTATTGATACTAATTACAATGAAAGATTC	420
Nb3	AAAGAAAATATAGTAAAAAAGGCGGACAAATGTATTGATACTAATTACAATGAAAGATTC	420
Sa1	AAAGAAAATATAGTAAAAAAGGCGGACAAATGTATTGATACTAATTACAATGAAAGATTC	417
Sa2	AAAGAAAATATAGTAAAAAAGGCGGACAAATGTATTGATACTAATTACAATGAAAGATTC	420
Sb1	AAAGAAAATATAGTAAAAAAGGCGGACAAATGTATTGATACTAATTACAATGAAAGATTC	420
Sb2	AAAGAAAATATAGTAAAAAAGGCGGACAAATGTATTGATACTAATTACAATGAAAGATTC	418

Fa1	-----	360
Fa2	-----	360
Fa3	-----	360
Fa4	-----	360
Fb1	-----	360
Fb2	-----	360
Fb3	-----	360
Nb4	-----	360
Na1	AAATTTTGTGTTTTTGCCTTTATTTTATAAAGGGCGATTGTTTTTTGCTTATTTTAAAA	480
Na2	AAATTTTGTGTTTTTGCCTTTATTTTATAAAGGGCGATTGTTTTTTGCTTATTTTAAAA	477
Na3	AAATTTTGTGTTTTTGCCTTTATTTTATAAAGGGCGATTGTTTTTTGCTTATTTTAAAA	479
Na4	AAATTTTGTGTTTTTGCCTTTATTTTATAAAGGGCGATTGTTTTTTGCTTATTTTAAAA	480
Nb1	AAATTTTGTGTTTTTGCCTTTATTTTATAAAGGGCGATTGTTTTTTGCTTATTTTAAAA	480
Nb2	AAATTTTGTGTTTTTGCCTTTATTTTATAAAGGGCGATTGTTTTTTGCTTATTTTAAAA	480
Nb3	AAATTTTGTGTTTTTGCCTTTATTTTATAAAGGGCGATTGTTTTTTGCTTATTTTAAAA	480
Sa1	AAATTTTGTGTTTTTGCCTTTATTTTATAAAGGGCGATTGTTTTTTGCTTATTTTAAAA	477
Sa2	AAATTTTGTGTTTTTGCCTTTATTTTATAAAGGGCGATTGTTTTTTGCTTATTTTAAAA	480
Sb1	AAATTTTGTGTTTTTGCCTTTATTTTATAAAGGGCGATTGTTTTTTGCTTATTTTAAAA	480
Sb2	AAATTTTGTGTTTTTGCCTTTATTTTATAAAGGGCGATTGTTTTTTGCTTATTTTAAAA	478

Fa1	-----	360
Fa2	-----	360
Fa3	-----	360
Fa4	-----	360
Fb1	-----	360
Fb2	-----	360
Fb3	-----	360
Nb4	-----	360
Na1	TCACTCTGTATGTCAAAAAATGCATAAAATATAGGGTGTTCATTTGGAAGATCAAGGAA	540
Na2	TCACTCTGTATGTCAAAAAATGCATAAAATATAGGGTGTTCATTTGGAAGATCAAGGAA	537
Na3	TCACTCTGTATGTCAAAAAATGCATAAAATATAGGGTGTTCATTTGGAAGATCAAGGAA	539
Na4	TCACTCTGTATGTCAAAAAATGCATAAAATATAGGGTGTTCATTTGGAAGATCAAGGAA	540
Nb1	TCACTCTGTATGTCAAAAAATGCATAAAATATAGGGTGTTCATTTGGAAGATCAAGGAA	540
Nb2	TCACTCTGTATGTCAAAAAATGCATAAAATATAGGGTGTTCATTTGGAAGATCAAGGAA	540
Nb3	TCACTCTGTATGTCAAAAAATGCATAAAATATAGGGTGTTCATTTGGAAGATCAAGGAA	540
Sa1	TCACTCTGTATGTCAAAAAATGCATAAAATATAGGGTGTTCATTTGGAAGATCAAGGAA	537
Sa2	TCACTCTGTATGTCAAAAAATGCATAAAATATAGGGTGTTCATTTGGAAGATCAAGGAA	540
Sb1	TCACTCTGTATGTCAAAAAATGCATAAAATATAGGGTGTTCATTTGGAAGATCAAGGAA	540
Sb2	TCACTCTGTATGTCAAAAAATGCATAAAATATAGGGTGTTCATTTGGAAGATCAAGGAA	538

Fa1	-----AAAGAAAATATAGTAAA	377
Fa2	-----AAAGAAAATATAGTAAA	377
Fa3	-----AAAGAAAATATAGTAAA	377
Fa4	-----AAAGAAAATATAGTAAA	377
Fb1	-----AAAGAAAATATAGTAAA	377
Fb2	-----AAAGAAAATATAGTAAA	377
Fb3	-----AAAGAAAATATAGTAAA	377
Nb4	-----AAAGAAAATATAGTAAA	377
Na1	GGATAAAAAAATTGAAAATAAATAAATTTAAAAAAATTTATAAAAAAAGAAAATATAGTAAA	600
Na2	GGATAAAAAAATTGAAAATAAATAAATTTAAAAAAATTTATAAAAAAAGAAAATATAGTAAA	597
Na3	GGATAAAAAAATTGAAAATAAATAAATTTAAAAAAATTTATAAAAAAAGAAAATATAGTAAA	599
Na4	GGATAAAAAAATTGAAAATAAATAAATTTAAAAAAATTTATAAAAAAAGAAAATATAGTAAA	600
Nb1	GGATAAAAAAATTGAAAATAAATAAATTTAAAAAAATTTATAAAAAAAGAAAATATAGTAAA	600
Nb2	GGATAAAAAAATTGAAAATAAATAAATTTAAAAAAATTTATAAAAAAAGAAAATATAGTAAA	600
Nb3	GGATAAAAAAATTGAAAATAAATAAATTTAAAAAAATTTATAAAAAAAGAAAATATAGTAAA	600
Sa1	GGATAAAAAAATTGAAAATAAATAAATTTAAAAAAATTTATAAAAAAAGAAAATATAGTAAA	597
Sa2	GGATAAAAAAATTGAAAATAAATAAATTTAAAAAAATTTATAAAAAAAGAAAATATAGTAAA	600
Sb1	GGATAAAAAAATTGAAAATAAATAAATTTAAAAAAATTTATAAAAAAAGAAAATATAGTAAA	600
Sb2	GGATAAAAAAATTGAAAATAAATAAATTTAAAAAAATTTATAAAAAAAGAAAATATAGTAAA	598

\*\*\*\*\*

Fa1	AAAGCGGACAAATGTATTGATACTAATTACAATGAAAGATTCAATTTTTGTGTTTTTGC	437
Fa2	AAAGCGGACAAATGTATTGATACTAATTACAATGAAAGATTCAATTTTTGTGTTTTTGC	437
Fa3	AAAGCGGACAAATGTATTGATACTAATTACAATGAAAGATTCAATTTTTGTGTTTTTGC	437
Fa4	AAAGCGGACAAATGTATTGATACTAATTACAATGAAAGATTCAATTTTTGTGTTTTTGC	437
Fb1	AAAGCGGACAAATGTATTGATACTAATTACAATGAAAGATTCAATTTTTGTGTTTTTGC	437
Fb2	AAAGCGGACAAATGTATTGATACTAATTACAATGAAAGATTCAATTTTTGTGTTTTTGC	437
Fb3	AAAGCGGACAAATGTATTGATACTAATTACAATGAAAGATTCAATTTTTGTGTTTTTGC	437
Nb4	AAAGCGGACAAATGTATTGATACTAATTACAATGAAAGATTCAATTTTTGTGTTTTTGC	437
Na1	AAAAGCGGACAAATGTATTGATACTAATTACAATGAAAGATTCAATTTTTGTGTTTTTGC	660
Na2	AAAAGCGGACAAATGTATTGATACTAATTACAATGAAAGATTCAATTTTTGTGTTTTTGC	657
Na3	AAAAGCGGACAAATGTATTGATACTAATTACAATGAAAGATTCAATTTTTGTGTTTTTGC	659
Na4	AAAAGCGGACAAATGTATTGATACTAATTACAATGAAAGATTCAATTTTTGTGTTTTTGC	660
Nb1	AAAAGCGGACAAATGTATTGATACTAATTACAATGAAAGATTCAATTTTTGTGTTTTTGC	660
Nb2	AAAAGCGGACAAATGTATTGATACTAATTACAATGAAAGATTCAATTTTTGTGTTTTTGC	660
Nb3	AAAAGCGGACAAATGTATTGATACTAATTACAATGAAAGATTCAATTTTTGTGTTTTTGC	660
Sa1	AAAAGCGGACAAATGTATTGATACTAATTACAATGAAAGATTCAATTTTTGTGTTTTTGC	657
Sa2	AAAAGCGGACAAATGTATTGATACTAATTACAATGAAAGATTCAATTTTTGTGTTTTTGC	660
Sb1	AAAAGCGGACAAATGTATTGATACTAATTACAATGAAAGATTCAATTTTTGTGTTTTTGC	660
Sb2	AAAAGCGGACAAATGTATTGATACTAATTACAATGAAAGATTCAATTTTTGTGTTTTTGC	658

\*\*\*.\*\*\*\*\*:\*\*\*\*\*

Fa1	CTTATTTTATAAAAAGGCGATTGTTTTTTTGCCTATTTTAAAATCACTCTGTATGTCAAAA	497
Fa2	CTTATTTTATAAAAAGGCGATTGTTTTTTTGCCTATTTTAAAATCACTCTGTATGTCAAAA	497
Fa3	CTTATTTTATAAAAAGGCGATTGTTTTTTTGCCTATTTTAAAATCACTCTGTATGTCAAAA	497
Fa4	CTTATTTTATAAAAAGGCGATTGTTTTTTTGCCTATTTTAAAATCACTCTGTATGTCAAAA	497
Fb1	CTTATTTTATAAAAAGGCGATTGTTTTTTTGCCTATTTTAAAATCACTCTGTATGTCAAAA	497
Fb2	CTTATTTTATAAAAAGGCGATTGTTTTTTTGCCTATTTTAAAATCACTCTGTATGTCAAAA	497
Fb3	CTTATTTTATAAAAAGGCGATTGTTTTTTTGCCTATTTTAAAATCACTCTGTATGTCAAAA	497
Nb4	CTTATTTTATAAAAAGGCGATTGTTTTTTTGCCTATTTTAAAATCACTCTGTATGTCAAAA	497
Na1	CTTATTTTATAAAAAGGCGATTGTTTTTTTGCCTATTTTAAAATCACTCTGTATGTCAAAA	720
Na2	CTTATTTTATAAAAAGGCGATTGTTTTTTTGCCTATTTTAAAATCACTCTGTATGTCAAAA	717
Na3	CTTATTTTATAAAAAGGCGATTGTTTTTTTGCCTATTTTAAAATCACTCTGTATGTCAAAA	719
Na4	CTTATTTTATAAAAAGGCGATTGTTTTTTTGCCTATTTTAAAATCACTCTGTATGTCAAAA	720
Nb1	CTTATTTTATAAAAAGGCGATTGTTTTTTTGCCTATTTTAAAATCACTCTGTATGTCAAAA	720
Nb2	CTTATTTTATAAAAAGGCGATTGTTTTTTTGCCTATTTTAAAATCACTCTGTATGTCAAAA	720
Nb3	CTTATTTTATAAAAAGGCGATTGTTTTTTTGCCTATTTTAAAATCACTCTGTATGTCAAAA	720
Sa1	CTTATTTTATAAAAAGGCGATTGTTTTTTTGCCTATTTTAAAATCACTCTGTATGTCAAAA	717
Sa2	CTTATTTTATAAAAAGGCGATTGTTTTTTTGCCTATTTTAAAATCACTCTGTATGTCAAAA	720
Sb1	CTTATTTTATAAAAAGGCGATTGTTTTTTTGCCTATTTTAAAATCACTCTGTATGTCAAAA	720
Sb2	CTTATTTTATAAAAAGGCGATTGTTTTTTTGCCTATTTTAAAATCACTCTGTATGTCAAAA	718

\*\*\*\*\*



Fa1	CT	679
Fa2	CT	679
Fa3	CT	679
Fa4	CT	679
Fb1	CT	679
Fb2	CT	679
Fb3	CT	679
Nb4	CT	679
Na1	CT	902
Na2	CT	899
Na3	CT	901
Na4	CT	902
Nb1	CT	902
Nb2	CT	902
Nb3	CT	901
Sa1	CT	899
Sa2	CT	902
Sb1	CT	902
Sb2	CT	899
	**	

## Supplementary File 4-2. Information about 27 candidates differentially expressed in the fast lines.

On chromosome 3, *C-factor* encodes a short-chain dehydrogenases/reductase (SDR) and is a member of SDR superfamily (Niu et al., 2022). In insects, SDR enzymes mainly participate in the synthesis of ecdysone in a specific Black Box step of ecdysteroid biosynthesis (Niwa et al., 2010) (Figure 4-37).

*SLC25-35-1*, *Melted* and *SLC25-35-2* are close to each other in the genome of *T. castaneum*. We did find significant differential expression of *Melted* and *SLC25-35-2*, but not of *SLC25-35-1*. By interacting with tuberous sclerosis 1 (Tsc1) and FOXO, *Melted* enhances insulin/TOR (target of rapamycin) activity (Teleman et al., 2005), a pivotal pathway enhancing growth rate (Baker and Thummel, 2007; Nijhout et al., 2014). It is unclear how the mitochondrial solute carrier *SLC25-35-2* would affect developmental speeds. Hence, it could be that *Melted* acted as the driver gene and *SLC25-35-2* as the hitchhiker.

CYP6 orthologs, including *Cyp6a14* and *Cyp6k1*, have been implicated to insecticide resistance in many insects, such as *D. melanogaster* (Daborn et al., 2002), *T. castaneum* (Ercan et al., 2020; Oppert et al., 2015), *Leptinotarsa decemlineata* (Scott et al., 2020), *Anopheles gambiae* (Nikou et al., 2003), *Myzus persicae* (Chiu et al., 2008) and *Periplaneta americana* (Zhang et al., 2016). However, it has never been reported that CYP6 orthologs participate in the regulation of development.

The calcitonin receptor is homologous to a subfamily of the seven-transmembrane domain, G-protein-coupled receptor superfamily (GPCRs) in family B. In function, family B proteins of GPCRs typically recognize regulatory peptides such as parathyroid hormone, secretin, glucagon, urocortin and vasoactive intestinal polypeptide (Harmar, 2001; McLatchie et al., 1998). In *Drosophila*, family B proteins of GPCRs regulate longevity and stress responses (Lin et al., 1998). In addition, calcitonin receptor regulates the body temperature rhythm in insects as well as in mammals (Goda et al., 2018).

Odorant receptors also belong to the GPCRs family but lack homology to GPCRs in vertebrates (Buck and Axel, 1991). They contain the odorant-binding site and interact with a vast chemicals (Hallem and Carlson, 2006). In insects, odor detection is mediated by a unique class of odorant-gated ion channels (Sato et al., 2008; Wicher et al., 2008). The members of GPCRs, *CalcitoninR* and *OR327* may participate in the regulation of development by recognizing regulatory peptides.

*Sec61a* is participating in the transport of polypeptides into the eukaryotic endoplasmic reticulum (Park and Rapoport, 2012). Here, down-regulation of *Sec61a* in fast developing embryos might indicate that the transport of polypeptides is not much required after dorsal closure. *Lac2* controls cuticle tanning in *Tribolium* (Arakane et al., 2005). So, fast developing embryos need to catalyze cuticle tanning in advance before hatching to larvae. Although *Skiv2* was significantly down-regulated during dorsal closure (Figure 4-5A), no reports on its function in insects are available.

On chromosome 9, the *metabotropic glutamate receptors (mGluR)* is a member of family C GPCRs. By mediating intracellular signal transduction, the *mGluR* carries out a variety of functions, such as mobilization of calcium, modulation of a variety of ion channels (calcium or potassium currents), and activation of protein kinase C, phospholipase D, protein kinase and TOR pathways (Conn and Pin, 1997; Niswender and Conn, 2010). Thus, the up-regulation of *mGluR* found in our study may indicate that intracellular signal transduction is very active during dorsal closure.

Suppression of tumorigenicity 18 protein (ST18) encodes a zinc finger transcription factor and is involved in apoptosis and inflammation. In human, it is mainly related to occurrence of disease, such as pemphigus vulgaris (Petzl-Erler, 2020) and Alzheimer's disease (Kim et al., 2021). As no publications on the function of St18 C2H2C in insects are available, we do not discuss it here.



The main function of cationic amino acid transporters (CATs) is participating in the transport of cationic amino acids into most cells, and mediating efflux of their substrates as well (Closs et al., 2006). In this study, gene expression profiles of three CATs, including *CAT1*, *CAT2* and *CAT3*, strongly suggested that all of them are possibly involved in fast embryonic development. They are orthologous to slimfast, an amino acid sensor that can overrule peripheral insulin/TOR activity by PI3K modulation (Colombani et al., 2003). They are thus likely candidates to affect developmental speed.

The *Drosophila* transcription factor, Adh distal factor-1 (Adf-1), containing a TAF-binding motif of Myb and Myb-related proteins, binds to upstream recognition elements in a diverse group of promoters to activate their transcription, such as dopa decarboxylase and antennapedia P1 (Cutler et al., 1998; England et al., 1990). Adf-1 is only detectable in most somatic cells of later stages embryos but not in very early embryos of *Drosophila* (England et al., 1992). Here, expression data suggested that Adf-1 plays a more important role during dorsal closure than after it. In *Bemisia tabaci*, silencing Adf-1 activates autophagy and apoptosis, therefore resulting in a significant decrease in the total number of bacteriocytes (Li et al., 2022).

Protein-L-isoaspartate O-methyltransferase (Pcmt) is used to accomplish L-isoaspartate methylation, thus repairing proteins by reformation of l-aspartate (Mishra and Mahawar, 2019). The down-regulation of *Pcmt* found in our study may suggest low investment in protein repair in fast developing embryos.

*LOC107397428*, *Chymase*, *Cyp18a1* and *Cyp306a1* are close to each other in the genome, too. As they are all differentially expressed, all of the could be the target of selection. However, our RNAi screen suggests that a deletion affecting *Cyp18a1* expression is the driving allele. *LOC107397428* is an uncharacterized gene in the NCBI gene database. As a member of neutral serine proteases, Chymase has been widely studied in mammals and is essentially unique to mast cells (Pejler, 2020; Welle, 1997). Down-regulation of *Chymase* may suggest fewer mast cells in fast developing embryos. See Discussion for *Cyp18a1* and *Cyp306a1* (*phantom*).

*Deadpan*, a gene encoding a helix-loop-helix protein, is one direct target of Notch signaling in *Drosophila* (Bier et al., 1992; San-Juán and Baonza, 2011). The Notch signaling is participating in many aspects of communication between cells and regulating metazoan development and tissue renewal (Kopan and Ilagan, 2009). Through Notch signaling, *Deadpan* could be involved in many aspects of dorsal closure.

Pancreatic triacylglycerol lipase (Lipase) fulfills a key function in fat metabolism by finally breaking down dietary lipids into monoglycerides and free fatty acids (Winkler et al., 1990). In this study, *Lipase* was up-regulated before dorsal closure, and down-regulated during and after it. This pattern may indicate that fat metabolism is highly required to start dorsal closure.

*Integrin aPS2* expression did not vary too much in the process of dorsal closure among the selection lines. The cell adhesion molecule integrin is likely to play an important role in morphogenetic movements such as dorsal closure (Münster et al., 2019).

Inositol hexakisphosphate kinase (Ip6k), with three isoforms in mammals but one isoform in *Drosophila*, participates in diverse cellular pathways via the synthesis of inositol pyrophosphates (Jadav et al., 2016). Inositol pyrophosphates can affect protein function by binding to protein itself or pyrophosphorylation of its  $\beta$ -phosphate to form pyrophosphoserine, thus participating in a diverse of metabolic, developmental, and signaling pathways (Shah et al., 2017).

Bone morphogenetic protein (BMP) and activin membrane-bound inhibitor (Bambi) is an inhibitor of the transforming growth factor- $\beta$  (TGF- $\beta$ ) signaling but a positive modulator of Wnt signaling (Carethers, 2009; Lin et al., 2008). BMPs are multifunctional growth factors and belong to the TGF- $\beta$

superfamily. As the negative regulator, Bambi inhibits BMP and activin signaling during *Xenopus* embryogenesis (Onichtchouk et al., 1999). In this study, significant up-regulation of *Ip6k* and *Bambi* found in our study indicates that many pathways are involved in finishing dorsal closure.

### Supplementary file 2 references

- Arakane, Y., Muthukrishnan, S., Beeman, R. W., Kanost, M. R. and Kramer, K. J.** (2005). Laccase 2 is the phenoloxidase gene required for beetle cuticle tanning. *Proceedings of the National Academy of Sciences* **102**, 11337-11342.
- Baker, K. D. and Thummel, C. S.** (2007). Diabetic larvae and obese flies—emerging studies of metabolism in *Drosophila*. *Cell metabolism* **6**, 257-266.
- Bier, E., Vaessin, H., Younger-Shepherd, S., Jan, L. Y. and Jan, Y. N.** (1992). deadpan, an essential pan-neural gene in *Drosophila*, encodes a helix-loop-helix protein similar to the hairy gene product. *Genes & Development* **6**, 2137-2151.
- Buck, L. and Axel, R.** (1991). A novel multigene family may encode odorant receptors: a molecular basis for odor recognition. *Cell* **65**, 175-187.
- Carethers, J. M.** (2009). Intersection of transforming growth factor- $\beta$  and wnt signaling pathways in colorectal cancer and metastasis. *Gastroenterology* **137**, 33-36.
- Chiu, T.-L., Wen, Z., Rupasinghe, S. G. and Schuler, M. A.** (2008). Comparative molecular modeling of *Anopheles gambiae* CYP6Z1, a mosquito P450 capable of metabolizing DDT. *Proceedings of the National Academy of Sciences* **105**, 8855-8860.
- Closs, E., Boissel, J.-P., Habermeier, A. and Rotmann, A.** (2006). Structure and function of cationic amino acid transporters (CATs). *The Journal of membrane biology* **213**, 67-77.
- Colombani, J., Raisin, S., Pantalacci, S., Radimerski, T., Montagne, J. and Léopold, P.** (2003). A nutrient sensor mechanism controls *Drosophila* growth. *Cell* **114**, 739-749.
- Conn, P. J. and Pin, J.-P.** (1997). Pharmacology and functions of metabotropic glutamate receptors. *Annual review of pharmacology and toxicology* **37**, 205-237.
- Cutler, G., Perry, K. M. and Tjian, R.** (1998). Adf-1 is a nonmodular transcription factor that contains a TAF-binding Myb-like motif. *Molecular and cellular biology* **18**, 2252-2261.
- Daborn, P., Yen, J., Bogwitz, M., Le Goff, G., Feil, E., Jeffers, S., Tijet, N., Perry, T., Heckel, D. and Batterham, P.** (2002). A single P450 allele associated with insecticide resistance in *Drosophila*. *Science* **297**, 2253-2256.
- England, B. P., Admon, A. and Tjian, R.** (1992). Cloning of *Drosophila* transcription factor Adf-1 reveals homology to Myb oncoproteins. *Proceedings of the National Academy of Sciences* **89**, 683-687.
- England, B. P., Heberlein, U. and Tjian, R.** (1990). Purified *Drosophila* transcription factor, Adh distal factor-1 (Adf-1), binds to sites in several *Drosophila* promoters and activates transcription. *Journal of Biological Chemistry* **265**, 5086-5094.
- Ercan, F. S., Azarkan, S. Y., Ercan, N. and Koc, M.** (2020). Sequence variants of CYP345a1 and CYP6a14 gene regions in *Tribolium castaneum* (Coleoptera: Tenebrionidae) adults treated with the novel characterized *Bolanthus turcicus* (Caryophyllaceae) extract. *Molecular Biology Research Communications* **9**, 105.
- Goda, T., Doi, M., Umezaki, Y., Murai, I., Shimatani, H., Chu, M. L., Nguyen, V. H., Okamura, H. and Hamada, F. N.** (2018). Calcitonin receptors are ancient modulators for rhythms of preferential temperature in insects and body temperature in mammals. *Genes & development* **32**, 140-155.
- Hallem, E. A. and Carlson, J. R.** (2006). Coding of odors by a receptor repertoire. *Cell* **125**, 143-160.
- Harmar, A. J.** (2001). Family-B G-protein-coupled receptors. *Genome biology* **2**, 1-10.
- Jadav, R. S., Kumar, D., Buwa, N., Ganguli, S., Thampatty, S. R., Balasubramanian, N. and Bhandari, R.** (2016). Deletion of inositol hexakisphosphate kinase 1 (IP6K1) reduces cell migration and invasion, conferring protection from aerodigestive tract carcinoma in mice. *Cellular signalling* **28**, 1124-1136.

- Kim, B.-H., Nho, K., Lee, J.-M. and Initiative, A. s. D. N.** (2021). Genome-wide association study identifies susceptibility loci of brain atrophy to NFIA and ST18 in Alzheimer's disease. *Neurobiology of Aging* **102**, 200. e201-200. e211.
- Kopan, R. and Ilagan, M. X. G.** (2009). The canonical Notch signaling pathway: unfolding the activation mechanism. *Cell* **137**, 216-233.
- Li, N.-N., Jiang, S., Lu, K.-Y., Hong, J.-S., Wang, Y.-B., Yan, J.-Y. and Luan, J.-B.** (2022). Bacteriocyte development is sexually differentiated in *Bemisia tabaci*. *Cell reports* **38**, 110455.
- Lin, Y.-J., Seroude, L. and Benzer, S.** (1998). Extended life-span and stress resistance in the *Drosophila* mutant methuselah. *Science* **282**, 943-946.
- Lin, Z., Gao, C., Ning, Y., He, X., Wu, W. and Chen, Y.-G.** (2008). The pseudoreceptor BMP and activin membrane-bound inhibitor positively modulates Wnt/ $\beta$ -catenin signaling. *Journal of Biological Chemistry* **283**, 33053-33058.
- McLatchie, L. M., Fraser, N. J., Main, M. J., Wise, A., Brown, J., Thompson, N., Solari, R., Lee, M. G. and Foord, S. M.** (1998). RAMPs regulate the transport and ligand specificity of the calcitonin-receptor-like receptor. *Nature* **393**, 333-339.
- Mishra, P. and Mahawar, M.** (2019). PIMT-mediated protein repair: Mechanism and implications. *Biochemistry (Moscow)* **84**, 453-463.
- Münster, S., Jain, A., Mietke, A., Pavlopoulos, A., Grill, S. W. and Tomancak, P.** (2019). Attachment of the blastoderm to the vitelline envelope affects gastrulation of insects. *Nature* **568**, 395-399.
- Nijhout, H. F., Riddiford, L. M., Mirth, C., Shingleton, A. W., Suzuki, Y. and Callier, V.** (2014). The developmental control of size in insects. *Wiley Interdisciplinary Reviews: Developmental Biology* **3**, 113-134.
- Nikou, D., Ranson, H. and Hemingway, J.** (2003). An adult-specific CYP6 P450 gene is overexpressed in a pyrethroid-resistant strain of the malaria vector, *Anopheles gambiae*. *Gene* **318**, 91-102.
- Niswender, C. M. and Conn, P. J.** (2010). Metabotropic glutamate receptors: physiology, pharmacology, and disease. *Annual review of pharmacology and toxicology* **50**, 295.
- Niu, L., Yan, H., Sun, Y., Zhang, D., Ma, W. and Lin, Y.** (2022). Nanoparticle facilitated stacked-dsRNA improves suppression of the Lepidopteran pest *Chilo suppressalis*. *Pesticide Biochemistry and Physiology* **187**, 105183.
- Niwa, R., Namiki, T., Ito, K., Shimada-Niwa, Y., Kiuchi, M., Kawaoka, S., Kayukawa, T., Banno, Y., Fujimoto, Y. and Shigenobu, S.** (2010). Non-molting glossy/shroud encodes a short-chain dehydrogenase/reductase that functions in the 'Black Box' of the ecdysteroid biosynthesis pathway. *Development* **137**, 1991-1999.
- Onichtchouk, D., Chen, Y.-G., Dosch, R., Gawantka, V., Delius, H. and Niehrs, C.** (1999). Silencing of TGF- $\beta$  signalling by the pseudoreceptor BAMBI. *Nature* **401**, 480-485.
- Oppert, B., Guedes, R. N., Aikins, M. J., Perkin, L., Chen, Z., Phillips, T. W., Zhu, K. Y., Opit, G. P., Hoon, K. and Sun, Y.** (2015). Genes related to mitochondrial functions are differentially expressed in phosphine-resistant and-susceptible *Tribolium castaneum*. *BMC genomics* **16**, 1-10.
- Park, E. and Rapoport, T. A.** (2012). Mechanisms of Sec61/SecY-mediated protein translocation across membranes. *Annu Rev Biophys* **41**, 21-40.
- Pejler, G.** (2020). Novel insight into the in vivo function of mast cell chymase: Lessons from knockouts and inhibitors. *Journal of Innate Immunity* **12**, 357-372.
- Petzl-Erler, M. L.** (2020). Beyond the HLA polymorphism: A complex pattern of genetic susceptibility to pemphigus. *Genetics and molecular biology* **43**.
- San-Juán, B. P. and Baonza, A.** (2011). The bHLH factor deadpan is a direct target of Notch signaling and regulates neuroblast self-renewal in *Drosophila*. *Developmental biology* **352**, 70-82.
- Sato, K., Pellegrino, M., Nakagawa, T., Nakagawa, T., Vosshall, L. B. and Touhara, K.** (2008). Insect olfactory receptors are heteromeric ligand-gated ion channels. *Nature* **452**, 1002-1006.

- Scott, I. M., Hatten, G., Tuncer, Y., Clarke, V. C., Jurcic, K. and Yeung, K. K.-C.** (2020). Proteomic Analyses Detect Higher Expression of C-Type Lectins in Imidacloprid-Resistant Colorado Potato Beetle *Leptinotarsa decemlineata* Say. *Insects* **12**, 3.
- Shah, A., Ganguli, S., Sen, J. and Bhandari, R.** (2017). Inositol pyrophosphates: energetic, omnipresent and versatile signalling molecules. *Journal of the Indian Institute of Science* **97**, 23-40.
- Teleman, A. A., Chen, Y.-W. and Cohen, S. M.** (2005). Drosophila Melted modulates FOXO and TOR activity. *Developmental cell* **9**, 271-281.
- Welle, M.** (1997). Development, significance, and heterogeneity of mast cells with particular regard to the mast cell-specific proteases chymase and tryptase. *Journal of leukocyte biology* **61**, 233-245.
- Wicher, D., Schäfer, R., Bauernfeind, R., Stensmyr, M. C., Heller, R., Heinemann, S. H. and Hansson, B. S.** (2008). Drosophila odorant receptors are both ligand-gated and cyclic-nucleotide-activated cation channels. *Nature* **452**, 1007-1011.
- Winkler, F., d'Arcy, A. and Hunziker, W.** (1990). Structure of human pancreatic lipase. *Nature* **343**, 771-774.
- Zhang, J., Zhang, Y., Li, J., Liu, M. and Liu, Z.** (2016). Midgut transcriptome of the cockroach *Periplaneta americana* and its microbiota: digestion, detoxification and oxidative stress response. *PloS one* **11**, e0155254.

### Supplementary File 4-3. The details on the mathematical modelling.

Here we provide a detailed derivation of the mathematical model of ecdysone dynamics. First we focus on the cross-talk between ecdysone and its own synthesis, i.e. the Halloween genes (Niwa and Niwa, 2016). A positive feedback of ecdysone into the Halloween has been well established, for instance for *phm* and *dib* (Moeller et al., 2013). In our model, we let *Spook* represent the Halloween genes. Also in *Tribolium*, there is a binding site for the ecdysone receptor just upstream of the *Spook* transcription start site, suggesting that ecdysone positively regulates transcription of *Spook*. This creates a positive feedback loop between Spook and ecdysone (*Figure S1* in this supplementary file).

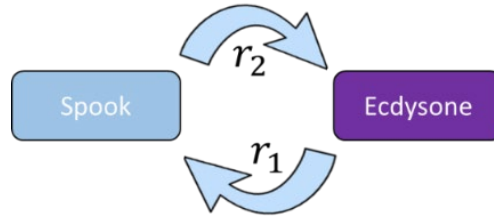


*Figure S1*. Diagram of the positive feedback loop between Spook and Ecdysone. The arrows indicate positive interactions.

Following the law of mass action (Lund, 1965), the reactions shown in *Figure S1* above translate to the set of ordinary differential equations,

$$\begin{cases} \frac{dS}{dt} = r_1 E - \beta_1 S, \\ \frac{dE}{dt} = r_2 S - \beta_2 E. \end{cases} \quad (1)$$

The first right-hand side terms of Eq. (1) represent the production of Spook ( $S$ ) and ecdysone ( $E$ ); the second right-hand side terms represent the degradation of Spook and ecdysone. To simplify the model and focus on ecdysone, we assume that ecdysone production and degradation is slow relative to Spook transcription and translation, such that the level of Spook can be expressed as an ecdysone-dependent steady state,  $S = \bar{S}(E)$ . The quasi-steady state assumption ( $d\bar{S}/dt = 0$ ) then yields that:

$$\bar{S}(E) = \frac{r_1}{\beta_1} E \quad (2)$$

Substituting Eq. (2) into Eq. (1), we have following equation:

$$\frac{dE}{dt} = \beta E. \quad (3)$$

where  $\beta = r_1 r_2 / \beta_1 - \beta_2$ . Thus Eq. (3) describes autocatalytic synthesis of ecdysone (*Figure S2* in this supplementary file, right panel).

Next we include the transcription, translation and activity of the ecdysone inactivating enzyme Cyp18a1 (denoted as  $C$ ). An increase of *Cyp18a1* expression follows the onset of high ecdysone (main Figure 4-14), suggesting that ecdysone upregulates Cyp18a1 production. To model inactivation of ecdysone, we assume a simple enzymatic breakdown. The full conceptual model then becomes as shown in *Figure S2* in this supplementary file.

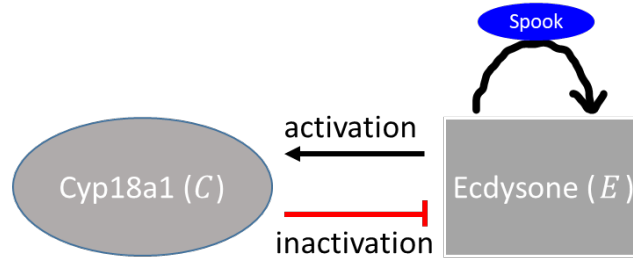


*Figure S2.* Diagrammatic representation of the regulation paths among the reactions of Spook, Ecdysone and Cyp18a1. The black arrows mean positive regulation and red arrow means negative regulation. The self-regulation of ecdysone is a simplified version of the feedback loops in *Figure S1* under the quasi-steady state assumption of Spook.

Mathematically, following the law of mass action (Lund, 1965) and ignoring Michaelis-Menten kinetics (Johnson and Goody, 2011), the reactions in *Figure S2* above are described by extending Eq. (3) as,

$$\begin{cases} \frac{dC}{dt} = f(E) - \lambda C, \\ \frac{dE}{dt} = bE - kCE. \end{cases} \quad (4)$$

In the first equation, we use an increasing function  $f(E)$  for the ecdysone-induced transcription and translation of Cyp18a1, and a first-order degradation of Cyp18a1. Ecdysone synthesis is due to an autocatalytic production ( $bE$ ; see Eq. 3), the term  $kCE$  is enzymatic degradation of ecdysone by Cyp18a1. For the form of the activation function  $f(E)$ , Zuin, J. et al. recently found that the gene transcription rate induced by promoter-enhancer contact satisfies a Sigmoid function (Zuin et al., 2022). Therefore, we assumed an explicit sigmoidal function

$$f(E) = \frac{V_{max}}{1 + \exp((\theta - E)/s)}. \quad (5)$$

To test the validity of our model, we used the least square method to fit Eq. (3) to the ecdysone timeseries for *Tribolium* eggs in presence of *Cyp18a1* pRNAi (*Figure S3a* in this supplementary file, see also main Figure 4-21). To include the effect of Cyp18a1 and to further test our model, by selecting appropriate values for  $\theta$  and  $s$  (*Table S1*), we next fitted the Eq. (4) to the timeseries of Cyp18a1 and ecdysone for normal *Tribolium* eggs (*Figure S3b* in this supplementary file, see also main Figure 4-14). The results show that our model fits very well with the data (*Figure S3a* and *Figure S3b* in this supplementary file).

In Sigmoid function (5), the regulation of ecdysone to Cyp18a1 expression, there are three parameters.  $V_{max}$  represents the maximal production rate of Cyp18a1,  $\theta$  is a threshold of ecdysone at which the production rate of Cyp18a1 is half of  $V_{max}$ , and  $s$  is the slope factor which controls the response sharpness (sensitivity) of Cyp18a1 production to ecdysone. With high sensitivity ( $s$  is high), Cyp18a1 production starts at low ecdysone levels, while the start of Cyp18a1 production requires higher ecdysone levels when  $s$  is low (main Figure 4-38C). In other words, we assume that the Slow allele containing two binding sites for the anchoring protein Tramtrack is more likely to establish or maintain enhancer-promotor interactions at low ecdysone levels (main Figure 4-39B), while the F allele is more refractory to low ecdysone levels (main Figure 4-39B).

In *Figure S4*, we present the dynamics of Cyp18a1 expression and ecdysone concentration with variations in parameters  $V_{max}$ ,  $\theta$  and  $s$ , respectively. We observed that, with the decrease of  $s$  (i.e., reduced sensitivity of Cyp18a1 production to ecdysone), *Cyp18a1* expression becomes delayed, but ecdysone peaks earlier and more highly, in agreement with the experimental data (main Figure 4-33, Figure 4-34 and *Figure S4c*). Collectively, these simulations support the idea that changing the reaction sensitivity of Cyp18a1 to ecdysone leads to the shift of the ecdysone peak.

*Table S1*. Parameters and initial values used for numerical simulations.

Estimated results of equation (3)	Par	Description	Value
	$\beta$	The net growth rate of ecdysone	0.03/h
	$E_0$	The initial value of equation (3)	592pg/ml
Parameters and initial values in equations (4) and in sigmodal function (5)	$b$	The relative growth rate of ecdysone	0.24/h
	$k$	Cyp18a1-mediated degradation rate of ecdysone	21.24/h
	$\lambda$	Degradation rate of Cyp18a1	0.0087/h
	$V_{max}$	Maximal production rate of Cyp18a1	0.0012/h
	$\theta$	Ecdysone concentration producing half maximal production rate of Cyp18a1	2500pg/ml
	$s$	Response sharpness (sensitivity) of Cyp18a1 to ecdysone	1000pg/ml
	$C_0$	Initial value of Cyp18a1 in Eq (4)	0.0032pg/ml
	$E_0$	Initial value of ecdysone in Eq (4)	89.52pg/ml

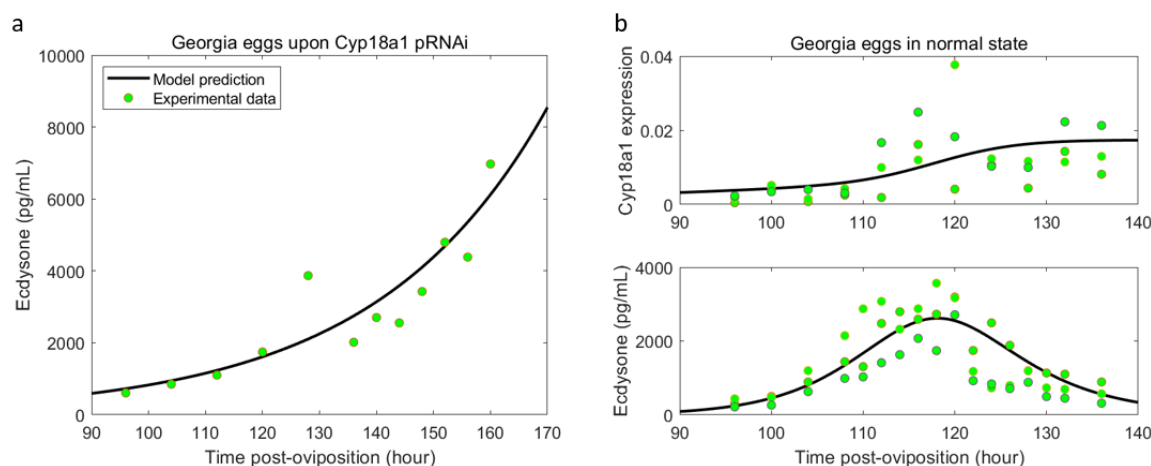


*Figure S3*. Data fitting and parameters estimation by matching equation (3) and equation (4) to the Cyp18a1 expression level and ecdysone concentration in Georgia eggs. **(a)** The time series of ecdysone in Georgia eggs upon Cyp18a1 pRNAi. **(b)** The dynamics of Cyp18a1 and ecdysone in wild type Georgia eggs. The growth of ecdysone in Georgia eggs exposed to Cyp18a1 pRNAi is exponential. In normal situation, ecdysone shows a peak when the level of Cyp18a1 is bigger than a certain level.

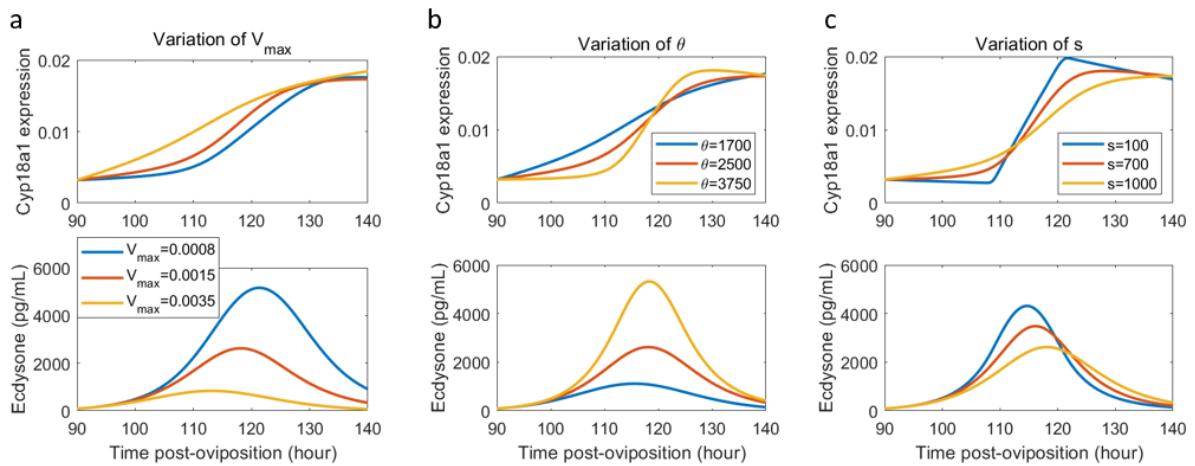


Figure S4. The dynamics of Cyp18a1 expression level and ecdysone concentration with variations in parameters  $V_{max}$  (a),  $\theta$  (b) and  $s$  (c) of the Sigmoid function.

### Supplementary file 3 references

- Johnson, K. A. and Goody, R. S.** (2011). The original Michaelis constant: translation of the 1913 Michaelis–Menten paper. *Biochemistry* **50**, 8264-8269.
- Lund, E. W.** (1965). Guldberg and Waage and the law of mass action. *Journal of Chemical Education* **42**, 548.
- Moeller, M. E., Danielsen, E. T., Herder, R., O'Connor, M. B. and Rewitz, K. F.** (2013). Dynamic feedback circuits function as a switch for shaping a maturation-inducing steroid pulse in *Drosophila*. *Development* **140**, 4730-4739.
- Niwa, Y. S. and Niwa, R.** (2016). Transcriptional regulation of insect steroid hormone biosynthesis and its role in controlling timing of molting and metamorphosis. *Dev Growth Differ* **58**, 94-105.
- Zuin, J., Roth, G., Zhan, Y., Cramard, J., Redolfi, J., Piskadlo, E., Mach, P., Kryzhanovska, M., Tihanyi, G. and Kohler, H.** (2022). Nonlinear control of transcription through enhancer–promoter interactions. *Nature* **604**, 571-577.





# Chapter 5

## Summary, discussion and perspective

### Summary

This thesis focuses on important life history traits and their trade-offs. Particularly, the trade-off between immune defense and embryonic developmental speed is a central theme of study. In short, the details of immune defenses during embryonic development of basal hexapods are studied in Chapter 2, the trade-off with developmental speed is studied in chapter 3 using selection lines of the red flour beetle *Tribolium castaneum*, while the genetics underlying developmental speed are studied in Chapter 4.

Several evolutionary innovations have made significant contributions to the extraordinary success of the insects (discussed in **Chapter 1**). However, an evolutionary novelty in insect eggs, the serosa, gets less attention from evolutionary biologists.

### The serosa and immune competence of springtail eggs

During insect embryonic development, immune protection is provided by the serosa, an extraembryonic epithelium (Jacobs et al., 2014a; Jacobs et al., 2022).

In **Chapter 2**, I expanded immune challenge to the non-insect springtail *Orchesella cincta* that does not possess a serosa, but is very close to insects in the phylogenetic tree (Figure 5-1). By injecting a mixture of Gram-positive and Gram-negative bacteria (*Micrococcus luteus* and *Escherichia coli*), I showed that immune genes in the eggs of *O. cincta* are upregulated upon infection. Thus, I concluded that the serosa is not an absolute prerequisite for an innate immune response and that other tissues produce antimicrobials in springtail eggs. Interestingly, it has been reported that eggs of the burying beetle *Nicrophorus vespilloides* lack an inducible innate immune response upon infection, despite possessing a serosa (Jacobs et al., 2014b). This further confirms that the presence or absence of a serosa in arthropod eggs does not necessarily mean presence or absence of an innate immune protection.

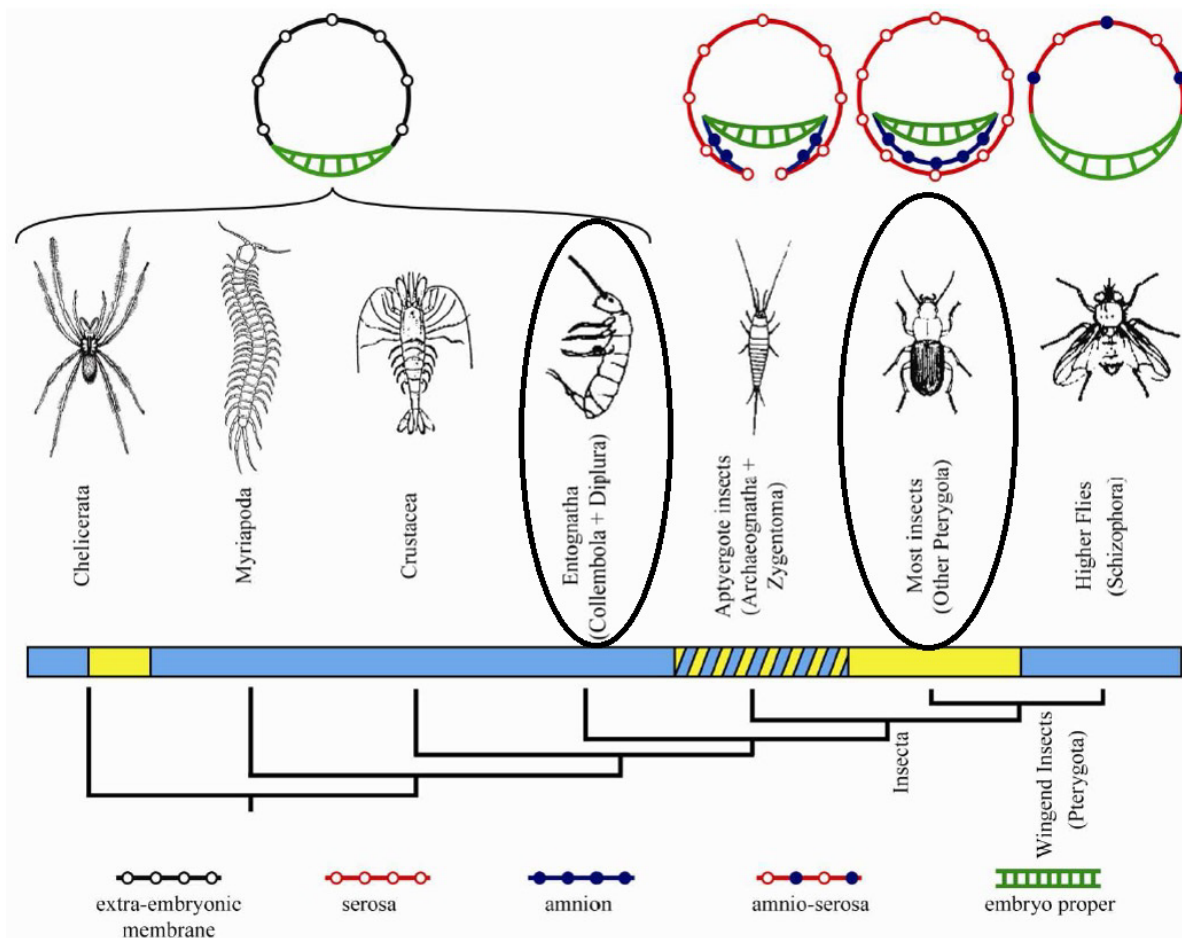


Figure 5-1. Phylogeny of all major arthropod groups. The bar under the groups shows that the eggs live in aquatic (blue), terrestrial (yellow) or humid environments (striped). The schematic drawings above illustrate the topology of embryo, amnion and serosa in these eggs. The springtails and insects are indicated with an oval in the phylogenetic tree. Adopted from (Jacobs et al., 2013).

### Trade-offs with developmental speed

The insects *N. vespilloides* and *Drosophila melanogaster* both develop extremely quickly as embryo, and both lost desiccation resistance and immune competence of the egg (Jacobs and van der Zee, 2013; Jacobs et al., 2014b). *Drosophila* has lost the serosa altogether. Thus, egg defense seems to trade off with developmental speed in insects. Trade-offs between growth and immune defense have been shown in several organisms (Brommer, 2004; Diamond and Kingsolver, 2011; Lozano-Durán et al., 2013).

In **Chapter 3**, I selected replicate outbred populations of *Tribolium castaneum* for fast and slow embryonic development. I was thereby able to test this possible trade-off between immune defense and the duration of embryonic development. I did not find the trade-off between immune defense and embryonic developmental time in the infected selection lines, even though all genes tested showed strong upregulation upon infection. By measuring fecundity of our *Tribolium* selection lines, however, we found a strong negative correlation between developmental speed and fecundity (Figure 5-2).

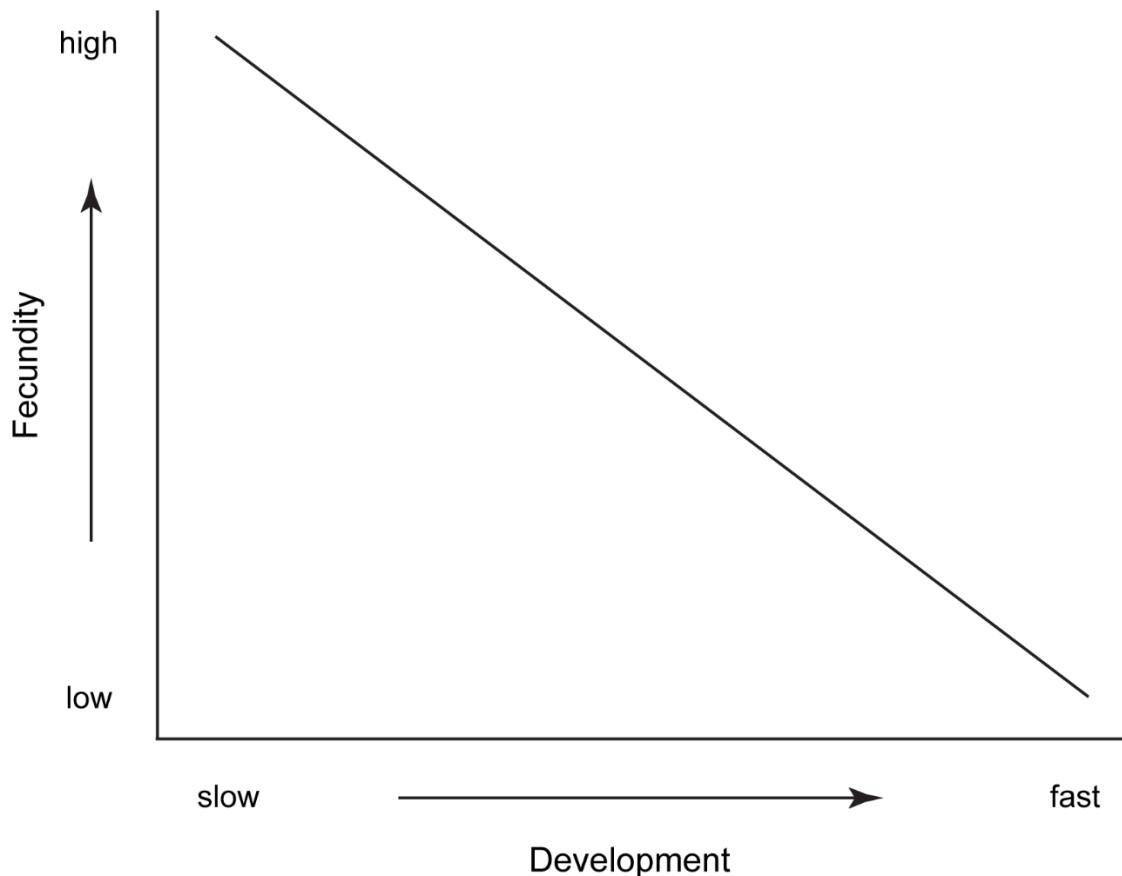


Figure 5-2. The trade-off between fast development and high fecundity found in our *Tribolium* selection lines.

### **A major life history allele in the beetle *Tribolium***

Most decisions of insects on physiological, developmental, and behavioral events are mediated by hormones (Gade et al., 1997; Ketterson and Nolan, 1999; Lösel and Wehling, 2003; Stearns, 1989). The steroid hormone ecdysone (20E) is such a crucial hormone in insects (Scaraffia and Miesfeld, 2013).

In **Chapter 4**, I show a clear divergence in embryonic developmental timing of the selection lines from the start of dorsal closure onwards. I also show that a high ecdysone peak during embryonic development induces dorsal closure. Consistently, the embryonic ecdysteroid peak of the fast lines occurred earlier than in the selection lines for slow embryonic development.

Combining pooled whole genome resequencing with gene expression and a functional RNAi screen, I show that *Cyp18a1*, the 20E degrading enzyme was a main target of selection. Particularly, I show that a 222 bp deletion (called F allele in Chapter 4) upstream of *Cyp18a1* (Figure 5-3B), has been under positive selection in the fast lines. The deletion is located in a cis-regulatory element containing Tramtrack and Broad transcription factor binding sites, and a binding site for the Ecdysone receptor forming an ecdysone-responsive enhancer regulating *Cyp18a1* expression (Figure 5-3). The alternative allele is the S allele in which no deletion is present, but a repeated sequence (Figure 5-3A).

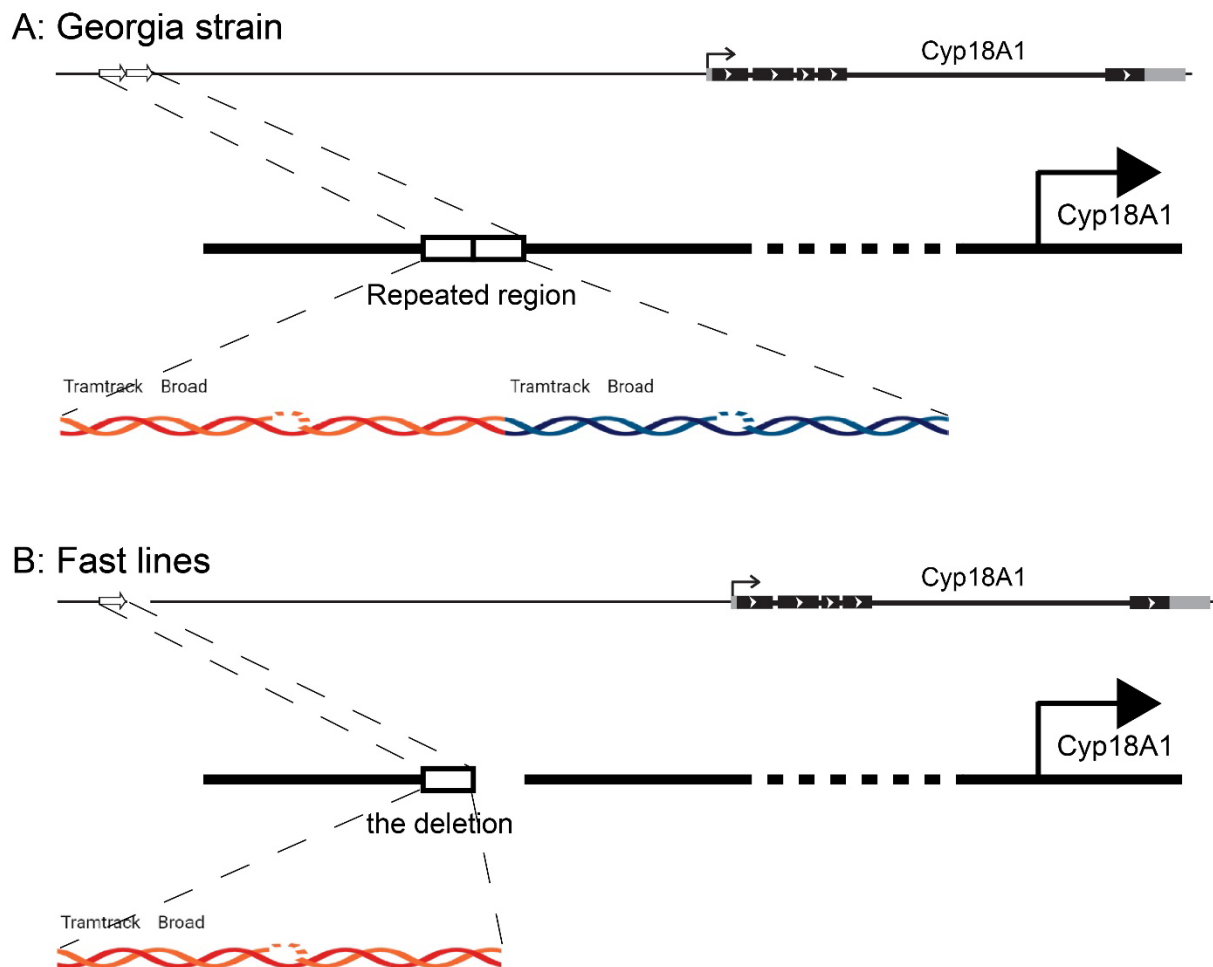


Figure 5-3. Schematic overview of the repeated region and the deletion in the upstream of *Cyp18a1*. A, The repeated region in the Georgia strain with double Tramtrack and Broad transcription factor binding sites (The S allele). B, the deleted region from the fast lines of the selection lines with single Tramtrack and Broad transcription factor binding sites (The F allele).

Interestingly, the Georgia lab strain is homozygous for the S-allele, which means that in all individuals, the 222 bp sequence is duplicated (Figure 5-3A). This gave me the chance to recreate this deletion in the homogenous genetic background of the Georgia strain using CRISPR-Cas9 technology. As a result, I show that this single deletion accelerates development, delays *Cyp18a1* expression, advances the ecdysone peak, and causes a trade-off with fecundity. As the slow allele contains two Tramtrack and two Broad binding sites, instead of one, we assume that the enhancer of the slow allele more easily establishes contact with the basal promoter. A mathematical model shows that reduced sensitivity to ecdysone of the fast allele delays *Cyp18a1* expression, but advances the ecdysone peak if one assumes that ecdysone levels depend on a self-regulatory positive feedback loop.

In conclusion, I could not show that developmental speed trades off with immune defense, but I demonstrated a clear trade-off with fecundity. This life-history trade-off is genetically mediated by a simple 222bp deletion upstream of the ecdysone degrading enzyme *Cyp18a1*.

## Discussion and perspective

We found ecdysone as main target of selection for altered developmental speed. On the one hand, ecdysone is well known to control developmental time (Rewitz et al., 2013; Yamanaka et al., 2013). But on the other hand, ecdysone is also involved in starting or potentiating immunocompetence, the topic of Chapter 2 and 3. Ecdysone upregulates, for instance, the receptor of the IMD pathway PGRP-LC (Rus et al., 2013), and also directly some antimicrobial peptides (Flatt et al., 2008; Meister and Richards, 1996). However, in our study, we did not find a trade-off between developmental speed and immune defense (Chapter 3). It could be that such trade-off is not present in our selection lines, but it could also be that our qPCR approach on a limited set of immune genes was not sufficient to reveal such a trade-off.

Ecdysone is a typical developmental timer. Indeed, growth rate (expressed in mg/days) is not significantly different between the fast and slow lines (Chapter 3); only developmental time is. However, among the targets of selection is also *meltd*, a protein that interacts with Tsc1 and FOXO to enhance insulin/TOR activity (Teleman et al., 2005). Insulin signalling is a pivotal pathway enhancing growth rate (Baker and Thummel, 2007; Nijhout et al., 2014). Another potential target identified is *CATI*. CAT is orthologous to slimfast, an amino acid sensor in the fat body that can overrule peripheral insulin/TOR activity by PI3K modulation affecting developmental time (Baker and Thummel, 2007; Colombani et al., 2003). Both *Meltd* and *CATI* RNAi lead to developmental delay (Figure 4-6).

These two major regulatory systems, ecdysone and insulin/TOR signalling could mutually regulate developmental speed. Upon stimulation by insulin and insulin-like growth factor (IGF) or amino acids, insulin and TOR pathways are activated. The second major target in our selection lines, *Meltd*, balances these two pathways (Baker and Thummel, 2007; Teleman et al., 2005), which in the end also has an output in ecdysone biosynthesis (Kannangara et al., 2021; Niwa and Niwa, 2016; Yamanaka et al., 2013) (Figure 5-4). With the activation of ecdysone signaling, developmental timing is also affected.

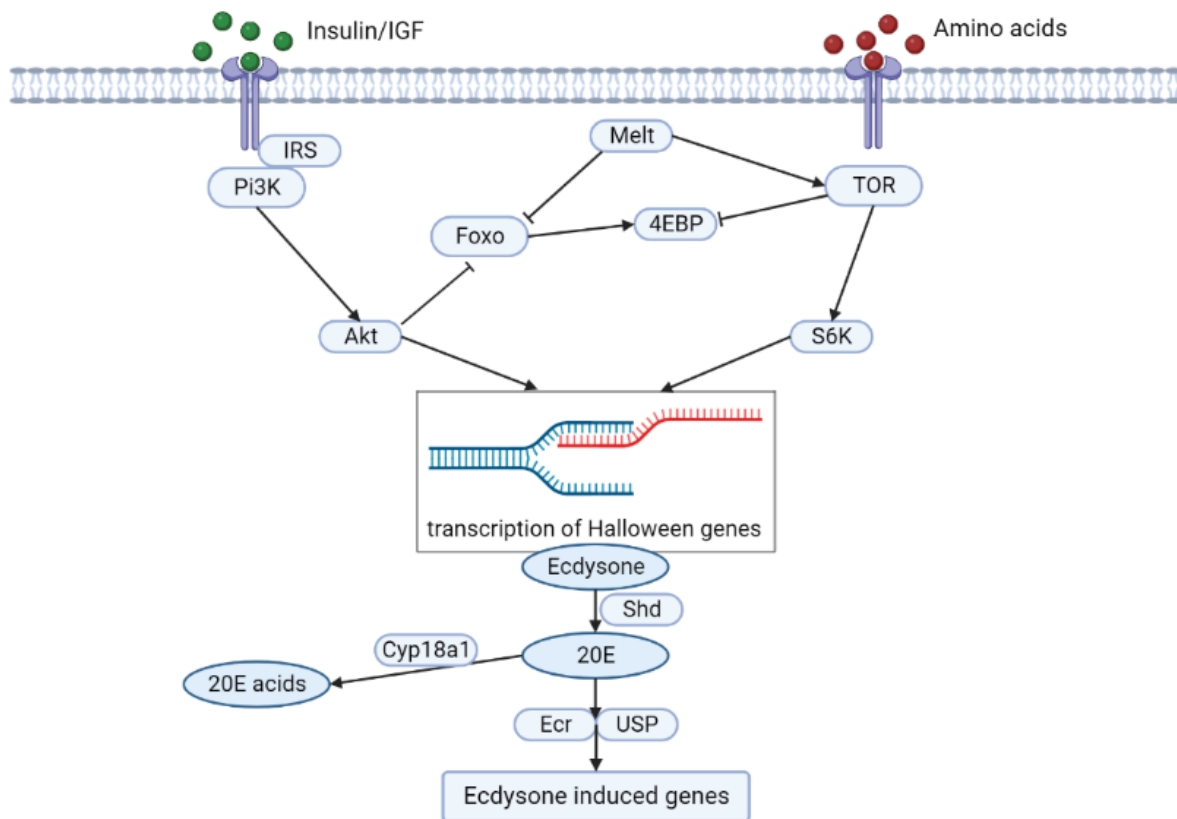


Figure 5-4. Cross talk between ecdysone signaling, insulin and target of rapamycin (TOR) pathways. Key: green balls, insulin and insulin-like growth factors; red balls, amino acids. These balls are transported through phospholipid bilayer into the cell as stimulation. After binding to the IRS or TOR, they will activate insulin and TOR pathways in the IRS/PI3K/Akt/Foxo and TOR/S6K signaling branches, respectively. Meanwhile, Melt attends to balance these two pathways by regulating Foxo and TOR. As a result, Akt and S6K turn on the transcription of Halloween genes, synthesizing ecdysone and activating 20E signaling pathway. IRS, insulin receptors; PI3K, phosphoinositide 3-kinase; Akt, protein Kinase B; FoxO, forkhead box O; Melt, protein melted; 4EBP, eukaryotic translation initiation factor 4E-binding protein; S6K, S6 Kinase; Ecr, ecdysone receptor; USP, Ultraspiracle.

So far, I did not have time to functionally study the role of insulin pathway in development in *Tribolium*. In future experiments, injections with a synthetic insulin peptide will be informative, as recently reported method to study roles of insulin in long-lived reproductive caste of ants (Yan et al., 2022). Finally, I did not find any evidence for involvement of another important hormone, juvenile hormone, which is responsible for growth, development and reproduction of insects as well (Jindra et al., 2013; Williams, 1956). In general, juvenile hormone and ecdysone have opposite roles on growth, immunity and reproduction in insects (Schwenke et al., 2016; Spindler et al., 2009). Thus, I speculate that juvenile hormone may be associated with slow embryonic development.

## Ecological importance

Current global warming is  $\sim 1.1^{\circ}\text{C}$  above preindustrial, which has raised concerns among scientists and the public. It is estimated that the warming will reach  $\sim 1.5^{\circ}\text{C}$  by 2030, and even  $\sim 2$  to  $3^{\circ}\text{C}$  expected under current policies by 2100. Strikingly, global warming of  $1.5$  to  $2^{\circ}\text{C}$  triggers multiple climate tipping points according to the Paris climate agreement. When reaching one of the tipping points, global warming may result in substantial Earth system impacts (Armstrong McKay et al., 2022).

When species respond differently to global warming, ecological mismatches in seasonal timing (“phenological mismatches”) occur. Such mismatches have also been reported for plants and their pollinators, leading to global threats for pollinators that are crucial to humans (Freimuth et al., 2022; Gérard et al., 2020). Phenological mismatches must exert strong selection on insect developmental

time (Renner and Zohner, 2018; Singer and Parmesan, 2010). My study has shown that polymorphisms affecting developmental speed are present in natural insect populations. This means that developmental timing may be much more evolvable than expected for such a supposedly highly optimized life history trait (Stearns, 2000). Maintenance of the polymorphism may be explained by balancing selection requiring rapid adult dispersal when food sources are temporary, or allowing slow development and higher fecundity in more stable ecological conditions (Charlesworth, 2015). Classically, quantitative traits are thought to be determined by many alleles of small effect (Charlesworth and Edwards, 2018). My work, however, has demonstrated that polymorphisms can be alleles of very large effect. In conclusion, insect populations may be able to adapt their developmental time and life histories rapidly to global warming.

However, I have also demonstrated that changes in key life history traits such as developmental timing are highly correlated to other traits. Although changes in developmental timing may not immediately affect immune defenses of insects, my work has clearly shown that climate-induced changes in developmental time will have consequences for weight and fecundity of insects. Such changes could still disrupt ecological networks. Nevertheless, my thesis has revealed substantial evolvability of insect developmental speed.

## Conclusions

In summary, it has been well established that insect eggs are immune-protected by the serosa. I have shown, however, that the serosa is not a prerequisite for an immune reaction in eggs, as infection upregulates immune genes in springtail eggs that do not possess a serosa. I could not find a trade-off between immune protection and developmental speed in insect eggs. I did, however, find a clear trade-off between developmental speed on the one hand and weight and fecundity on the other hand in selection lines of the beetle *Tribolium castaneum*. Strikingly, a single natural allele mediates this trade-off to a large extent, as demonstrated by CRISPR/Cas9 reconstruction. Such alleles may play a crucial role when insects have to adapt their developmental speed to current climate change.

## References

- Armstrong McKay, D. I., Staal, A., Abrams, J. F., Winkelmann, R., Sakschewski, B., Loriani, S., Fetzer, I., Cornell, S. E., Rockström, J. and Lenton, T. M. (2022). Exceeding 1.5° C global warming could trigger multiple climate tipping points. *Science* **377**, eabn7950.
- Baker, K. D. and Thummel, C. S. (2007). Diabetic larvae and obese flies—emerging studies of metabolism in *Drosophila*. *Cell metabolism* **6**, 257-266.
- Brommer, J. E. (2004). Immunocompetence and its costs during development: an experimental study in blue tit nestlings. *Proceedings of the Royal Society of London. Series B: Biological Sciences* **271**, S110-S113.
- Charlesworth, B. (2015). Causes of natural variation in fitness: Evidence from studies of *Drosophila* populations (vol 112, pg 1662, 2015). *Proceedings of the National Academy of Sciences of the United States of America* **112**.
- Charlesworth, B. and Edwards, A. W. F. (2018). A century of variance. *Significance* **15**, 20-25.
- Colombani, J., Raisin, S., Pantalacci, S., Radimerski, T., Montagne, J. and Léopold, P. (2003). A nutrient sensor mechanism controls *Drosophila* growth. *Cell* **114**, 739-749.
- Diamond, S. E. and Kingsolver, J. G. (2011). Host plant quality, selection history and trade-offs shape the immune responses of *Manduca sexta*. *Proceedings of the Royal Society B: Biological Sciences* **278**, 289-297.
- Flatt, T., Heyland, A., Rus, F., Porpiglia, E., Sherlock, C., Yamamoto, R., Garbuzov, A., Palli, S. R., Tatar, M. and Silverman, N. (2008). Hormonal regulation of the humoral innate immune response in *Drosophila melanogaster*. *Journal of Experimental Biology* **211**, 2712-2724.
- Freimuth, J., Bossdorf, O., Scheepens, J. and Willems, F. M. (2022). Climate warming changes synchrony of plants and pollinators. *Proceedings of the Royal Society B* **289**, 20212142.



- Gade, G., Hoffmann, K.-H. and Spring, J. H.** (1997). Hormonal regulation in insects: facts, gaps, and future directions. *Physiological reviews* **77**, 963-1032.
- Gérard, M., Vanderplanck, M., Wood, T. and Michez, D.** (2020). Global warming and plant–pollinator mismatches. *Emerging topics in life sciences* **4**, 77-86.
- Jacobs, C. G., Rezende, G. L., Lamers, G. E. and van der Zee, M.** (2013). The extraembryonic serosa protects the insect egg against desiccation. *Proceedings of the Royal Society B: Biological Sciences* **280**, 20131082.
- Jacobs, C. G., Spaink, H. P. and van der Zee, M.** (2014a). The extraembryonic serosa is a frontier epithelium providing the insect egg with a full-range innate immune response. *elife* **3**, e04111.
- Jacobs, C. G., van der Hulst, R., Chen, Y.-T., Williamson, R. P., Roth, S. and van der Zee, M.** (2022). Immune function of the serosa in hemimetabolous insect eggs. *Philosophical Transactions of the Royal Society B* **377**, 20210266.
- Jacobs, C. G. and van der Zee, M.** (2013). Immune competence in insect eggs depends on the extraembryonic serosa. *Developmental & Comparative Immunology* **41**, 263-269.
- Jacobs, C. G., Wang, Y., Vogel, H., Vilcinskis, A., van Der Zee, M. and Rozen, D. E.** (2014b). Egg survival is reduced by grave-soil microbes in the carrion beetle, *Nicrophorus vespilloides*. *BMC Evolutionary Biology* **14**, 1-8.
- Jindra, M., Palli, S. R. and Riddiford, L. M.** (2013). The juvenile hormone signaling pathway in insect development. *Annual review of entomology* **58**, 181-204.
- Kannangara, J. R., Mirth, C. K. and Warr, C. G.** (2021). Regulation of ecdysone production in *Drosophila* by neuropeptides and peptide hormones. *Open Biology* **11**, 200373.
- Ketterson, E. D. and Nolan, J., Val** (1999). Adaptation, exaptation, and constraint: a hormonal perspective. *the american naturalist* **154**, S4-S25.
- Lösel, R. and Wehling, M.** (2003). Nongenomic actions of steroid hormones. *Nature reviews Molecular cell biology* **4**, 46-55.
- Lozano-Durán, R., Macho, A. P., Boutrot, F., Segonzac, C., Somssich, I. E. and Zipfel, C.** (2013). The transcriptional regulator BZR1 mediates trade-off between plant innate immunity and growth. *elife* **2**, e00983.
- Meister, M. and Richards, G.** (1996). Ecdysone and insect immunity: the maturation of the inducibility of the dipterin gene in *Drosophila* larvae. *Insect biochemistry and molecular biology* **26**, 155-160.
- Nijhout, H. F., Riddiford, L. M., Mirth, C., Shingleton, A. W., Suzuki, Y. and Callier, V.** (2014). The developmental control of size in insects. *Wires Dev Biol* **3**, 113-134.
- Niwa, Y. S. and Niwa, R.** (2016). Transcriptional regulation of insect steroid hormone biosynthesis and its role in controlling timing of molting and metamorphosis. *Development, growth & differentiation* **58**, 94-105.
- Renner, S. S. and Zohner, C. M.** (2018). Climate change and phenological mismatch in trophic interactions among plants, insects, and vertebrates. *Annual review of ecology, evolution, and systematics* **49**, 165-182.
- Rewitz, K. F., Yamanaka, N. and O'Connor, M. B.** (2013). Developmental checkpoints and feedback circuits time insect maturation. *Current topics in developmental biology* **103**, 1-33.
- Rus, F., Flatt, T., Tong, M., Aggarwal, K., Okuda, K., Kleino, A., Yates, E., Tatar, M. and Silverman, N.** (2013). Ecdysone triggered PGRP-LC expression controls *Drosophila* innate immunity. *The EMBO journal* **32**, 1626-1638.
- Scaraffia, P. and Miesfeld, R.** (2013). Insect Biochemistry/Hormones. In *Encyclopedia of Biological Chemistry: Second Edition*, pp. 590-595: Elsevier Inc.
- Schwenke, R. A., Lazzaro, B. P. and Wolfner, M. F.** (2016). Reproduction–immunity trade-offs in insects. *Annual review of entomology* **61**, 239.
- Singer, M. C. and Parmesan, C.** (2010). Phenological asynchrony between herbivorous insects and their hosts: signal of climate change or pre-existing adaptive strategy? *Philosophical Transactions of the Royal Society B: Biological Sciences* **365**, 3161-3176.
- Spindler, K.-D., Hönl, C., Tremmel, C., Braun, S., Ruff, H. and Spindler-Barth, M.** (2009). Ecdysteroid hormone action. *Cellular and molecular life sciences* **66**, 3837-3850.
- Stearns, S. C.** (1989). Trade-offs in life-history evolution. *Functional ecology* **3**, 259-268.

- (2000). Life history evolution: successes, limitations, and prospects. *Naturwissenschaften* **87**, 476-486.
- Teleman, A. A., Chen, Y.-W. and Cohen, S. M.** (2005). Drosophila Melted modulates FOXO and TOR activity. *Developmental cell* **9**, 271-281.
- Williams, C. M.** (1956). The juvenile hormone of insects. *Nature* **178**, 212-213.
- Yamanaka, N., Rewitz, K. F. and O'Connor, M. B.** (2013). Ecdysone control of developmental transitions: lessons from Drosophila research. *Annual review of entomology* **58**, 497-516.
- Yan, H., Opachaloemphan, C., Carmona-Aldana, F., Mancini, G., Mlejnek, J., Descostes, N., Sieriebriennikov, B., Leibholz, A., Zhou, X. and Ding, L.** (2022). Insulin signaling in the long-lived reproductive caste of ants. *Science* **377**, 1092-1099.



# Nederlandse samenvatting

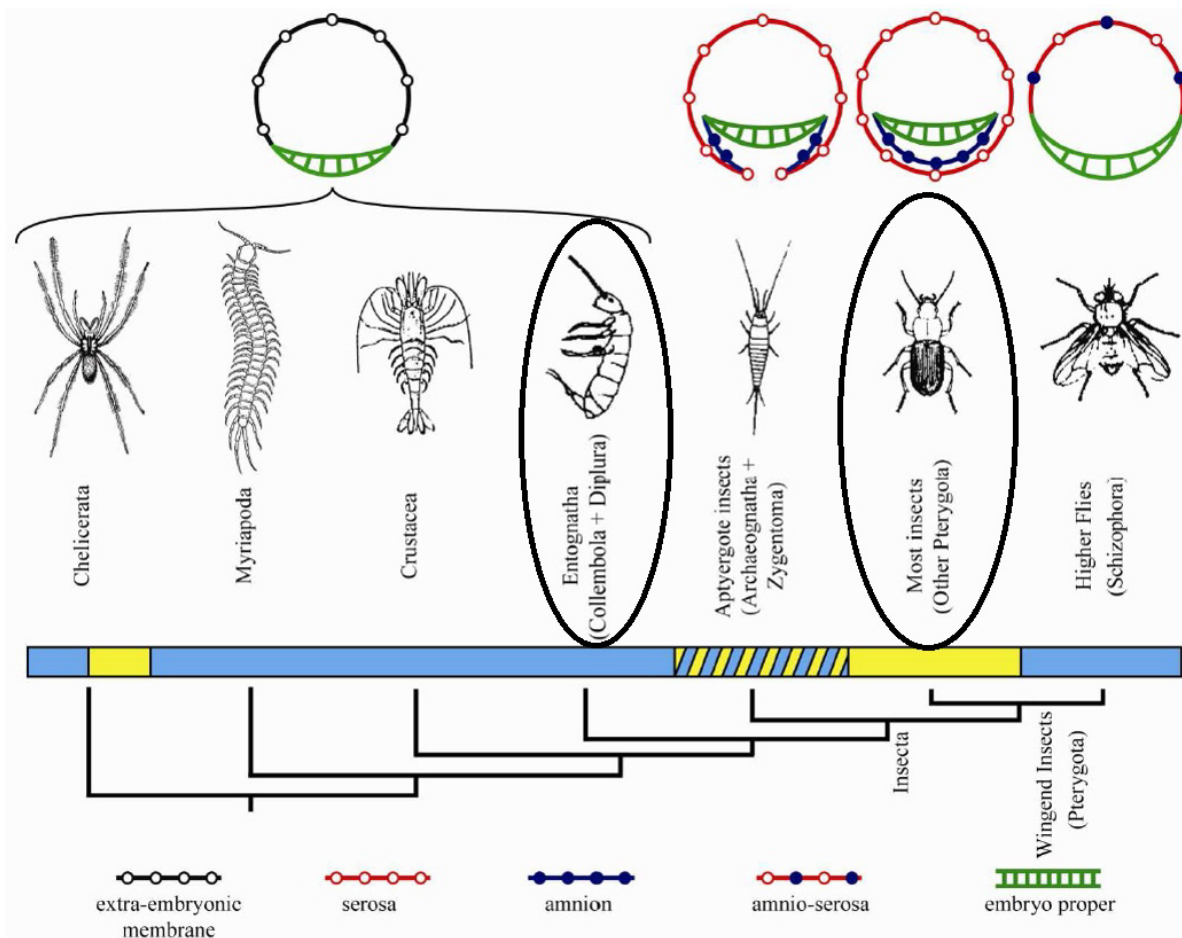
Dit proefschrift richt zich op kenmerken van de levensgeschiedenis van organismen en hun wederzijdse afhankelijkheid. In het bijzonder staat de balans tussen ontwikkelingssnelheid en de sterkte van het immuunantwoord centraal. Kort samengevat onderzoek ik de immuunafweer tijdens de embryonale ontwikkeling van een hexapode in hoofdstuk 2, onderzoek ik in hoofdstuk 3 de compromissen ('*trade-offs*') die samenhangen met verhoogde ontwikkelingssnelheid in selectielijnen van de rijstmeelkever *Tribolium castaneum* en onderzoek ik de genetische basis van deze compromissen in hoofdstuk 4.

Diverse evolutionaire innovaties hebben bijgedragen aan het buitengewone succes van de insecten (besproken in hoofdstuk 1). Een evolutionaire innovatie in het ei van insecten, de serosa, krijgt echter minder aandacht van evolutiebiologen.

## **De serosa en immunocompetentie in eieren van springstaarten**

Gedurende de embryonale ontwikkeling van insecten wordt immunologische bescherming geboden door de serosa, een extraembryonaal membraan.

In **hoofdstuk 2** onderzoek ik de immuunafweer in de springstaart *Orchesella cincta*, een organisme dat geen insect is en dus geen serosa heeft, maar wel nauw verwant is aan de insecten (Figuur 5-1). Door een mix van Gram-positieve en Gram-negatieve bacteriën (*Micrococcus luteus* en *Escherichia coli*) te injecteren, laat ik zien dat infectie de transcriptie van immuogenen verhoogt in eieren van *O. cincta*. Ik concludeer dat de serosa dus niet strikt noodzakelijk is voor een immuunantwoord en dat andere weefsels antimicrobiële eiwitten produceren in *O. cincta* eieren. Een hier interessante andere publicatie toont aan dat eieren van de doodgraver *Nicrophorus vespilloides* geen immuunantwoord laten zien, hoewel ze wel degelijk een serosa bezitten. Dit ondersteunt dat de aanwezigheid of afwezigheid van een serosa in eieren van geleedpotigen niet noodzakelijkerwijze betekent dat immuunafweer aanwezig of afwezig is.

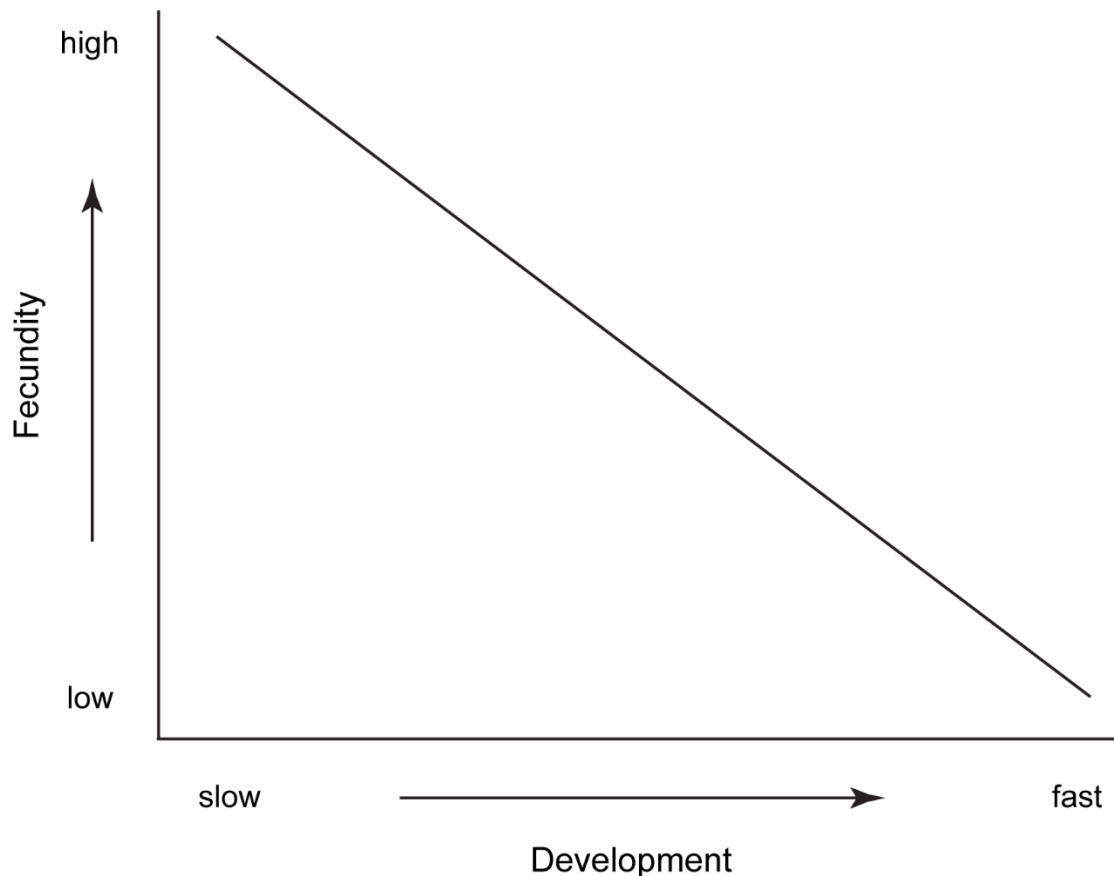


Figuur 5-1. Stamboom van de grote groepen geleedpotigen. De balk laat zien of eieren van deze groepen in aquatisch (blauw) terrestrisch (geel) of vochtig milieu ontwikkelen. De schematische tekeningen erboven laten de topologie van embryo, serosa en amnion zien in deze eieren. De springstaarten en insecten zijn omcirkeld in de stamboom.

### Trade-offs met ontwikkelingssnelheid

De doodgraver *N. vespilloides* en de fruitvlieg *D. melanogaster* ontwikkelen beide extreem snel als embryo en beiden hebben dus immunocompetentie in het ei verloren. In *Drosophila* is zelfs de gehele serosa verloren gegaan tijdens de evolutie. Het lijkt er dus op dat er een trade-off is tussen ontwikkelingssnelheid en immuunafweer. Trade-offs tussen groei en immuunafweer zijn al aangetoond in meerdere organismen.

In **hoofdstuk 3** voerde ik kunstmatige selectie uit op uitgekruiste populaties van *Tribolium castaneum* voor langzame en snelle embryonale ontwikkeling. Hierdoor was ik in staat om de wederzijdse afhankelijkheid van ontwikkelingssnelheid en sterkte van het immuunantwoord te testen. Hoewel infectie in alle lijnen leidde tot verhoogde expressie van immuunogenen, vond ik geen trade-off tussen ontwikkelingssnelheid en immuunafweer in de selectielijnen. Ik kon echter duidelijk aantonen dat er een trade-off bestaat tussen ontwikkelingssnelheid en fecunditeit (Figuur 5-2).



Figuur 5-2. De trade-off tussen ontwikkelingssnelheid en fecunditeit zoals gevonden in onze selectielijnen.

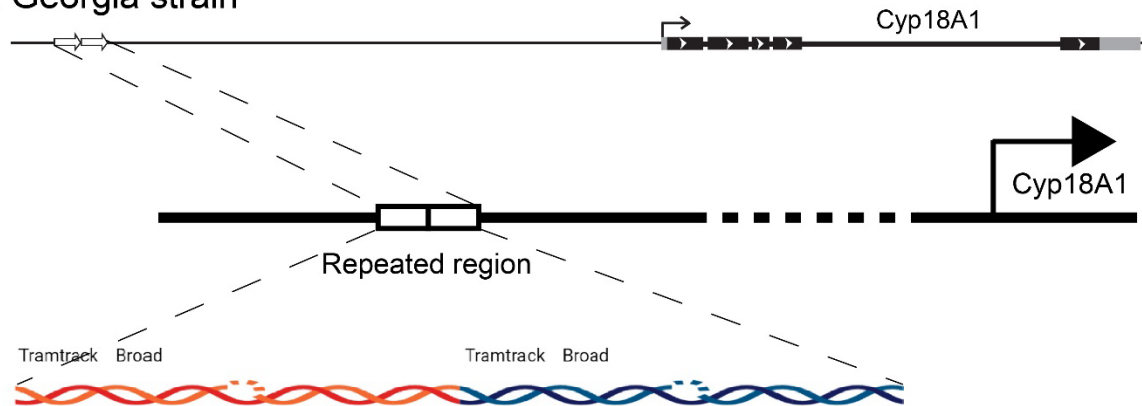
### Een belangrijk allel dat levensgeschiedenis bepaalt in *Tribolium*

De meeste beslissingen in de fysiologie, ontwikkeling en gedrag van insecten worden gestuurd. Het stereoïde hormoon ecdysone (20E) is zo'n cruciaal hormoon in insecten.

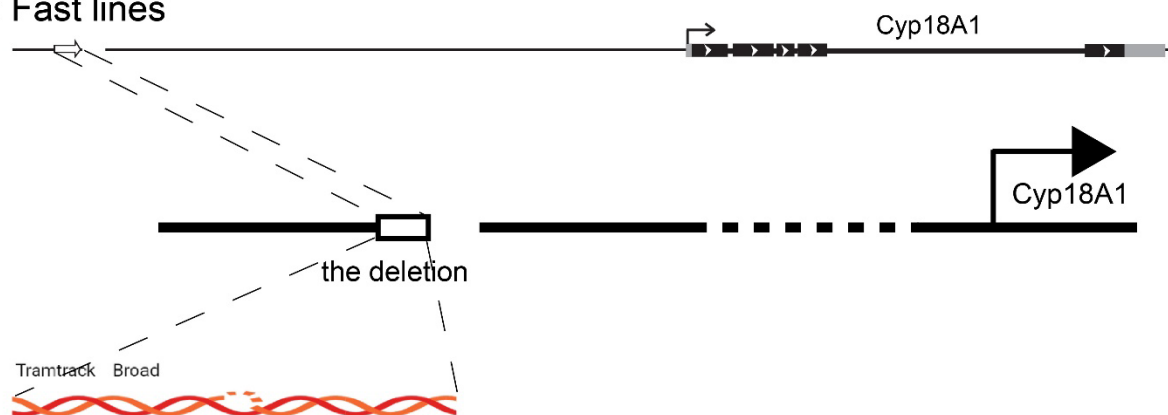
In **hoofdstuk 4** laat ik zien dat de embryonale ontwikkeling van de selectielijnen begint te divergeren in timing rond het begin van de dorsale sluiting van het embryo. Ik laat ook zien dat een puls van ecdysone tijdens de embryonale ontwikkeling de dorsale sluiting induceert. Consistent hiermee vindt de piek van ecdysone vroeger plaats in de lijnen die geselecteerd waren voor snelle embryonale ontwikkeling dan in de lijnen die geselecteerd waren voor langzame embryonale ontwikkeling.

Door *pooled whole genome resequencing* te combineren met genexpressie studies en een RNAi screen, kon ik laten zien dat een enzym dat ecdysone afbreekt, *Cyp18a1*, onder selectie heeft gestaan. Om precies te zijn heeft een deletie van 222 basenparen, die een stuk vóór *Cyp18a1* ligt, onder positieve selectie gestaan in de snelle lijnen (dit allel noemen we het F allel). Deze deletie ligt in een regulator element van *Cyp18a1* dat bindingsplaatsen voor Tramtrack, Broad en de ecdysone receptor bevat die samen een ecdysone-gevoelige enhancer vormen (Figuur 5-3). Het alternatieve allel is het S-allel waarin geen deletie aanwezig is, maar een herhaalde sequentie (Figuur 5-3A)

### A: Georgia strain



### B: Fast lines



Figuur 5-3. Schematische representatie van de regio met een herhaalde sequentie (het S allel) en een deletie (het F allel) een stuk vóór *Cyp18a1*. (A) De herhaalde sequentie in de Georgia lijn met dubbele bindingsplaatsen voor Tramtrack en Broad. (B) De deletie in dezelfde regio die alleen nog maar enkele bindingsplaatsen heeft voor Tramtrack en Broad (het F allel).

Het is interessant dat de Georgia lijn homozygoot is voor het S allel, zodat de herhaalde sequentie aanwezig is in alle individuen (Figuur 5-3A). Dit gaf mij de mogelijkheid om de deletie te reconstrueren in de homogene genetische achtergrond van de Georgia-lijn met behulp van CRISPR-Cas9 technologie. Ik laat zien dat deze deletie de embryonale ontwikkeling versnelt, de expressie van *Cyp18a1* vertraagt, maar de piek van ecdysone vervroegt en een trade-off met fecunditeit teweeg brengt. Omdat het S allel dubbele bindingsplaatsen voor Tramtrack en Broad bevat, neem ik aan dat de enhancer van het S allel makkelijker bindt met basale promotor van *Cyp18a1*. Een wiskundig model laat zien dat verminderde gevoeligheid voor ecdysone van het F allel leidt tot vertraging van *Cyp18a1* expressie, maar juist tot een eerdere piek van ecdysone als we veronderstellen dat ecdysone een positieve feedback heeft op de eigen synthese.

Samenvattend kon ik niet laten zien dat er een trade-off is tussen ontwikkelingssnelheid en sterkte van het immuunantwoord. Ik kon echter een duidelijke trade-off met fecunditeit aantonen. Deze trade-off wordt genetisch gestuurd door een eenvoudige deletie van 222 baseparen een stuk vóór het gen *Cyp18a1*.

## Curriculum Vitae

Shixiong Cheng (Chinese: 程世雄) was born in Gangu, Gansu province, China on April 12<sup>th</sup>, 1993. After graduating from high school in Gangu county, he studied aquaculture at Dalian Ocean University in Dalian, Liaoning for his bachelor and master studies from 2011 to 2018. In June 2015, he gained his bachelor degree of Science in Agriculture. He then joined in the Key Laboratory of Mariculture & Stock Enhancement in North China's Sea, Ministry of Agriculture, under the supervision of Prof. dr. Y. Chang. He continued to study aquaculture until June 2018 at the same university, with a thesis focusing on the cloning, expression analysis and functional characterization of a thioredoxin-like protein gene from sea cucumber *Apostichopus japonicas*. This thesis had been selected as 2018 excellent thesis of master graduates in Liaoning Province in May 2019.

In December 2018, Shixiong was awarded the Chinese Government Scholarship to pursue his PhD research for a period of 4 years at the Institute of Biology, Leiden University, the Netherlands. The PhD project focused on innate immunity, developmental speed and their trade-offs in two hexapod models, under the supervision of Dr. M. van der Zee and Prof. dr. H. P. Spaank. Shixiong spent most of his PhD time to study the genetic basis of embryonic developmental speed in artificial selection lines of the beetle *Tribolium castaneum*, a.o. by applying CRISPR-Cas9 technology. In December 2022, he was also funded by the Institute of Biology, Leiden University for a period of 6 months to finish the work. In August 2023, this work has been orally presented at the International Conference on Insect Science (ICIS2023) in Baoding, China, which was rewarded with the best PhD student presentation prize. The results of his work at Leiden University are presented in this thesis.





## List of publications

**Cheng S**, Jacobs CGC, Mogollón Pérez E, Chen D, van de Sanden J, Bretscher K, Verweij F, Bosman J, Hackmann A, Merks R, van den Heuvel J, and van der Zee M. A life-history allele of large effect shortens developmental time in a wild insect population. *Nature Ecology & Evolution*, accepted for publication with minor revision.

Wang M., Rücklin M., Poelmann R. E., de Mooij C. L., Fokkema M., Lamers G. E., de Bakker M. A., Chin E., Bakos L. J., Marone F., Wisse B. J., de Ruiter M. C., **Cheng S**, Nurhidayat L, Vijver M. G., and Richardson M. K. Nanoplastics causes extensive congenital malformations during embryonic development by passively targeting neural crest cells. *Environment International*. 2023 Mar 6:107865.

Wang Y\*, **Cheng S\***, Chang Y, Li K, Chen Y, Wang Y. Identification and expression analysis of a TLR11 family gene in the sea urchin *Strongylocentrotus intermedius*. *Immunogenetics*. 2018 May;70(5):337-46. (\* **co-first authors**)

**Cheng S**, Chen Y, Chang Y, Li K, Zhang X, Shang S, Li G, Li L. Cloning and expression analysis of a stomatin gene from the sea cucumber *Apostichopus japonicus*. *Invertebrate Survival Journal*. 2017 Oct 25;14(1):414-22.

**Cheng S**, Chang Y, Wang Y, Li G, Chen Y, Ning J, Li K. Molecular cloning and functional characterization of a calreticulin gene from the sea cucumber *Apostichopus japonicus*. *Invertebrate Survival Journal*. 2017 Sep 18;14(1):363-74.

**Cheng S**, Li C, Wang Y, Yang L, Chang Y. Characterization and expression analysis of a thioredoxin-like protein gene in the sea cucumber *Apostichopus japonicus*. *Fish & Shellfish Immunology*. 2016 Nov 1;58:165-73.